# Defining the Landscape of the PARKIN- and PINK1-Dependent Ubiquitin-Modified Proteome in Response to Mitochondrial Dysfunction

Dissertation Advisor: Professor J. Wade Harper Shireen Akhavan Sarraf

Abstract

**Defining the landscape of the PARKIN- and PINK1-dependent ubiquitin-modified proteome in response to mitochondrial dysfunction**

Parkinson's disease (PD) is a progressive neurological disorder resulting from loss of dopaminergic neurons of the substantia nigra, in part due to mitochondrial dysfunction. The E3 ubiquitin ligase, PARKIN, and mitochondrial kinase, PINK1, found mutated in familial early onset recessive forms of PD play central roles in mitochondrial homeostasis, thus maintaining control of a diversity of cellular processes, including energy metabolism, calcium buffering, and cell death. Together, PARKIN and PINK1 control mitochondrial homeostasis via a signaling cascade in which depolarization-induced PINK1 stabilization and activation on the mitochondrial outer membrane (MOM) promotes recruitment of PARKIN. Consequently, the outer mitochondrial membrane is extensively decorated with ubiquitin, ultimately resulting in removal of the damaged organelles via mitophagy, the selective autophagic removal of mitochondria. While PARKIN has been demonstrated to ubiquitylate Porin, Mitofusin, and Miro proteins on the MOM, the full repertoire of PARKIN substrates – the PARKIN-dependent ubiquitylome – remains poorly defined. Here, large-scale quantitative diGlycine (diGly) capture proteomics was used to identify PARKIN-dependent ubiquitylation on lysine residues in proteins modified upon mitochondrial depolarization. Hundreds of ubiquitylation sites in dozens of proteins were identified, with strong enrichment for MOM proteins, indicating that PARKIN activity has the capacity to dramatically alter the ubiquitylation status of the mitochondrial proteome. Complementary interaction proteomics identified physical association of PARKIN with a cohort of MOM ubiquitylation targets, autophagy receptors, and the proteasome, interactions which were completely dependent upon mitochondrial damage and drastically reduced upon mutation

of the active site residue, C431, found mutated in PD patients. Furthermore, structural and evolutionary analysis of PARKIN-dependent ubiquitylation events revealed extensive conservation of target sites on cytoplasmic domains in vertebrate and *D. melanogaster* MOM proteins. Parallel PINK1 interaction proteomics identified numerous subunits of the translocase of the outer mitochondrial membrane (TOMM) and a novel interactor, CLU1, shown to regulate mitochondrial morphology in lower eukaryotes. Positive genetic interaction between CLU1, PINK1, and PARKIN suggests the potential of a newly identified node of regulation for the PINK1/PARKIN pathway. These studies define how PARKIN and PINK1 re-sculpt the proteome to support mitochondrial homeostasis, ultimately contributing toward an improved understanding of their role in the progression of disease.

**Table of contents**

**List of Figures and Tables**

**Chapter 1: Introduction**



**Chapter 2: Global profiling of the PARKIN modified proteome in response to mitochondrial depolarization**

**Supplementary Table 2.** Complete list of all proteins and sites identified and quantified from all experiments from this study, as well as Tier1, 2, and 3 and Class1 and Class 2 site lists. Excel Spreadsheet.

**Supplementary Table 3.** Proteomic analysis of HA-FLAG-PARKIN associated proteins in 293T cells in response to depolarization using CompPASS. This file contains all the WDN-scores, Z-scores, and APSMs for the PARKIN immunoprecipitation data from 293T cells (WT and PARKIN mutants). Excel Spreadsheet.

**Supplementary Table 4.** Proteomic analysis of HA-FLAG-PARKIN associated proteins in HeLa cells in response to depolarization using CompPASS. This file contains all the WDN-scores, Z-scores, and APSMs for the PARKIN immunoprecipitation data from HeLa cells. Excel Spreadsheet.

**Supplementary Table 5.** Conservation and structural analysis of selected candidate PARKIN substrates. Excel spreadsheet containing Protein DataBase (PDB) identifiers, the identity of ubiquitylation sites that change in response to depolarization, and the conservation of sites in M. musculus, D. rerio, and D. melanogaster. Excel Spreadsheet.

**Supplementary Table 6.** Quantification of the PARKIN-mitochondrial overlap for the imaging experiments in Figure 2.15. Excel Spreadsheet.

**Supplementary Table 7.** Phospho-proteomic analysis of HA-FLAG-PARKIN associated proteins in 293T cells. This file contains all phosphorylation sites identified from all AP-MS experiments performed in 293T cells. Excel Spreadsheet.

**Supplementary Table 8.** RNAi screen of PARKIN substrates and interactors. This file contains lists of classes for PARKIN translocation screen and mitophagy screen performed in HeLa-N-HA-PARKIN cells. Excel Spreadsheet.

**Supplementary Table 9.** Proteomic analysis of PINK1-HA-FLAG associated proteins in 293T and HeLa cells in response to depolarization using CompPASS. This file contains all the WDN-scores, Z-scores, and APSMs. Excel Spreadsheet.

**Supplementary Table 11.** Proteomic analysis of CLU1-HA-FLAG, HA-FLAG-CLU1, and CLU1-HA-FLAG truncation mutants. This file contains all identified associated proteins in 293T cells using CompPASS. This file contains all the WDN-scores, Z-scores, and APSMs. Excel Spreadsheet.

**Acknowledgments**

Working with Wade Harper has been an extremely valuable experience for which I am grateful. From him, I have learned everything from how to properly design an experiment to analytically examining the results of those experiments (and never believing them the first time). Wade has guided me while at the same time allowing me independence to develop my own ideas and skills which has made me a more confident and self-reliant scientist and thinker. Wade has always provided an example of hard work and shown me what it takes to be a successful scientist. His constant support and willingness to help have made my achievements possible.

Much of what I have learned in graduate school is due to the generosity, of time and knowledge, of a number of current and former members of the Harper lab. Malavika Raman and I joined the lab on the same day. Since then, I have had both a great friend and a wonderful scientist to learn from and work with. Mat Sowa has expertise in so many areas and has always been willing to share it. His encouragement has been invaluable from the beginning of my time in the Harper lab. Every member of the lab has left their mark on my career and I appreciate the opportunity to work with each of them. Eric Bennett, Brenda O'Connell, and Chris Behrends were all post-docs when I started, taught me a great deal and I am glad to have worked with them. Former graduate students, Jen Svendsen and Lulu Ang and my fellow current graduate student, Marcus Tan, were always supportive and helpful, providing me wonderful examples of what to aim for. Virginia Guarani-Pereira, Seb Hayes, John Lydeard, Firaz Mohideen, Christian Munch, Jin-Mi Heo, Laura Pontano-Vaites, Anne White, Myriam Boukhali, Alban Ordureau, and Joe Mancias have all been special labmates and I have learned from every one of them.

I would also like to thank Steve Gygi and all of the members of his lab for our successful collaboration. Their generosity with their time and skills contributed greatly to my success. In particular, Woong Kim operated the Orbitrap, shot all of my diGly samples, and instructed me in diGly analysis. Ed Huttlin's bioinformatics and statistics expertise have made my project

possible and his willingness to explain them has allowed me to better understand methods for large data processing and analysis.

Thank you to my DAC committee, Randy King, Jim DeCaprio, and Wenyi Wei, who were always supportive and instructive, especially when my project was less than successful. Their suggestions have consistently been helpful and I always left my committee meetings feeling better than I went in. I would also like to acknowledge my defense committee, Randy King, Tom Schwarz, Dan Finley and Grace Gill for their time and willingness to take part in this final step of my graduate career.

Finally, I would like to thank my family, the people who deserve the most credit for my success. My parents, Mohammad and Catherine Sarraf, continue to inspire me with their intelligence, kindness and hard work. From them, I have received unwavering support in all my endeavors and the best role models possible. My brother, Darius, and my sister, Suzy, have also been constant sources of support and encouragement and have always been there for me when I needed them. Finally, David Collier has been a great influence in my life. Even through his own efforts to complete his PhD, he made it clear that he would always be there to help and support me and I cannot imagine how I could have completed this journey without him.

**Contributions**

I have had the opportunity to work with many talented and generous individuals while completing my project. Some colleagues helped me to complete specific areas of my project both by offering their expertise and guidance and their hands-on skills. Malavika Raman designed and carried out the RNAi screening and microscopy we undertook to examine the effects of individual PARKIN substrates on PARKIN translocation and mitophagy (Figure 2.22). Together, we worked with Tiao Xie of the Image Data and Analysis (IDAC) core at Harvard Medical School wrote the custom script allowing us to analyze the RNAi data. Virginia Guarani-Pereira contributed Figure 2.13 validating PARKIN-interacting proteins. The PARKIN web tools

described in Figure 2.18 were constructed by Mat Sowa who also designed the *CompPASS* software that provides the basis for much of our work in the Harper lab. Mark Kankel, from the Artavanis-Tsakonas lab, performed the Drosophila experiments detailed in Figure 3.6.

# CHAPTER 1

## Introduction

## 1.1 Parkinson's Disease

In 1871, James Parkinson published his account of "the shaking palsy," a description of the disease which was eventually named for him (Parkinson, 2002). Nearly 200 years later, it was estimated that the number of people over the age of 50 afflicted with Parkinson's disease (PD) in the world's 10 most populous nations was between 4.1 and 4.6 million in 2005 and will double to between 8.7 and 9.3 million by 2030 as worldwide life expectancy and population increase (Dorsey et al., 2007). Second only to Alzheimer's disease, Parkinson's is the most common neurodegenerative disorder whose social and economic burden on individuals and societies is increasing; the current estimate of prevalence in the US alone is 1.5 million cases (Hirtz et al., 2007; Thomas and Beal, 2007). Though recognized so many years ago, the causes of Parkinson's disease are still largely unknown though a number of genetic and environmental risk factors have been identified. Understanding of the etiology of PD has been advanced over the last two decades through the identification of several gene mutations which have provided insight into the molecular pathways of the disease.

## 1.2 Etiology of Parkinson's disease

Parkinson's disease is a neurodegenerative disorder diagnosed clinically by the presence of motor symptoms including bradykinesia, hyperkinesia, rigidity, resting tremor, and postural instability; however, non-motoric symptoms can also occur, including autonomic, cognitive, and psychiatric difficulties. These motor deficiencies are attributed to the progressive and ultimately severe impairment or loss of dopaminergic neurons of the substantia nigra pars compacta (SNpc) (Thomas and Beal, 2007) (Figure 1.1a). When functioning normally, DA neurons produce the neurotransmitter, dopamine (DA), which is transmitted between the substantia nigra and the corpus striatum to coordinate smooth controlled muscle movement. Correspondingly, decreased levels of DA result in ineffective signaling, abnormal nerve functioning, and loss of the ability to properly regulate movement (Schwartz and Sabetay, 2012)

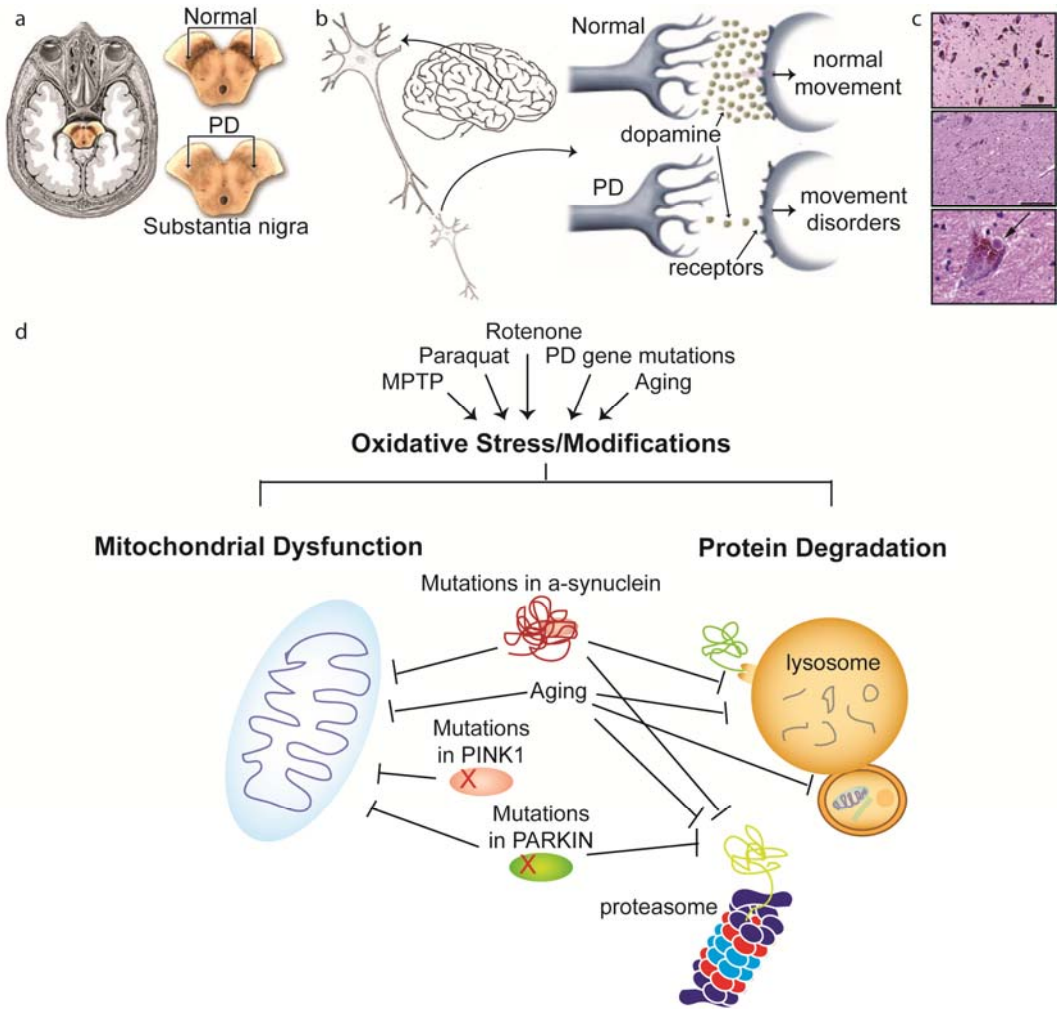


Figure 1.1 Overview of Parkinson's disease. (PD). a, Left: Location of the substantia nigra in a horizontal cross section of the brain. Right: Difference between healthy and PD-affected substantia nigra. b, Dopamine levels are decreased in PD resulting in decreased signaling and movement disorders (adapted from http://www.science.ca/scientists). c, Normal substantia nigra (top panel), PD-affected substantia nigra, note extensive loss of pigmented neurons (middle panel), high magnification of PD neuron containing Lewy body (arrow) (bottom panel) (adapted from http://missinglink.ucsf.edu/lm/ids_104_neurodegenerative.htm). d, Risk factors for PD include environmental, genetic, and endogenous influences which can trigger oxidative modifications, mitochondrial dysfunction, and impaired protein degradation which together contribute to DA neuron cell death and the progression of neurodegeneration.

(Figure 1.1b). It is estimated that at the onset of symptoms nearly 60% of SNpc DA neurons have already been lost and dopamine levels may be depleted by 80%. Though excessive loss of DA neurons does occur, the neurodegeneration extends to noradrenergic, serotonergic, and cholinergic systems as well as the cerebral cortex though it is unclear when this occurs relative to DA neuron injury or death, but is thought to occur in later stages of disease (Dauer and

Przedborski, 2003). Possibly a causal factor in the loss of DA neurons is a main pathological hallmark of idiopathic Parkinson's – the presence of α-synuclein-immunoreactive inclusions in neuronal perikarya (Lewy bodies) and processes (Lewy neurites) (Figure 1.1c). These deposits are composed of insoluble aggregates of alpha-synuclein in association with other proteins, including ubiquitin, and are believed to represent an aggresome response which may ultimately be lethal to the cell (Kalia et al., 2012).

Though there is no apparent genetic linkage in nearly 95% of cases of Parkinson's disease, the cause(s) of idiopathic disease, the most common form of the illness, remain essentially unidentified. It is generally thought that a number of environmental factors may potentially contribute to the disease, particularly when genetic susceptibility may be present (Figure 1.1d). The environmental hypothesis proposes that PD-related neurodegeneration results from exposure to a dopaminergic toxin. A clue into the pathogenesis of the disease emerged when the neurotoxin, 1-methyl-4-phenyl-1,2,3,6-tetrahydropyridine (MPTP), was discovered to cause a parkinsonian syndrome in intravenous drug users upon exposure to contaminated drug preparations (Langston et al., 1983). Follow-up studies in animals have shown that exposure to MPTP, a mitochondrial Complex I inhibitor, induces dopaminergic neurodegeneration and parkinsonism (Cannon and Greenamyre, 2011; Malkus et al., 2009). Similarly, rotenone and paraquat, also inhibitors of Complex I, are commonly used to model PD in animals. However, whether any specific toxin is truly a cause of sporadic PD is yet unproven. Another proposed initiator of the disease is an endogenous toxin, potentially produced by disturbances in the balance of normal metabolism, which then generates damaging reactive oxygen species (ROS) thus harming cells. Though the contribution of this premise is unconfirmed, polymorphisms in the xenobiotic detoxifying enzyme cytochrome P450 have been linked to greater risk of developing early-onset PD (Dauer and Przedborski, 2003; Sandy et al., 1996). Despite the uncertainty associated with these hypotheses, much edifying and productive

research based on these studies has focused on oxidative stress, mitochondrial respiration defects, and aberrant protein aggregation in DA neurons (Figure 1.1d).

### 1.3 Pathogenesis of Parkinson's disease

Though the initial causes are yet unknown, studies based on the models proposed lend support to two major hypotheses which may contribute to PD-associated neurodegeneration. First, protein misfolding and aggregation are toxic to SNpc DA neurons and second, that mitochondrial dysfunction causes oxidative stress, which ultimately results in cell death (Dauer and Przedborski, 2003) (Figure 1.1d). Clearly, these hypotheses are not mutually exclusive and it is quite likely that aspects of each play roles in SNpc neuron death and development of PD. Discovery of the overlap between these hypotheses may be the key to understanding the initiation and progression of the disease. For example, it has been shown that oxidative damage can encourage misfolding and aggregation of alpha-synuclein (Giasson et al., 2000).

#### 1.3.1 Misfolded proteins and aggregates

The presence of abnormally folded proteins in brain tissue, a characteristic of a number of neurodegenerative diseases, though the proteins involved and the location of deposits differ, suggests that this common attribute may be toxic to neuronal cells. The avenues through which misfolded proteins may harm cells are numerous, including direct damage by distortion of cellular structures or interference with intracellular processes. Aggregates could also trap and sequester vital proteins, preventing them from carrying out crucial functions. Though logical, evidence shows that there is little correlation between protein inclusions and cell death (Cummings et al., 1999; Saudou et al., 1998). In fact, it now seems more likely that inclusions may be produced as a result of active sequestration of soluble misfolded proteins, created to keep toxic soluble misfolded proteins at bay, and thus they may not actually be a causal factor in disease (Cummings et al., 1999; Dauer and Przedborski, 2003).

Little progress was made into illuminating the molecular underpinnings of PD until efforts in recent years uncovered parallels between sporadic and genetic Parkinson's. In patients with inherited PD, pathogenic mutations are thought to directly affect the folding of mutated proteins, thereby interfering with their normal functions. Furthermore, identification of single gene mutations in proteins involved in the ubiquitin proteasome system (UPS) has focused attention on the role of protein degradation, quality control, and homeostasis in the development of PD, thus linking the UPS to the production of misfolded proteins and development of inclusions.

### 1.3.2 Ubiquitin system and 26S proteasome in neurodegeneration

Ubiquitin conjugation is well-known for its prominent role in targeting cellular proteins to the 26S proteasome for degradation, allowing precise control over a variety of functions, including gene regulation, cell cycle progression, signaling pathways, endocytosis, and homeostatic turnover of proteins (Hershko and Ciechanover, 1998; Pickart and Eddins, 2004). The conjugation of ubiquitin to a substrate lysine requires an ATP-dependent enzymatic cascade carried out by E1 (ubiquitin activating), E2 (ubiquitin conjugating) and E3 (ubiquitin ligating) enzymes (Ciechanover et al., 1982; Hershko and Ciechanover, 1998; Hershko et al., 1983; Pickart and Eddins, 2004) (Figure 1.2). Conjugation of ubiquitin can have a variety of downstream consequences, depending on the type of ubiquitin chain linkage formed, including endocytosis, signaling, autophagy, and proteasomal degradation.

The 26S proteasome is a 2.4 MDa complex composed of two multisubunit subcomplexes: the 20S proteasome, which is the core protease, and the 19S regulatory particle, which can cap the 20S subunit at either end. As its name suggests, the 19S regulatory particle is responsible for regulating the activity of the proteasome by controlling access to the catalytic core. Additionally, the 19S controls recognition, deubiquitylation, and unfolding of substrates fated for degradation. ATP-dependent interaction of the hexameric ring-shaped

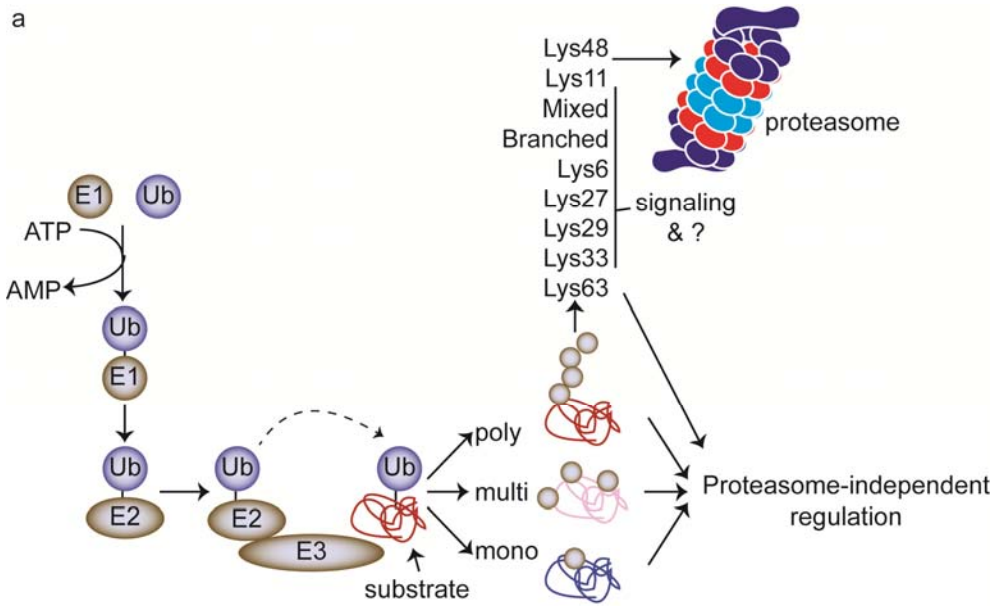


**Figure 1.2 Ubiquitin Proteasome System.** Ubiquitin conjugation occurs through an ATP-dependent enzyme cascade (see text). Conjugation can target cellular proteins to the 26S proteasome for degradation or function in non-proteolytic pathways depending on the type of ubiquitin chain linkage.

"base" subunit of the 19S with the 20S causes channel opening and allows substrate access to the catalytic core (Finley et al., 2012; Smith et al., 2006). Proteasome-mediated degradation is a well-defined mechanism in which the 19S ubiquitin-binding subunits capture polyubiquitylated substrates leading to subsequent removal of ubiquitin chains by the proteasome-associated deubiquitylating enzymes and finally unfolding and feeding of the substrate into the 20S core by the AAA-ATPase subunits of the 19S base (Demartino and Gillette, 2007; Finley, 2009; Pickart and Cohen, 2004; Tanaka and Tsurumi, 1997). Proteasomal degradation clears misfolded proteins from the cell in contrast to the chaperone system, which binds exposed hydrophobic regions of unfolded or partially folded proteins, thus shielding them from degradation or aggregation and allowing them more time to fold properly (Ross and Pickart, 2004). Coupled with the presence of misfolded or aggregated proteins found in SNpc DA neurons, the discovery of mutations in genes encoding enzymes in the UPS indicates the probable significance of the UPS in the molecular pathogenesis of PD.

As described earlier, though protein aggregates are found in many neurodegenerative diseases, they do not appear to be the cause of cell death, but are thought instead to be a protective response aimed at sequestering misfolded proteins that have escaped degradation (Huang and Figueiredo-Pereira, 2010). The requirement for unfolding prior to proteolysis suggests that proteins that arrive at the proteasome but cannot be unfolded have the potential to act as dominant inhibitors of its function, thus incapacitating the proteasome and potentially leading to accumulation (Bennett et al., 2005; Bennett et al., 2007). In fact, decreased proteasome activity is associated with aging, the major risk factor for PD, and has also been shown in post-mortem extracts of the substantia nigra from PD-afflicted patients (McNaught et al., 2004). Consistent with this hypothesis, when overexpressed in cultured cell, mutated forms of alpha-synuclein have been shown to inhibit proteasome activity, though it is not clear how this may work in disease progression. However, there is likely interplay between the accumulation of misfolded proteins, the UPS, damage to cellular organelles, such as the mitochondria, and the production of ROS.

### 1.3.3 Mitochondrial dysfunction in SNpc DA neurons and Parkinson's disease

Over a century ago, the significance of mitochondria was recognized when they were described as "elementary organisms" alive inside cells carrying out vital functions (Ernster and Schatz, 1981). However, the symbiotic origin of mitochondria was dismissed until the 1960s with the discovery of mitochondrial DNA (mtDNA) which corroborated the theory that mitochondria were descendants of endosymbiotic bacteria (DiMauro and Schon, 2003; Pallen, 2011; Sagan, 1967). Electron microscopy studies in the 1950s captured the ubiquitous bean-shaped organelles and revealed the ultrastructural features of mitochondria, including double lipid membranes, the intermembrane space, and the matrix (Palade, 1953) (Figure 1.3a). The importance of these unique structural features became evident once the major function of mitochondria was understood – to provide the chemical energy essential for biosynthetic and

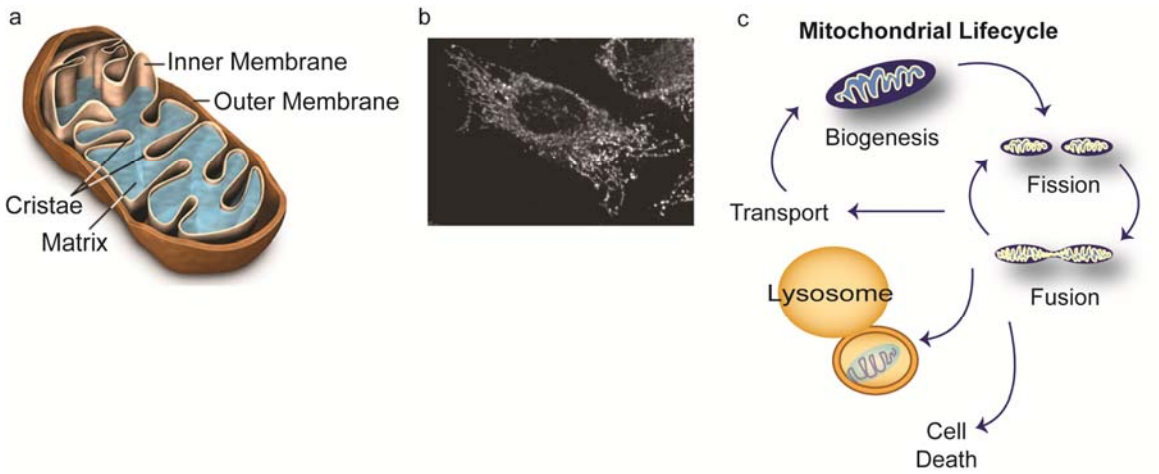


**Figure 1.3 Features of the mitochondria. a**, Cartoon depicting structural aspects of the mitochondria (adapted from http://micro.magnet.fsu.edu/cells/mitochondria.html). **b**, Mitochondrial tubular network in HeLa cells. Mitochondria are visualized by staining with antibody targeting the mitochondrial protein, TOMM20. **c**, Healthy mitochondria undergo dynamic fusion-fission cycles resulting in exchange of membrane, membrane proteins, and contents.

motor activities of the cell by means of the electron-transport chain and oxidative phosphorylation. Additionally, the mitochondria carry out numerous duties, such as pyruvate oxidation, the Krebs cycle, amino acid, fatty acid, and steroid metabolism, regulation of calcium homeostasis, and control of apoptosis (Ernster and Schatz, 1981).

More recent studies have shown that mitochondria are not the solitary organelles captured in static micrographs but rather dynamic interconnected tubular networks of organelles varying widely in size and shape (Figure 1.3b). Their morphology can differ based on cell type, cell cycle stage, localization within the cell, or can depend on any number of metabolic or chemical states existing in the cell or organelle itself (Detmer and Chan, 2007). Imaging studies performed in living cells have demonstrated that mitochondria are constantly in motion and that mitochondrial tubules move with their long axes aligned along cytoskeletal tracks (Hollenbeck and Saxton, 2005). Upon encountering each other during these movements, mitochondria may undergo fusion leading to the unification of the double membranes and the resultant mixing of both the lipid membranes and the interior contents (Figure 1.3c). This mixing can be problematic in the case of mitochondrial damage and cells have evolved intricate pathways in order to sequester or remove damaged organelles from the larger population. Mitochondria can also

divide by fission to produce numerous smaller organelles which can be actively transported to alternate subcellular locations (Detmer and Chan, 2007). Under steady state conditions, the cycles of fusion and fission are balanced, maintaining a healthy population of mitochondria within the cell.

As stated, neurons bear a high metabolic burden compared to other cells of the body. It has been suggested that SNpc DA neurons, which are at greatest risk in PD, have a distinctive physiological phenotype that may contribute to their vulnerability. Explanations for a variety of cell-specific stresses have been proposed. One of these theories is that extended opening of L-type calcium channels during autonomous pacemaking results in sustained calcium entry into the cytoplasm of SNpc DA neurons causing an elevated basal level of mitochondrial oxidant stress. It is thought that mitochondria are capable of dealing with this stress in the short term; however, this increased oxidant stress may eventually increase DNA damage and accelerate aging - a metabolically expensive strategy that taxes mitochondria and thus SNpc DA cells (Surmeier et al., 2010). Furthermore, since neurons in the SNpc are postmitotic, they are at risk of accumulating mitochondrial damage over an organism's lifetime, resulting in progressive mitochondrial dysfunction and ultimately increased oxidative stress, decreased calcium buffering capacity, decreased ATP production, and, eventually, cell death—unless quality control processes are enacted.

Another characteristic of SNpc DA neurons that may put them at higher risk of oxidant stress is their large axonal field. It is estimated that a typical SNpc DA neuron has a mean axonal length of 470mm and supports approximately 370,000 synapses (Arbuthnott and Wickens, 2007; Matsuda et al., 2009). Consequently, it has been suggested that the increased need for axonal protein trafficking leads to elevated proteostatic stress, potentially leading to the accumulation of pathogenic aggregates, thus intertwining the UPS and mitochondrial fitness. Additionally, synaptic terminals are metabolically demanding subcellular locations which require a high density of ATP-producing mitochondria to power synaptic transmission and regulate

calcium homeostasis. In comparison to other neuronal cell types, SNpc DA neurons display lower mitochondrial density in the somatodendritic region (Liang et al., 2007). This dearth of mitochondria in the cell body may lead to lower spare oxidative capacity, thus loss of the ability to protect against reactive oxygen species, and insufficient ATP production, possibly inducing an energy crisis and contributing to age-related decline of the mitochondria (Nicholls, 2008; Surmeier et al., 2010). Furthermore, to achieve this non-uniform distribution, neurons rely heavily on active transport to recruit mitochondria and other organelles to synapses, which requires properly regulated mitochondrial dynamics and transport.

The discovery that toxins such as MPTP and paraquat, which cause parkinsonism, block the electron transport chain (ETC) by inhibiting mitochondrial complex 1 was a compelling indication that defects in oxidative phosphorylation may play a role in the pathogenesis of PD (Nicklas et al., 1987). This was further corroborated by studies identifying abnormalities or deficiencies in complex I in PD and *in vitro* studies which indicated that defects in complex I could cause oxidative stress and mitochondrial failure in cells (Greenamyre et al., 2001; Janetzky et al., 1994). Furthermore, biological markers of oxidative stress and reduced staining for complex I have been identified in PD SNpc neurons examined post-mortemly (Dauer and Przedborski, 2003; Hattori et al., 1991). As a result of mitochondrial respiration, potent oxidants, such as superoxide radicals and hydrogen peroxide, are produced as byproducts. When complex I is not functional, the production of ATP decreases while that of ROS increases which can cause damage to cellular proteins, DNA, lipids, and thus all organelles. It is proposed that the mitochondrial ETC itself may be targeted by these reactive species, thus generating a cycle of mitochondrial damage and further production of ROS (Cohen, 2000). The presence of increased mitochondrial ROS production and oxidative stress is interconnected with defects in the UPS and protein folding. The result of this proliferation in reactive species causes damage to proteins, increasing unfolding, thus escalating strain on the UPS and chaperones. SNpc neurons may be acutely affected by this scenario since the metabolism of DA is known to

produce ROS and furthermore these cells contain a low anti-oxidant capacity (Exner et al., 2012; Graham et al., 1978). Still, despite proof of mitochondrial dysfunction in PD tissue and animal models, until the discovery of commonalties between sporadic and genetic PD, little was understood of whether mitochondrial damage and increased oxidative stress were causative or additional symptoms of disease.

### 1.4 Genetics of Parkinson's disease

Though they explain but a small proportion of disease, the discovery of several monogenic mutations causally linked to the development of PD have fostered research into molecular mechanisms that may be common to both genetic and idiopathic disease. Mitochondrial impairment, oxidative stress, and dysfunction of protein folding or degradation appear to play a central role in PD pathogenesis in both types of disease, induced either by single gene dysfunction or in the case of sporadic PD, by factors such as age or environmental exposure, though genetic factors are still thought to modulate sensitivity (Lim et al., 2002). Accumulating evidence suggests that disorder of mitochondrial quality control may play a fundamental role in both idiopathic and genetic PD (Dawson and Dawson, 2003; Exner et al., 2012). Accumulation of damage to the mitochondria in neuronal cells, which bear a high metabolic load, may lead to loss of mitochondrial homeostasis and ultimately cell death. Of the fewer than twenty proteins implicated genetically in PD, 6 have roles in mitochondrial homeostasis, and many of the remainder, when mutated, lead to toxic aggregates that may indirectly affect mitochondrial health (Martin et al., 2011) (Table 1.1).

The amount of risk of Parkinson's that can be attributed to genetic causes is highly variable depending on the risk loci and population studied. For example, a very large proportion of risk, nearly 40%, is accounted for by mutations in leucine-rich repeat kinase 2 (LRRK2) G2019S and glucosecerebrosidase (GBA) in Ashkenazi Jewish populations; similarly LRRK2 G2019S is highly implicated in Arab populations. In East Asian cohorts, approximately 10% of

**Table 1.1 Genes and loci associated with parkinsonism**

| PARK locus | Gene | Inheritance | Map position | Clinical phenotype | Pathology |
|---|---|---|---|---|---|
| PARK1/4 | SNCA | Dominant | 4q21 | Parkinsonism with common dementia | Lewy bodies |
| PARK2 | Parkin | Recessive | 6q25-q27 | Early-onset, slowly progressing parkinsonism | Lewy bodies |
| PARK3 | Unknown | | 2p13 | Late-onset parkinsonism | Lewy bodies |
| PARK5 | UCHL1 | | 4p14 | Late-onset parkinsonism | Unknown |
| PARK6 | PINK1 | Recessive | 1p35-p36 | Early-onset, slowly progressing parkinsonism | One case with Lewy bodies |
| PARK7 | DJ-1 | Recessive | 1p36 | Early-onset parkinsonism | Unknown |
| PARK8 | LRRK2 | Dominant | 12q12 | Late-onset parkinsonism | Lewy bodies (usually) |
| PARK9 | ATP13A2 | Recessive | 1p36 | Early-onset parkinsonism with Kufor-Rakeb syndrome | Unknown |
| PARK10 | Unknown | | 1p32 | Unclear | Unknown |
| PARK11 | GIGFY2 | | 2q36-q37 | Late-onset parkinsonism | Unknown |
| PARK12 | Unknown | | Xq | Unclear | Unknown |
| PARK13 | Omi/HTRA2 | | 2p13 | Unclear | Unknown |
| PARK14 | PLA2G6 | Recessive | 22q13.1 | Parkinsonism with additional features | Lewy bodies |
| PARK15 | FBXO7 | | 22q12-q13 | Early-onset parkinsonism | Unknown |
| PARK16 | Unknown | | 1q32 | Late-onset parkinsonism | Unknown |
| FTDP-17 | MAPT | Dominant | 17q21.1 | Dementia, sometimes parkinsonism | Neurofibrillary tangles |
| SCA2 | Ataxin 2 | Dominant | 12q24.1 | Usually ataxia, sometimes parkinsonism | Unknown |
| SCA3 | Ataxin 3 | Dominant | 14q21 | Usually ataxia, sometimes parkinsonism | Unknown |
| Gaucher's locus | GBA | High-risk locus | 1q21 | Late-onset parkinsonism | Lewy bodies |
| SPG11 | Spatacsin | Recessive | | Usually spastic paraplegia; some complex parkinsonism, addl features | Unknown |

Adapted from (Hardy, 2010; Martin et al., 2011)

PD has been associated with a number of LRRK2 mutations. In outbred European populations, association of LRRK2 and GBA mutations with increased risk is near 8% (Hardy, 2010). Loss-of-function mutations or deletions in PARKIN and PTEN-induced putative kinase (PINK1) which explain nearly 50% of early-onset disease (before age 40), account for perhaps only 1-2% of PD overall ((Martin et al., 2011). Taken together, Mendelian and high risk loci identified via genome wide association studies (GWAS) explain perhaps 10-40% of PD risk across most populations that have been studied (Hardy, 2010; Martin et al., 2011).

As more and more studies uncover genetic contributions to PD, the proportion of risk assigned to the environment has consistently decreased. Table 1.1 lists the loci at which pathogenic mutations have been linked to parkinsonism, both those conventionally termed "Parkinson loci," such as PARK2, PINK1, SNCA, LRRK2, DJ-1, and FBXO7 and others, including UCHL1, MAPT, SCA2, SCA3, and SPG11, which can clinically present as Parkinson disease but are also often clinically distinct (Hardy, 2010; Martin et al., 2011). Because Parkinson's disease has traditionally been defined clinically, it can be difficult to unambiguously distinguish. The majority of idiopathic cases exhibit Lewy bodies, though this is not the case with the genetic forms of disease and obviously impossible to document in living patients (Hardy, 2010). However, a small number of cases of PD caused by PARKIN and PINK1 mutations have been reported to contain typical Lewy bodies, suggesting some commonality in the pathogeneses of the two forms of the disease (Farrer et al., 2001). Nevertheless, PARKIN- and PINK1-associated disease is very distinct from typical idiopathic PD, presenting with a prolonged and benign disease duration, profound dopamine sensitivity, and sleep benefit (Dawson and Dawson, 2010).

### 1.5 Parkinson's disease genes are linked to mitochondrial quality control

As is often the case, studies of genes associated with Mendelian disease have provided insight into the molecular pathogenesis of PD. Deficits in mitochondrial respiration, morphology,

trafficking, and quality control, probably triggered by a combination of environmental factors and genetic susceptibility, have long been implicated in the pathogenesis of idiopathic PD. Dysfunction of mitochondria due to complex 1 deficiency resulting in impaired electron transfer in the substantia nigra as well as mutations in mitochondrial proteins and mtDNA deletions have all been identified in PD patients (Keane et al., 2011). In recent decades, the identification of numerous genes, some mitochondrial, linked to PD have highlighted the importance of mitochondrial quality control in the etiology of the disease. The discovery of these distinct genetic loci which contain pathogenic mutations associated with PD has accelerated the understanding of mechanisms of disease pathogenesis, which appear to be common to both genetic and sporadic disease. The most apparent pathways revealed include mitochondrial damage and quality control and the UPS (Figure 1.1d).

PARKIN, an E3 ubiquitin ligase acts downstream of PINK1, a mitochondrial kinase, in a pathway which is involved in the selective elimination of damaged mitochondria, termed mitophagy (Narendra et al., 2008) (Figure 1.4a). Similarly, DJ-1 may move to the mitochondria in response to oxidative stress in order to help maintain mitochondrial function (Canet-Aviles et al., 2004; Cookson, 2010; McCoy and Cookson, 2011). The role of FBXO7, a component of another E3 ligase complex, is yet unclear, but it is thought that it may also be involved in mitochondrial physiology (Hardy, 2010; Paisan-Ruiz et al., 2010; Zhao et al., 2011). It is unresolved as to whether the proteins produced by these genes are directly involved the same or parallel mitochondrial maintenance pathways, but it is a striking commonality that all of these genes are engaged in a mitochondrial damage response. Another prominent pathway which appears to play a role in the development of PD involves lysosomes. Both GBA and ATP13A2 are lysosomal enzymes found mutated in Parkinson's (Paisan-Ruiz et al., 2010). It is tempting to imagine that these proteins act downstream in the elimination of damaged mitochondria via autophagy – thus the role for lysosomes; however, a relationship between these loci and the mitochondrial loci is not obvious at this point.

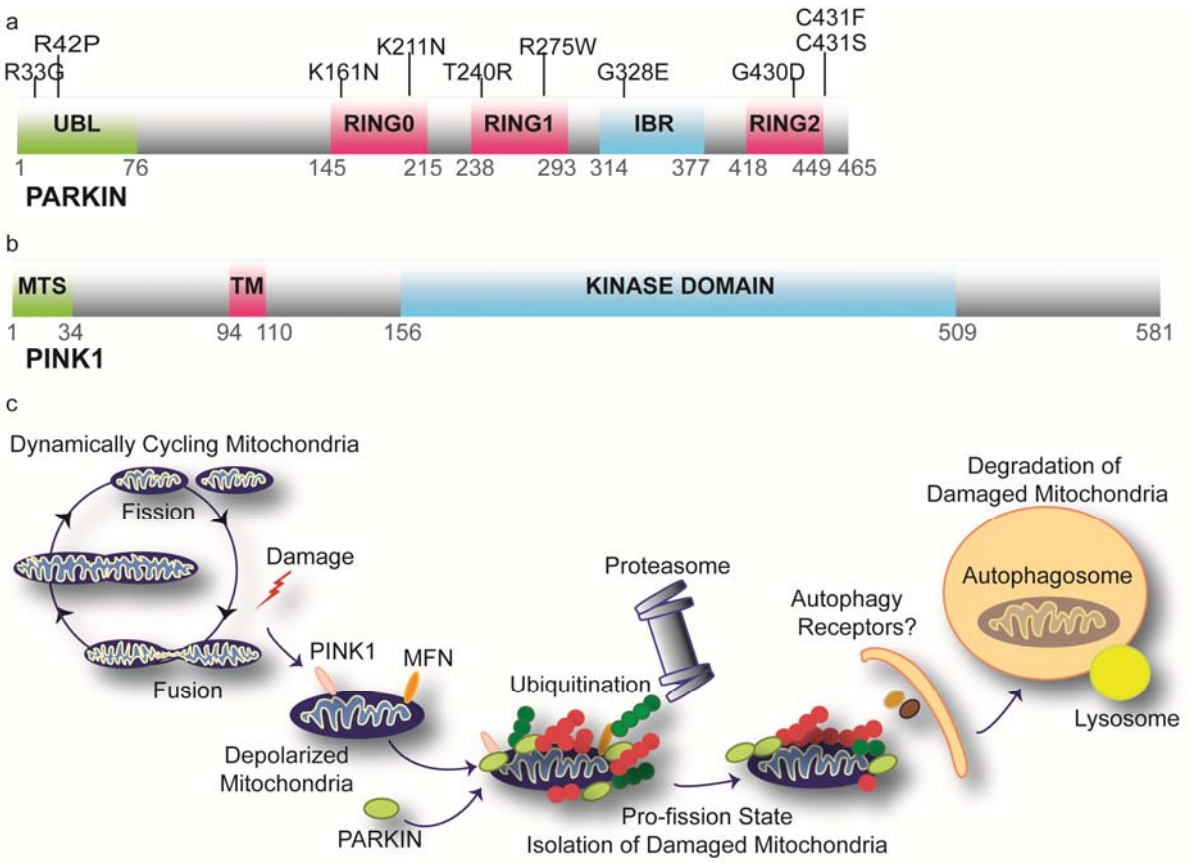


**Figure 1.4 PARKIN and PINK1 in mitophagy. a**, The E3 ligase, PARKIN contains a UBL domain, two RING domains, and an in-between-RING (IBR) domain. PARKIN associates with the proteasome through the UBL and with the E2, UbcH7 through RING1. PD-associated mutations span the entire protein and are found within each domain. A small sample of patient mutations is shown. **b**, PINK1 is a serine/threonine kinase with an N-terminal mitochondrial targeting sequence (MTS), transmembrane domain (TM), and C-terminal kinase domain. **c**, Model depicting PINK1 and PARKIN in mitophagy. Upon mitochondrial membrane depolarization, full-length PINK1 accumulates at the outer mitochondrial membrane promoting PARKIN translocation to the mitochondria, leading to PARKIN-dependent mitochondrial ubiquitylation. Ubiquitylation promotes degradation of some proteins, like MFN, creating a pro-fission environment promoting the isolation of damaged organelles. Ubiquitylation also recruits autophagic machinery to the mitochondria, possibly through interaction with ubiquitin receptors, resulting in the ultimate removal of damaged mitochondria via autophagy.

### 1.6 Phosphatase and tensin (PTEN)-induced putative kinase 1 (PINK1) (PARK6)

Mutations in PINK1, a serine, threonine kinase cause early-onset familial PD (Valente et al., 2004). PINK1 is a 581 amino acid protein that contains an N-terminal mitochondrial targeting sequence, a transmembrane domain, and a highly conserved protein kinase domain, similar to serine/threonine kinases of the Ca2+ calmodulin family (Figure 1.4b). Nearly 30 pathogenic mutations in PINK1 have been identified, among them missense, non-sense, or frameshift

mutations, deletions or rearrangements which for the most part impair kinase activity or reduce the stability of the protein (Corti et al., 2011).Though it has been reported to be found in both the cytosol and both outer and inner mitochondrial membrane, PINK1 does contain an N-terminal mitochondrial targeting sequence (MTS) and staining patterns appear to be consistent with mitochondrial localization (Gandhi et al., 2006; Haque et al., 2008; Lin and Kang, 2008; Muqit et al., 2006; Narendra et al., 2010b). Only as of 2006 was PINK1 shown to be important at the mitochondria; knockout (KO) of the Drosophila PINK1 homolog resulted in male sterility, muscle degeneration, defects in mitochondrial morphology, and increased sensitivity to oxidative stress (Clark et al., 2006). The same study also showed mitochondrial localization of WT PINK1 and fragmentation of cristae upon knockout. Upon loss of PARKIN, a similar phenotype was seen, though PARKIN overexpression could rescue PINK1 deficiency, thus placing PARKIN downstream of PINK1 in the same pathway and underscoring the significance of mitochondrial disorder as a fundamental mechanism of PD pathogenesis (Clark et al., 2006; Park et al., 2006; Yang et al., 2006). Whether PINK1 and PARKIN interact directly, or if PINK1 phosphorylates PARKIN and/or PARKIN ubiquitylates PINK1 is a controversial issue, supported by some studies but refuted by others (Kim et al., 2008b; Lazarou et al., 2012; Moore, 2006; Sha et al., 2010; Shiba et al., 2009; Um et al., 2009).

In the few years since it was determined that PINK1 played a vital role in maintaining mitochondrial well-being, numerous details of its processing and function have been discovered. It is proposed that under steady state conditions, PINK1 is targeted by its MTS for import via the TOM/TIM23 complexes into the inner mitochondrial membrane where it is cleaved by an intermembrane protease, presenilin-associated rhomboid like protease (PARL), and ultimately degraded by an MG132-senstive protease (Deas et al., 2011; Jin et al., 2010). It is not yet clear where this proteolysis occurs, but if in fact the proteasome is responsible, PINK1 must presumably be removed from the mitochondria via reverse translocation. Evidence suggests that perturbation of the mitochondrial membrane potential results in cleavage of the MTS on a

PINK1 import intermediate still associated with the TOMM complex, thus preventing import into the inner mitochondrial membrane and PARL-mediated processing (Narendra et al., 2010b). Additionally, upon mitochondrial depolarization, inner membrane proteases are thought to be rendered nonfunctional, resulting in PINK1 stabilization and accumulation in the outer mitochondrial membrane (Jin et al., 2010). PINK1 can then move laterally into the outer mitochondrial membrane and extend its kinase domain into the cytoplasm, which is essential for the recruitment of PARKIN to the mitochondria (Meissner et al., 2011; Narendra et al., 2010b). A recent study has shown that PINK1 is associated with the TOMM complex in depolarized mitochondria, potentially enabling rapid reimport of PINK1 after repolarization to terminate the mitophagy response (Lazarou et al., 2012).

Loss of PINK1 in mice increases sensitivity of DA neurons to MPTP treatment which can be abrogated by overexpression of PARKIN or DJ-1 (Haque et al., 2008). Correspondingly, PINK1 has been shown to increase cellular resistance to a diverse array of stresses and in addition to its role in PD, may act as tumor suppressor (Devine et al., 2011). Obviously, unearthing the identity of PINK1 targets is essential and a number of studies have been conducted to do so. TNF receptor-associated protein 1 (TRAP1), a mitochondrial chaperone of the Hsp90 family, and HtrA2/Omi, a mitochondria serine protease, were both identified as substrates and shown to play roles in mediating protection against oxidative stress (Plun-Favreau et al., 2007; Pridgeon et al., 2007). Recently, the Rho-like GTPase, Miro, was identified as a PINK1 substrate after mitochondrial depolarization (Wang et al., 2011b). Miro, located in the outer mitochondrial membrane, binds Milton, an adaptor protein, which bridges an interaction with kinesin heavy chain, thus allowing mitochondria to be trafficked along microtubules for axonal transport (Glater et al., 2006; Guo et al., 2005). Working in rat hippocampal neurons or Drosophila larval neurons, Wang et al. (2011) found that PINK1 or PARKIN overexpression could arrest mitochondrial transport and that PINK1 may directly modify Miro by phosphorylation after mitochondrial depolarization, thus targeting it for

proteasome-mediated degradation after PARKIN-mediated ubiquitination. These observations support the model that PINK1 and Miro play opposing roles in mitochondrial trafficking in which degradation of Miro induced by PINK1 and PARKIN arrests mitochondrial movement and sequesters damaged mitochondria prior to elimination by mitophagy.

Much progress has been made, yet the precise mechanism by which PINK1 is regulated and how it promotes PARKIN activity is incompletely understood. It is evident that PINK1 is essential for PARKIN recruitment to mitochondria after CCCP treatment (Narendra and Youle, 2011). Recent reports support direct phosphorylation of PARKIN by PINK1, but the *in vivo* functional consequences of reported sites have not yet been elucidated (Kondapalli et al., 2012). By determining interactors, regulators, and additional substrates of PINK1 in the presence or absence of mitochondrial depolarization, we hope to elucidate how PINK1 regulation of Parkin occurs. Our initial analysis has uncovered a candidate PINK1 regulatory factor, CLU1, which has been genetically linked to the PARKIN/PINK1 pathway in Drosophila (Cox and Spradling, 2009). Loss of CLU1 orthologs identified in Drosophila, *Dictyostelium*, and *S.cerevisiae* results in mitochondrial clustering and altered morphology (Cox and Spradling, 2009; Fields et al., 1998; Zhu et al., 1997). To our knowledge, our findings provide the first evidence of direct interaction between PINK1 and CLU1 and we are investigating whether CLU1 may control the activity, stability, or localization properties of PINK1. Furthermore, we are examining whether phosphorylation of candidate Parkin substrates by PINK1 promotes ubiquitination in vivo and in vitro.

### 1.7 Role of the PARKIN E3 ligase in Parkinson's disease and mitophagy

#### 1.7.1 PARKIN is mutated in autosomal recessive early-onset PD

Parkin is commonly mutated in autosomal recessive forms of early-onset PD, often referred to as autosomal recessive juvenile PD (ARJPD), and accounts for a large proportion, nearly 50% of familial early onset PD cases (Abbas et al., 1999; Kitada et al., 1998). In addition

to its established role in PD, Parkin is also a putative tumor suppressor located adjacent to a fragile chromosome site frequently lost in a number of human cancers (Devine et al., 2011). The full length protein is widely expressed in a variety of tissues, though predominantly in muscle and brain (Kitada et al., 1998). Pathogenic mutations in PARKIN are scattered throughout the full length protein, with clusters apparent in each of the domains (Figure 1.4a). Mutations include missense, exon duplications, rearrangements, deletions, and truncations, all seemingly causative of ARJPD (Dawson and Dawson, 2010; Kitada et al., 1998).

Most patient mutations appear to impact E3 ligase activity or interactions with E2 enzymes leading to a loss-of-function phenotype. Evidence also exists that PARKIN can be inactivated by dopaminergic, nitrosative, and oxidative stress in sporadic PD (Martin et al., 2011). Clinically, patients with PARKIN mutations present classical signs of Parkinson's but with striking sleep benefit, abnormal dystonic movements, and a good response to levodopa. Pathologically, patients show a characteristic loss of SNpc DA neurons most often without Lewy bodies (Dawson and Dawson, 2010). It is yet unclear precisely how loss of PARKIN function contributes to DA neuron dysfunction, but it is thought that accumulation of as yet unidentified PARKIN substrate(s) and failure of proteolysis mediated by the UPS may cause neuronal death. Research in recent years uncovering PARKIN's role in mitochondrial homeostasis has energized the field and suggests that the significance of PARKIN and PINK deficiencies in PD pathogenesis is indeed strongly shaped by a loss of mitochondrial quality control (Narendra et al., 2008). PARKIN and PINK1 substrates at the mitochondria may be key to resolving those proteins vital for SNpc neuron survival.

### 1.7.2 PARKIN is a member of the RBR E3 ligase family RING/HECT hybrid

Parkin is a 465 amino acid protein and a member of the RING-between-RING (RBR) family of E3 ligases, which contain an RBR domain, composed of two RING fingers plus an In-Between-RING (IBR) domain (Eisenhaber et al., 2007; Marin et al., 2004) (Figure 1.4a). Based

on structural analysis of the human homologue of *Drosophila* Ariadne (HHARI), the RING2 domain appears to bind only a single zinc ion and so it was thought that RING2 of Parkin would behave similarly (Capili et al., 2004). However, RING1 of PARKIN is thought to bind two zinc ions and to fold into a classical RING finger while RING2 has also been recently shown to bind two zinc ions suggesting that diversity exists within these domains (Beasley et al., 2007; Hristova et al., 2009; Marin et al., 2004). Parkin also contains a unique regulatory domain, RING0, and the IBR domain, which both also bind two zinc ions and an N-terminal ubiquitin-like (UBL) domain which may mediate interactions with proteins containing ubiquitin binding domains (UBDs), such as the ubiquitin receptor, S5a/Rpn10, and the proteasome (Dachsel et al., 2005; Hristova et al., 2009; Safadi and Shaw, 2010; Um et al., 2010). The E2 ubiquitin-conjugating enzyme, UbcH7 is thought to interact with PARKIN through RING1 while the RBR domain mediates protein-protein interaction (Beasley et al., 2007). RING E3s typically carry out ubiquitin transfer directly from an activated E2 to a lysine on a substrate protein while the hallmark of HECT-type ubiquitin transfer is the formation of an E3 ubiquitin thioester intermediate (Deshaies and Joazeiro, 2009; Metzger et al., 2012). Though they contain RING domains, some RBRs appear to function like RING/HECT hybrids, in which they bind E2 s via a RING domain, but transfer ubiquitin to substrates through an E3 thioester-linked ubiquitin intermediate requiring a cysteine residue in RING2 (Wenzel et al., 2011). The identification of the requirement for cysteine 431 in PARKIN's enzymatic activity as well as a recent report that an oxyester intermediate can be seen on recombinant PARKIN C431S *in vitro* supports the validity of this cysteine as the site of a ubiquitin thioester intermediate (Lazarou et al., 2013; Wenzel et al., 2011).

### 1.7.3 PARKIN E3 ligase activity and regulation

Parkin was originally shown to have ubiquitin ligase activity through *in* vitro autoubiquitination assays, thus it was thought to be constitutively active (Shimura et al., 2000;

Zhang et al., 2000). However, consistent with the model that PARKIN is activated upon mitochondrial depolarization; recent studies have shown that PARKIN may exist in an autoinhibited state until triggered by post-translational modification. The closed conformation of this autoinhibited state is maintained by an intramolecular interaction between the N-terminal UBL domain and the C-terminal RING regions (Chaugule et al., 2011) (Figure 1.5a, b). Notably, the C-terminal RING regions have been shown to interact with ubiquitin and are required for efficient ligase activity. The RING2 domain, which contains C431, is essential for ligase activity and truncations or mutations which disrupt the folding of the zinc-coordinating residues result in inactive Parkin. However, N-terminal truncations leaving only the IBR-RING2 domains are active, which supports the notion that in the absence of the N-terminus, autoinhibition is relieved (Chaugule et al., 2011). Furthermore, some studies have shown that the presence of an N-terminal affinity tag results in constitutively active PARKIN, presumably because it disrupts the intramolecular interaction (Burchell et al., 2012; Chew et al., 2011). Clearly, the N-terminal UBL and RING0 domains are not required for basal Parkin activity, but are likely necessary for regulating its activity (Hampe et al., 2006; Matsuda et al., 2006). Collectively, these data support a model wherein PARKIN is autoinhibited by internal binding of the N-terminal domain which inhibits autoubiquitination and presumably substrate interaction and ubiquitination (Figure 1.5b, c).

In recent years, PINK1 was shown to be necessary for PARKIN recruitment to the mitochondria after depolarization (Narendra et al., 2008). Several groups have found evidence to support the hypothesis that PINK1 kinase activity is necessary for phosphorylation and translocation of PARKIN, though it has been difficult to prove direct phosphorylation (Matsuda et al., 2010; Narendra et al., 2010b). An alternative hypothesis proposes that PINK1-dependent activation of mitochondrial ubiquitination reflects phosphorylation of substrates, which PARKIN may then recognize and in fact, evidence has shown that the mitochondrial GTPase, Miro, is phosphorylated by PINK1 at Ser156 and

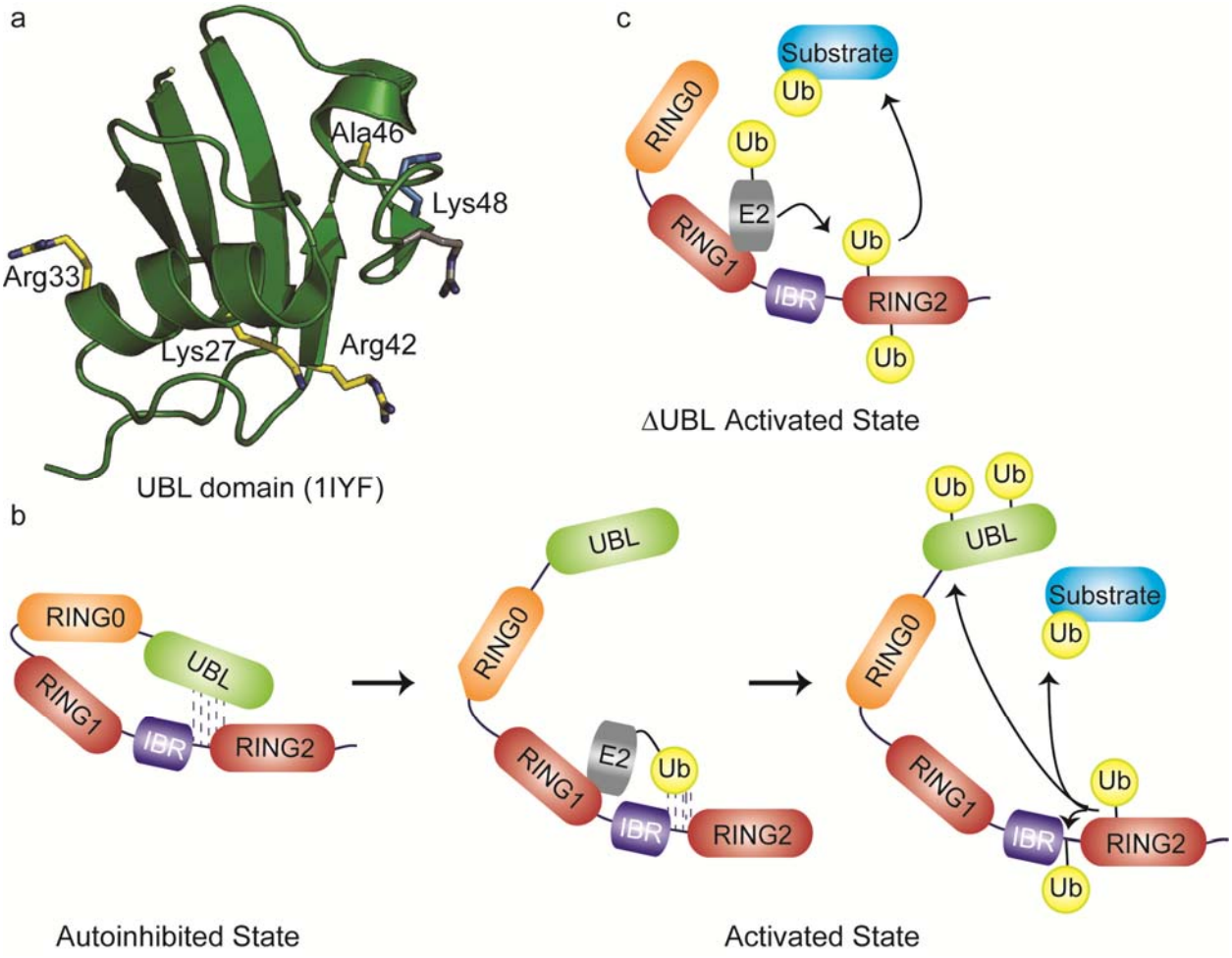


**Figure 1.5 Regulation of PARKIN E3 ligase activity. a**, PD mutations (yellow) in the UBL domain of PARKIN relieve autoinhibition. Ubiquitylation of lys27 and lys48 (blue) was identified in our study and may contribute to PARKIN activation (PDB code 1IYF (Sakata et al., 2003)). **b**, In the absence of stimulation, PARKIN exists in an autoinhibited state in which the UBL domain folds over to bind the C-terminus of the protein in a region harboring UBL-domain/Ubiquitin binding capacity. A ubiquitin-conjugated E2 enzyme may interfere with this interaction and allow substrate ubiquitination and/or Parkin autoubiquitination. PINK1 may also contribute to activation via phosphorylation of various sites within PARKIN. **c**, PARKIN lacking the UBL is thought to be constitutively active.

subsequently ubiquitylated by PARKIN after mitochondrial depolarization (Wang et al., 2011b). However, another study has found this site to be nonessential for PARKIN-dependent Miro degradation (Liu et al., 2012). More recently, one group utilizing recombinant PINK1 found that the highly conserved residue serine 65 within the UBL domain of Parkin was directly targeted by PINK1 *in vitro.* Furthermore, phosphorylation of Ser65 enhanced PARKIN's E3 ligase activity in

an *in vitro* ubiquitylation reaction and was also detected by mass spectrometry on immunoprecipitated PARKIN after mitochondrial depolarization in the presence of PINK1 (Kondapalli et al., 2012). Though obviously regulated in a mitochondrial depolarization- and PINK1-dependent manner, the full functional consequence of phosphorylation of PARKIN at Ser65 is completely clear. Because the activity and substrate specificity of PARKIN is likely to be integrated with its mechanism of activation, it is essential to fully characterize how PARKIN is activated.

Numerous PARKIN interactors and substrates have been reported over the years, however, during this time, the mechanism of autoinhibition was yet unknown and PARKIN was thought to be constitutively active. Furthermore, PARKIN itself is reported to be prone to misfolding, a complicating factor when attempting to study it in cells, particularly with overexpressed protein (Wang et al., 2005). Misfolded PARKIN may interact with other poorly folded proteins, aggregate, or bind proteins involved in quality control under these conditions thus obscuring identification of actual specific interactors. Numerous early studies have proposed candidate Parkin substrates, including CCNE, AIMP2, DJ-1, and RANBP2, though many of these and their functional consequences have not been reliably substantiated most likely due to the varying methods used, including yeast 2-hybrid assays, mass spectrometry, and co-immunoprecipitation from a diversity of cell types or tissues (Dawson and Dawson, 2010).

Another unanswered question is how ubiquitin chain linkage type produced by PARKIN is controlled and how it impinges on the fate of substrates. PARKIN has been reported to build numerous types of ubiquitin chains, including K27, K48, and K63 (Chan et al., 2011; Geisler et al., 2010). This has several implications that include not only the mechanism of PARKIN E3 ligase activity, but also the processes that occur post-ubiquitylation, such as proteasome-mediated degradation or downstream signaling. The means by which PARKIN might be capable of producing multiple different types of chain linkages may be a property of its unique RBR

structure. One mechanism which has been established for other RING-IBR-RING and HECT domain E3s may explain how PARKIN could also create distinct chain linkages. The presence of C-terminal surfaces that are able to bind distinct faces of ubiquitin may be able to orient acceptor ubiquitin molecules on substrates for attack on the donor ubiquitin thioester; thus the use of a weak ubiquitin binding site, such as that which PARKIN utilizes for autoinhibition, may allow assembly of distinct chain linkages (Chaugule et al., 2011; Kulathu and Komander, 2012) (Figure 1.5b).

### 1.7.4 Models used to study PINK1 and PARKIN

Unexpectedly, neither PINK1 nor Parkin knockout mice present with a morphological or behavioral phenotype; however, *Drosophila* KO models do exhibit age-dependent loss of DA neurons and mitochondrial dysfunction and both Parkin and PINK1-deficient cultured cells show increased vulnerability to mitochondrial damage (Casarejos et al., 2006; Haque et al., 2012; Rosen et al., 2006; Sandebring et al., 2009). Because vertebrate KO models do not display age-related loss of DA neurons, they may not faithfully recapitulate human PD pathogenesis. However, subtle phenotypes have been recorded, including abnormalities in the DA nigrostriatal circuit or noradrenergic system (Goldberg et al., 2003; Itier et al., 2003; Von Coelln et al., 2004). Interestingly, transgenic mice expressing Parkin mutants exhibited age-dependent DA neuron degeneration and hallmark characteristics of PD, suggesting that dominant toxicity of a Parkin mutant is sufficient to elicit PD symptoms, though this model requires further study but has been corroborated in flies (Lu et al., 2009; Sang et al., 2007; Wang et al., 2007). In 2011, Shin et al. produced a conditional Parkin KO mouse which showed that loss of Parkin function in adult mice led to progressive degeneration of DA neurons, suggesting that the lack of effects of germline Parkin KO in previous models had been masked by developmental compensation (Shin et al., 2011). Knockout of Parkin in *Drosophila* leads to mutant flies with reduced lifespan, male sterility, defects in muscle, and reduced mitochondria with loss of cristae structure.

Furthermore, degeneration of DA neurons with abnormal mitochondria was seen in both Parkin and PINK1-null flies and both are sensitive to oxidative stress and show increased levels of cellular ROS (Clark et al., 2006; Greene et al., 2003). Transgenic expression of Parkin is able to rescue PINK1 deficiency though the reverse is not true, confirming that PARKIN lies downstream of PINK1 in a common pathway.

Cellular models examining PARKIN and PINK1 have often used HeLa cells because they do not endogenously express PARKIN, thus conveniently providing a null background on top of which to exogenously express the protein (Denison et al., 2003). Mitochondrial depolarization in HeLa cells exposed to the uncoupling agent carbonyl cyanide 3-chlorophenylhydrazone (CCCP) results in PINK1 processing and PARKIN translocation to the mitochondria and the induction of mitophagy (Narendra et al., 2008). In fibroblasts from PINK1-null mice, PARKIN translocation is abrogated (Narendra et al., 2010b). Though HeLa cells are extremely useful for establishing the mechanisms of the PARKIN/PINK1 pathway, these studies have met with some criticism because there is little way of knowing if they are physiologically relevant, both because of the cell type used and because of the huge assault on the cellular population of mitochondria achieved by CCCP treatment. To address this, studies in neurons, which may more closely recapitulate the cellular environment in which PD arises, have examined whether PINK1 activation and PARKIN translocation are relevant. Results have been controversial; for example, one group has shown impaired recruitment of lentivirally-expressed Parkin to mitochondria in induced pluripotent stem (iPS) cells taken from fibroblasts of PD patients with PINK1 gene mutations that were differentiated into dopaminergic neurons (Seibler et al., 2011). However, others have presented evidence that endogenous levels of Parkin are not sufficient to initiate mitophagy after mitochondrial depolarization in human primary fibroblasts and iPS-generated neurons from controls and PINK1 mutant patients (Rakovic et al., 2013; Van Laar et al., 2011). These negative results however, are called into question by reports that Pink1-dependent Parkin translocation does occur in mouse cortical neurons in

response to a variety of mitochondrial damaging agents but only in the absence of antioxidants in the neuronal culturing medium, implicating a key role of ROS in the response (Joselin et al., 2012). Further studies have shown PINK1 stabilization and PARKIN recruitment to mitochondria in rat cortical neurons, rat hippocampal neurons, and mature cortical neurons treated with both CCCP and less globally damaging agents, such as Antimycin A, a complex I inhibitor (Cai et al., 2012b; Narendra et al., 2010b; Wang et al., 2011b). Of note, when compared with non-neuronal cells, neuronal mitophagy occurs much more slowly and is a compartmentally restricted process, coupled with reduced anterograde mitochondrial transport. Ultimately, Parkin-targeted mitochondria accumulate in somatodendritic regions where mature lysosomes are located (Cai et al., 2012a; Cai et al., 2012b). A compartmentalized focus on damaged mitochondria in neurons is consistent with the likely mode of damage in living cells, in which a population of cellular mitochondria are damaged and selectively targeted for degradation. Though it has been suggested that mitophagy differs between human non-neuronal and neuronal cells and between endogenous and PARKIN-overexpressing cellular models, strong evidence is accumulating to suggest that this model does in fact represent a physiological response to mitochondrial damage.

### 1.7.5 General features of autophagy and mitophagy

Autophagy broadly refers to multiple pathways in the cell which exist to perform bulk degradation of cytosolic components and organelles. Macroautophagy, the main type of autophagy, which is well conserved from yeast to mammals is generally induced by cellular starvation and operates to provide the cell with essential nutrients. In juxtaposition with this, selective autophagy, such as mitophagy, acts to clear damaged or excess organelles, including mitochondria (Kim et al., 2007). Both processes employ a similar mechanism in which a double membrane structure, termed a phagophore, is formed around the cytosolic contents or targeted organelle. The membrane is eventually extended until closed, forming an autophagosome which

ultimately fuses with a lysosome to form an autolysosome, in which degradation of the autophagosome contents occurs via by lysosomal hydrolases (Levine and Klionsky, 2004; Yang and Klionsky, 2010b) (Figure 1.6). The basic autophagic machinery employed by macroautophagy is also used in mitophagy, however there are aspects of the specific pathways that differ or are yet unknown, for example, how the phagophore is selectively recruited to mitochondria is unclear. Autophagy consists of several sequential steps, initiation of the phagophore membrane and isolation of the contents, elongation and closure of the membrane to form the autophagosome, transport to lysosomes, fusion of the autophagosome and lysosome, and lysosomal degradation of the contents (Mizushima, 2007).

First identified in yeast, nearly 30 ATG proteins acting in autophagy have been identified (Nakatogawa et al., 2009). The majority of these are also essential in mitophagy (Kanki et al., 2010). ATG proteins are grouped based on their functions; the Atg1p-Atg13p-Atg17p kinase complex, the ULK1 complex in mammals, is normally inhibited by target of rapamycin complex 1 (TORC1) which blocks Atg1 interaction with Atg13, thus controlling early steps in autophagosome formation (Figure 1.6). In mammalian cells, mitophagy can also be stimulated by the Hsp90-Cdc37 complex which acts through ULK1 for initiation (Ashrafi and Schwarz, 2013). The next steps in assembly of the autophagosome are regulated by phosphatidyl inositol triphosphate (PIP3) signals which are controlled by the vacuolar protein sorting Vps34-Vps30p-Atg14 complex in yeast, and it mammalian counterpart PIK3C3-BECN1 (beclin1). This PI3K-mediated organization of PIP3-rich membrane domains is essential for nucleation of the isolation membrane, though it has been shown that stress-induced bulk autophagy and mitophagy can occur independently of Beclin1, however the mechanism of this is not understood (Ashrafi and Schwarz, 2013; Chu et al., 2007). A ubiquitin-like protein (UBL) conjugation cascade, comprised of the E1 enzyme Atg7p, the E2 enzymes (Atg10p and Atg3p) and two UBLs (Atg8p and Atg12p) is required for maturation of autophagosomes via elongation

of isolation membranes and cargo recruitment (Nakatogawa et al., 2009). At this step, the Atg12p-Atg5p complex binds to Atg16p, which moves to the isolation membrane to promote

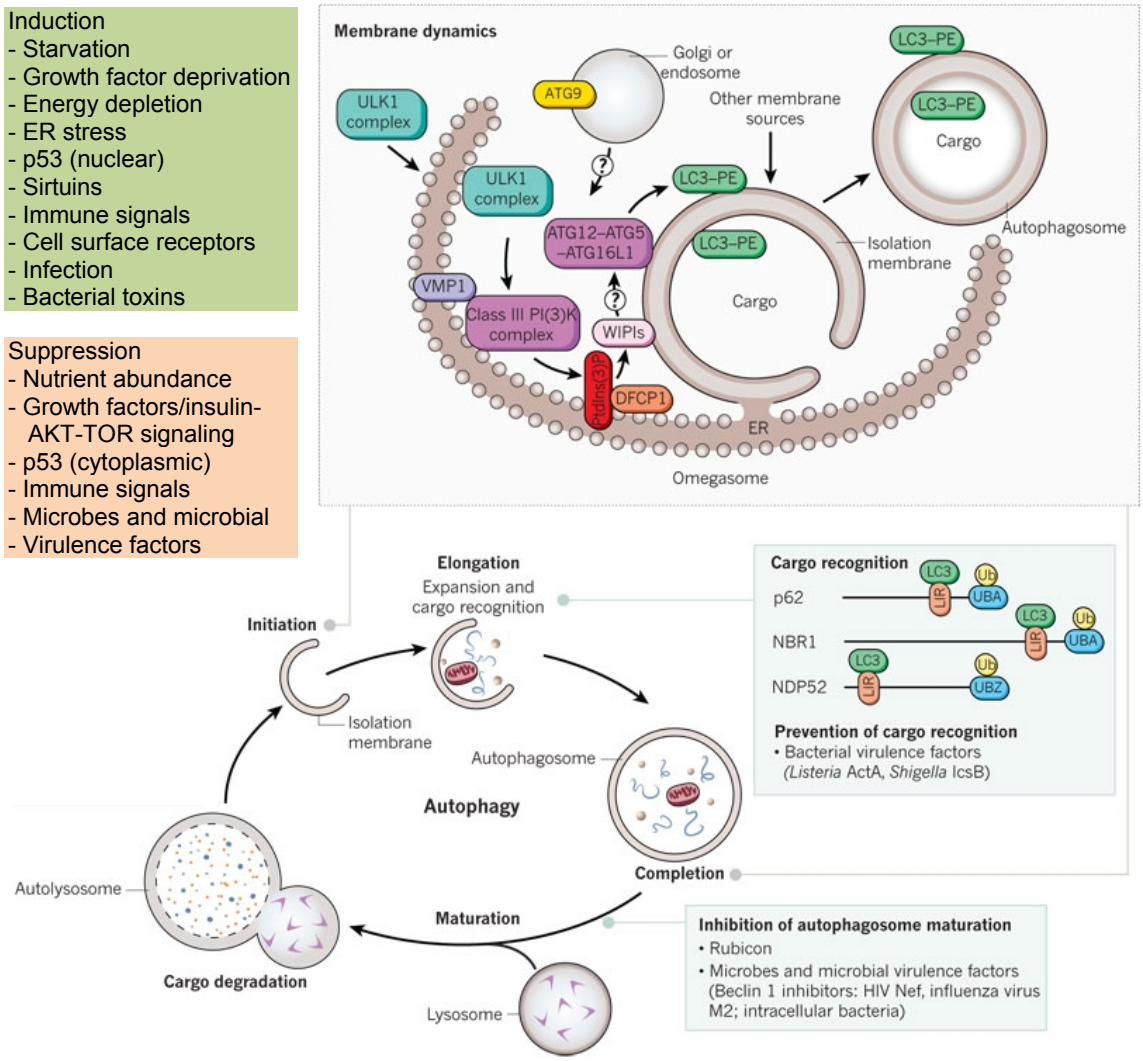


**Figure 1.6 Overview of the autophagy pathway.** The top right box depicts the molecular events involved in membrane initiation, elongation and completion of the autophagosome. After induction of autophagy, the ULK1 complex (ULK1–ATG13–FIP200–ATG101) (downstream of the inhibitory mTOR signaling complex) translocates to the ER and transiently associates with VMP1, resulting in activation of the ER-localized autophagy-specific class III phosphatidylinositol-3-OH kinase (PI(3)K) complex, and the phosphatidylinositol-3-phosphate (PtdIns(3)P) formed on the ER membrane recruits DFCP1 and WIPIs. WIPIs and the ATG12–ATG5–ATG16L1 complex are present on the outer membrane, and LC3–PE is present on both the outer and inner membrane of the isolation membrane, which may emerge from subdomains of the ER. The cellular events that occur during autophagy are depicted in the bottom diagram, including the major known cellular and microbial proteins that regulate autophagy initiation, cargo recognition and autophagosome maturation. Only those cellular proteins known to be adaptors for targeting microbes are shown; other proteins (not shown) also function in cargo recognition of mitochondria and other organelles. LIR, LC3-interacting region (motif); Ub, ubiquitin; UBA, ubiquitin-associated domain; UBZ, ubiquitin-binding zinc finger (adapted by permission from Macmillan Publishers Ltd: Nature (Levine et al., 2011)).

conjugation of Atg8p to phosphatidylethanolamine (PE) acting as a linker influencing formation and elongation of the phagophore membrane (Xie and Klionsky, 2007). The Atg5 complex can also promote incorporation of Atg8-PE (MAP1LC3 in mammals) into autophagosomes, which can then promote closure of autophagosomes as well as cargo recruitment. LC3 is synthesized in the pro-LC3 form, cleaved by Atg4b to produce LC3-I, and then conjugated to PE to form LC3-II which is required for membrane elongation and closure to form mature autophagosomes (Behrends et al., 2010; Yang and Klionsky, 2010b). LC3-II localizes selectively to forming and newly formed autophagosomes, thus it is often used as an autophagosomal marker.

Because it is known that most of the autophagy core machinery is required for mitophagy, studies have tried to discern how discrimination is introduced for selective autophagy in yeast (Itakura et al., 2012; Kanki et al., 2010). Nearly 40 genes found to be essential for mitophagy but not autophagy were identified, including Atg11 and Atg32, thought to function as adaptors between the mitochondria and Atg8 (LC3C) thus bridging the selected organelle and the canonical autophagy machinery (Kanki et al., 2009; Kanki et al., 2010). Though no homologs have been found in higher eukaryotes, possible functional homologs have been identified. The ubiquitin-binding adaptor protein p62 (SQSTM1) accumulates on damaged mitochondria and may aid in recruitment of mitochondria to the autophagosome by binding to LC3, though it does not appear to be essential for mitophagy (Geisler et al., 2010; Narendra et al., 2010a). Another known mitophagy adaptor is Nix (also known as BNIP3L), a mitochondrial protein, which is required for programmed mitophagy during reticulocyte maturation (Sandoval et al., 2008; Schweers et al., 2007). Nix directly binds LC3, possibly serving the function of both Atg11 and Atg32. The autophagy interactor is NBr1, which can cooperate with p62 and Nix, and is essential for pexophagy, the selective autophagy of peroxisomes, plays no known role in mitophagy as yet (Deosaran et al., 2012; Kirkin et al., 2009; Lamark et al., 2009).Some also consider PARKIN to be a mitophagy receptor, however, it is more likely that PARKIN serves to

designate damaged mitochondria for removal via attachment of ubiquitin, which is then recognized and targeted by ubiquitin-binding autophagy receptors.

### 1.7.6 PARKIN targets damaged mitochondria for removal by mitophagy

Though mitochondria were first seen in autophagosomes in the 1950s, this degradation was thought to be a general response to cellular stress or starvation (Yang and Klionsky, 2010a). While mitophagy does occur to regulate mitochondria size and number under steady-state conditions, it is also utilized by the cell to eliminate sperm-derived mitochondria after fertilization and during the process of erythrocyte maturation (Al Rawi et al., 2011; Sandoval et al., 2008). Because both the dopaminergic neurons of the substantia nigra appear to be especially sensitive to mitochondrial damage and genes found mutated in PD appear to play a role in mitochondrial quality control, mitophagy is being more thoroughly examined. Upon injury, mitochondria cannot maintain the electric potential gradient across the inner membrane, resulting in depolarization, a state which can be achieved through aberrant protein activity or the use of numerous drugs, such as CCCP or rotenone, treatment with which has been shown to reproduce features of Parkinson's disease in animal models (Betarbet et al., 2000; Sherer et al., 2003). Furthermore, mitophagy in yeast can be activated by mutations that diminish the electrochemical gradient across the inner membrane (Nowikovsky et al., 2007; Priault et al., 2005). Upon PINK1 stabilization at the mitochondrial outer membrane (MOM) after depolarization, PARKIN, normally a soluble cytosolic protein, is recruited to the MOM, in a PINK1-kinase dependent manner (Figure 1.4c). Subsequently, the damaged mitochondria are extensively decorated with ubiquitin, a process requiring PARKIN E3 ligase activity, thus selectively targeting damaged mitochondria for degradation via mitophagy (Matsuda et al., 2010; Narendra et al., 2008).

More specifically, it has been shown in HeLa cells expressing exogenous PARKIN that upon mitochondrial depolarization, PARKIN is recruited to the mitochondria in under an hour

and mitochondria are ultimately cleared from the cell by selective autophagy at around 24 hours post-drug (Geisler et al., 2010; Narendra et al., 2008). PINK1 kinase activity is required; however, membrane localized PINK1 may be sufficient to induce selective autophagy since PINK1 targeted to peroxisomes and lysosomes was able to recruit PARKIN and trigger the pathway (Lazarou et al., 2012). Thus, it is unclear whether selectivity is assured by targeting PINK1 via an MTS to the mitochondria or if PARKIN maintains any form of substrate specificity. So far, the best understood PARKIN substrates are MFN1/2 and RHOT1/2 (also called MIRO1/2), two MOM-tethered GTPases whose PARKIN-dependent proteasome turnover alters fission-fusion cycles and microtubule-dependent trafficking of mitochondria, respectively (Narendra et al., 2012; Tanaka et al., 2010; Wang et al., 2011b). The MOM porin proteins VDAC1/2/3 are also ubiquitylated by PARKIN, and are required for PARKIN localization on mitochondria through a poorly understood mechanism (Sun et al., 2012) Proteomic studies of purified mitochondria have also identified additional proteins whose abundance is either decreased or increased upon PARKIN activation or depolarization, but precisely how these proteins are regulated and the extent to which ubiquitin is involved is unclear (Chan et al., 2011). At this point, we do not have a comprehensive understanding of cellular PARKIN targets, which will be critical for elucidating how PARKIN promotes mitochondrial homeostasis.

An obvious role for PARKIN and PINK1 in maintaining a healthy population of cellular mitochondria is through sequestration of damaged organelles by regulation of fusion/fission cycles and trafficking. As mitochondrial homeostasis involves continuous cycles of fusion and fission which result in mixing of membranes and contents, any event which affects mitochondria may have implications for the entire mitochondrial population (Detmer and Chan, 2007; Okamoto and Shaw, 2005). Fusion and fission are controlled by separate members of a family of conserved GTPases. Dynamin-related protein 1 (Drp1) is a dynamin-like GTPase which oligomerizes into ring-like structures around the outer membrane of mitochondrial tubules, then constricts and severs the mitochondria (Okamoto and Shaw, 2005). Fission requires slightly

more machinery in order to fuse both the inner and outer mitochondrial membranes. Mitofusin 1 and 2 (Fzo in yeast) are the only conserved outer membrane proteins involved in fusion (Liesa et al., 2009). In order to promote fusion, mitofusins on adjacent mitochondria form homotypic and heterotypic complexes that tether the mitochondria ultimately leading to full fusion (Chen et al., 2003). Optic atrophy 1 (Opa1) (Mgm1 in yeast) is required for fusion of the inner mitochondrial membrane. An extremely important consequence of fusion and fission is the distribution of mtDNA and proteins throughout the mitochondrial network (Detmer and Chan, 2007). Though ubiquitination of the mitofusins and their removal from the MOM by p97 may help to sequester damaged mitochondria by preventing re-fusion with the healthy network, evidence suggests that this process is more complicated and studies have shown that in MFN-null MEFs, mitophagy is still completely blocked by proteasome inhibitor, indicating that degradation of additional proteins is essential for mitophagy caused by Parkin activation (Chan et al., 2011; Tanaka et al., 2010). It is possible that degradation of other outer membrane proteins, such as RHOT1, may also be necessary – in the case of RHOT1, degradation appears to halt axonal trafficking of damaged mitochondria, possibly another step in sequestration before removal.

A recent study using a quantitative proteomic approach found a significant increase in both Lys48- and Lys63-linked polyubiquitin chains on depolarized mitochondria of HeLa cells overexpressing PARKIN (Chan et al., 2011). How PARKIN can direct two different chains linkages and which substrates receive each type of linkage is still a mystery. As expected, total levels of MFN1, MFN2, RHOT1 (Miro1), and RHOT2 (Miro2) decreased, supporting the notion that decreased MFN1/2 and RHOT1/2 protein levels can alter both mitochondrial dynamics and transport. However, proteasomal degradation of MOM proteins appears to be essential for the progression of PARKIN-dependent mitophagy as evidenced by proteasome inhibition, which blocks mitophagy (Chan et al., 2011; Yoshii et al., 2011). However, even in the absence of MFN1/2 tested using null mouse embryonic fibroblasts (MEFs), mitophagy was not impeded, suggesting that these are nonessential determinants in the progression of mitophagy.

Alternatively, it is possible that widespread, potentially nonspecific ubiquitination of mitochondrial proteins facilitates mitophagy by remodeling the MOM in bulk in response to depolarization (Sun et al., 2012; Tanaka et al., 2010). Ultimately this proteasome-mediated degradation coupled with nondegradative ubiquitin signals which presumable attract ubiquitin-binding proteins that recruit the autophagy machinery, somehow selectively to the mitochondria.

### 1.8 Unanswered questions in PINK1 and PARKIN-mediated mitophagy

Though great progress has been made in deconstructing the intricacies of the autophagic clearance of mitochondria, clearly there must be numerous players and steps in the pathways that are yet to be discovered. Though both PARKIN and PINK1 have been shown to be required for mitophagy, it is yet unknown how these proteins selectively target mitochondria for autophagic degradation. The ubiquitination of mitochondrial proteins is clearly important, but the topology of the ubiquitin linkages and control of the ultimate recruitment of the autophagosome is still a mystery. The extent to which proteasomal degradation of PARKIN substrates versus recruitment of ubiquitin binding proteins to relevant ubiquitylated substrates is critical for mitophagy requires examination. Numerous early studies have proposed candidate PARKIN substrates, though many of these have not been reliably substantiated. However, more recent work is beginning to define some highly validated PARKIN substrates, though not clearly the ones important to mitophagy.

Proteomic studies of purified mitochondria have also identified additional proteins whose abundance is either decreased or increased upon PARKIN activation or depolarization but precisely how these proteins are regulated and the extent to which ubiquitin is involved is unclear (Chan et al., 2011). We do not have a comprehensive understanding of cellular PARKIN targets, which is critical for elucidating how PARKIN promotes mitochondrial homeostasis, nor how PARKIN and PINK1, together with the proteasome, sculpt the MOM proteome to alter mitochondrial fate. Moreover, for the vast majority of E3s, including PARKIN, the extent to which

ubiquitin transfer is site-specific and signal-dependent is largely unknown, and we do not have a global understanding of site-specificity across a wide range of substrates for a single E3. Such information, however, is necessary for decoding the topology of E3 function and for defining how the ubiquitin system re-sculpts the proteome.

A number of mysteries remain to be solved. For example, to what extent does PARKIN activate mitophagy by causing the degradation of MOM proteins or by ubiquitylating proteins on the mitochondrial surface? How do PINK1 and PARKIN interact with one another and with substrates on the mitochondrial surface to cause mitophagy? Is PARKIN-mediated ubiquitination required for mitophagy? Which targets and modes of ubiquitination are implicated in this process? Do certain PARKIN targets trigger mitophagy? How are autophagosomes directed selectively to mitochondria?

We set out to systematically identify cellular PARKIN-dependent ubiquitylation targets and the dynamics of modification in a site-specific manner using quantitative diGly (QdiGly) proteomics and synthetic isotopic labeling with amino acids in culture (SILAC) to identify ubiquitylation sites that are dynamically induced upon mitochondrial depolarization. The diverse list of PARKIN substrates identified in the past implicates PARKIN in a range of cellular pathways, though confirmation or reproducibility of many substrates has been unsuccessful or conflicting. Therefore, identification of true PARKIN substrates and interactors and how these change in the presence of disease mutants is essential in order to gain real insight into the development of PD. PARKIN has been shown to ubiquitylate some proteins on the MOM, however, the complete PARKIN-dependent ubiquitylome remains poorly defined. We applied large-scale quantitative diGlycine capture proteomics to identify PARKIN-dependent ubiquitylation upon mitochondrial depolarization. We identified hundreds of ubiquitylation sites in dozens of proteins, many of which are located at the mitochondria, illustrating PARKIN's capacity to radically remodel the ubiquitylation status of the mitochondrial proteome. We used parallel complementary interaction proteomics to further explore the roles of both PARKIN and

PINK1 in mitochondrial homeostasis. We found that PARKIN physically associated with a reproducible assembly of MOM proteins, many of which were also ubiquitylation targets, upon mitochondrial depolarization. Interactions with potential autophagy receptors and the proteasome were also wholly dependent upon mitochondrial damage. To understand the significance of our findings, we mapped ubiquitylation sites onto available protein structures highlighting PARKIN's role at the MOM and the evolutionary conservation of ubiquitylation sites. In sum, our studies illuminate PARKIN and PINK1 modify the proteome to maintain mitochondrial homeostasis.

# CHAPTER 2

**Global profiling of the PARKIN modified proteome in response to mitochondrial depolarization**

Based on: Sarraf SA, Raman M, Guarani-Pereira V, Sowa M, Huttlin EL, Gygi SP, Harper JW. Landscape of the PARKIN-dependent ubiquitin modified proteome in response to mitochondrial depolarization. Nature. 2013 Apr 18;496(7445):372-6. doi: 10.1038/ nature12043. Epub 2013 Mar 17.

## Chapter 2: Contributions

**Figure 2.13** Validation of PARKIN interactors identified via interaction proteomics. Experiments performed by Virginia Guarani-Pereira.

**Figure 2.18** Web-tool for interrogation and structural analysis of candidate PARKIN targets. Web tool designed and constructed by Mathew Sowa.

## 2.1 Introduction

Parkinson's disease is a degenerative disorder of the central nervous system resulting from the cumulative loss of dopaminergic neurons, the distinct causes of which are not fully understood. Defects in mitochondrial homeostasis have been well documented for many years, and appear to be common to both sporadic and genetic PD (Dawson and Dawson, 2010). In this scenario, mechanisms that serve to remove damaged mitochondria from cells may be defective thus selectively harming neurons, cells which maintain a high metabolic load. Ultimately, it is thought that this accumulated damage, which occurs as a result of defects in mitochondrial homeostasis, may induce cell death. The protein kinase, PINK1, and the E3 ubiquitin ligase, PARKIN, are both found mutated in early onset familial PD and act in the same pathway to regulate mitochondrial homeostasis (Narendra et al., 2008). Both proteins appear to be vital in the regulation of mitochondrial quality by directing degradation of damaged mitochondria via mitophagy. It has been shown that the kinase activity of PINK1 and the E3 ligase activity of PARKIN are both essential to this process; however, the molecular workings of numerous aspects of the pathway and the underlying mechanisms are poorly understood. One very important aspect of the pathway about which little is known is how the ubiquitin signal generated by PARKIN on damaged mitochondria is translated into a signal which activates and recruits autophagy machinery. Thus, to begin exploration of this question, we surveyed the effects of PARKIN activation using a variety of proteomic and cell biological approaches.

Based on previous studies, we know that ubiquitination at the mitochondria after damage is both PARKIN-dependent and necessary for mitophagy (Narendra et al., 2009). In spite of years of work, many aspects of this pathway remain poorly understood. While a number of substrates have been identified for PARKIN, the full repertoire of PARKIN targets on the mitochondria as well as the effect of ubiquitination on the fate of individual substrates, are largely unknown. In fact, the actual physiological substrates of PARKIN's ubiquitin ligase activity important for its quality control functions remain poorly defined, and in some cases controversial

(Dawson and Dawson, 2010). How PARKIN together with the proteasome sculpts the mitochondrial outer membrane proteome to alter mitochondrial fate remains one of the most pressing questions for the field. To explore these issues, we utilized proteomic approaches and numerous cell biological approaches in an attempt to provide a systematic and definitive understanding of the PARKIN-modified proteome. Our ultimate goal was to contribute information about how the PINK1-PARKIN pathway remodels the MOM proteome to control mitochondrial fate. To this end, we performed an unbiased quantitative proteomics analysis of cellular proteins that are ubiquitylated in response to mitochondrial damage in a PINK1-PARKIN-dependent manner. This analysis revealed hundreds of candidate ubiquitylation sites in dozens of MOM and cytoplasmic proteins, including both novel and previously identified PARKIN substrates. Together with interaction proteomic studies and analysis of PARKIN disease mutants, these studies have provided the first integrated topological view of how the PARKIN pathway re-sculpts the MOM of damaged mitochondria. We believe our efforts provide the first systematic compendium of PARKIN targets as a resource for the Parkinson's disease field. And we hope it can contribute to the understanding of the physiological functions of PARKIN in cells experiencing oxidative stress, for example as a consequence of aging or mitochondrial malfunction, and potentially provide targets or mechanisms which will aid in PD drug discovery.

### 2.1.1 Complementary integrative proteomic approaches to study PARKIN and PARKIN targets

In order to better understand PARKIN's role in modifying damaged mitochondria and effecting its removal, we have used two complementary approaches, an interaction proteomics method developed in our lab to identify high-confidence candidate interaction proteins (HCIPs) and quantitative diGlycine (diGly) capture proteomics coupled with stable isotope labeling of amino acids in culture (SILAC) and liquid chromatography-mass spectrometry (LC-MS) to

determine specific targets of PARKIN ubiquitination after mitochondrial damage. These methods allow us both to identify substrates of PARKIN in response to mitochondrial depolarization as well as to determine those proteins with which PARKIN interacts, thus clarifying potential enzymatic partners, regulators, or substrates. This comprehensive approach allows us to examine multiple players in the pathway and to evaluate both their regulation and their targets. Furthermore, we demonstrate that quantitative diGly capture proteomics can be used to identify substrates for a single E3 ubiquitin ligase.

**Quantitative diGlycine (diGly) capture proteomics**

Historically, identifying targets of ubiquitylation has been very challenging. The ubiquitin modification is relatively large, at ~8800 Daltons (Da), when compared to other post-translational modifications, such as phosphorylation, which adds only 80 Da to the mass of a protein. Furthermore, because ubiquitylation is often a signal for degradation of the modified protein, the turnover of ubiquitylated proteins is often very rapid, making it difficult to capture and detect modified proteins under steady-state conditions. Most studies have relied on either the use of ubiquitin binding domains, antibodies or overexpression of epitope-tagged ubiquitin in an attempt to capture ubiquitylated proteins for identification by mass spectrometry. Attempts to identify the total cellular ubiquitylome or changes in response to various stimuli, though have had limited success actually identifying or quantifying peptides containing a ubiquitin modification (Table 2.1) (Argenzio et al., 2011; Danielsen et al., 2011; Matsumoto et al., 2005; Meierhofer et al., 2008; Peng et al., 2003; Tagwerker et al., 2006). In most studies, tagged ubiquitin has been overexpressed in cells, after which ubiquitin is usually immunoprecipitated, thus allowing identification of the modified peptide. Though substrates have been identified using this method, we cannot be sure that modification and substrates found in the presence of overexpressed epitope-tagged ubiquitin truly represent endogenous circumstances. There is a concern that the excess ubiquitin may disrupt endogenous ubiquitin modification pathways to some degree and the extent to which overexpression may affect the occupancy and specificity

**Table 2.1 Identification of ubiquitin sites by mass spectrometry.** Previous studies have predominantly relied upon exogenous expression of epitope-tagged ubiquitin.

| Organism | Method | Proteins | Sites | Study |
|---|---|---|---|---|
| Yeast | His-Ub | 1075 | 110 | (Peng et al., 2003) |
| HEK293 | His-Ub | 22 | 4 | (Kirkpatrick et al., 2005b) |
| HEK293T | Ub-antibody | 670 | 18 | (Matsumoto et al., 2005) |
| Yeast | HB-Ub | 258 | 20 | (Tagwerker et al., 2006) |
| Liver cells | GST-UIM | 83 | 19 | (Tan et al., 2008) |
| HeLa | HB-Ub | 669 | 44 | (Meierhofer et al., 2008) |
| HeLa, Mouse Fibroblast | Ub-antibody, Flag-His-Ub | 1472 | 31 | (Argenzio et al., 2011) |
| U2OS – HEK293T | Strep-HA-Ub | 5756 | 753 | (Danielsen et al., 2011) |

of ubiquitylation is unclear. Even with the application of these methods by numerous groups, the overall number of modification sites identified is small, particularly in comparison to the extent of acetylation and phosphorylation identified (Choudhary et al., 2009; Huttlin et al., 2010). This leaves us with the question, what are the endogenous sites of modification?

Early work performed using tagged ubiquitin demonstrated that ubiquitin site identification is aided by the presence of a Gly-Gly remnant which is present as an isopeptide linkage with lysine residues in ubiquitylated proteins. This characteristic can be used diagnostically to identify ubiquitylated peptides by mass spectrometry (Peng et al., 2003). The Gly-Gly remnant is created by trypsin proteolysis of a ubiquitin-conjugated protein producing the two amino acid signature peptide at the ubiquitination site which is derived from the C-terminus of ubiquitin (Figure 2.1). The Gly-Gly remnant remains covalently attached to the target lysine residue via an isopeptide bond and results in a mass shift at the lysine residue of 114.1 Da as well as a missed proteolytic cleavage because trypsin proteolysis cannot occur at the modified lysine. Peng et al. demonstrated the utility of these signature peptides by using them to identify

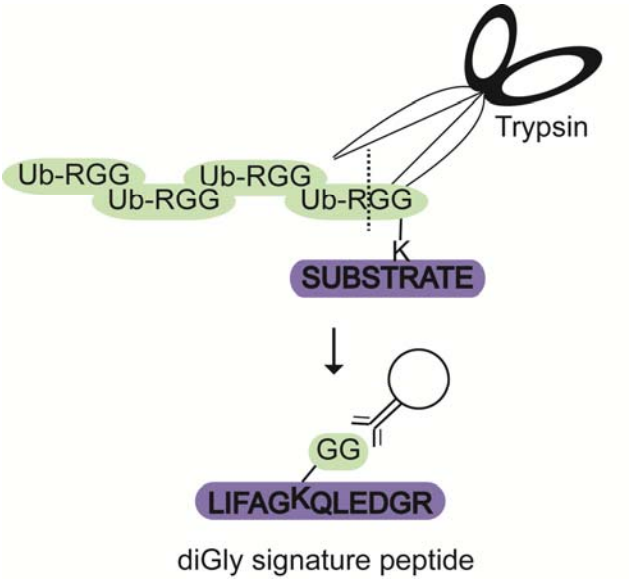


**Figure 2.1 Generation of the diGly remnant enables antibody-based capture of endogenous ubiquitylated proteins.** Proteolysis with trypsin produces the unique diGly signature peptide which is then recognized by an antibody allowing quantitative examination of alterations in the ubiquitinome.

epitope-tagged ubiquitin conjugates in yeast with mass spectrometry (Peng et al., 2003). Even with this precise and sensitive technique, the low occupancy of ubiquitylation makes detection of endogenously modified proteins extremely challenging in the absence of overexpression of either ubiquitin or substrate.

Another challenge is the ability to detect substrates for a single E3 ubiquitin ligase. To date, the majority of E3 substrates have been identified based on a physical interaction between the E3 and the substrate followed by mutational analysis to identify candidate ubiquitylation sites in the targets. Often, both affinity techniques and bioinformatics approaches used to discover ligase substrates are unsuccessful both because substrates are not abundant and because affinity of ligase for the substrates is likely to be low. Furthermore, recognition elements in substrates are often poorly defined and may not be conserved, thus minimizing the probability that bioinformatic approaches will consistently identify E3 substrates. However, these approaches have worked fairly reliably on a small scale but do not always provide a direct route to the actual sites of endogenous ubiquitylation *in vivo*, due to the possibility of cryptic sites or

artifactual effects of overexpression. Furthermore, confirmation of the ubiquitylation of these substrates and identification of the modified sites has lagged further behind. Our study provides evidence that diGly capture proteomics can be used to identify substrates of a single E3 ligase *in vivo*. Unlike most previous approaches aimed at identifying ubiquitylated proteins which have relied on exogenously expressed tagged ubiquitin, our system relies on antibody-based capture of endogenous diGly-containing peptides to quantitatively monitor alterations in the ubiquitylome in response to mitochondrial depolarization and PARKIN activation (Figure 2.1).

Our goal was to globally monitor changes in the ubiquitylated proteome after PARKIN activation; in order to address this question in the context of the limitations detailed above, we used a newly developed approach to enrich for and identify ubiquitylated peptides. Combination of a monoclonal antibody that specifically recognizes the diGly remnant of ubiquitylated proteins resulting from trypsinolysis with metabolic labeling in cell culture allowed us to identify and quantify ubiquitylated proteins and their sites of modification on a global scale. Using this method, a recent study was able to identify roughly 19,000 ubiquitylation sites in nearly 5000 proteins in the process of monitoring temporal changes in diGly site abundance in response to proteasome inhibition, thus creating an extraordinary resource for the identification and classification of ubiquitin-modified lysine residues in both known UPS substrates and newly identified substrates (Kim et al., 2011). Using a similar approach with a different antibody, another group was able to map 11,000 endogenous ubiquitylation sites on more than 4,000 human proteins, thus confirming the efficacy of the method (Wagner et al., 2011). Compared to previously used methods, such as western blotting or other MS-based approaches, our approach provides several advantages for ubiquitylation site mapping. For example, we are able to perform an efficient single-step enrichment for ubiquitylated peptides which enables the detection of low abundant modification sites. Furthermore, this method allows deep sampling and quantification of a proteome-wide analysis of endogenous ubiquitylation.

Deeper examination of the data produced from these studies shows that while they produce vast datasets consisting of endogenous ubiquitylation sites, the degree of overlap between biological duplicates is not necessarily as high as might be expected; however, amongst those sites repeatedly sampled, correlation of the fold-change in modification is high. Because previous papers published showed little success in the identification of substrates of a single E3, we performed preliminary experiments to determine how well the diGly approach might work for PARKIN (Lee et al., 2011). Due to what we expected to be the stochastic nature of the diGly capture, we chose to investigate an E3 which exhibits signal-dependent activity and which targets an abundant substrate population at the mitochondria. Through repeated sampling, we have identified the strengths and limitations of this technology, revealing that extensive sampling of the cellular ubiquitylome is required to fully populate the substrate list for a single E3 ligase because the diGly approach relies on antibody-based capture of substrates from the massive pool of ubiquitylated proteins available. Sampling of proteins from this immense pool results in repeated identification of abundant ubiquitylated proteins along with stochastic identification of less abundant ubiquitylated proteins (Figure 2.2). However, with increased sampling, less abundant proteins can be identified, though stochastically, meaning that a substantial number of peptides are identified only in a single replicate experiment. We have striven to circumvent the stochastic nature of the diGly approach by both repeated sampling and execution of multiple replicate experiments in numerous cell lines. This repeated sampling has allowed us to routinely capture and validate ubiquitylation sites present at high abundance while gradually populating the list with additional sites of lesser abundance, which we have a lower probability of identifying numerous times. By creating a large enough experimental pool, we are able to delve deeper into the substrate population to identify those lesser abundant, though truly ubiquitin-modified, substrates. Thus, the limitation we aimed to address is a detection limit or a limitation of capture, not an issue of noise or of sorting true from false identification.

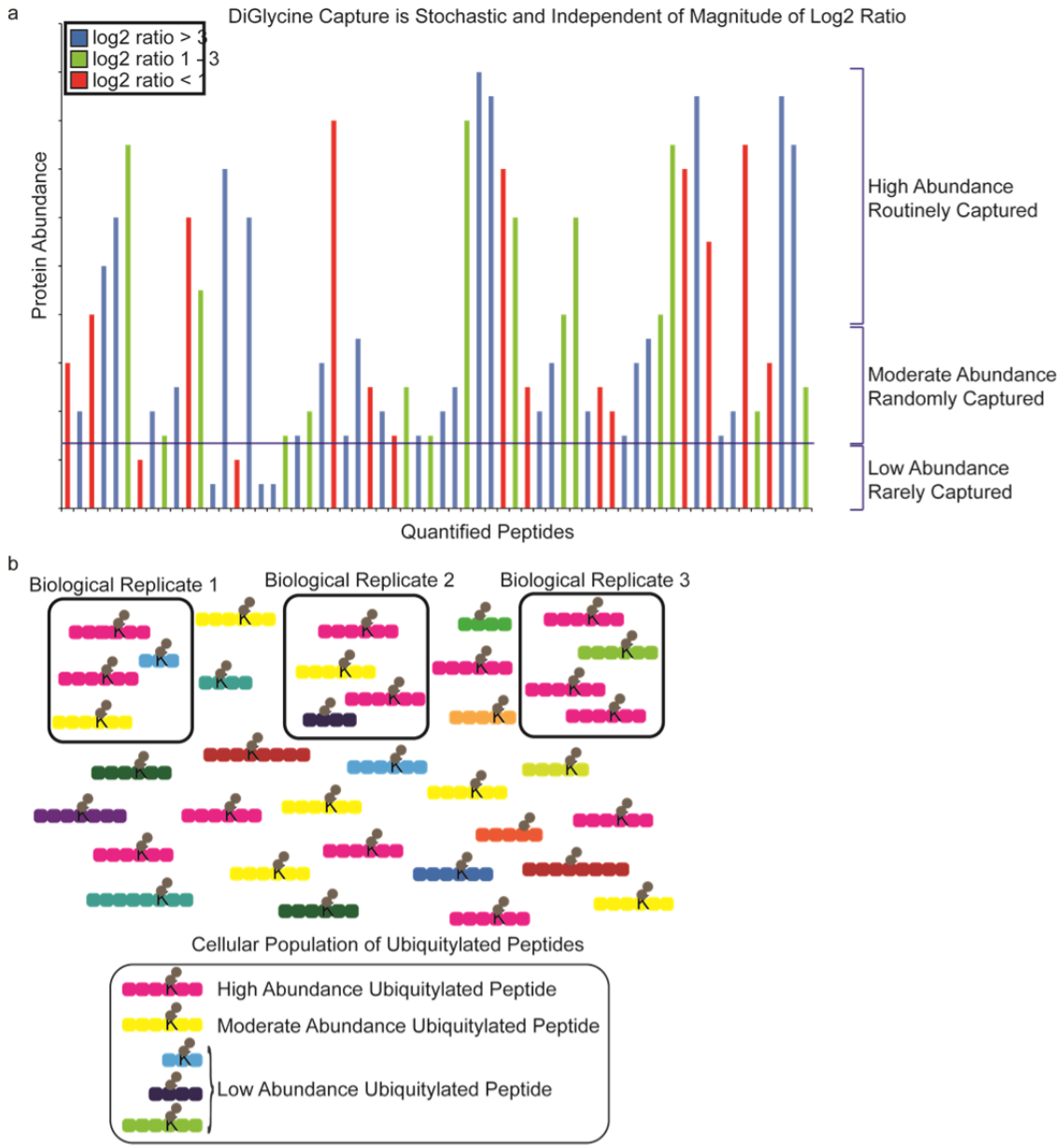


**Figure 2.2 Schematic representation of stochasticity in the diGly capture approach.** **a**, Schematic displaying the basis for stochastic retrieval of low abundance peptides that nevertheless have high log2 (H:L) ratios in a SILAC experiment. Abundant proteins may be routinely sampled by diGly antibody regardless of their log2 (H:L) ratio but lower abundance proteins may be rarely captured, even though they may be highly regulated in response to a signal (log2 (H:L) ratio >3). Thus, multiple experiments may be required to substantially sample a wide cross section of ubiquitylation sites. **b**, Basis for stochastic capture of peptides across biological replicates, with peptides from abundant proteins being detected routinely whereas peptides for low abundance proteins are only captured within a subset of experiments.

**Affinity-purification mass spectrometry (AP-MS) to determine PARKIN interactors**

Direct interrogation of physiological protein complexes can be achieved through interaction proteomics. Typically, this approach entails purification of a protein of interest and identification of co-purifying proteins or complexes via liquid chromatography-tandem mass spectrometry (LC-MS/MS). A major pitfall of this approach is that a large number of nonspecific interacting proteins typically dominate the mass spectral analysis of purified complexes (Ewing et al., 2007). Our lab has sought to address this issue through the creation of a proteomic analysis software platform, termed CompPASS, which employs an unbiased comparative approach to identify high-confidence candidate interacting proteins from the hundreds of proteins typically identified in and AP-MS experiment. Any potential interactors then identified are then scored based on abundance, uniqueness, and reproducibility in order to pull out the true interactors (Sowa et al., 2009). Using this method, we performed a series of studies to complement the quantitative proteomics approach described above. We examined interactors of PARKIN in the presence or absence of mitochondrial depolarization to identify depolarization-dependent high confidence candidate HA-PARKIN-interacting proteins in numerous cell lines. We found depolarization-dependent PARKIN association with numerous MOM targets, autophagy receptors, and the proteasome in a manner that required the active site of PARKIN. We also examined a series of mutations found either in patients with PD or designed to affect PARKIN activation and dynamics.

Integration of the quantitative and interaction proteomic methods together with cell biological studies has allowed us to perform a series of studies that have revealed the PARKIN-modified proteome, including hundreds of ubiquitylation sites on dozens of proteins, including known and novel targets. Using these methods, we have identified approximately 10,000 ubiquitylation sites in more than 2,000 proteins. Many of these candidate PARKIN targets are located on the MOM, where all sites identified are located on the cytoplasmic face, while other substrates identified are thought to be primarily cytoplasmic. Parallel interaction proteomic and *in vivo* functional

studies revealed signal dependent association of PARKIN with a cohort of MOM proteins in a manner that depends upon functionality of the active site of PARKIN. Our data suggest that PARKIN interacts with and promotes the site-specific ubiquitylation of numerous mitochondrial and cytoplasmic proteins, thereby extending previous studies examining abundance of mitochondrially-enriched proteins, thus allowing us to place candidate PARKIN-dependent ubiquitination targets into a structural and functional framework. This global and quantitative examination of proteins targeted for ubiquitylation after mitochondrial depolarization provides a dynamic readout of how the entire proteome is remodeled in response to this form of cellular stress as well as the identification of substrates for an individual E3 ligase implicated in multiple devastating diseases.

## 2.2 Results

### 2.2.1 PARKIN is recruited to depolarized mitochondria resulting in clearance via mitophagy

To begin our investigation of the global effects of PARKIN activation, we sought to confirm previously published work describing the translocation of PARKIN to mitochondria after CCCP-induced mitochondrial depolarization and resultant mitophagy. Therefore, we created stably expressed N-HA-FLAG-PARKIN HeLa cell lines in which we observed a shift from cytoplasmic to mitochondrial-associated PARKIN and extensive colocalization with TOMM20, a mitochondrial outer membrane protein, after 1 hour of CCCP treatment (Figure 2.3a) which we confirmed using transiently expressed N-GFP-PARKIN in HeLa cells (Figure 2.3b). Furthermore, upon PARKIN translocation, the mitochondria are extensively labeled with ubiquitin, which we confirmed using multiple antibodies to detect endogenous ubiquitin as well as an HA-ubiquitin construct (Figure 2.3c, d). Almost complete colocalization of PARKIN on

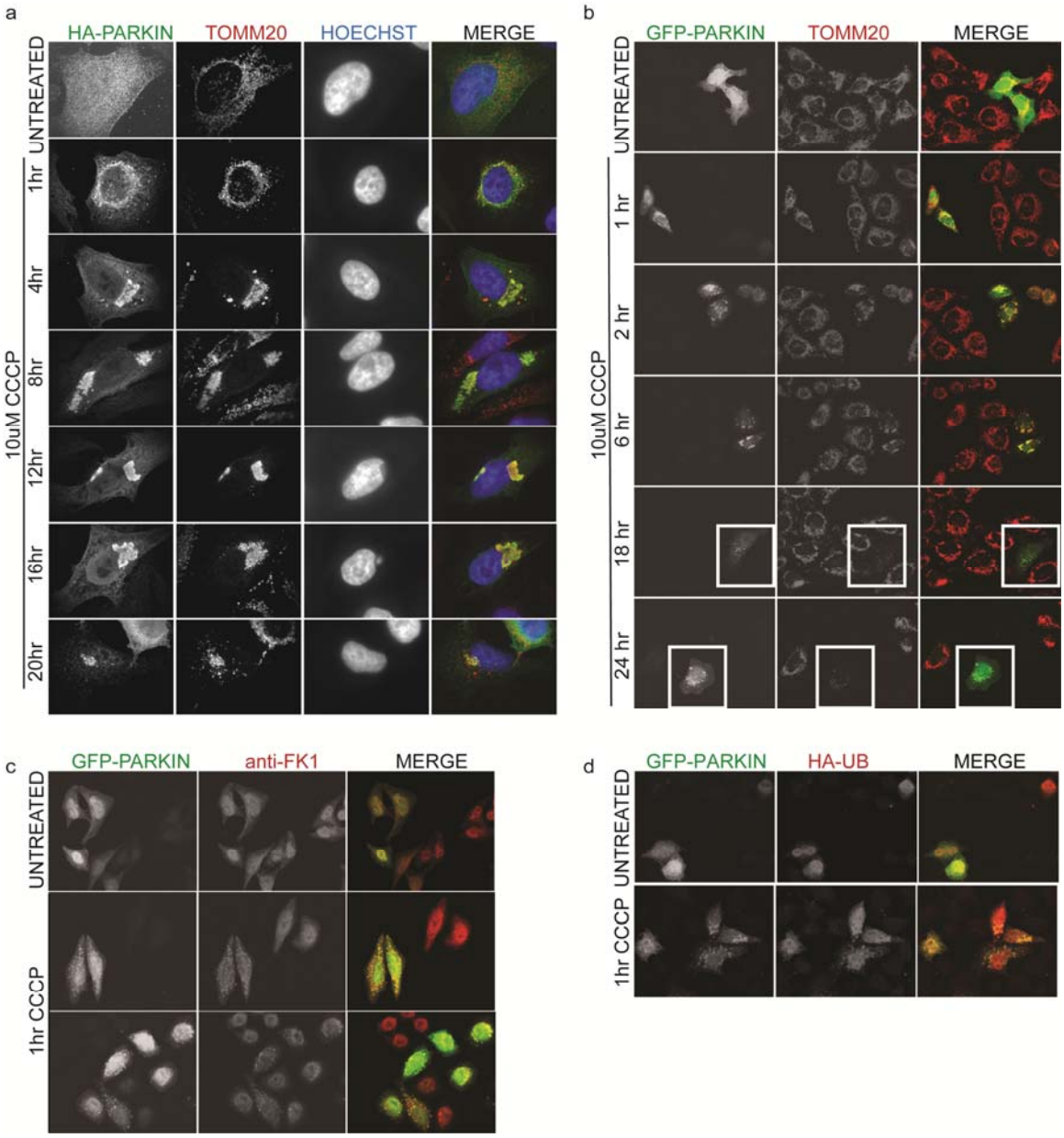


**Figure 2.3 Mitochondrial depolarization results in translocation of PARKIN to the mitochondria and mitochondrial ubiquitylation. a**, N-HA-Flag-PARKIN stably expressed in HeLa cell line treated with 10μM CCCP for various time points immunostained for HA-PARKIN (green) or a mitochondrial marker, TOMM20 (red). **b**, N-GFP-PARKIN transfected HeLa cells treated with 10μM CCCP for various time points immunostained with anti-TOMM20 (red). The white boxes highlight GFP-PARKIN expressing cells with decreased levels of mitochondria. **c**, Stably expressed GFP-PARKIN HeLa cell line stained with anti-FK1 to detect colocalization of PARKIN with endogenous ubiquitin after 1 hour of 10μM CCCP treatment. **d**, Stably expressed GFP-PARKIN colocalizes with HA-ubiquitin (red) after 1 hour 10μM CCCP.

clustered mitochondria and endogenous or tagged ubiquitin could be detected after as little as one hour (Figure 2.3c, d).

To verify that the mitochondria were being removed from cells via mitophagy, we treated transiently transfected HeLa cells with GFP-PARKIN or stable N-HA-FLAG-PARKIN and treated with CCCP for 1, 2, 18, and 24 hours. As expected, GFP-PARKIN translocated to the mitochondria within 1 hour of CCCP treatment and was still visible at 6 hours post-drug (Figure 2.3b). However, by 18 hours, though some GFP-PARKIN foci were still observable, the amount of signal was decreased. Furthermore, mitochondrial staining of TOMM20 also decreased in those cells transfected with GFP-PARKIN and by 24 hours, mitochondrial mass appeared to be significantly reduced (Figure 2.3b). To confirm that the removal of mitochondria occurred via autophagy, we treated cells with Bafilomycin A (BafA), which prevents maturation of autophagic vacuoles by inhibiting fusion between autophagosomes and lysosomes. Upon BafA treatment for 6 or 24 hours, we observed an increase in the number of cells containing mitochondrial GFP-PARKIN and ubiquitin foci when compared to untreated cells, suggesting that the loss of mitochondrial from these cells was indeed through an autophagic mechanism (Figure 2.4).

### 2.2.2 Quantitative profiling of the PARKIN-modified proteome

We set out to systematically identify and quantify cellular PARKIN-dependent ubiquitylation targets and the dynamics of modification in a site-specific manner using quantitative diGly (QdiGly) capture proteomics. QdiGly merges antibody-based capture of “diGly remnant” containing peptides and SILAC to identify ubiquitylation sites that are dynamically induced, in this case, upon mitochondrial depolarization. To overcome the inherent stochasticity of diGly capture and ensure that we sampled low abundance ubiquitylated peptides, we designed a 3-tiered approach in which we performed 73 independent QdiGly profiling experiments using 4 different cell lines allowing us to compare the effects of endogenous and overexpressed PARKIN which we used in order to increase the ability to detect mechanistically

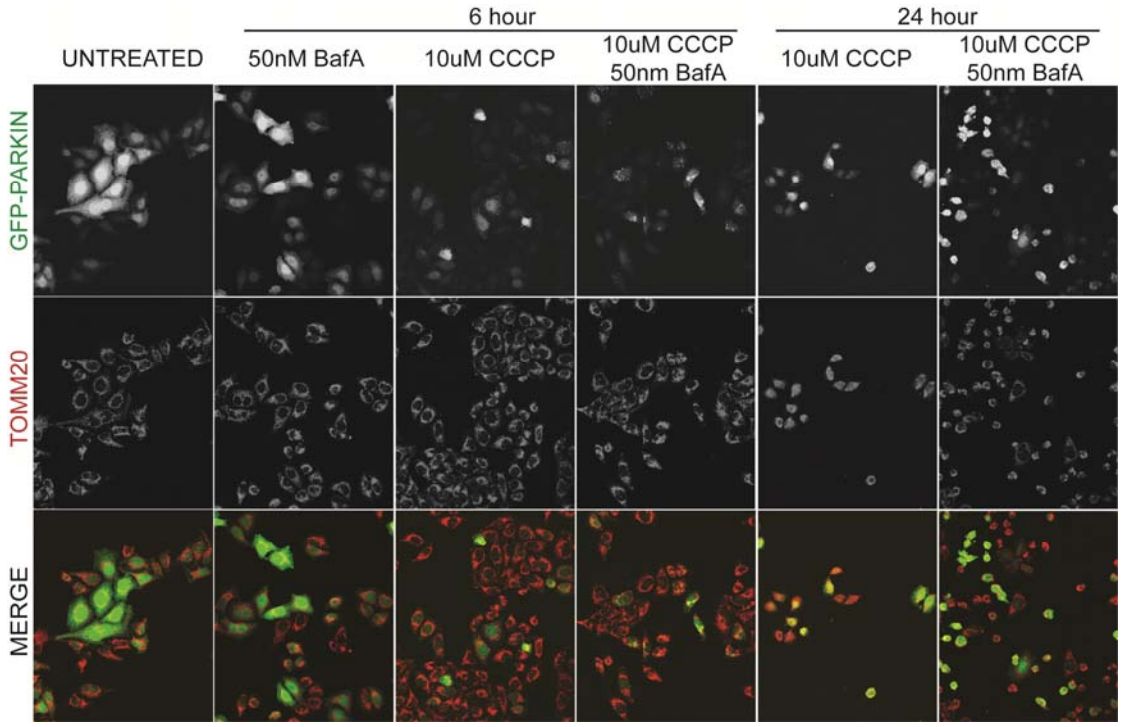


**Figure 2.4 Mitochondria are removed from PARKIN-expressing cells via mitophagy. a,** HeLa GFP-PARKIN cell line treated with 10uM CCCP and/or 50nM BafA for 0, 6, 0r 24 hours.

relevant ubiquitylation sites (Figure 2.5, Supplementary Table 1). We used 2 epithelial cell lines, HCT116 and HeLa, and one neuronal, SH-SY5Y, which has commonly been used to model PD in the past (Borland et al., 2008; Lopes et al., 2010; Xie et al., 2010). Both HCT116 and SH-SY5Y cells express low levels of endogenous PARKIN while HeLa cells do not express any PARKIN due to a chromosomal rearrangement (Figure 2.6a-c) (Denison et al., 2003). Tier 1 consisted of the epithelial colon cancer-derived HCT116 cell line stably expressing HA- FLAG-PARKIN ($HCT116^{PARKIN}$) at levels approximately 10-fold greater than endogenous, the expectation being that elevated PARKIN levels would allow us to identify mechanistically relevant ubiquitylation events that might otherwise not be detectable with lower levels of signal seen physiologically (Figure 2.5, Figure 2.6a). Tier 2 examined HeLa cells with or without lentiviral- expression of HA-FLAG-PARKIN ($HeLa^{PARKIN}$) to formally identify PARKIN-dependent ubiquitination events among those found globally with depolarization (Figure 2.5, Figure 2.6b,c).

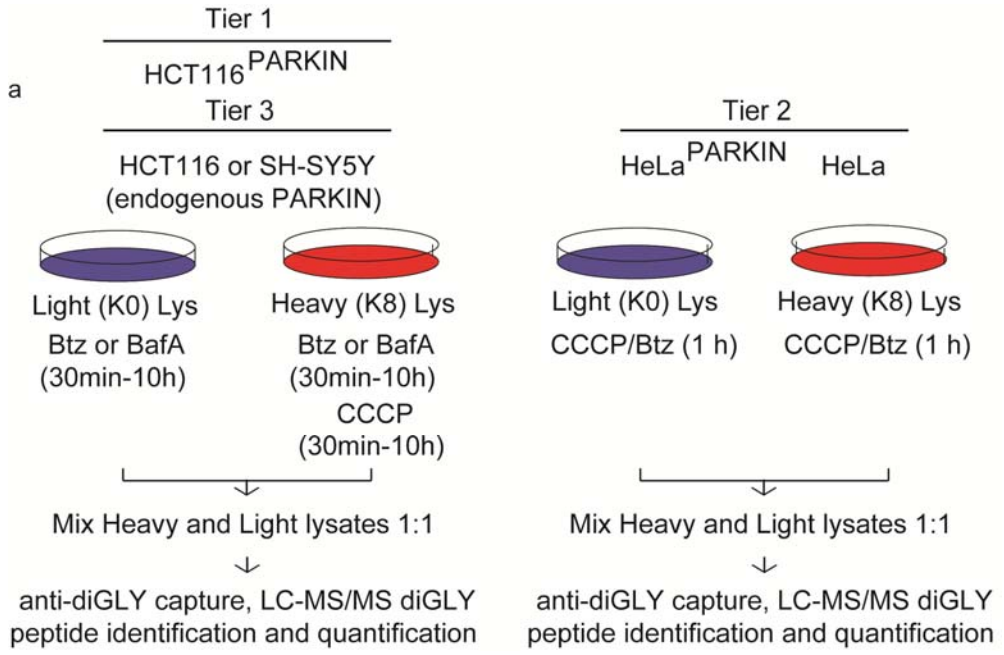


**Figure 2.5 Experimental scheme for QdiGly proteomics to determine PARKIN-dependent ubiquitylation**.

Tier 3 identified ubiquitylation events in HCT116 and SH-SY5Y cells expressing endogenous PARKIN, thus serving to validate sites found to be PARKIN-dependent in HeLa$^{PARKIN}$ cells, and depolarization dependent in HCT116$^{PARKIN}$ cells (Figure 2.5, Figure 2.6a,c). Using this SILAC-based tiered system, we examined the log2 ratio of Heavy:Light (H:L) diGly-containing peptides in cells with or without the addition of the uncoupling agent carbonyl cyanide 3-chlorophenylhydrazone (CCCP). In order to increase the likelihood of detecting ubiquitylated peptides, turnover was blocked by proteasome inhibition with bortezomib (Btz) or autophagy inhibition with BafA in some instances (Supplementary Table 1). This approach allowed us to identify both potential substrates of PARKIN in response to mitochondrial depolarization as well as the modified lysine(s) within the substrates.

Using this approach, we generated a comprehensive list of mitochondrial depolarization-dependent PARKIN-modified proteins, identifying a total of 10,287 non-redundant sites of ubiquitylation in 2268 proteins and quantifying 7821 sites in 2116 proteins across all cell lines (Figure 2.7a, Supplementary Table 2). From the 34 Tier 1 control and QdiGly profiling

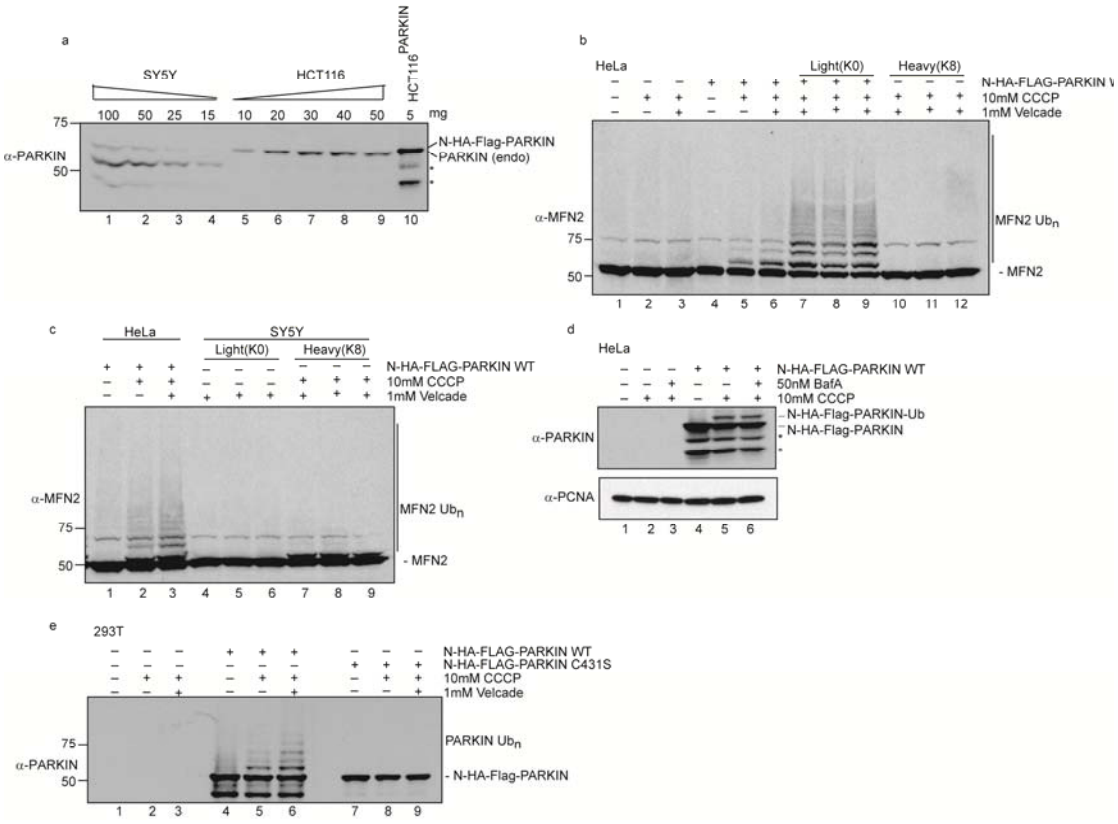


**Figure 2.6 Characterization of PARKIN expression in cell lines employed in this study.** Extracts from the indicated cell lines were subjected to SDS-PAGE and immunoblotting with anti-PARKIN antibodies. **a,** Determination of the relative levels of PARKIN in SH-SY5Y, HCT116, and HCT116$^{PARKIN}$ cell lines. **b,** Characterization of N-HA-FLAG-PARKIN expression in 293T and HeLa cells used for interaction proteomics. **c,** Demonstration of MFN2 ubiquitylation in HeLa$^{PARKIN}$ cells used for QdiGly profiling. **d,** Demonstration of MFN2 ubiquitylation in SH-SY5Y cells used for QdiGly profiling. *, PARKIN breakdown product.

experiments performed in HCT116$^{PARKIN}$ cells, we identified 6934 sites in 1993 proteins, quantifying 4772 sites, in 1654 proteins (Figure 2.7a, Supplementary Table 2). Though we performed experiments at multiple time points, we have mainly compared one hour of CCCP/Btz treatment across cell lines. In 18 experiments using HCT116$^{PARKIN}$ cells treated for 1 hour with CCCP/Btz, we quantified 443 ubiquitylated sites (261 proteins) with a H:L log2 ratio greater than or equal to 1.0, which represents a 2-fold increase in ubiquitylation status in at least one experiment (Figure 2.7a-c). Comparison of two representative experiments displayed a Pearson's correlation of 0.69, suggesting a good deal of overlap between experiments (Figure 2.7d); similar overlap was observed among biological replicates in HCT116$^{PARKIN}$ cells (Figure

**Figure 2.7 QdiGly proteomics of the PARKIN-dependent ubiquitin modified proteome**. **a**, diGly sites identified and quantified across 73 experiments. FDR, false discovery rate. **b**, $log_2$(H:L) plots for quantified diGly peptides for HCT116$^{PARKIN}$ (experiment 17) or HeLa$^{PARKIN}$ (experiment 57) cells. **c**, Distribution of ubiquitylation sites (log2(H:L) ≥ 1) and proteins identified up to 6 times across 18 independent HCT116$^{PARKIN}$ QdiGly experiments (1h 10μM CCCP, 1μM Btz). **d**, Pearson's Correlation plots for 2 representative QdiGly experiments from HCT116$^{PARKIN}$ cells (left panel) and HeLa$^{PARKIN}$ cells (right panel). **e**, Overlap of ubiquitylation sites found in the three deepest sampling data sets of HCT116$^{PARKIN}$ biological replicates (1 h 10μM CCCP, 1μM Btz) (Supplementary Tables 1, 2). **f**, Overlap between ubiquitylation sites and proteins for the various extended time point HCT116$^{PARKIN}$ QdiGly profiling experiments and the HCT116$^{PARKIN}$ 1h QdiGly profiling experiments. See Table S1 for conditions of the extended time course experiments. **g,** Heatmap of Log2(H:L) values for selected diGly peptides from untreated HCT116$^{PARKIN}$ cells at 1 and 8 h post CCCP treatment. Data are shown for those peptides that were quantified at both time points and in which at least one time point had a log2(H:L) value ≥1.0. **h**, Overlap of ubiquitylation sites in HeLa$^{PARKIN}$ biological triplicates (1 h 10μM CCCP, 1μM Btz). **i**, Overlap between triplicate QdiGly profiling experiments in SH-SY5Y cells (1 h 10μM CCCP, 1μM Btz).

a

| Cell line | Sites ID (FDR,%) | Proteins ID (FDR,%) | Sites Quant (FDR,%) | Proteins Quant (FDR,%) | All Sites (Proteins) log2(H:L)>1 | 1h CCCP/Btz Sites (Proteins) log2(H:L)>1 |
|---|---|---|---|---|---|---|
| HCT116-PARKIN | 6934 (0.61) | 1993 (0.85) | 4772 (0.23) | 1654 (0.36) | 807 (438) | 443(261) |
| HeLa-PARKIN | 3286 (0.40) | 1220 (0.74) | 2802 (0.29) | 1066 (0.38) | 617(325) | 582(303) |
| HCT116 | 6419 (0.31) | 1927 (0.88) | 4808 (0.12) | 1645 (0.36) | 838(391) | 108 (78) |
| SH-SY5Y | 3450 (0.17) | 1329 (0.68) | 2687 (0.15) | 1120 (0.54) | 337(235) | 284 (204) |
| Total (Non-redundant) | 10287 (0.59) | 2295 (1.00) | 7821 (0.31) | 2132 (1.08) | 1978(879) | 1112 (576) |

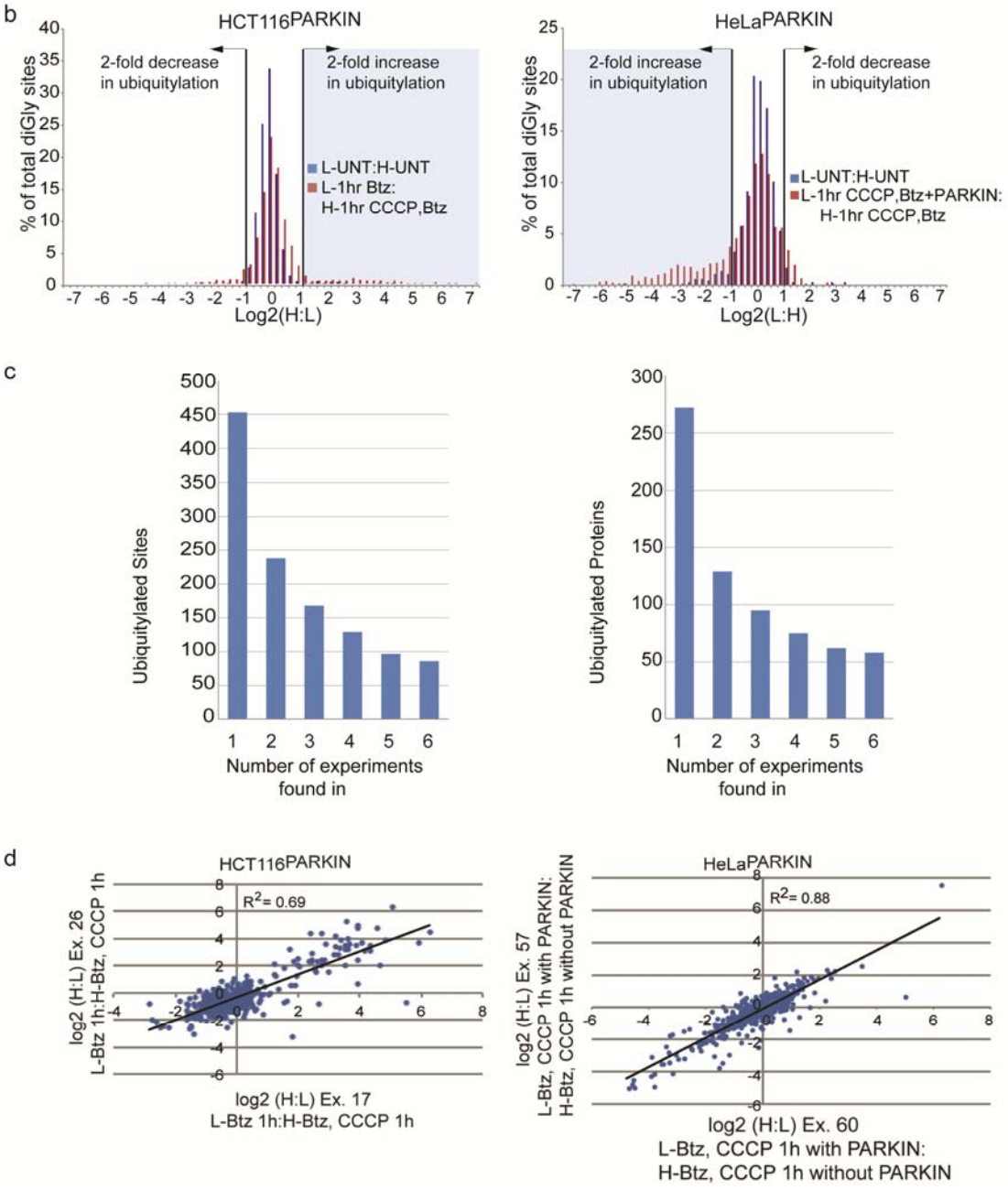


**Figure 2.7 (Continued)**

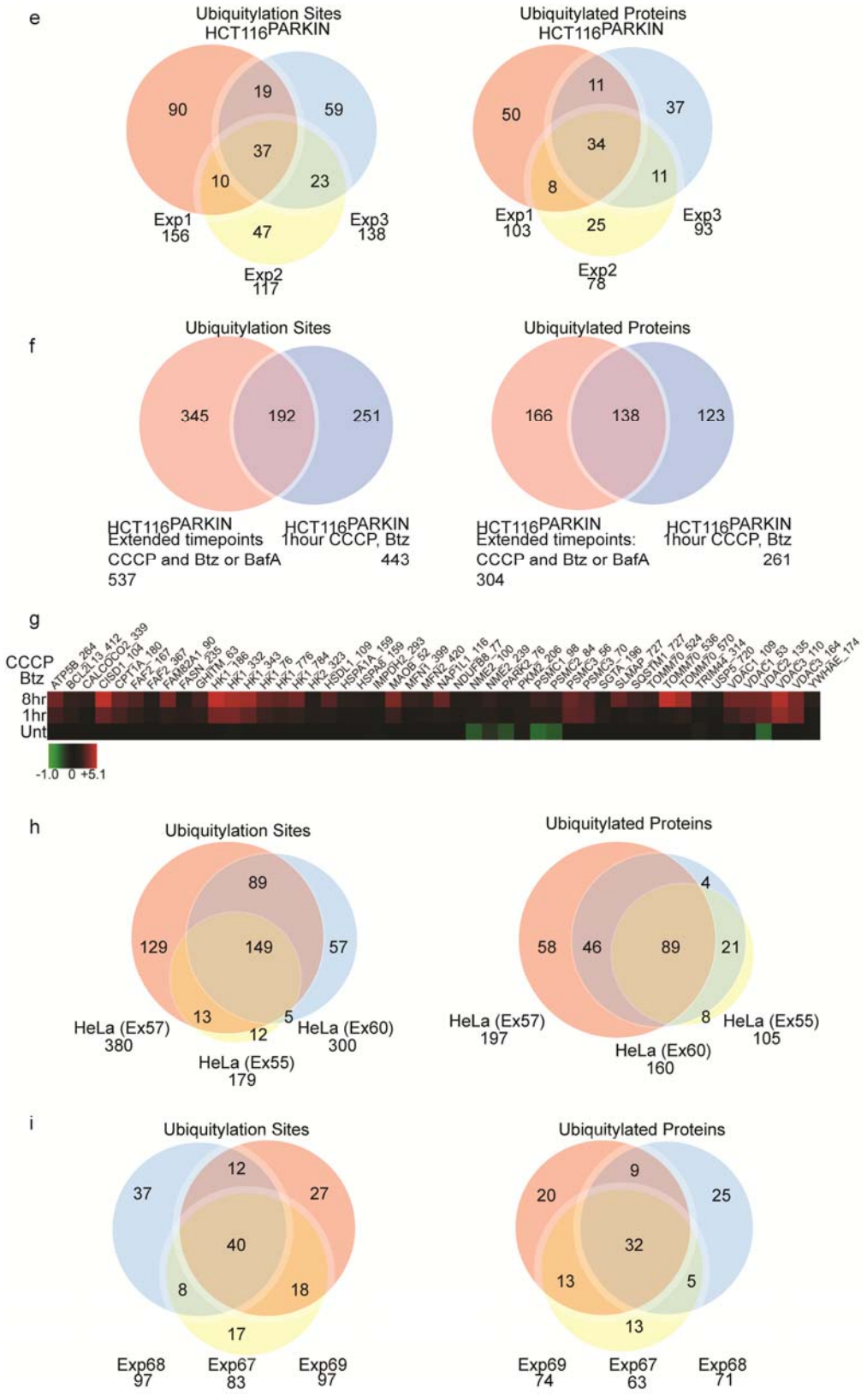


**Figure 2.7 (Continued)**

2.7e). In sixteen additional Tier 1 experiments with depolarization treatment of up to 10 hours, we identified 537 non-redundant diGly sites (304 proteins), including 192 diGly sites (138 proteins) also identified at 1h (Figure 2.7f, Supplementary Table 1). Furthermore, upon comparison of log2(H:L) ratios from 48 Tier 1 sites in 36 proteins at 1 and 8 h post CCCP/Btz treatment from parallel experiments, we found persistent or increased ubiquitylation for 34 sites (Figure 2.7g).

To differentiate between PARKIN-dependent and depolarization-dependent ubiquitylation events, we performed 9 control or 1 hour CCCP/Btz-treated QdiGly experiments in HeLa versus HeLa$^{PARKIN}$ cells and reversed the light and heavy amino acid labeling in these experiments to control for potentially inherent differences in ubiquitylation site abundance between heavy and light cultures that would otherwise contribute to false positives (Tier 2) (Figure 2.5, Figure 2.6b, c, Supplemental Table 1). As expected, depolarization induced ubiquitylation of MFN2 was wholly dependent on exogenous expression of PARKIN in HeLa cells (Figure 2.6b, c). We identified 582 PARKIN-dependent diGly peptides (303 proteins) with a log2 (H:L) ratio ≤ 1.0, consistent with a 2-fold increase in ubiquitylation (Figure 2.7a, b, Supplemental Table 2). Duplicate samples produced a Pearson's correlation of 0.88 (Figure 2.7d) and similarly, we saw significant overlap across biological triplicates (Figure 2.7h). Strikingly, 165 diGly sites (99 proteins) were common to Tiers 1 and 2 at 1 hour of mitochondrial depolarization (Figure 2.8a). This increased to 191 sites (144 proteins) when all Tier1 and Tier 2 data were compared (Supplementary Table 2). We have termed the overlapping set of ubiquitylation sites with 1 hour of depolarization and their associated proteins as Class 1 candidate PARKIN-dependent targets. Proteins found in both cell lines but with different sites of ubiquitylation are referred to as Class 2 (Supplementary Table 2).

We set a 2-fold increase in H:L ratio as the threshold for regulated ubiquitylation; however, many sites of modification were induced 30 to 60-fold upon mitochondrial depolarization (Figure 2.8b, Supplementary Table 2), indicating highly dynamic target

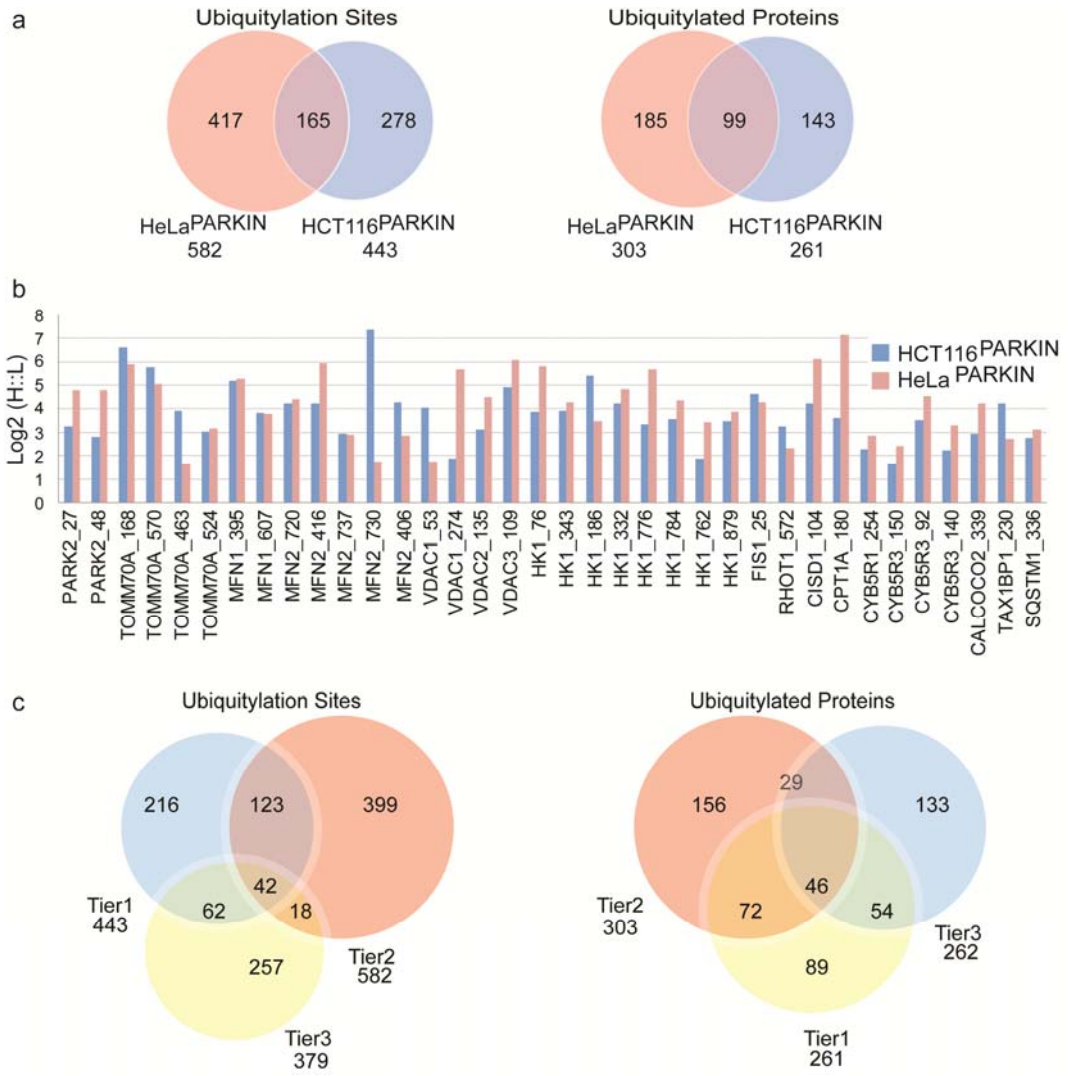


**Figure 2.8 Analysis of QdiGly proteomics to determine the PARKIN-dependent ubiquitin modified proteome**. **a**, Ubiquitylation site and protein overlap between all HCT116$^{PARKIN}$ and HeLa$^{PARKIN}$ experiments treated with 10μM CCCP, 1μM Btz for 1 h (Tier 1). **b**, $Log_2$(H:L) ratios for selected diGly sites from HCT116$^{PARKIN}$ (Ex17) and HeLa$^{PARKIN}$ (Ex57) (1 h 10μM CCCP, 1μM Btz). **c**, Overlap between Tier 1, 2 and 3 experiments (1 h 10μM CCCP, 1μM Btz). Venn diagram corresponds to diGly sites with log2(H:L) ≥ 1.0 and the corresponding proteins. Ex, experiment.

modification via PARKIN. Furthermore, we found that Class 1 targets were highly enriched for mitochondrial proteins ($p < 1.76 \times 10^{-17}$) (FIGURE 2.9a). In total, 60 Class 1 and 2 targets were linked with mitochondria or ER-type membranes, including 36 MOM proteins (Figure 2.9b). Consistent with previous studies, we repeatedly identified MFN1/2, RHOT1/2 (Miro), and VDAC1/2/3 proteins as PARKIN substrates in numerous experiments, both suggesting the efficacy of our approach and providing evidence that diGly capture routinely and efficiently

**Figure 2.9 PARKIN-dependent ubiquitylation sites revealed by QdiGly proteomics. a,** Class 1 target Gene Ontology Enrichment, determined used DAVID functional annotation enrichment tools. **b,** Class 1 sites are in black font. Additional sites found in Class 1 proteins are in red ($HCT116^{PARKIN}$) or blue font ($HeLa^{PARKIN}$). Site overlap in HCT116 and/or SH-SY5Y: magenta, orange, and green octagons. Dotted lines: interacting proteins. Rectangles represent Class 2 substrates. Red or blue boxes refer to additional sites identified in either $HCT116^{PARKIN}$ and $HeLa^{PARKIN}$ cells (Supplementary Table 2). * and **^**, protein levels decrease or increase, respectively, upon depolarization in a previous study by Chan et al., 2011.

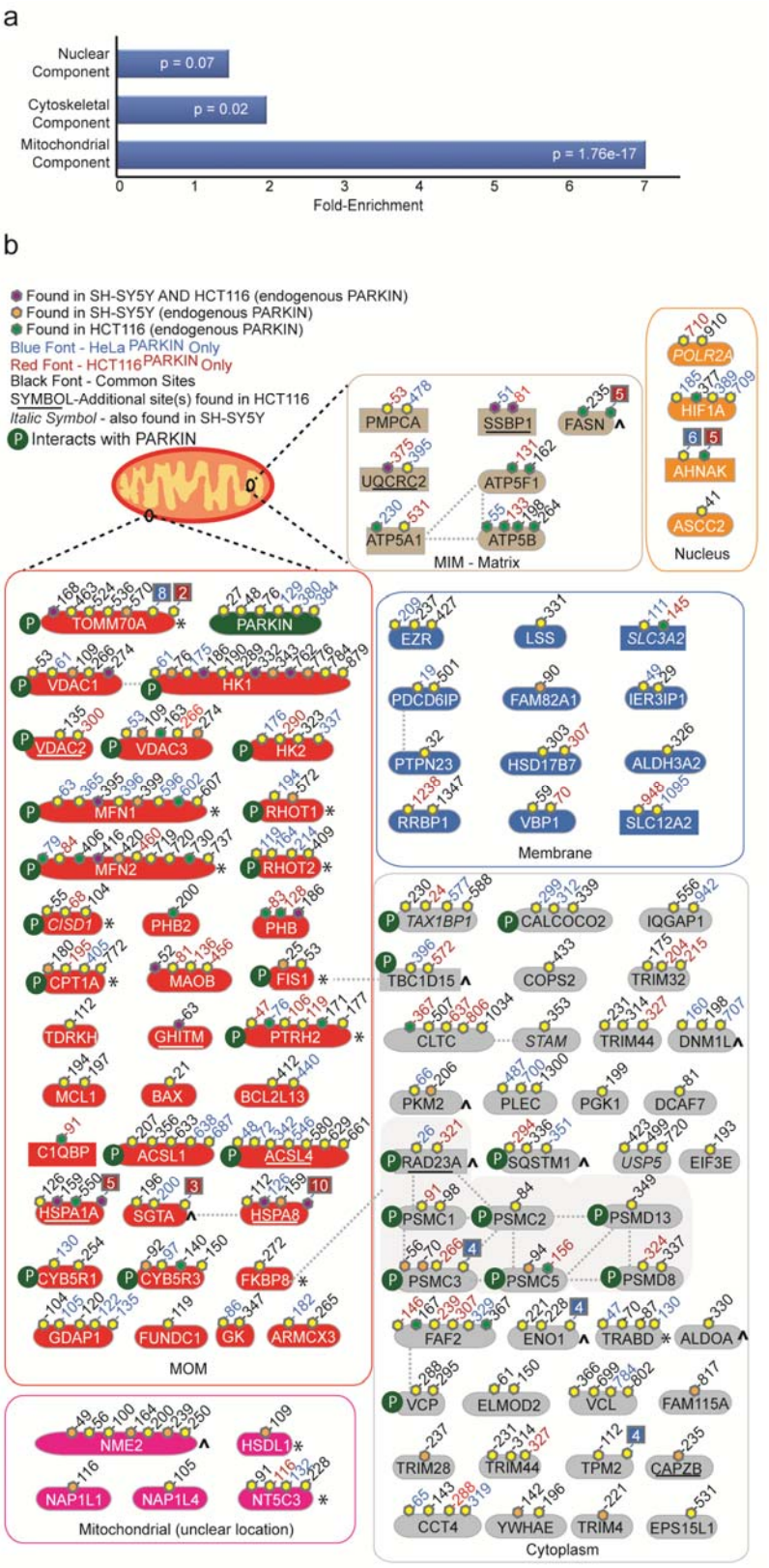


**Figure 2.9 (Continued)**

identifies those highly abundant substrates which were detectable by other methods in the past. However, using repeated sampling in conjunction with diGly capture, we were able to identify numerous additional proteins which have been impossible to distinguish in previous studies. Though enrichment for mitochondrial proteins was expected due to PARKIN translocation, we also identified numerous cytoplasmic proteins (Figure 2.9b). Of particular interest, candidate cytoplasmic targets included proteasome subunits, the VCP/p97 AAA ATPase, and the proposed autophagy adaptors (SQSTM1, CALCOCO2/NDP52, and TAX1BP1) (Figure 2.9b).

To validate our findings in HCT116$^{PARKIN}$ and HeLa $^{PARKIN}$ cells, we performed 22 QdiGly experiments using HCT116 and SH-SY5Y cells expressing endogenous PARKIN (Tier 3) (Figure 2.5, Figure 2.6a, c, Supplementary Table 1). By western blot, we were primarily able to detect only mono-ubiquitylated forms of MFN2 ubiquitylation in these cell lines upon mitochondrial depolarization presumably due to low levels of endogenous PARKIN (Figure 2.6c). Out of 4,808 sites (1,645 proteins) quantified in HCT116 cells, we found a total of 838 sites (391 proteins) whose log2 (H:L) ratios were ≥ 1.0 after mitochondrial depolarization in the presence of either Btz or BafA (Figure 2.7a, Supplementary Table 1, Supplementary Table 2). Under similar experimental conditions using SH-SY5Y cells, we quantified a total of 2687 sites (1120 proteins) from which 337 ubiquitylation sites in 235 proteins showed increased log2 (H:L) ratios (Figure 2.7a, Supplementary Table 1, Supplementary Table 2). Among biological triplicates in SH-SY5Y cells at 1 hour of CCCP/Btz we saw high degrees of overlap, again suggesting that the most abundant diGly sites are most easily reproducibly captured (Figure 2.7i). When compared to Tier 1 and Tier 2 data sets, we found broad overlap with the Tier 3 data (Figure 2.8c, Supplementary Table 2). Additionally, fifteen CCCP-dependent diGly sites in 12 Class 1 or 2 PARKIN target proteins were found in both the HCT116 and SH-SY5Y cell lines. Individually, 29 sites in 27 Class 1 or 2 proteins were detected in SH-SY5Y cells and 27 sites in 17 Class 1 or 2 proteins were detected in HCT116 cells (Figure 2.9b, Supplementary Table 2). Moreover, 124 sites identified in Tier 3 experiments were located in 29 Class 1 or 2 proteins,

though the sites themselves were distinct from Class 1/2 sites, possibly suggesting promiscuity of PARKIN targeting at the site level; regardless, Tier 3 provided extensive confirmation of many PARKIN-dependent diGly sites and proteins at endogenous PARKIN levels.

To further confirm that proteins identified via diGly capture were being ubiquitylated in a depolarization-dependent manner, we stably expressed a subset of C-terminally HA-Flag-tagged substrates in HCT116 cells. We were able to confirm depolarization-dependent ubiquitylation of C1QBP, UQCRC2, FAF2, PHB, PHB2, VDAC3, NDUFA9, and ATP5F1 in HCT116 cells via immunoblotting at either 1 hour or 8 hours post-CCCP or CCCP/Btz treatment (Figure 2.10c). For some substrates, e.g. C1QBP, we could easily detect ubiquitylation at 1 hour in the presence of CCCP, regardless of Btz addition. However, for others, such as NDUFA9, we were unable to detect ubiquitylation at 1 hour, though the modification was detectable by 8 hours (Figure 2.10c). For a subset of substrates, UQCRC2, C1QBP, ATP5F1, and PHB, we demonstrated that ubiquitylation was either greatly reduced or eliminated by RNAi-mediated depletion of PARKIN, suggesting PARKIN-dependent ubiquitylation (Figure 2.10a, b, d). Though we are able to validate PARKIN targets identified via QdiGly capture using this system, it often required longer time points after depolarization to detect the ubiquitylation modifications. Though this may at first appear to be a perplexing discrepancy, we believe this is accounted for by differences in sensitivity of the techniques used as well as the use of HCT116 cell lines expressing low levels of endogenous PARKIN which may require a longer period of time to produce detectable levels of ubiquitylation activity.

### 2.2.3 Interaction Proteomics: PARKIN interaction is mitochondrial depolarization-dependent

To complement the QdiGly capture substrate identification and to determine whether PARKIN might stably associate with candidate substrates, we employed anti-HA affinity purification and mass spectrometry in 293T and HeLa cells stably expressing N-terminally tagged HA-Flag-

**Figure 2.10 Validation of candidate PARKIN targets. a,** Validation of siRNAs targeting PARKIN by immunofluorescence. HeLa cells stably expressing HA-FLAG-PARKIN were transfected with PARKIN siRNAs and the depletion of PARKIN examined by confocal microscopy after immunostaining with anti-HA and anti-TOMM20 antibodies. Nuclei were stained with Hoechst dye. **b**, Validation of siRNAs targeting PARKIN by immunoblotting. The indicated siRNAs were transfected into HCT116 expressing endogenous levels of PARKIN or HeLa cells stably expressing HA-FLAG-PARKIN cells and after 72 h, cell extracts were immunoblotted with anti-PARKIN, anti-HA, or anti-PCNA antibodies. **c**, HCT116 cells stably expressing the indicated candidate PARKIN targets as C-terminal HA-FLAG-tagged fusions were treated with CCCP (10μM) and/or Btz (1μM) for the indicated period of time prior to harvesting proteins in 8 M urea. Extracts were subjected to immunoblotting with the indicated antibodies. **d**, HCT116 cells stably expressing the indicated candidate PARKIN targets as C-terminal HA-FLAG-tagged fusions were transiently transfected with either control siRNA or a validated siRNA targeting PARKIN. After 72 h, cells were treated with CCCP (10μM) and/or Btz (1μM) for the indicated period of time prior to harvesting proteins in 8 M urea. Extracts were subjected to immunoblotting with the indicated antibodies.

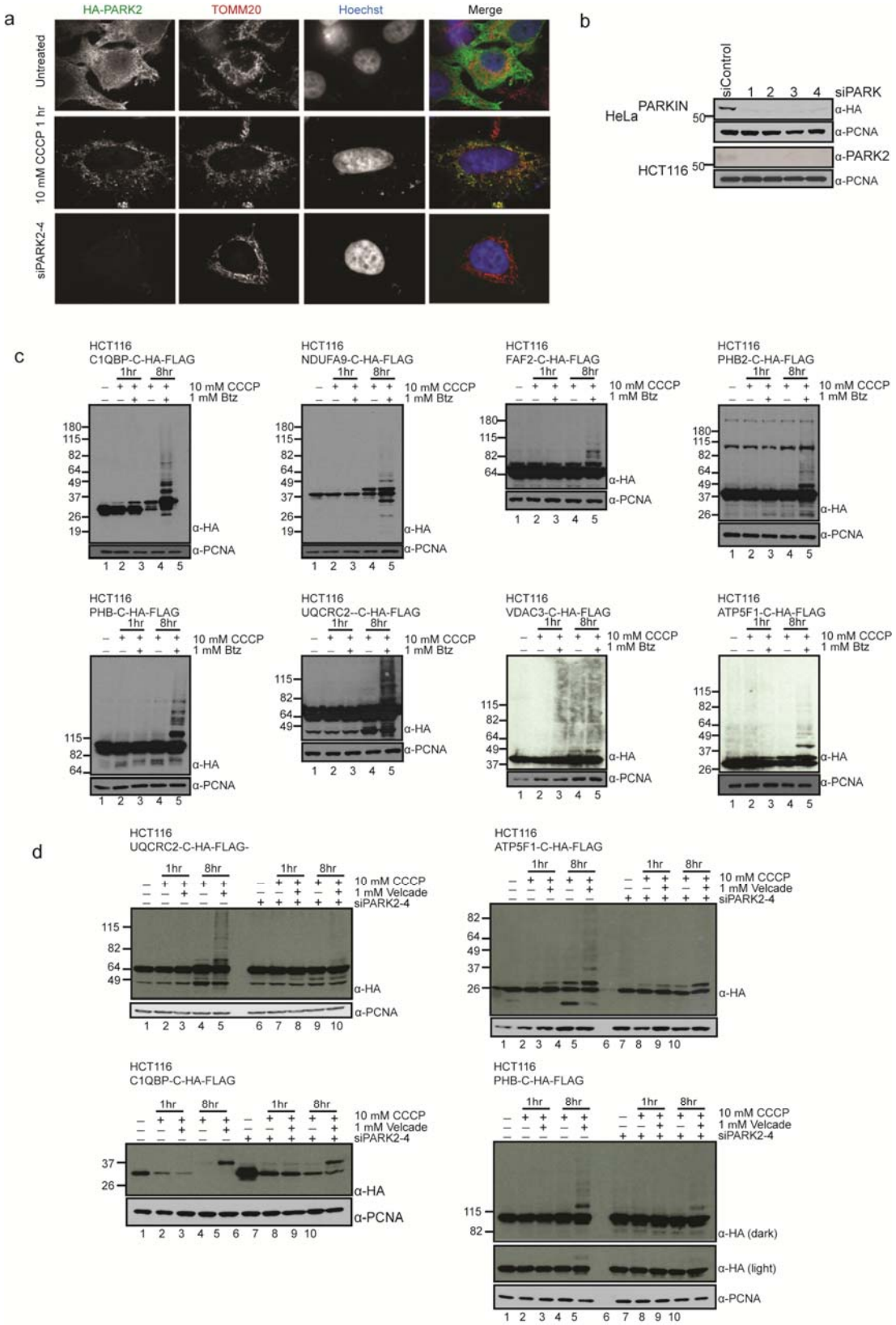


**Figure 2.10 (Continued)**

PARKIN (Figure 2.6d, e). Analysis of the proteomic data with *CompPASS* identifies high-confidence candidate interacting proteins based on the abundance (average assembled peptide spectral matches, APSMs), reproducibility, and frequency of interactors found in numerous parallel AP-MS experiments using both NWD and Z-scores (Sowa et al., 2009). Presumably, PARKIN interactors will vary throughout any time course experiment due to a number of possible reasons, including transient or low affinity enzyme:substrate interactions, degradation of interactors or PARKIN itself by the proteasome after ubiquitylation or autoubiquitylation, respectively, or destruction via mitophagy. Because we expected PARKIN action to by dynamic, we examined 293T N-HA-Flag-PARKIN cells treated with CCCP alone or with the addition of Btz to inhibit proteasomal degradation, or BafA, to inhibit autophagy for 1, 4, or 8 hours in biological duplicate (Figure 2.11). To allow a semi-quantitative assessment of interactions, we

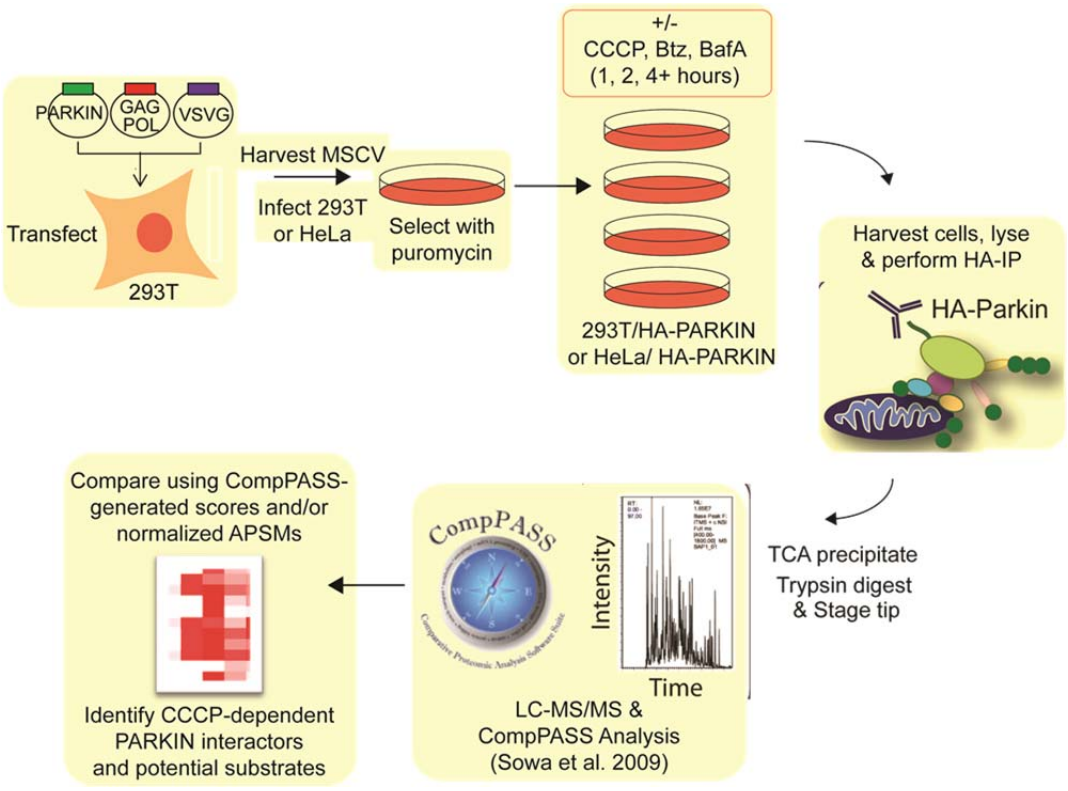


**Figure 2.11 Schematic illustration of the major steps in our interaction proteomics platform.** (see Chapter 5: Materials and Methods).

compared bait-normalized APSMs for proteins that were HCIPs under at least one condition examined unless otherwise noted. PARKIN did not reproducibly interact with any proteins in the absence of depolarization, suggesting that PARKIN requires activation and may need to overcome an autoinhibited state as described previously (Figure 2.12a, Supplementary Table 3) (Chaugule et al., 2011). Strikingly, after one hour of CCCP-induced mitochondrial depolarization, we identified more than 15 mitochondrial proteins that pass our *CompPASS* parameters to be classified as HCIPs (Figure 2.12a, b, Supplementary Table 3).

In response to depolarization, 4 major classes of HCIPs were identified under at least one of the conditions examined: 1) twenty mitochondrial outer membrane proteins involved in fusion-fission cycles and trafficking, metabolism, and protein or small molecule translocation across the MOM, 2) autophagy adaptors, 3) numerous components of the 26 proteasome, and 4) the VCP/p97 AAA+-ATPase implicated in MFN1 turnover. Amongst the mitochondrial proteins identified were known PARKIN substrates, MFN1/2, RHOT1, and VDAC1/2/3; however, we also identified FIS1, RHOT2, and MARCH5, additional proteins involved in control of mitochondrial membrane fusion and organelle trafficking (Figure 2.12a, b, Supplementary Table 3). Marking of these proteins for degradation may be an early step in PARKIN-mediated remodeling of the outer mitochondrial membrane. Additionally, we identified 2 components of the MOM translocase (TOMM70A and TOMM20), which act as receptors and mediators for protein import across the outer mitochondrial membrane, the autophagy adaptor SQSTM/p62, and several proteins involved in metabolism, including HK1/2 (Figure 2.12a, b, Supplementary Table 3). TOMM70A and HK1, as well as multiple subunits of the proteasome, and VCP were identified under all conditions examined whereas other proteins including the candidate autophagy receptors CALCOCO2 and TAX1BP1, and the RAB7 GAP TBC1D15, which is known to interact with FIS1 to promote mitochondrial fission cycles, were primarily detected at either late time points or in response to BafA treatment (Figure 2.12a, b, Supplementary Table 3). CALCOCO2 is a Ca+2 binding protein that functions to remove bacteria from cells via

**Figure 2.12 PARKIN associates with mitochondrial proteins and the proteasome in response to depolarization**. **a**, Heat map of HCIPs (represented by APSMs) for 293T HA–Flag–PARKIN cell lines (left panel) and HeLa HA-Flag-PARKIN cell line (right panel) in response to mitochondrial depolarization, with or without Btz or BafA. Proteins indicated had weighted and normalized *D*-scores ≥ 1.0, *Z*-score ≥ 5, and APSMs ≥ 2 for 293T biological duplicates unless otherwise noted (see Methods). HeLa data is from single experiments and proteins indicated had weighted and normalized *D*-scores ≥ 1.0 unless otherwise noted (see Methods). **b**, Summary of PARKIN-interacting proteins in 293T and HeLa cell lines and integration with diGly sites.

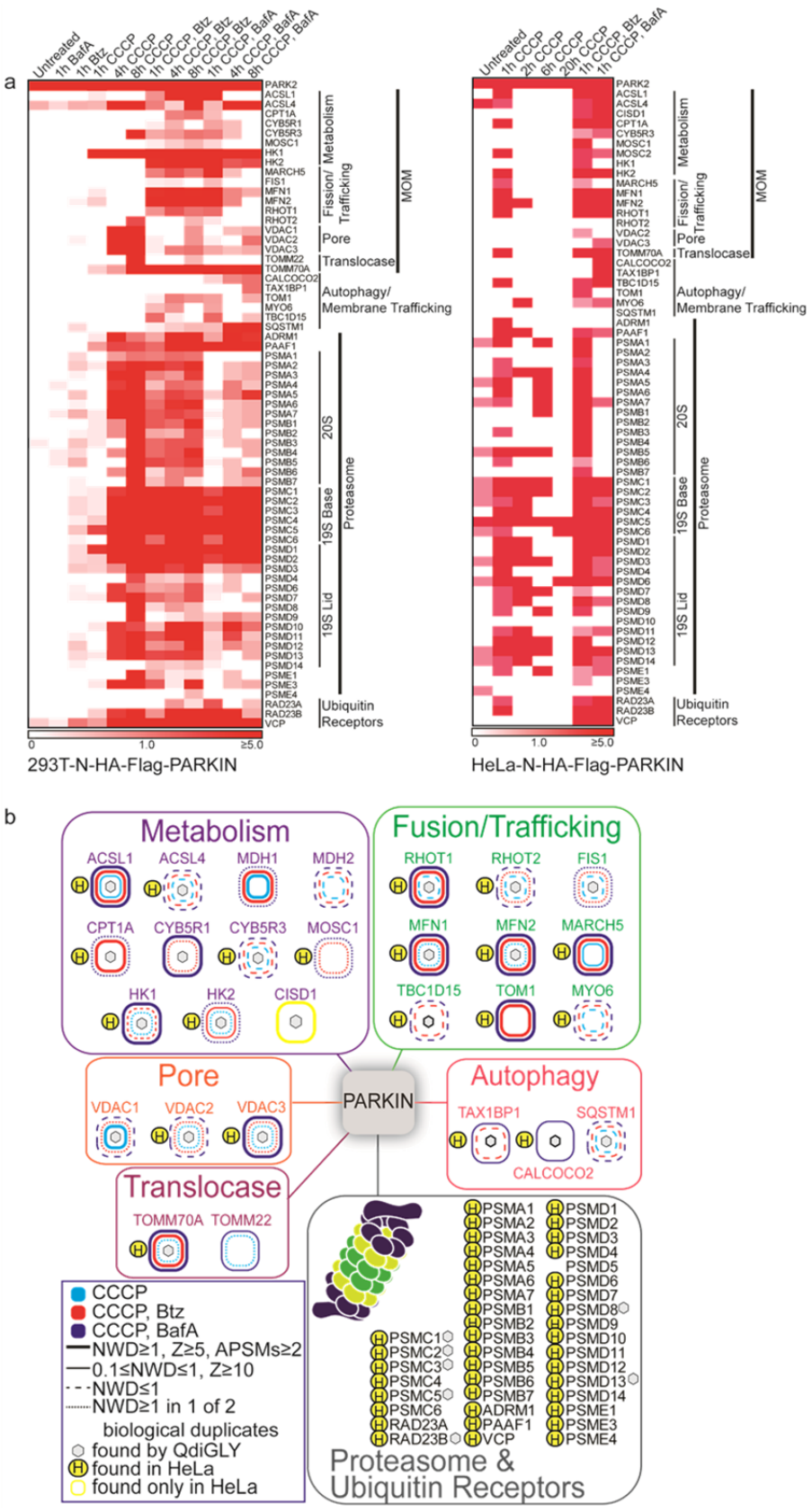


**Figure 2.12 (Continued)**

autophagy by binding to ubiquitin on bacteria and to ATG8 (LC3) on autophagosomes, thereby recruiting ubiquitylated bacteria to the autophagosome. TAX1BP1 is also a ubiquitin binding protein involved in innate immunity that has only recently been linked with autophagy (Newman et al., 2012); however, their copurification with PARKIN after depolarization, but only in the presence of autophagy inhibitor, suggests that they might act as cargo adaptors for mitophagy.

While components of all sub-complexes of the proteasome co-purified with PARKIN after mitochondrial depolarization, proteins comprising the 19S regulatory particle (PSMC and PSMD) were most prominent (Figure 2.12a, b, Supplementary Table 3). Additionally, proteasome regulators, including RAD23, ADRM1, and the proteasome activator subunit PAAF1, appeared as PARKIN interactors after depolarization, suggesting that after activation, PARKIN may translocate to the mitochondria where it ubiquitylates substrates while bringing them in close proximity to the proteasome. In fact, the abundance of several proteins purified in association with PARKIN was reduced at 4 or 8 hours post-depolarization in samples treated with BafA, such as MFN2 and RHOT1/2, consistent with these proteins being targeted to the proteasome (Figure 2.12a, b, Supplementary Table 3).

Numerous proteins identified as PARKIN HCIPs were validated as interactors in HeLa cells stably expressing N-HA-PARKIN treated with CCCP and either Btz or BafA from 1 to 20 hours post CCCP treatment (Figure 2.12a, Supplementary Table 4).. Strikingly, in the absence of Btz, the majority of these interactions were lost starting as early as 2 hours post CCCP treatment. This decrease in association was largely blocked by addition of Btz or BafA (Figure 2.12a, Supplementary Table 4), suggesting a possible role for the proteasome and autophagy in loss of these proteins. Nevertheless, 19 of the 26 mitochondrial and autophagy proteins and 39 of 40 proteasome subunits found in 293T cells were identified in at least one condition examined in HeLa cells (Figure 2.12b). As in 293T cells, the interaction of PARKIN with CALCOCO2 and TAX1BP1 in HeLa cells was only seen in the presence of BafA.

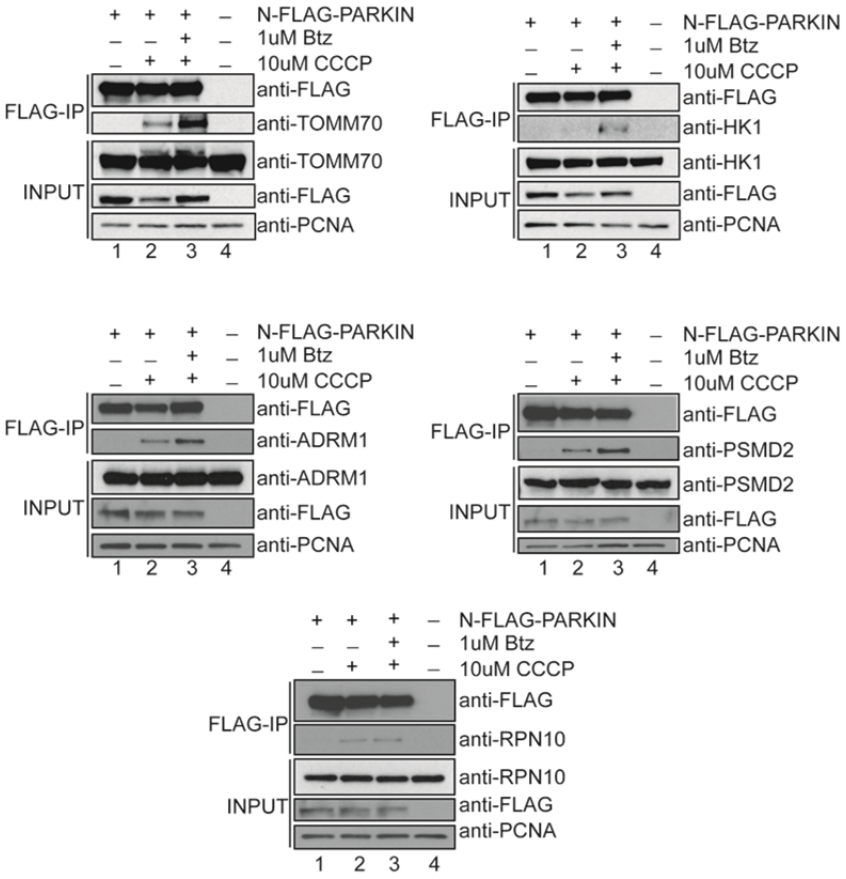


**Figure 2.13 Validation of PARKIN interactors identified via interaction proteomics**. Validation of PARKIN interaction with TOMM70, HK1, and proteasomal subunits ADRM1, RPN10, and PSMD2. Extracts from 293T cells stably expressing HAFLAG-PARKIN with or without treatment with CCCP (10 μM) or CCCP and Btz (Velcade) (1 μM) were immunoprecipitated with anti-FLAG antibodies and immunoblotted with the indicated antibodies. Anti-PCNA was used as a loading control. Experiments were performed by Virginia Guarani-Pereira.

Because antibodies that efficiently immunoprecipitate endogenous PARKIN were not available, we further validated a subset of the depolarization-dependent interactions using a 293T N-HA-Flag-PARKIN stable cell line together with anti-FLAG antibodies. Anti-Flag immunoprecipitation of stably expressed HA-FLAG-PARKIN confirmed depolarization-dependent interaction between PARKIN and HK1, TOMM70, and the proteasome subunits ADRM1, RPN10, and PSMD2 (Figure 2.13).

Remarkably, of the mitochondrial and autophagy proteins identified by AP-MS, all but 2 (MARCH5 and TBC1D15) were also identified as candidate PARKIN substrates by QdiGly proteomics (Figure 2.9, Figure 2.12b, Supplementary Table 2). Moreover, multiple subunits of

the regulatory particle of the proteasome, ubiquitin receptors (RAD23B), and VCP were found to be ubiquitylated in a PARKIN-dependent manner by QdiGly proteomics (Figure 2.9b, Figure 2.12b, Supplementary Table 2). Together with the QdiGly proteomics, we have constructed a PARKIN interactome and PARKIN-modified proteome providing a vast resource to the field and identifying numerous candidates for further characterization.

### 2.2.4 Interaction Proteomics: effects of PARKIN mutations

Because PARKIN is so clearly regulated upon mitochondrial depolarization, we questioned whether PARKIN mutations would affect the interaction landscape. To examine how structural and functional elements within PARKIN contribute to interaction with its binding partners and the proteasome, we performed AP-MS experiments with 4 mutants: 1)ΔUBL, in which the N-terminal UBL domain (residues 1-80) implicated in auto-inhibition is deleted (Chaugule et al., 2011), 2) K27R, K48R, which replaces two sites of regulated ubiquitylation identified by QdiGly profiling, 3) S65A or S65E, which blocks PINK1-dependent phosphorylation in a process that has been implicated in PARKIN activation *in vitro*, (Kondapalli et al., 2012) and 4) C431S, wherein the active site cysteine in the second RING domain (reported to be required for ubiquitin thioester formation (Wenzel et al., 2011) is replaced by serine, thereby rendering the protein inactive as an E3 (Figure 2.14a). This mutation is reminiscent of a PD patient mutation, C431F, which fails to localize to mitochondria in response to depolarization (Cookson et al., 2003).

Interestingly, mutation of cysteine 431 resulted in loss of regulatable PARKIN activation; the mutant neither translocated to the mitochondria upon CCCP treatment nor was able to promote ubiquitination of MFN2 in response to mitochondrial depolarization (Figure 2.14b, c Figure 2.15a, Supplementary Table 3). We were particularly interested in mutants in the ubiquitin-like domain of PARKIN due to recent reports implicating the UBL in autoinhibition, specifically S65, phosphorylation of which was reported to be required for activation of PARKIN

**Figure 2.14 Functional properties and interaction partners of PARKIN mutants**. **a**, Summary of functional experiments on selected PARKIN mutant proteins. ΔUBL-PARKIN, residues 81-465. **b**, MFN2 ubiquitylation by selected PARKIN mutants in 293T cells. *, PARKIN breakdown products. **c,** Heatmaps for a series of interacting proteins with a WDN-score ≥ 1.0, Z-score ≥ 5, APSMs ≥ 2, and found in biological duplicates for various PARKIN mutants, unless otherwise noted (see Methods).

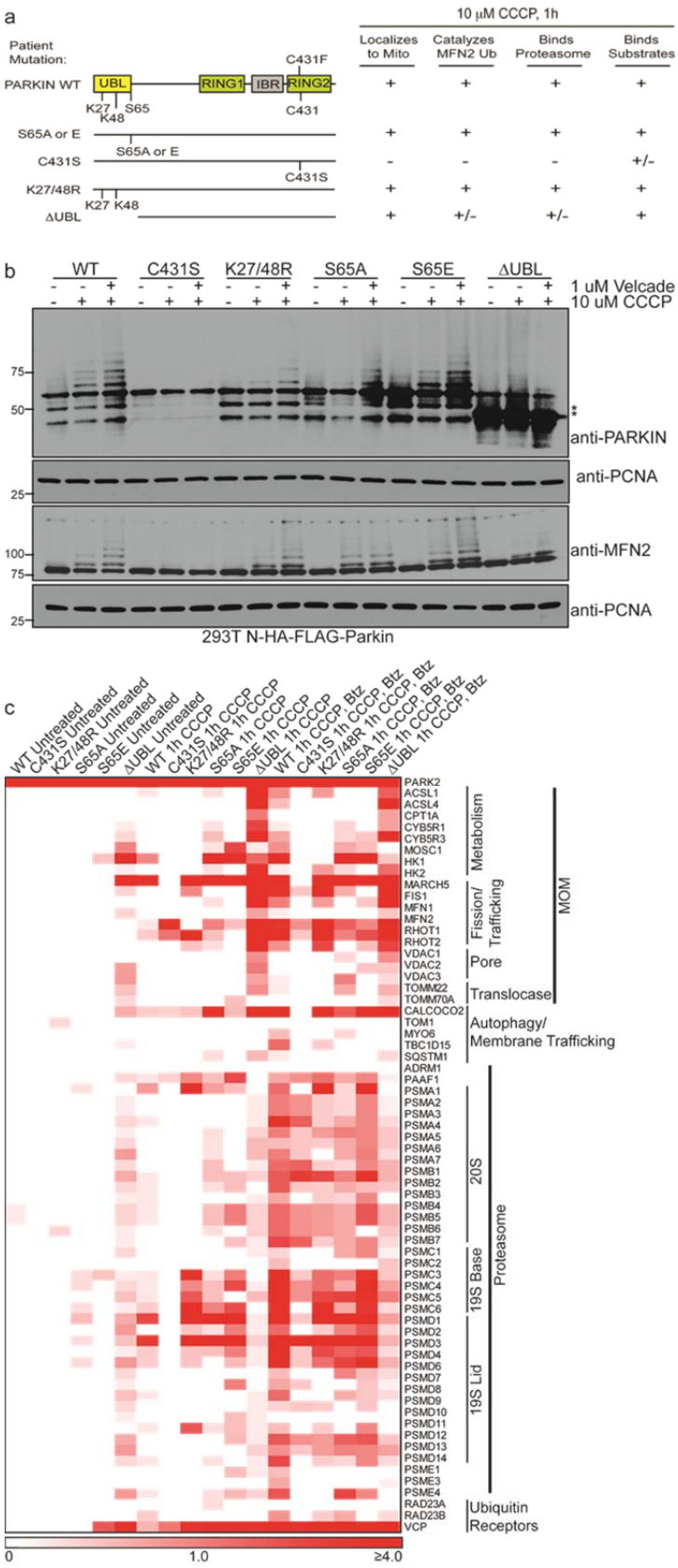


**Figure 2.14 (Continued)**

(Chaugule et al., 2011; Kondapalli et al., 2012). Additionally, the sites we identified via QdiGly, K27 and K48, lie in the UBL of PARKIN and are ubiquitylated in a depolarization-dependent manner. Unlike C431S, we found that ΔUBL, S65A/E, and K27/48R mutants maintained their ability to localize to mitochondria and to promote ubiquitination of MFN2 in response to depolarization (Figure 2.14b, c Figure 2.15a).

Our AP-MS results are generally consistent with these results in that the ΔUBL, S65A/E, and K27/48R mutants retained strong interactions with mitochondrial proteins and the proteasome upon depolarization in the presence of Btz (Figure 2.14c, Supplementary Table 3). Interestingly, the ΔUBL mutant more efficiently captured mitochondrial proteins in response to CCCP when compared with wild-type (WT) PARKIN, consistent with this mutant displaying enhanced activity, possibly as a result of removal of auto-inhibition through this domain. Conversely, its interaction with the proteasome was decreased relative to WT PARKIN (Figure 2.14c, Supplementary Table 3). Unexpectedly, we found that all of the PARKIN UBL mutants were still regulated, showing translocation to the mitochondria only upon depolarization and associating with the same proteins identified in the WT AP-MS experiments only after mitochondrial depolarization (Figure 2.14b, c, Supplementary Table 3). Though we cannot discount possible autoinhibition by the ΔUBL, it does not appear to be wholly essential for regulation of substrate interaction or depolarization-mediated translocation. Thus phosphorylation of S65 by PINK1 does not appear to be absolutely required for these aspects of PARKIN function *in vivo*, although we cannot rule out a kinetic effect of these mutations. However, consistent with the absence of mitochondrial localization of the C431S mutant, depolarization resulted in strong reduction in capture of mitochondrial proteins relative to WT PARKIN. Thus, the catalytic activity of PARKIN may be required for activation via depolarization and PINK1.

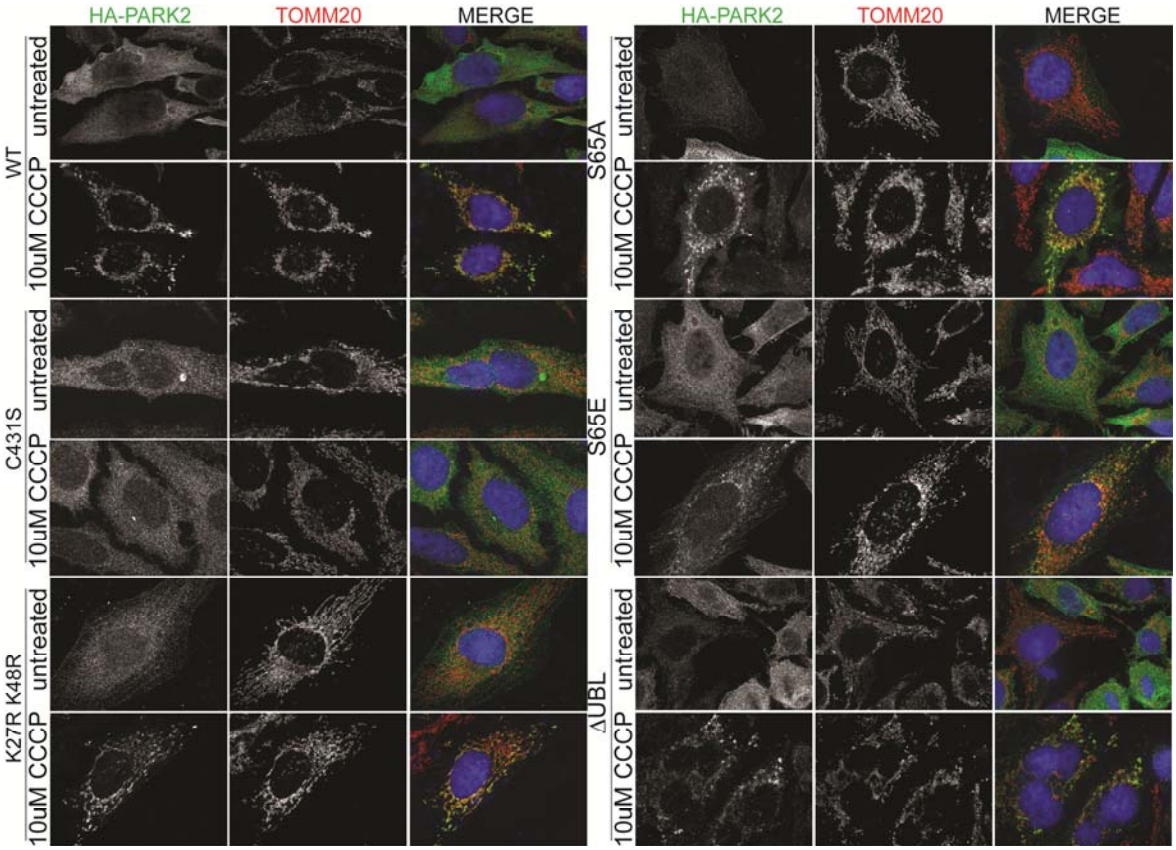


| Cell Line | Construct | Condition | % of Parkin Colocalization with TOMM20 |
|---|---|---|---|
| HeLa | N-HA-PARK2 WT | untreated | 38.74 |
| | | 1hrCBtz | 85.19 |
| HeLa | N-HA-PARK2 K27RK48R | untreated | 37.75 |
| | | 1hrCBtz | 90.88 |
| HeLa | N-HA-PARK2 C431S | untreated | 54.97 |
| | | 1hrCBtz | 31.86 |
| HeLa | N-HA-PARK2 S65A | untreated | 10.35 |
| | | 1hrCBtz | 96.93 |
| HeLa | N-HA-PARK2 S65E | untreated | 23.6 |
| | | 1hrCBtz | 76.38 |
| HeLa | N-HA-PARK2 dUBL | untreated | 28.61 |
| | | 1hrCBtz | 74.27 |

**Figure 2.15 Localization of PARKIN and selected mutants to mitochondria in response to depolarization.** HeLa cells stably expressing wild-type PARKIN or the indicated PARKIN mutants as HA-FLAG fusion proteins were treated with CCCP (10 μM, 1h), cells were fixed, stained with anti-HA (green) and anti-TOMM20 (red), and nuclei stained with Hoechst 33342. Images of representative cells were collected using a Nikon confocal microscope and percent colocalization calculated. See Methods and Supplementary Table 6 for details of quantification. Percent colocalization determined by Malavika Raman.

### 2.2.5 Analysis of PARKIN target site conservation and structural topology

Our data suggest that PARKIN interacts with and promotes the site-specific ubiquitylation of numerous mitochondrial and cytoplasmic proteins; therefore, in order to gain a

better understanding of the relationship between PARKIN and its interacting partners and substrates, we sought to examine PARKIN ubiquitylation targets in the context of their conservation and *in vivo* organization. We explored the spatial relationship between protein localization, structure, and conservation for 90 Class 1 sites on 36 candidate PARKIN substrates (Figure 2.16a-e, Supplementary Table 5). Overall, we found extensive conservation of ubiquitylated lysine resides in PARKIN targets for the 29 proteins displaying clear orthologs. In mouse (Mus *musculus*), 90% of sites were conserved, compared to 78% in zebrafish (Danio *rerio*), and 51% in Drosophila *melanogaster*, one of the lowest eukaryotes known to contain an active PARKIN-PINK1 pathway. Additionally, 38% of sites were conserved in all three species and in 22 out of the 36 proteins examined, at least one site was conserved from human to D. *melanogaster* (Figure 2.16a-e).

We then examined the protein domains containing ubiquitylation sites to determine whether there was any pattern to PARKIN's substrate targeting. We found that ubiquitylation sites primarily occurred in globular domains and were not restricted to any particular structural feature; sites were observed on all three major classes of structural elements (α-helices, β-sheets, and loops). Using MOTIFX, we analyzed the sequence motifs of all Class 1 candidate PARKIN targets for a consistent pattern; however, we found no conserved sequence motifs, suggesting that PARKIN specificity may be driven by its activation and recruitment to the mitochondria and substrates rather than a particular target sequence within substrates.

We therefore wanted to better understand the relationship between PARKIN-mediated sites of ubiquitylation and the physical structures of the mitochondrial and cytoplasmic proteins

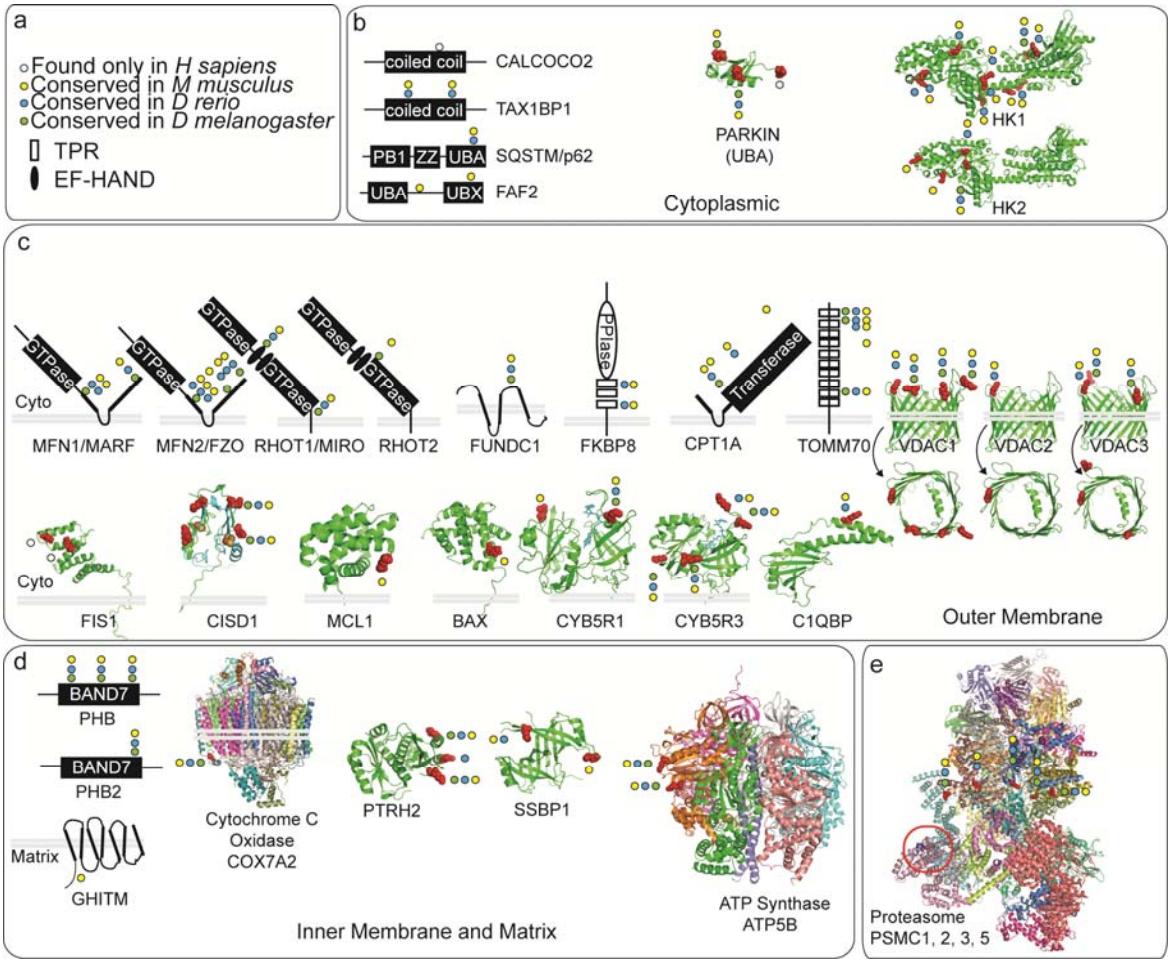


**Figure 2.16 Structural anatomy and conservation of PARKIN-dependent diGly sites.** Structures or domain schematics are shown for Class 1 depolarization and PARKIN-dependent diGly sites (PDB codes, Supplementary Table 5). **a**, Legend for color-coded circles that indicate the conservation of Lys at homologous positions in *M. musculus*, *D. rerio* and *D. melanogaster* (Supplementary Table 5). For structures, regulated sites are shown in red space-filled models. **b**, Cytoplasmic proteins. **c**, MOM proteins. **d**, MIM and matrix proteins. **e**, Proteasome, RPN10, red circle.

targeted. To do so, we mapped the positions of ubiquitylation onto existing 3-D structures of proteins in the Protein Database (PDB) allowing us to examine the sites as they appear on substrate proteins. Of the 17 MOM targets whose structures or membrane orientations are defined, all identified ubiquitylation sites were presented on the cytoplasmic surface (Figure 2.16c), consistent with the idea that PARKIN re-sculpts the MOM proteome after translocation from the cytoplasm. Fifty-nine percent of Class 1 and 2 targets had one or two sites of ubiquitylation while 41% of targets had 3-15 sites that were PARKIN-dependent based on Tier 2

analysis (Figure 2.17a). Of the 8 Class 1 and Class 2 sites identified in MFN1, all but 2 are located in helical motifs flanking the 2 C-terminal membrane-spanning regions, suggesting localized ubiquitylation (Figure 2.9b, Figure 2.16c). We detected 14 Class 1 and 2 sites in HK1, but unlike MFN1, these sites were comparatively delocalized across both globular domains in HK1 (Figure 2.16b). Similarly, TOMM70 was decorated extensively over its 10 cytoplasmic TPR motifs (Figure 2.9b, Figure 2.16c). VDAC ubiquitylation occurred at multiple sites on the cytoplasmic lip of its central transmembrane pore, suggesting a potential regulatory effect on small-molecule transport upon depolarization in a PARKIN-dependent manner (Figure 2.16c).

In addition to the numerous mitochondrial outer membrane proteins that we identified, we also observed modifications on mitochondrial inner membrane and matrix proteins (Figure 2.16d). It is possible that these proteins are trapped outside the mitochondria prior to import. However, in some cases (e.g. components of ATP synthase), the extent of ubiquitylation increased substantially at longer time points after depolarization (Supplementary Table 2), potentially reflecting disruption of mitochondrial structure allowing the ubiquitylation machinery access to this compartment. Additionally, the diGly sites we identified in each of the three

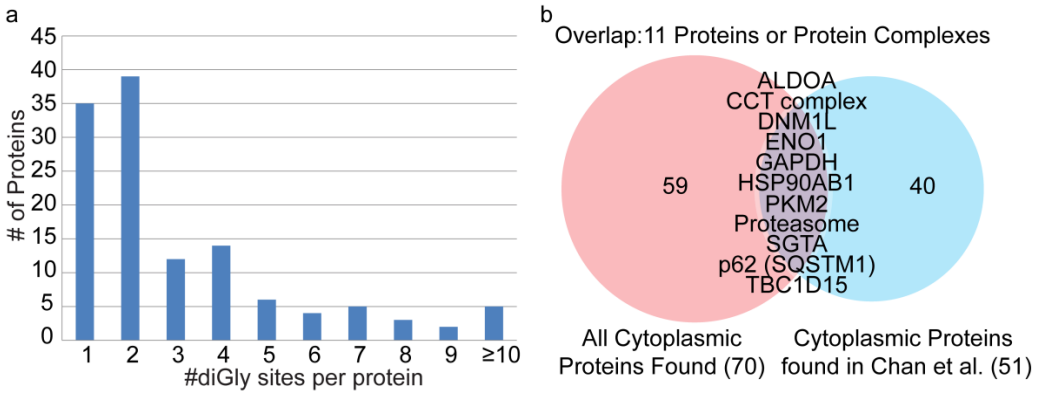


**Figure 2.17 Characteristics of candidate PARKIN targets. a,** Distribution of the number of Class 1 and 2 ubiquitylation sites identified across all Class 1 and 2 targets. **b**, Comparison between cytoplasmic proteins identified as PARKIN targets (Class 1 and 2) in this study, and proteins whose abundance accumulated in mitochondria as determined by SILAC-based proteomics (Chan et al., 2011).

ATPase subunits of the regulatory particle of the proteasome (PSMC1/RPT2, PSMC2/RPT1, and PSMC3/RPT5) occur within extended helices that form coiled-coils with neighboring RPT subunits and are clustered together on a surface of the regulatory particle that is proximal to the RPN10 subunit (Figure 2.9b, Figure 2.16e). Previous studies have reported an interaction between the C-terminal UIM domain of RPN10 and the UBL domain of PARKIN (Sakata et al., 2003). Thus, our finding that association of PARKIN with the proteasome is greatly stimulated by mitochondrial depolarization suggests that PSMC ubiquitylation is likely linked to assembly of PARKIN with the proteasome, as association of PARKIN with the RPN10 subunit is likely to favor ubiquitylation of nearby PSMC subunits (Figure 2.16e).

In order to place candidate PARKIN-dependent ubiquitination targets into a structural and functional framework, we have created an interactive resource that integrates dynamic ubiquitylation data with available structural information (Figure 2.18a, b and METHODS). This tool can be used to visualize sites of ubiquitination in proteins with known structures as well as examine the magnitudes of induction of modifications (log2 (H:L) ratio) across the 73 experiments we performed. These data suggests that PARKIN activation leads to widespread ubiquitylation of a dozens of proteins, including a cohort of proteins associated with mitochondria. By examining the sites as they appear on substrate proteins, we are able to place targets into a structural and contextual framework and form a comprehensive view of the entire pathway.

### 2.2.6 Development of PARKIN *in vitro* assay and substrate validation

To facilitate both mechanistic examination of the PARKIN enzymatic process as well as validation of substrates identified via QdiGly proteomics, we developed a system allowing us to recapitulate PARKIN activity *in vitro*. Preliminary experiments showed extensive post-translational modifications on PARKIN after mitochondrial depolarization with CCCP which were sensitive to both the deubiquitylating enzyme, USP2, and λ phosphatase treatment (Figure

**Figure 2.18 Web-tool for interrogation and structural analysis of candidate PARKIN targets. a**, Web tool. In order to aid in the analysis of the PARKIN-dependent ubiquitin modified proteome, a web-based tool was developed for retrieval, plotting of data for individual sites across multiple experiments, and visualization of structures for candidate PARKIN targets. On the front page (panel a), you can enter 3 analysis areas: structural analysis, plotting of ubiquitylation sites across experiments, and access to tables and retrieval of data. Panel **b**, shows an example of a plot of log2 SILAC ratios for a MFN2 site across several experiments using Site-Surveyor. For structural analysis, individual experiments can be selected from a drop-down menu, which then populates a table collecting PDB identifiers for proteins having structures in the PDB. Individual PDB identifiers are linked to a page, which collects relevant quantitative proteomics data (principally the log2 ratio for identified and quantified peptides and the peptide sequences), and displays the structure in a new window, allowing 3-D rotation and visualization (Panel **c**). Lysines that were identified as ubiquitylated are shown in space-filling models and are color-coded based on the log2 ratio for regulated sites (sites showing an increased diGly ratio in red. Sites that are identified but not quantified are shown in white. The web tool can be accessed at http://harper.hms.harvard.edu. Web tool designed and constructed by Mathew Sowa.

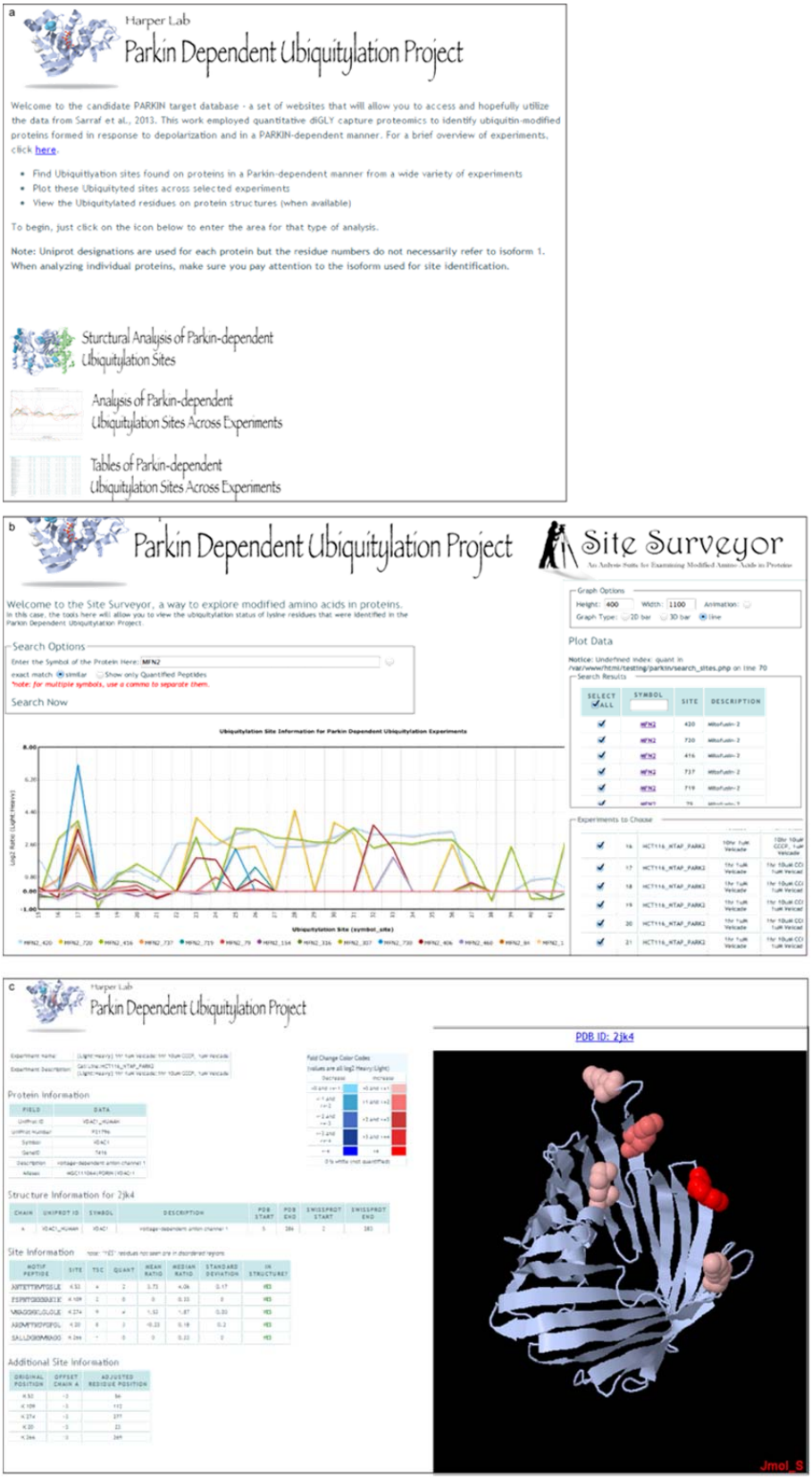


**Figure 2.18 (Continued)**

2.19a). Therefore, we reasoned that because PARKIN activity requires activation by PINK1 and/or another unidentified enzyme, which were presumably absent in bacterial or insect cell preps as these produced highly insoluble protein with little activity. Therefore, we isolated HA-Flag-PARKIN WT or catalytically defective HA-Flag-PARKIN C431S from 293T cells either

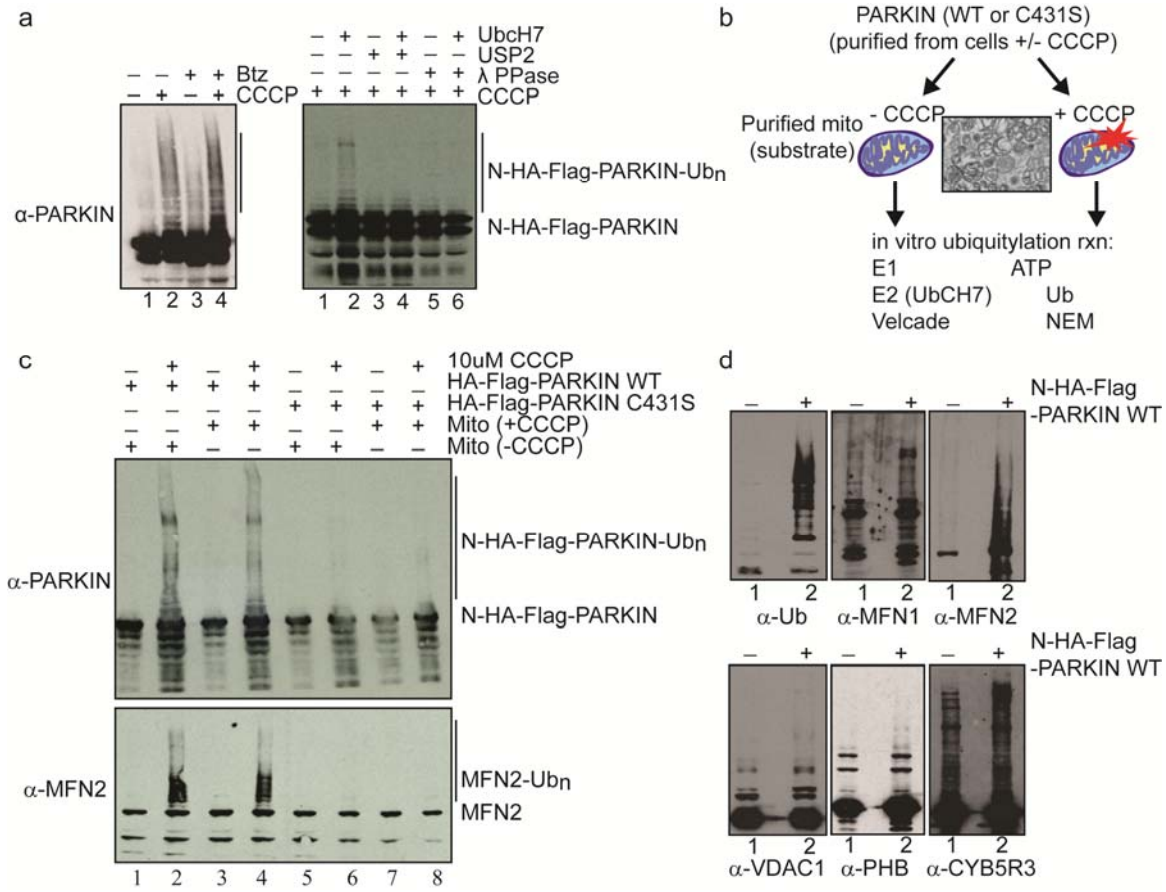


**Figure 2.19 Development of an *in vitro* system for PARKIN validation. a**, N-HA-Flag-PARKIN purified from 293T cells after 1 h 10μM CCCP and/or 1μM Btz (left panel). N-HA-Flag-PARKIN purified from 293T cells (1 h 10μM CCCP) treated with USP2 or λ phosphatase followed by *in vitro* ubiquitylation reaction (right panel). **b**, Scheme of *in vitro* approach. Inset photograph contains an example of purified mitochondria verified by electron microscopy. **c**, *In vitro* ubiquitylation reaction using either PARKIN WT or C431S purified from 293T cells (1h 10μM CCCP) and purified mitochondria as substrate. Mitochondrial protein MFN2 is used as a readout of PARKIN activity on the mitochondria (bottom panel). PARKIN autoubiquitylation is shown in the top panel. **d**, *In vitro* ubiquitylation reactions were performed as described above and blotted for mitochondrial candidate PARKIN targets.

untreated or treated with CCCP for 1 hour. In parallel, we isolated intact mitochondria from either untreated or depolarized HeLa cells which do not contain endogenous Parkin and further removed any existing ubiquitin conjugates using treatment with USP2, followed by NEM treatment to block USP2 activity (Figure 2.19b). We then performed *in vitro* ubiquitylation reactions using this purified mitochondria as substrate and found that only HA-Flag-PARKIN purified from depolarized cells (Figure 2.19c, lane 2, 4), but not from untreated cells (lanes 1, 3) was capable of ubiquitylating MFN2 on mitochondria. Interestingly, MFN2 ubiquitylation occurred regardless of whether the mitochondria itself was purified from depolarized or untreated cells (Figure 2.19c, lanes 2, 4). As expected, HA-Flag-PARKIN C431S did not promote MFN2 ubiquitylation (Figure 2.19c, lanes 5-8). Compared to previously published work featuring bacterial recombinant PARKIN protein, our method of purification post-CCCP treatment appears to result in more robust and stronger Parkin activity. Using this system, we can detect increased ubiquitylation of QdiGly-identified PARKIN substrates *in vitro* including MFN1, MFN2, VDAC1, CYB5R3, PHB, and PARKIN via immunoblotting with antibodies against the endogenous proteins. Western blot for total ubiquitin also shows increased ubiquitylation on mitochondria which have been exposed to CCCP-treated PARKIN WT (Figure 2.19d).

After careful analysis of AP-MS data obtained from PARKIN WT and C431S cell lines, we realized that there was a possibility that WT PARKIN purified from depolarized cells had the potential to co-purify with ubiquitylated MFN2, thus there was the possibility of obtaining a false positive; though, due to the extent of ubiquitylation seen on MFN2, unlikely. To address this issue, we set up a number of experiments which will allow us to definitively confirm our *in vitro* ubiquitylation result. The first approach is based on the *in vitro* assay described above. We have developed a parallel approach that seeks to quantitatively examine PARKIN-dependent MOM ubiquitylation *in vitro* via a PARKIN-dependent “heavy-label transfer” approach (Figure 2.20a). The key to this method is the use of uniformly isotopically heavy-labeled ubiquitin in the *in vitro* reaction thus allowing us to distinguish between it and any pre-existing “light” ubiquitin. If

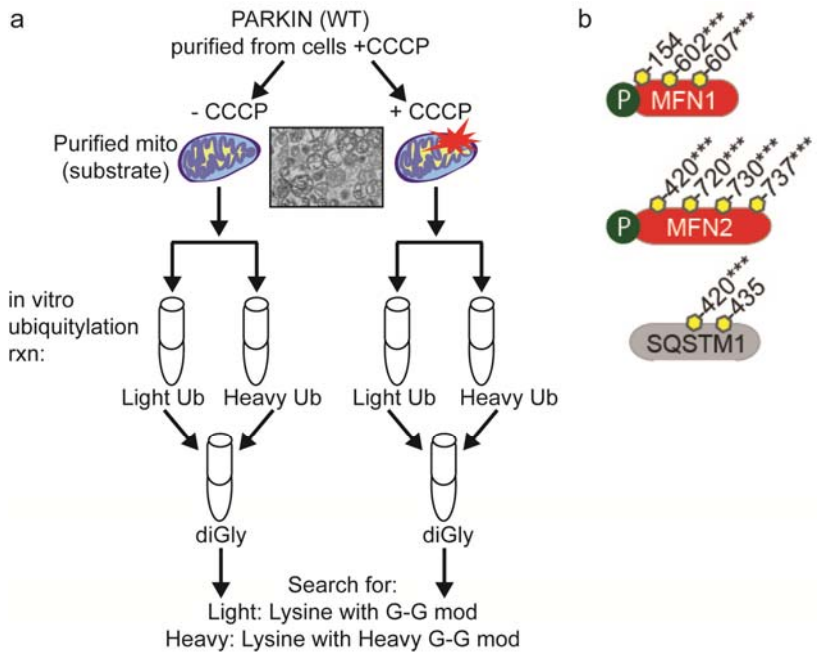


**Figure 2.20 Quantitative *in vitro* system for PARKIN target validation. a**, Scheme for *in vitro* system utilizing heavy-labeled ubiquitin to "mark" *in vitro* PARKIN-mediated ubiquitylation events. **b**, Heavy-label ubiquitin transfer sites identified and quantified on MFN1, MFN2, and SQSTM1. *** sites regulated *in vivo*.

successful, the *in vitro* ubiquitylation reaction produces a diGly tag on PARKIN substrates with a 6 Da increase in mass relative to any pre-existing ubiquitin modifications on the mitochondria, thus allowing *in vitro* PARKIN-dependent events to be identified by MS. We have performed a pilot experiment using this method allowing us to quantitatively examine PARKIN-dependent MOM ubiquitylation *in vitro* via this PARKIN-dependent "heavy-label transfer" approach. In this preliminary experiment, we identified 3, 4 and 2 heavy-label transfer sites for MFN1, MFN2, and SQSTM1, respectively (Figure 2.20b). Seven of these sites were found to increase in abundance in at least one *in vivo* diGly IP experiment. Recently, another group published a similar assay, thus confirming the validity of our approach in demonstrating activation of PARKIN's enzymatic activity toward mitochondria (Lazarou et al., 2013). However, our approach further demonstrates a method to quantitatively measure this activity on intact purified mitochondria *in vitro*, which will allow extensive future investigation of PARKIN targets and

activity, especially in regards to how these are affected by mutations found in Parkinson's disease.

In order to improve the efficiency of the *in vitro* reaction to make it useful for validation of PARKIN targets found via QdiGly proteomics, our second approach employs the ongoing development of a variety of new reagents to optimize the assay. To avoid the need to purify activated PARKIN from mammalian cells, we are expressing full length (FL), ΔUBL, or C431S PARKIN constructs together with mammalian PINK1 in Sf9 insect cells. Purified PARKIN and PINK1 will then be mixed with purified mitochondria in an *in vitro* ubiquitylation reaction will can then be assayed by immunoblotting and mass spectrometry. These approaches are allowing us to simultaneously develop an important *in vitro* system for studying PARKIN function while providing a means by which to validate targets of PARKIN and to demonstrate that they are direct.

### 2.2.7 PARKIN is post-translationally modified in response to mitochondrial depolarization

Reports in recent years have suggested that under normal conditions, PARKIN exists in an autoinhibited state in which the N-terminal UBL domain binds a ubiquitin/UBL binding site in the C-terminal portion of the protein thus both keeping the protein closed and preventing binding to ubiquitin (Chaugule et al., 2011). Upon mitochondrial damage, PARKIN activation occurs, requiring phosphorylation by PINK1, potentially on multiple sites; activity also appears to require the active site Cys of PARKIN. This supports the possibility of a multi-step mechanism of activation in which initial PINK1-dependent phosphorylation events are followed by PARKIN auto-ubiquitylation, both of which might be required for activation of maintenance of an "open" state. As PINK1 is known to be required for PARKIN activation, much effort has been devoted to identification of PINK1 phosphorylation sites on PARKIN; however, confirmation of direct phosphorylation has been difficult and many of the reports remain unsubstantiated (Kim et al., 2008b; Kondapalli et al., 2012; Lazarou et al., 2013; Sha et al., 2010; Shiba et al., 2009; Um et

al., 2009). In the last year, new data has suggested that phosphorylation of S65 in the PARKIN UBL domain can promote ubiquitin-transfer by PARKIN *in vitro* (Kondapalli et al., 2012). However, we have found that this residue is not essential for MFN2 ubiquitylation *in vivo*, PARKIN translocation to the mitochondria, or for interaction with substrates, indicating involvement of potential additional PINK1-dependent events (Figure 2.14b, c, Figure 2.15). We have observed USP2- and λ-phosphatase-sensitive CCCP-induced modification on PARKIN purified from 293T cells (Figure 2.19a). Therefore, we re-examined our AP-MS data utilizing search conditions optimized for identification of phosphorylation modifications. We identified additional phosphorylation and ubiquitylation sites in PARKIN, many of which lie outside of the UBL domain and may contribute to activation (Figure 2.21, Supplementary Table 7). In total, we found 24 phosphorylation sites occurring on serines, threonines, and tyrosine residues. Not all of the sites appear to be depolarization-dependent; however, we are in the process of testing whether any of these sites are necessary for PARKIN activation *in vivo*. Additionally, we found

that depolarization is not sufficient to induce robust association of PARKIN C431S with the cohort of MOM proteins normally bound by PARKIN under these conditions (Figure 2.14c). We believe PARKIN activation may involve a two-step mechanism in which PINK1 phosphorylation promotes partial loss of auto-inhibition via the UBL domain or possibly at

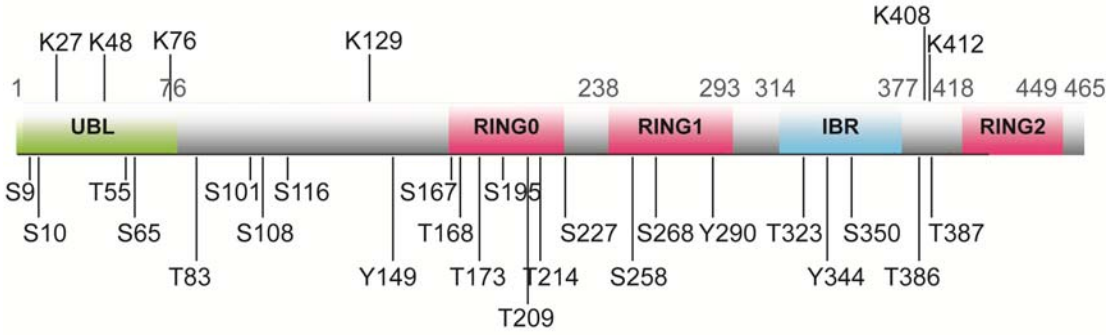


**Figure 2.21 Post-translational modification of PARKIN.** Phosphorylation and ubiquitylation sites identified on PARKIN via AP-MS.

additional sites outside this domain, and subsequent auto-ubiquitylation completes the process. This proposed model will be examined both *in vivo* and using the *in vitro* system through the analysis of phosphorylation and ubiquitylation site mutants.

### 2.2.8 Determining the role of candidate PARKIN targets in initiation or progression of mitophagy

The steps that occur downstream of PINK1 and PARKIN activation remain unknown. How PARKIN gets to the mitochondria and how ubiquitylation of mitochondrial outer membrane or other proteins leads to mitophagy is unclear. To systematically test proteins identified in our studies, we have begun RNAi-mediated depletion and high-throughput microscopic screening to determine whether a subset of the proteins identified as PARKIN interactors or targets are important in these processes (Figure 2.22a). First, we created a clonal HeLa-N-HA-Flag-PARKIN cell line to minimize variability throughout the screening process (Figure 2.22b). To determine if any of the proteins of interest were essential for PARKIN translocation after mitochondrial depolarization, we treated cells with siRNA for 72 hours prior to treatment with CCCP for 2 hours, after which cells were stained and imaged. To measure PARKIN translocation, we are working with Tiao Xie (IDAC) to create a custom script that measures the percent of PARKIN signal which colocalizes with the mitochondria. Though screening and analysis are still ongoing, preliminary analyses have allowed us to classify genes based on the percent of PARKIN colocalization compared to siControl. Proteins whose RNAi-mediated depletion results in 75% or greater loss of PARKIN translocation are termed Class 1 and those proteins whose depletion results in 50% or greater loss of translocation are Class 2 proteins (Figure 2.22c, e, Supplementary Table 8). Within each Class, we further ranked genes based on the number of siRNAs out of four giving a positive result for each gene. Amongst the proteins we identified at the most stringent cut-off are the hexokinases and IMMT, a protein known to mediate outer and inner membrane dynamics.

We also want to determine whether one or more PARKIN interactors or substrates is required for the initiation or progression of mitophagy. To do so, we are using a very similar approach to that described above employing RNAi-mediated depletion and high-throughput microscopic screening (Figure 2.22a). This second portion of our screen employs siRNA-mediated depletion of candidate mitophagy regulators in HeLa-N-HA-FLAG-PARKIN cells for 48 hours prior to treatment with CCCP for 24 hours, followed by fixation and imaging. We first looked at the overall changes in the average mitochondrial area per cell in comparison to control cells (Figure 2.22d). Depletion of the majority of genes did not have a drastic effect on mitochondrial area, which will allow us focus on those with greater changes for follow-up studies, for example those with at least a 1.25-fold increase. If a gene is necessary in the progression of mitophagy, we would expect that RNAi-mediated knockdown would result an increase in total mitochondrial area compared to siPINK1- or siPARK2-treated cells. These proteins are most likely not targeted for degradation by PARKIN, but instead may be modified with ubiquitin for another purpose, such as signaling or regulation. To identify these genes, we compared mean mitochondrial mass per cell to that observed in cells treated with either siRNA targeting PINK1 or PARKIN. Because siPINK1 consistently evoked a more drastic phenotype than siPARKIN, we set the threshold for Class 1 genes at this level. These are considered the highest confidence targets in terms of a potential effect on progression of mitophagy. Class 2 genes passed the threshold set by cells treated with siPARKIN. Within each class, genes were further ranked based on how many siRNAs of out four provided a positive result (Figure 2.22e, Supplementary Table 8). Based on these classifications, Class 1 genes for which >2 shRNAs reduce mitophagy will be primary targets for future studies and fully characterized.

In contrast, it is also possible that depletion of certain PARKIN substrates might result in increased levels of mitophagy thus resulting in decreased total mitochondrial area compared to siControl-treated cells.. Such a result might indicate the loss of an inhibitor of mitophagy – a protein likely to be targeted for degradation in a PARKIN-dependent manner. To determine

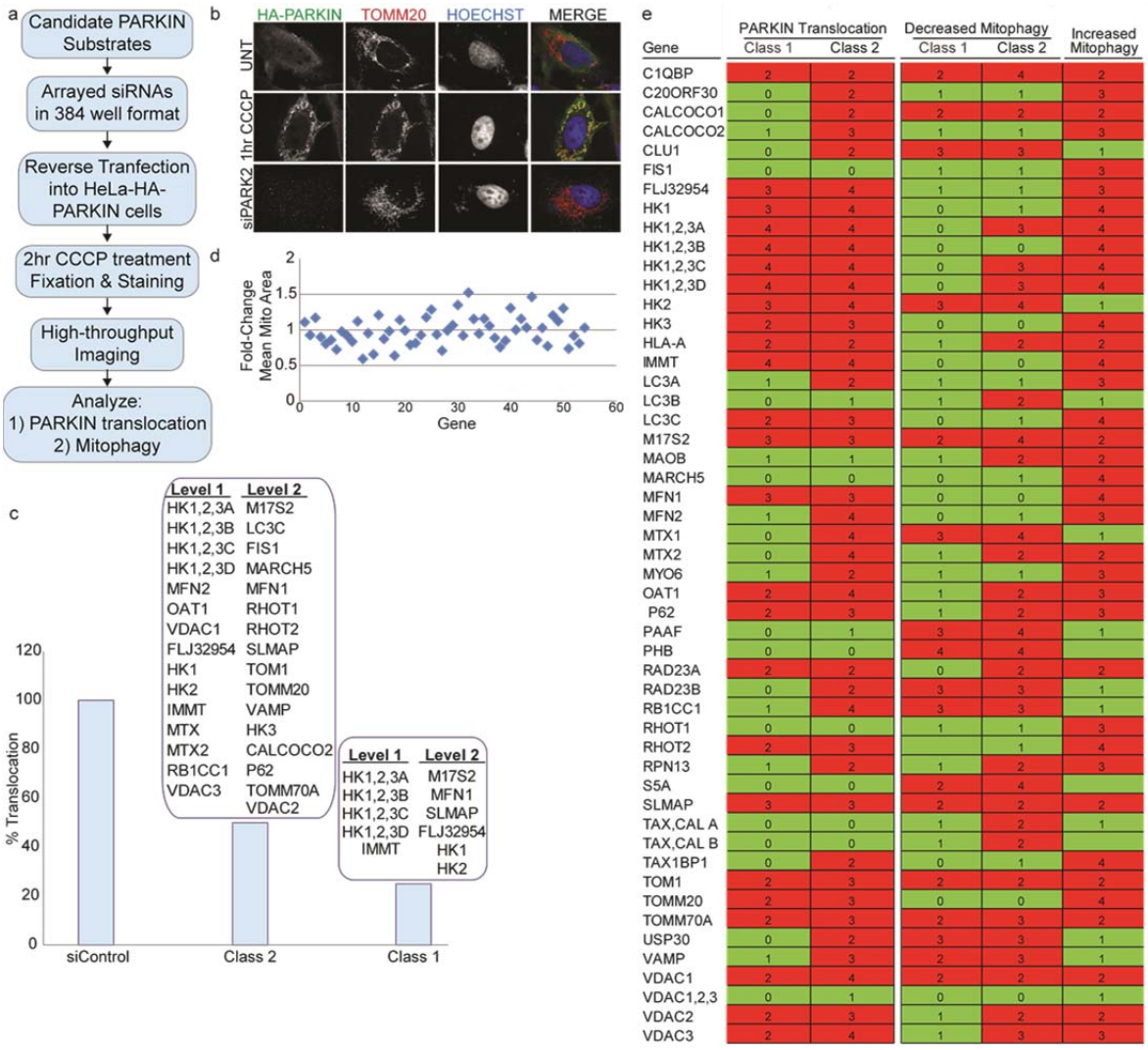


**Figure 2.22 RNAi screening with candidate-PARKIN substrates and interactors. a**, Flow chart of high-throughput RNAi screen used to determine effects of candidate PARKIN-target depletion on PARKIN translocation or mitophagy. **b**, Staining of HA-PARKIN (green), TOMM20 (red), or nuclei (blue) in the clonal HeLa N-HA-Flag-PARKIN cell line used in this study. Cells were either untreated, treated with 1hr 10μM CCCP, or 72h siPARK2 and 1h 10μM CCCP. **c**, Graph depicting Class 1 and Class 2 hits for PARKIN translocation screen. Class 1, 75% decrease in translocation compared to siControl, Class 2, 50% decrease in translocation compared to siControl, Level 1, 4/4 positive siRNAs for a given gene, Level 2, 3/4 positive siRNAs. **d**, Mitophagy screen: dot-plot of fold-change in mean mitochondrial area compared to siControl for all genes tested. **e**, Shown are the numbers of individual siRNAs targeting each gene that scored positive in each screen. Red, genes with 2 or more positive siRNAs; Green, genes with <2 positive siRNAs. siRNA screening and microscopy performed by Malavika Raman. Custom script written by Tiao Xie (IDAC).

genes which might play these roles, we again used a custom script to compare the total mitochondrial area per cell for each siRNA-treated well with siControl-treated cells and those genes whose depletion resulted in less mitochondrial area than control cells were considered positive. Figure 22.2 displays the results of this analysis, including the number of positive siRNAs per gene. We are the process of repeating this analysis with a newly created cell line which exhibits a greater degree of mitophagy than the current cell line being used, providing a greater dynamic range that allow us to make better comparisons and higher confidence predictions of proteins important in this process. Because we cannot rule out the possibility that depletion of some of these proteins may result in toxicity to the mitochondria or the cell as a whole, a second portion of our screen is underway examining the same outcomes in the absence of CCCP-induced depolarization, thus distinguishing siRNA-mediated defects in the presence and absence of depolarization. Thus, we are still in the process of analyzing and collecting all the data generated from these screens and repeating portions which require optimization.

### 2.3 Discussion

Here we describe systematic target identification and ubiquitylation site-specificity for the E3 ligase, PARKIN, thereby revealing the diversity and complexity of PARKIN function after mitochondrial depolarization. Using integrated approaches to identify both interactors and substrates of PARKIN, we have constructed the first quantitative description of the PARKIN-modified proteome. Our analysis reveals both increased ubiquitylation of mitochondrial targets and a distinct set of mitochondrial PARKIN-interactors present only after mitochondrial depolarization. Our work contributes to numerous areas of Parkinson disease research, illuminating aspects of mitochondrial quality control and regulation, PARKIN function on the MOM and in the cytoplasm, and PARKIN regulation. Our data represents a powerful resource for the identification and classification of ubiquitin-modified lysine residues and proteins after

PARKIN activation allowing for direct future interrogation of individual sites and proteins in both the mechanism by which PINK1-PARKIN pathway remodels the MOM proteome to control mitochondrial fate and how this remodeling may affect the initiation or progression of Parkinson's disease.

### 2.3.1 Potential impact of mitochondrial outer membrane protein ubiquitylation by PARKIN on the activity of individual proteins

By examining ubiquitylation sites on substrate proteins, we were able to place targets into a structural and contextual framework thus forming a comprehensive view of the entire pathway. We have consistently found that PARKIN is targeting outer membrane proteins on the mitochondrial surface; some of these proteins are most likely being targeted for degradation by the proteasome. For example, among the proteins we consistently identified are MFN1/2 and RHOT1/2, known PARKIN substrates involved in outer membrane dynamics which have been shown to be degraded in a PARKIN-dependent manner after mitochondrial depolarization. We also identified the VDAC proteins as both PARKIN substrates and interactors. Strikingly, when we mapped the ubiquitylation sites we identified onto existing VDAC structures, we determined that ubiquitylation occurred at multiple sites on the cytoplasmic rim of its central transmembrane pore. The VDAC proteins regulate the exchange of metabolites between the mitochondria and the cytosol which is tightly coupled to cell survival (Colombini et al., 1996). Since VDAC1 is the most abundant protein of the mitochondrial outer membrane, it may act as a hub for PARKIN recruitment or activity at the mitochondria. Because some of the ubiquitylation sites we identified may block the pore, we suspect that PARKIN is potentially mediating both the function and the fate of this substrate. Blocking metabolite conductance through VDAC could affect respiration or apoptotic factors, highlighting the potential for a PARKIN-dependent regulatory effect on small-molecule transport. Closure of VDAC in the mitochondrial outer membrane has been shown to occur after various cellular stresses resulting in global suppression of mitochondrial metabolism

and respiration (Lemasters and Holmuhamedov, 2006), thus insight into the mechanism by which VDAC may be regulated by the binding of PARKIN will be of immense value.

Previous studies indicate that PINK1 interacts stably with the TOMM complex through TOMM40 (Lazarou et al., 2012). Together with our findings that TOMM70 and TOMM22 are depolarization-dependent PARKIN-interacting proteins in addition to the identification of PARKIN-dependent ubiquitylation sites on TOMM70 (Figure 2.9b, Figure 2.12b), these data suggest that the TOMM complex may serve as a nexus for regulation of PARKIN by PINK1. Additionally, translocase function, for example, interaction with transport substrates, may be dynamically altered by ubiquitylation of numerous TPR repeats in TOMM70. Previous studies have shown regulation of the TOMM complex by phosphorylation (Schmidt et al., 2011), thus it seems likely that ubiquitylation could also act as a regulatory signal on these proteins. We intend to investigate the potential impact of PARKIN recruitment to the TOMM complex on mitochondrial protein import using *in vitro* import assays; we believe that PARKIN may be shutting down mitochondrial protein import after depolarization.

Also of interest, we identified ubiquitylation sites in each of three ATPase subunits of the regulatory particle of the proteasome (PSMC1/RPT2, PSMC2/RPT1, and PSMC3/RPT5) (Figure 2.9b, Figure 2.16e). These ubiquitylation events occur within extended helices that form coiled-coils with neighboring RPT subunits and are clustered together on a surface of the regulatory particle proximal to the RPN10 subunit. Previous studies indicate that the C-terminal UIM domain of RPN10 associates with the UBL domain of PARKIN (Sakata et al., 2003). Thus, our finding that association of PARKIN with the proteasome is greatly stimulated by mitochondrial depolarization suggests that PSMC ubiquitylation is likely linked to assembly of PARKIN with the proteasome, as association of PARKIN with the RPN10 subunit is likely to favor ubiquitylation of nearby PSMC subunits. Determination of whether this modification affects proteasome assembly or function downstream of PARKIN activation or is merely a “bystander effect” is crucial to resolve.

In addition to modification of MOM proteins, we also observed modification of proteins resident in the MIM or matrix (Figure 2.16d). Ubiquitylation of these proteins may reflect disruption of mitochondrial structure, which could allow MIM or matrix proteins to escape into PARKIN's vicinity. Alternatively, membrane disruption might permit the ubiquitylation machinery to gain access to these compartments (Yoshii et al., 2011). We observed a number of instances in which the extent of ubiquitylation increased substantially at longer times of depolarization, for example with components of ATP synthase, potentially reflecting local disruption of mitochondrial structure after extended exposure to CCCP. However, we cannot exclude the possibility that PARKIN's association with the TOMM complex allows ubiquitylation of proteins whose transport is stalled as a result of depolarization or PARKIN-dependent TOMM70 ubiquitylation. If this occurs, the repeated identification of the same subset of sites in multiple experiments employing 1 hour of depolarization would suggest a highly stereotypical ubiquitylation mechanism. Investigation of this phenomenon will require additional QdiGly experiments involving both mitochondrial depolarization and inhibition of protein synthesis in order to determine the cellular compartment or source of the ubiquitylated proteins. Furthermore, import assays described above will also clarify the role of the TOMM complex and potentially PARKIN's interactions with mitochondrial matrix or inner membrane proteins.

### 2.3.2 PARKIN targets in the cytoplasm

PARKIN may promote rapid turnover of some targets but not others. We identified a number of proteins in our Class 1 and 2 lists including MFN1/2 and RHOT1/2, which have been shown to undergo proteasomal turnover (Chan et al., 2011; Liu et al., 2012; Tanaka et al., 2010; Wang et al., 2011b). Most likely, a number of the proteins we identified, such as C1QBP1, FIS1 and CISD1, are also degraded after mitochondrial depolarization, as their total levels are also decreased upon PARKIN activation (Chan et al., 2011; Narendra et al., 2012). In contrast, a previous study identified 50 preferentially cytoplasmic proteins or protein complexes that are

enriched in mitochondria in response to depolarization (Chan et al., 2011). Consistent with this, we identified 11 of these proteins or components of protein complexes as Class 1 or 2 targets (Figure 2.17b), possibly reflecting an under-appreciated dynamic recruitment process affecting mitochondrial homeostasis. These include the autophagy adaptor p62, previously linked with mitochondrial clustering after damage, as well as TBC1D15 and DNML1, which are known to interact with FIS1 to regulate fission–fusion cycles (Narendra et al., 2010a; Onoue et al., 2012). In addition to p62, we also identified candidate autophagy receptors, CALCOCO2 and TAX1BP1, which are ubiquitylated upon depolarization and associate with PARKIN in the presence of BafA. Because CALCOCO2 has been shown to target bacteria for autophagy (Shpilka and Elazar, 2012; von Muhlinen et al., 2012), it is an attractive candidate for involvement in mitophagy and we currently in the process of examining it. Additionally, it is possible that additional cytoplasmic proteins identified here as PARKIN-dependent targets are transiently recruited to mitochondria but below the level of detection in previous studies. It is also likely that ubiquitylation of PARKIN targets alters their enzymatic properties or functions before their turnover by the proteasome or autophagy.

### 2.3.3 Relationship of PARKIN to other potential ubiquitin ligases acting on mitochondria.

We have identified numerous proteins on the MOM and in the cytoplasm that are ubiquitylated in a depolarization and PARKIN-dependent manner. In addition, we demonstrated that a substantial fraction of these proteins are captured as PARKIN-associated proteins by affinity chromatography-MS. However, we did not detect a substantial number of candidate substrates in physical association with PARKIN. This could reflect low abundance, difficulty in extraction from the MOM, or transient association with PARKIN. However, we are not able to conclude that all depolarization and PARKIN-dependent proteins are direct substrates. Another prominent mitochondrial E3 is MARCH5. Interestingly, we have identified MARCH5 as a PARKIN-associated protein (Figure 2.12), although we did not identify any PARKIN- or

depolarization-dependent ubiquitylation sites in MARCH5. Previous studies have implicated MARCH5 in cell cycle dependent control of MFN1 turnover (Park et al., 2010). While we cannot rule out a role for MARCH5 in ubiquitylation events seen here, our studies did not directly examine cell cycle dependent changes in ubiquitylation-site occupancy. Further studies will be required to fully understand the involvement of MARCH5 in the PARKIN-dependent ubiquitin modified proteome.

### 2.3.4 Parkin regulation and activity

Under normal conditions, PARKIN seems to exist in an autoinhibited state in which the UBL domain folds back upon the protein to interact with a ubiquitin/UBL binding site in the C-terminal portion of PARKIN (Chaugule et al., 2011). Activation requires PINK1 kinase activity as well as PARKIN ligase activity. Many studies have attempted to identify PINK1 phosphorylation sites on PARKIN; however, confirmation of direct phosphorylation has been difficult and remains unsubstantiated *in vivo* (Kim et al., 2008b; Kondapalli et al., 2012; Lazarou et al., 2013; Sha et al., 2010; Shiba et al., 2009; Um et al., 2009). Recent data suggests that phosphorylation of Ser65 in PARKIN's UBL domain promotes activation of PARKIN Ub-transfer activity *in vitro* (Kondapalli et al., 2012); however, we have not found Ser65 to be essential for MFN2 ubiquitylation *in vivo*, nor does mutation to Ala appear to affect substrate interaction, indicating the potential for additional PINK1-dependent events. In support of this idea, we have identified additional phosphorylation sites in PARKIN which we believe could contribute to activation, potentially in collaboration with Ser65. Furthermore, the ΔUBL mutant we examined more efficiently captured mitochondrial proteins compared to WT PARKIN in response to mitochondrial depolarization, potentially suggesting a loss of autoinhibition (Figure 2.14). However, the ΔUBL was still regulated, showing translocation to the mitochondria upon depolarization and associating with the same proteins identified in the WT AP-MS experiments after mitochondrial depolarization. We cannot discount possible autoinhibition by the ΔUBL or

potentially kinetic defects in both the ΔUBL and S65A mutants; however, neither appears to be absolutely essential for control of substrate interaction or depolarization-mediated translocation. We also found that PARKIN C431S failed to associate with the cohort of MOM proteins normally bound by WT PARKIN under depolarizing conditions, suggesting that PARKIN ligase activity is also required for activation. These observations lead us to support the presence of a multi-step activation mechanism in which PINK1 phosphorylation promotes partial loss of auto-inhibition via the UBL domain, and subsequent auto-ubiquitylation completes the process.

In addition to previously unidentified phosphorylation sites, we also discovered 6 sites of ubiquitylation spanning the length of the protein on PARKIN itself after mitochondrial depolarization (Figure 2.21). Two of the sites, Lys27 and Lys48 are located in the UBL domain; however, mutation of both sites to arginine does not appear to affect PARKIN interaction with MOM proteins after CCCP treatment. We believe that both phosphorylation of sites other than S65 by PINK1 as well as ubiquitylation on internal lysines is likely to be required for both activation of PARKIN, mitochondrial recruitment and interaction, and target ubiquitination. We are in the process of testing this proposed model through the analysis of phosphorylation and ubiquitylation site mutants using both *in vivo* methods and the *in vitro* system described earlier. The wealth of studies that have examined PARKIN regulation and activity have employed an extensive array of recombinant proteins, cell types, organisms, and techniques resulting in an abundance of information, often conflicting or unsubstantiated. The majority of studies examining PARKIN regulation have utilized bacterially purified recombinant protein. While useful, these systems most likely do not recapitulate the complexity of PARKIN activation and regulation that occurs in vivo. Questions remain regarding direct phosphorylation by PINK1 and whether autoubiquitylation truly occurs *in vivo* and is required for either activation or degradation of PARKIN, or possibly there is a threshold which regulates both. An understanding of the native state of Parkin in cells is emerging, and our data contributes to the understanding of how activity may change after activation.

### 2.3.5 Role of PARKIN targets in initiation and progression of mitophagy

Though our screening for PARKIN interactors or targets that are required for PARKIN translocation or the progression of mitophagy is not yet completed, we have started more focused studies on some proteins of interest. As described above, CALCOCO2 has been shown to be necessary to target bacteria for autophagy (Shpilka and Elazar, 2012; von Muhlinen et al., 2012); therefore, it is an appealing to speculate that it may play a role in mitophagy. We have shown that candidate autophagy receptors, CALCOCO2 and TAX1BP1, are ubiquitylated upon depolarization and associate with PARKIN in the presence of BafA. We propose that these related autophagy adaptor proteins may be dynamically recruited to the MOM and may link the depolarization response to the recruitment of autophagy machinery. These proteins did not score highly in the RNAi screen. However, we believe that co-depletion of these proteins may be required to see the true effect on mitophagy. However, codepletion appears to cause toxicity, thus underscoring the importance of these proteins, but making it difficult to study them.

Our expectation is that one or more PARKIN substrates will be ubiquitylated in a form that is recognized by the autophagy machinery, potentially CALCOCO2 or TAX1BP1/CALCOCO3. Developmental mitophagy requires NIX to bridge an interaction with ATG8/LC3 and ATG32 has been shown to play this role in yeast, however, corresponding proteins in mammalian cells are unknown (Kanki et al., 2009; Schweers et al., 2007). The requirement for p62 in mitophagy remains somewhat controversial – it has been shown both to be required for mitochondrial removal or merely for mitochondrial clustering after damage (Geisler et al., 2010; Narendra et al., 2010a). CALCOCO2 removes bacteria from cells via autophagy.by binding to ubiquitin on bacteria and to ATG8/LC3 on autophagosomes, thereby recruiting ubiquitylated bacteria to the autophagosome (von Muhlinen et al., 2012). TAX1BP1 is a ubiquitin binding proteins that is involved in innate immunity and only recently linked to autophagy (Newman et al., 2012; Thurston et al., 2009). Alignment of these two proteins shows

that the sequence in CALCOCO2 that interacts with LC3C is conserved in TAX1BP1. We intend to test whether mutation of this sequence may block mitophagy or affect mitochondrial clustering. Using both proteomics and immunofluorescence, our lab and others have shown that both CALCOCO2 and TAX1BP1 localize to autophagosomes, that TAX1BP1 colocalizes with P62, and CALCOCO2 with LC3B, supporting their role as cargo adaptors for autophagy (Newman et al., 2012), thus making these two proteins likely candidates for potential mitophagy receptors.

### 2.3.6 Comparison of PARKIN interaction data and candidate substrates with historical studies

Using interaction proteomics, we identified a reproducible cohort of depolarization-dependent PARKIN-interacting proteins and candidate substrates, many of which are mitochondrial, consistent with the model of PINK1-dependent recruitment of PARKIN to the mitochondria after damage. While we cannot exclude the possibility that some ubiquitylation events occur downstream of PARKIN activation, the fact that we find many of the targets as PARKIN-interacting proteins is consistent with direct ubiquitylation. Identification of ubiquitylation sites on many of these proteins via QdiGly analysis further supports the view that these proteins both interact with and are substrates of PARKIN. However, a number of candidate PARKIN binding proteins and substrates reported prior to the discovery of this PINK1-dependent conversion of PARKIN from an inactive to active form - including CCNE, AIMP2, DJ-1, and RANBP2 - were not detected here, and some of these interactions have been called into question as PARKIN targets based on other grounds (Dawson and Dawson, 2010). In contrast, activated PARKIN displays robust signal-dependent association with MOM-derived proteins, consistent with a primary role in mitochondrial ubiquitylation in response to this particular type of cellular challenge.

### 2.3.7 Conclusion

We have identified a wide cross-section of ubiquitylation sites and target proteins in 3 distinct cell lines. To our knowledge, this is only the third paper which has used the diGly capture approach to perform dynamic measurements of ubiquitylation. To complement this data, we have also systematically examined PARKIN interacting proteins. This work, together with previous studies, supports a model wherein PINK1-dependent recruitment of PARKIN allows its interactions with and ubiquitylation of numerous MOM proteins, likely resulting in widespread alterations in protein-protein interactions and turnover rates for many key mitochondrial proteins. Our data highlight a number of areas that will require future research. Numerous questions remain to be addressed, both on a global level and more specifically about PARKIN regulation and activation. We look forward to better understanding how PARKIN activity may create a signal which triggers mitophagy. Another question that arises is how PARKIN recognizes such a diverse array of substrates – are they all directly targeted? Perhaps some of the interacting proteins identified act as substrate-binding adaptors. To fully understand PARKIN activity, there are a number of issues to resolve, for example, does PARKIN interact with multiple E2 ubiquitin conjugating enzymes, possibly to affect the type of ubiquitin chain produced? Questions remain as the field progresses towards a better understanding of PARKIN and its role in PD. We have produced a compendium of PARKIN-dependent ubiquitylation sites and interactors, thus providing a resource for further dissection of the PARKIN-dependent and depolarization-dependent ubiquitin modified proteome. We hope our work will contribute toward a deeper understanding of how PARKIN contributes to mitochondrial homeostasis thus furthering efforts to overcome Parkinson's disease.

# CHAPTER 3

**Insight into the PINK1/PARKIN pathway through examination of PINK1 and a novel interacting protein, CLU1**

## Chapter 3: Contributions

**Figure 3.6** Genetic interactions between *clu*, *park*, and *Pink1*. Data obtained in collaboration with the Artavanis-Tsakonas lab with all *Drosophila* experiments performed by Mark Kankel.

### 3.1 Introduction

Evidence has shown that defects in mitochondrial homeostasis may be largely responsible for the accumulation of damaged mitochondria in dopaminergic neurons, ultimately leading to the cell death seen in Parkinson's disease (Dawson and Dawson, 2010). It is known that both PARKIN and PINK1 are commonly mutated in recessive forms of genetic Parkinson's disease (Corti et al., 2011) contributing to a pathology in which mechanisms which function to remove damaged mitochondria from cells may be defective. Both proteins appear to be vital in the regulation of mitochondrial quality by directing degradation of damaged mitochondria via mitophagy (Narendra et al., 2008). Though much of our work has focused on determining the effects of PARKIN activation, it is truly essential to clarify as much of the pathway involved as possible in order to progress in our understanding of Parkinson's disease, therefore, to complement our studies of PARKIN, we sought to expand current knowledge regarding the role of PINK1 in relation to PARKIN and mitochondrial homeostasis. As we have described, PARKIN has been shown to translocate to the mitochondria after membrane depolarization in a PINK1-kinase dependent manner. Under normal conditions, PINK1 is constitutively degraded; however, it is stabilized at the mitochondrial outer membrane upon mitochondrial depolarization where it acts to recruit PARKIN. Consequently, the outer mitochondrial membrane is extensively decorated with ubiquitin and the damaged organelles are eliminated via mitophagy. In order to better understand the role of PINK1 in this process, we have used mass spectrometry (LC-MS/MS) and the Comparative Proteomics Analysis Software Suite (CompPASS) to identify high-confidence candidate interacting proteins (HCIPs) of PINK1 after CCCP-induced mitochondrial depolarization.

Using our interactive proteomics platform we identified CLU1 as a PINK1-interacting protein. We have demonstrated that depletion of CLU1 in HeLa cells disrupts mitochondrial morphology and identified a genetic interaction between *Pink1* and *Clu,* and *Parkin* and *Clu* in *Drosophila*. Though we have not yet completed our investigation of the role of CLU1 in the

PINK1/PARKIN pathway, evidence suggests that it may be a regulatory factor controlling the activity or localization properties of PINK1.

### 3.1.1 PINK1 regulation and activation

Though it accounts for a lesser percentage of cases than PARKIN, numerous mutations in PINK1 have been shown to cause early-onset familial Parkinson's disease (Valente et al., 2004). Originally identified as a PTEN-induced gene in cancer cells, PINK1 contains an N-terminal MTS, putative transmembrane region, Ser/Thr kinase domain, and C-terminal regulatory domain (Chu, 2010) (Figure 3.1a). Bioinformatic analysis has revealed unique sequences within the kinase domain and functional motifs in the C-terminal region that may be involved in unique regulation of kinase activity, substrate selectivity and stability (Mills et al., 2008). PD mutations span the protein with varying effects on its function including stability of the protein, expression levels, truncation, association with chaperones such as HSP90, and importantly, activity of the kinase domain (Mills et al., 2008). PINK1 overexpression is protective against proteasome inhibitor-mediated cell death, MPTP and rotenone toxicity, and oxidative stress (Haque et al., 2008; Pridgeon et al., 2007; Valente et al., 2004; Wang et al., 2011a), effects which are eliminated by PD-associated mutations (Chu, 2010). Additionally, PINK1 may protect against injury associated with dominant genetic PD models as it has been shown to reduce α-synuclein-mediated retinal degeneration in *Drosophila* (Todd and Staveley, 2008, 2012), while knockdown of PINK1 appears to contribute to proteasomal impairment and α-synuclein aggregation in tissue culture cells (Liu et al., 2009a). Despite these striking effects on survival, little was known about PINK1 regulation, activation, or targets until recently and still, only a few target pathways have been identified. Evidence supporting the involvement of PINK1 in regulating mitochondrial function, trafficking, and structure is now well confirmed, however, how PINK1 is regulated and how PINK1 exerts its neuroprotective function remain unclear.

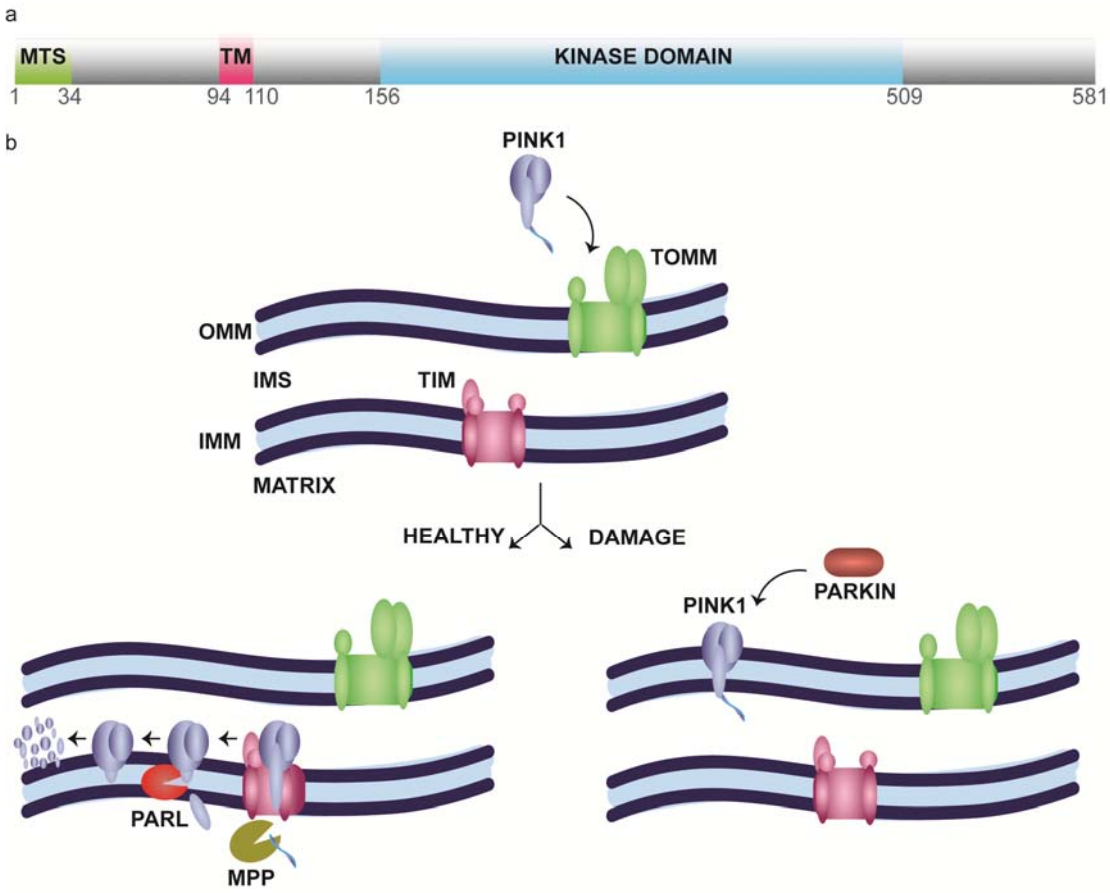


**Figure 3.1 PINK1 protein, import and processing**. PINK1 contains a mitochondrial targeting sequence (MTS), transmembrane domain (TM), and kinase domain. **b**, Model for PINK1 import and processing. PINK1 is targeted to the mitochondria by the N-terminal MTS and imported into the inner mitochondrial membrane via the general mitochondrial import machinery, TOMM and TIM23 complexes. Under normal conditions, MPP cleaves the MTS to generate a 60-kD ΔMTS-PINK1. PINK1 is then cleaved to a 52-kD form within the inner mitochondrial membrane by PARL. The 52-kD PINK1 is then degraded by an MG132-sensitive protease. Upon damage, When mitochondrial membrane potential is dissipated, PINK1 accumulates as a 63-kD full-length form on the OMM where it can recruit PARKIN to impaired mitochondria. OMM, outer mitochondrial membrane; IMM, inner mitochondrial membrane.

Reports assert that PINK1 carries out both cytoplasmic and mitochondrial functions (Gandhi et al., 2006; Haque et al., 2008; Lin and Kang, 2008; Muqit et al., 2006; Narendra et al., 2010b). For example, cytosolic PINK1 was shown to confer resistance to MPTP-induced stress in dopaminergic neurons (Haque et al., 2008), though staining of the WT protein supports mitochondrial localization (Gandhi et al., 2006; Haque et al., 2008; Lin and Kang, 2008; Muqit et al., 2006; Narendra et al., 2010b). Since the determination that PINK1 played a role in

mitochondrial function, a number of studies have been undertaken in attempts to understand its regulation. Under normal conditions with a healthy population of cellular mitochondria, PINK1 is constitutively degraded in a manner dependent upon mitochondrial membrane potential (Narendra et al., 2010b). Though rapidly turned over, PINK1 is targeted to the mitochondria by its MTS and imported via the general mitochondrial import machinery of the TOM/TIM23 complexes into the inner mitochondrial membrane where it is cleaved by the mitochondrial processing protease (MPP) to produce a 60 kD ΔMTS-PINK1 (Figure 3.1b). A hydrophobic region downstream of the MTS may impede complete translocation of PINK1 across the inner membrane (Becker et al., 2012). Import is followed by a second cleavage within the inner mitochondrial membrane by presenilin-associated rhomboid like protease (PARL) which produces a 52 kD form of the protein that is subsequently degraded by an MG132-sensitive protease, presumably the proteasome (Deas et al., 2011; Jin et al., 2010; Meissner et al., 2011). Though evidence supporting this processing of PINK1 is compelling, it is not yet clear where the proteolysis occurs; however, if the proteasome is responsible, PINK1 is presumably removed from the mitochondria via reverse translocation.

Exposure to ionophores, such as CCCP or valinomycin, results in mitochondrial depolarization, meaning the coupled reactions of electron transfer and H+ migration are uncoupled, allowing H+ ions to bypass ATP synthase and diffuse through the inner membrane thus destroying the pH and electrical gradients. Upon depolarization, full-length 63 kD endogenous PINK1 is immediately stabilized at the mitochondria in HeLa cells while no increase in PINK1 is seen in the cytoplasm (Narendra et al., 2010b). A similar phenomenon was observed in rat cortical neurons expressing tagged exogenous PINK1 (Narendra et al., 2010b; Zhou et al., 2008). Another approach used MFN1/2 null MEFS, which contain a heterogeneous mitochondrial population, some of which are bioenergetically uncoupled and others which are intact (Chen et al., 2005). As with treatment with uncoupling drugs, MFN1/2-/- mitochondria exhibit low membrane potential resulting in accumulation of PINK1 only on those affected

subsets of the population, an effect also observed after paraquat-induced oxidative stress, thus validating the selective stabilization of full-length PINK1 on mitochondria with low membrane potential (Cocheme and Murphy, 2008; Narendra et al., 2010b). Thus, perturbation of the mitochondrial membrane potential results in accumulation of the full-length 63 kD form of PINK1 on the outer mitochondrial membrane where it can extend its kinase domain into the cytoplasm.

Evidence suggests that inner membrane proteases are nonfunctional after depolarization, potentially explaining how PINK1 escapes degradation (Jin et al., 2010). Furthermore, the C-terminus of the protein is thought to promote retention of PINK1 at the outer membrane (Becker et al., 2012). After being transferred laterally into the outer mitochondrial membrane, PINK1's kinase domain is exposed to the cytoplasm allowing recruitment of PARKIN, which in turn, induces the degradation of the damaged mitochondria (Meissner et al., 2011; Narendra et al., 2010b). This model of PINK1 regulation and activation provides an explanation of how the cytoplasmic protein, PARKIN, is itself selectively recruited to damaged mitochondria and explains how PARKIN distinguishes injured from healthy mitochondria. A recent study in HeLa cells showed that after repolarization, PINK1 is rapidly reimported and degraded, presumably via lateral opening of the TOMM complex which permits PINK1 to re-enter the import pathway (Harner et al., 2011). Thus, association with the TOMM complex in depolarized mitochondria mediates rapid reimport and allows precise regulation of PINK1 levels resulting in displacement of mitochondrial PARKIN and rescue of repolarized mitochondria from the mitophagy response (Lazarou et al., 2012).

Upon stabilization, PINK1 is active at the outer mitochondrial membrane, where it may target substrates, itself, or both, though few substrates have been reported or confirmed and reports of autophosphorylation have conflicted. A recent reported showed that autophosphorylation on PINK1 Ser228 and Ser402 after a decrease in membrane potential was essential for efficient mitochondrial localization of PARKIN (Okatsu et al., 2012). However, other groups have identified several other sites of autophosphorylation, including the depolarization-

dependent modification of Thr257, though it does not appear to be required for PINK1 activation and is not highly conserved (Kondapalli et al., 2012). It is not clear how many and precisely which sites may be required for full activation of depolarization-dependent PINK1 kinase activity or if some of these sites may be off-target or nonessential consequences of kinase activation. In terms of PINK1 targets, very few have been identified. TNF receptor-associated protein 1 (TRAP1), a mitochondrial chaperone of the HSP90 family, and HtrA2/Omi, a mitochondria serine protease, were both identified as substrates and shown to play roles in mediating protection against oxidative stress (Plun-Favreau et al., 2007; Pridgeon et al., 2007). Miro, a Rho-like GTPase located in the outer mitochondrial membrane, is also a PINK1 substrate targeted after mitochondrial depolarization (Wang et al., 2011b). Through binding to Milton, Miro promotes an interaction with kinesin heavy chain which results in trafficking of mitochondria along microtubules for axonal transport (Glater et al., 2006; Guo et al., 2005) (Figure 3.2). Overexpression or activation of PINK1 results in degradation of Miro and arrest of mitochondrial transport, contributing to the sequestration of the damaged population of mitochondria (Wang et al., 2011b). Obviously the best studied candidate substrate of PINK1 is PARKIN. Though PINK1 kinase activity is required for PARKIN recruitment to the mitochondria and induction of mitophagy after depolarization, evidence for direct phosphorylation has been unsubstantiated and remains somewhat controversial (Becker et al., 2012; Kim et al., 2008b; Lazarou et al., 2012; Moore, 2006; Sha et al., 2010; Shiba et al., 2009; Um et al., 2009). A recent report using recombinant insect PINK1 found direct phosphorylation on Ser65 of PARKIN leading to activation of its E3 ligase activity in an *in* vitro ubiquitylation assay (Kondapalli et al., 2012). However, though we do identify Ser65 phosphorylation in a depolarization-dependent manner, our *in vivo* data does not support an essential role for it in PARKIN activation.

Mitochondria are actively transported throughout the cytosol, mainly along microtubules in mammalian cells (Frederick and Shaw, 2007). In neurons, movement is regulated both by active transport and fusion/fission cycles (Sheng and Cai, 2012; Wang et al., 2011b). Through

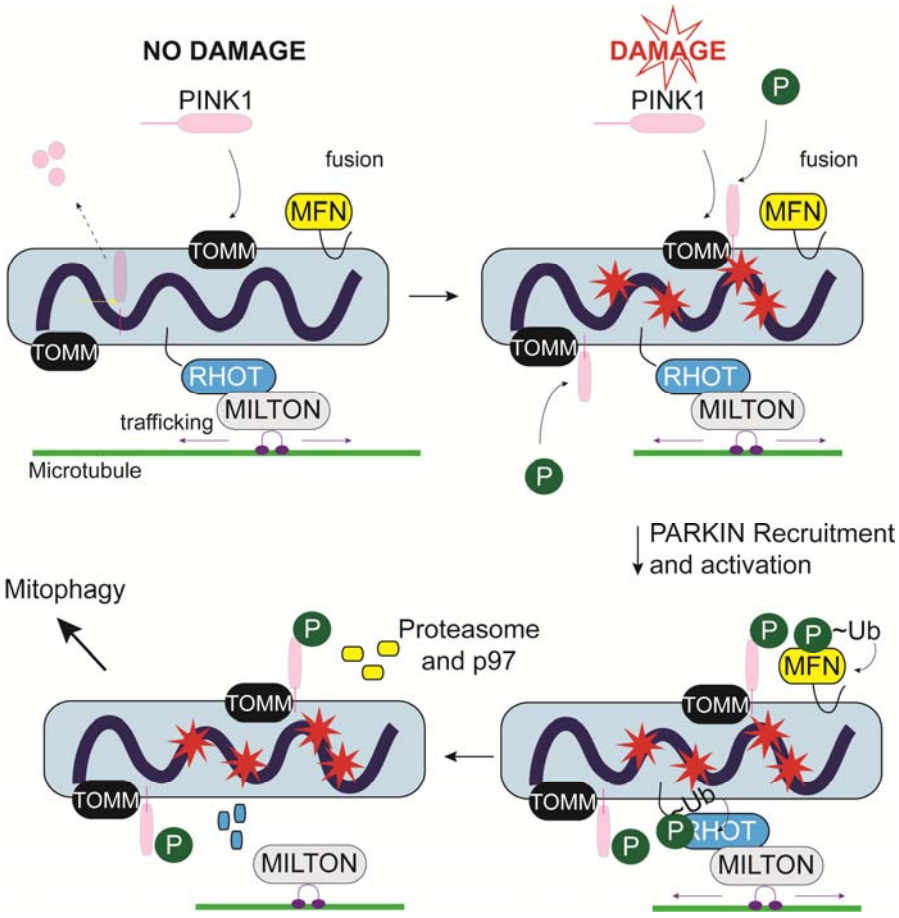


**Figure 3.2 PINK1/PARKIN-dependent arrest of mitochondrial trafficking.** Mitochondrial depolarization stabilizes PINK1 on the OMM were it both recruits PARKIN and interacts with Miro. PINK1 phosphorylation of Miro appears to target it for PARKIN-mediated ubiquitylation and subsequent degradation by the proteasome. Milton and kinesin, which bridge the interaction with microtubules, are released from the mitochondria resulting in arrest of movement.

effects on trafficking and fusion, PINK1 and PARKIN work together to affect mitochondrial localization (Figure 3.2); loss of balance between these proteins and their substrates leads to striking effects. For example, co-overexpression of PARKIN and PINK1 has been shown to disrupt the normally tubular mitochondrial network resulting in aggregation and perinuclear clustering of mitochondria (Vives-Bauza et al., 2010). Treatment with the microtubule depolarizing agent, nocodazole, causes dispersal of clustered mitochondria, thus underscoring the importance of microtubule transport networks in mitochondrial transport and maintenance of

the cellular pool of mitochondria (Vives-Bauza et al., 2010). It is also possible that mitophagy requires trafficking of damaged mitochondria to the perinuclear region for degradation, particularly in neurons, where the mitochondria may be dispersed at synaptic terminals, however, this retro-translocation of mitochondria remains controversial (Vives-Bauza et al., 2010). Regardless, association with microtubules is essential in mitochondrial trafficking, response to injury, and the preservation of a healthy population of mitochondria.

### 3.1.2 CLU1, a novel PINK1 interactor

Though it is well substantiated that PINK1 is essential for PARKIN recruitment to mitochondria after CCCP treatment (Narendra and Youle, 2011), the specifics of PINK1 regulation and its promotion of Parkin activity are incompletely understood. The ability to determine candidate interactors, regulators, or substrates of PINK1 may allow us to better understand how PINK1 regulation of PARKIN occurs. Through a proteomic approach, we have identified a candidate PINK1 regulatory factor, CLU1, shown to interact genetically with *parkin* in Drosophila (Cox and Spradling, 2009). Furthermore, mutation or depletion of CLU1 orthologs identified in Drosophila, *Dictyostelium*, and *S.cerevisiae* result in similar mitochondrial defects (Cox and Spradling, 2009; Fields et al., 1998; Zhu et al., 1997).

First identified in *Dictyostelium discoideum, the cluA* gene encodes a 150 kDa protein which, when depleted, results in clustering of normally uniformly dispersed mitochondria in the center of the cell (Figure 3.3a, b) (Zhu et al., 1997). The *cluA*- mutant also displays an increase in multinucleated cells, potentially suggesting a cytokinesis defect (Zhu et al., 1997). These observations led to the hypothesis that *cluA* may link mitochondria and the cytoskeleton. Under normal conditions, mitochondria are generally dispersed throughout eukaryotic cells, though they can also be found concentrated in areas with high levels of ATP consumption. The position of microtubules within cells have been shown to determine mitochondrial distribution as well as ensure proper mitochondrial replication, division, and transport to daughter cells (Berger and

Yaffe, 1996). Both cytoskeletal elements and components of mitochondrial membranes have been shown to be required for proper mitochondrial morphology and trafficking, especially in neurons which require a high density of mitochondria at synaptic terminals thus relying heavily on axonal trafficking of mitochondria (Glater et al., 2006; Itoh et al., 2013; Matsuda et al., 2009). By immunostaining, cytoskeletal structures appear normal in *cluA*- cells and the phenotype is not mimicked by cytoskeletal disruptive drugs (Fields et al., 2002). However, the clustered mitochondria in *cluA*- cells were often found to be interconnected by narrow membranous strands suggesting a blockage at a very late step in fission of the outer mitochondrial membrane (Fields et al., 2002).

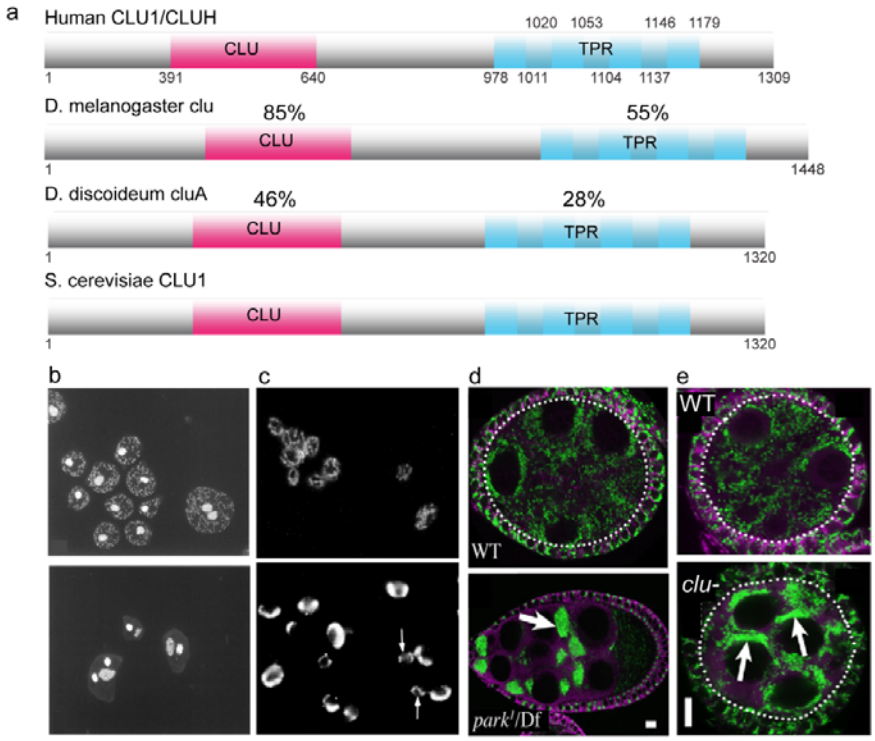


**Figure 3.3 CLU1 domain structure and mitochondrial phenotype. a**, CLU1 orthologs are highly conserved. Percentages indicate amino acid identity of the CLU and TPR domains. CLU, CLUstered mitochondria domain, TPR, tetratricopeptide repeat. **b**, WT *Dictyostelium* cells stained with DAPI to visualize nuclei and mitochondria (top panel). Mitochondria are clustered near the cell center in *cluA*- cells (bottom panel). **c**, Anti-porin staining of wild-type (*CLU1*) cells displays normal branched mitochondrial morphology (top panel). Staining of mutant (*clu1*Δ) cells displays clustered mitochondrial phenotype. **d**, Wild-type stage 5 follicles lack clustered mitochondria (green) (top panel). Extreme mitochondrial clustering in a stage 9 park1/Df follicle (bottom panel). **e**, Wild-type stage5 nurse cells in a cyst contain dispersed mitochondria (top panel) but cluster (arrows) in *clu-* nurse cells (bottom panel). Microscopy images adapted from (Cox and Spradling, 2009; Fields et al., 1998; Zhu et al., 1997).

In *Saccharomyces cerevisiae,* the identification of a large protein, 27% identical and 50% similar to *cluA*, termed *CLU1*, also showed mitochondrial defects upon disruption (Fields et al., 1998) (Figure 3.3a, c). In *clu1*Δ cells, the normally highly reticulated mitochondria are condensed to one side of the cell; however, upon transformation of *CLU1* into *cluA-D.discoideium* cells, normal cell cycle is restored and mitochondria are once again dispersed throughout the cell, confirming that *CLU1* is a functional homolog of *cluA (*Fields et al., 1998). Homology with the predicted sequence of the *cluA* gene product is also found in metazoans, for example *friendly mitochondria* (*fmt*) in Arabidopsis, shown to be required to prevent mitochondria from clustering. Also identified are the *C. elegans* gene *clu-1* and the human ortholog, KIAA0664 (CLU1), though neither of these has been studied. Though *clu* appears to be highly conserved, little functional information has emerged. In 1999, it was identified as a possible component of the translation initiation factor eIF3 in yeast via co-immunoprecipitation and referred to as the gene, TIF31, and protein, p135 (Vornlocher et al., 1999). However, *clu1*Δ cells had no defect in activity of the eIF3 enzyme complex and it was later shown that homologs of CLU1 did not co-purify with the eIF3 complex from human or plant cells (Browning et al., 2001).

The PINK1/PARKIN pathway is known to be conserved in *Drosophila*, therefore it has commonly been used as a model for Parkinson's disease. PARKIN null flies exhibit shortened life span, male sterility, and locomotor defects (Greene et al., 2003). The decreased fertility occurs due to a defect in spermatogenesis while apoptotic muscle generation causes the flight and climbing defects (Greene et al., 2003). Both phenotypes result from altered mitochondrial structure which affects both the germ line and muscle degeneration, indicating the potential significance of mitochondrial dysfunction in PD. The ortholog of *cluA, clueless* (*clu*), which encodes a highly conserved protein has been identified in Drosophila and is 53% identical to human Clu (Cox and Spradling, 2009) (Figure 3.3a). Similar to orthologous proteins in Dictyostelium and yeast, loss of Drosophila *clu* results in mitochondrial clustering (Figure 3.3d),

possibly at microtubule plus ends. In their effect on mitochondrial function, *clu* mutations resemble *parkin* mutations with null animals exhibiting decreased life span, sterility, and severe mitochondrial abnormalities in flight muscle (Figure 3.3c) (Cox and Spradling, 2009).

Though mammalian CLU1 is a large protein, approximately 150 kD, it contains few identifiable motifs. However, it does contain four highly conserved tetratricopeptide (TPR) repeats; TPR repeats usually fold together to produce a single, linear solenoid TPR domain which can form scaffolds to mediate protein–protein interactions or assembly of multiprotein complexes. CLU1 also contains an uncharacterized CLU (CLUstered mitochondria) domain unique to eukaryotic CLU1 orthologs (Figure 3.3a). Though not well studied, the CLU domain appears to be essential for proper mitochondrial function and the full-length protein is required for a late stage of MOM fission in Dictyostelium (Fields et al., 2002). Genetic interaction between *parkin* and *clu* was demonstrated by enhanced mitochondrial clustering in *park/+*; *clu/+* trans-heterozygotes (Cox and Spradling, 2009). A role for CLU in mitochondrial localization and possibly mitochondrial dynamic and fusion/fission is strongly supported by evidence in multiple species. To our knowledge, our findings provide the first evidence of direct interaction between PINK1 and CLU1 and we are currently investigating whether CLU1 may control the activity, stability, or localization properties of PINK1.

Protein networks are increasingly serving as tools to unravel the molecular basis of disease allowing the identification of new disease genes and identifying disease-related subnetworks. In order to better understand the PINK1/PARKIN pathway as a whole, we have again utilized the interaction proteomics method developed in our lab to identify high-confidence candidate interacting proteins of PINK1. Direct interrogation of physiological PINK1 protein complexes can be achieved through this approach allowing us to determine the interactors, regulators, or substrates of PINK1 with and without the induction of mitochondrial depolarization. Coupled with a variety of cell biological approaches, we hope to better understand how PINK1 regulation of PARKIN or other targets occurs. Using these methods, we

identified depolarization-independent PINK1 interactors located on the MOM, cytoplasmic interactors, such as CLU1, and the proteasome. PARKIN and PINK1-mediated remodeling of the outer mitochondrial membrane signifies an important step in the progression of mitophagy. An understanding of the networks surrounding these proteins may ultimately provide information about the progression and possible treatment of neurodegenerative disorders.

## 3.2 Results

### 3.2.1 Identification of novel PINK1 interactors

In order to better appreciate PINK1's contribution to the PINK1/PARKIN pathway, we utilized AP-MS and our interactive proteomics platform, *CompPASS* to interrogate this node of the pathway. After verifying mitochondrial localization and depolarization-dependent processing of C-HA-Flag-tagged PINK1 in 293T cells (Figure 3.4a), we performed HA-immunoprecipitation followed by mass spectrometry both in the presence and absence of 1 hour of CCCP. Using our interactive proteomics platform, we have identified candidate interactors, regulators, or potential substrates of PINK1, including both mitochondrial and cytoplasmic proteins. Under both untreated and depolarized conditions, PINK1 interacted with multiple components of the TOMM complex, including TOMM40, TOMM22, TOMM70, TOMM6 and TOMM34. Furthermore, PINK1 co-purified with a number of proteasome subunits and numerous mitochondrial outer membrane proteins, such as VDAC2, in addition to cytoplasmic proteins (Figure 3.4b, Supplementary Table 9). A number of other MOM proteins, including HK1, HK2, and HK3 were also identified but did not pass our stringent threshold for HCIPs. Of particular interest was KIAA0664, or CLU1, which was identified as a high confidence interacting protein under both treatment conditions.

Numerous proteins identified as PINK1 HCIPs were validated as interactors in HeLa cells stably expressing PINK1-C-HA-Flag which were either untreated or subjected to mitochondrial depolarization by treatment with CCCP for 1 hour (Figure 3.4b). As in 293T cells,

the majority of PINK1 interactors in HeLa cells, including subunits of the TOMM complex and CLU1, were seen both in the presence and absence of CCCP.

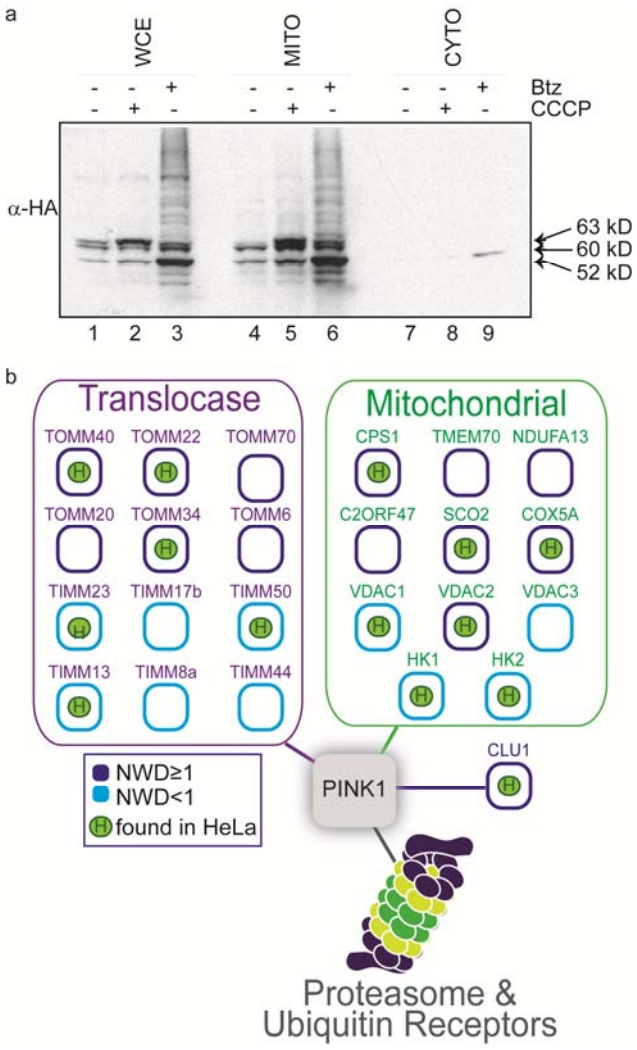


**Figure 3.4. PINK1 interaction proteomics. a**, Fractionation of C-HA-Flag-tagged PINK1 stable cell line used in this study. WCE, whole cell extract, MITO, mitochondrial fraction, CYTO, cytoplasmic fraction. Cells were either untreated or treated with 10μM CCCP and/or 1μM Btz for 1 h. Arrows indicate PINK1 full-length protein (63 kD) and cleavage products, 60 kD, which is lacking the MTS, and 52 kD. **b**, Summary of subset of PINK1-interacting proteins found under both untreated and depolarized conditions (1h 10μM CCCP and/or 1μM Btz) in 293T and HeLa cell lines. Full dataset is included in Supplementary Table 9.

### 3.2.2 CLU1 is a bona fide PINK1 interactor

Based on the interaction data generated from both 293T and HeLa cells lines stably expressing PINK1, we identified CLU1 as a candidate PINK1 interacting protein. Because

antibodies that efficiently immunoprecipitate endogenous CLU1 were not available, we further validated the interaction of CLU1 with endogenous PINK1 in HeLa cells transiently transfected with N-MYC-CLU1 either untreated or treated with CCCP for 1 hour. Using anti-MYC agarose to purify N-MYC-CLU1, we confirmed depolarization-independent interaction with endogenous PINK1 via immunoblotting (Figure 3.5).

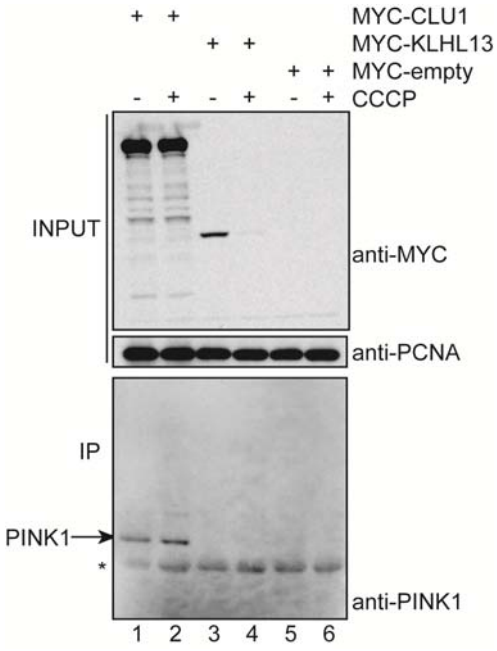


**Figure 3.5 Validation of interaction between CLU1 and PINK1**. Reciprocal interaction between CLU1 and PINK1 was identified in HeLa cells transiently transfected with N-MYC-CLU1. After 48h, cells were treated with 1h CCCP (10μM) and subjected to immunoprecipitation with anti-MYC agarose and immunoblotted with the indicated antibodies.

### 3.2.3 *clueless* interacts genetically with both *pink1* and *park* in Drosophila

A previous report identified a genetic interaction between *clueless* and *park* in Drosophila (Cox and Spradling, 2009). In collaboration with the Artavanis-Tsakonas lab, we sought both to confirm this finding in Drosophila and to examine the relationship between the fly orthologs, *clueless (clu)* and *pink1*. We examined three Exelixis *clueless* alleles for modification of the held out wing phenotype of tubGAL4 directed expression of multiple UAS-*parkin*$^{RNAi}$ and

UAS-*Pink1*$^{RNAi}$ alleles. *Clu* alleles tested included the null alleles, d08713 and f04554, and a hypomorph, f04554, based on Cox and Spradling, 2009 (Figure 3.6a, b). The penetrance of the phenotypes of the sample genotypes, *clueless/tubGAL4-parkin* and *clueless/tubGAL4-Pink1* were calculated (Figure 3.6c, Supplementary Table 10). In addition to validating the *clueless* and *park* interaction, we also determined that *clueless* null mutations enhance the classic "held out wing" phenotype seen in tubGAL4:UAS*pink1RNAi* and tubGAL4:UAS-*parkRNAi* flies, thus establishing that a genetic interaction may exist between clueless and PINK1.

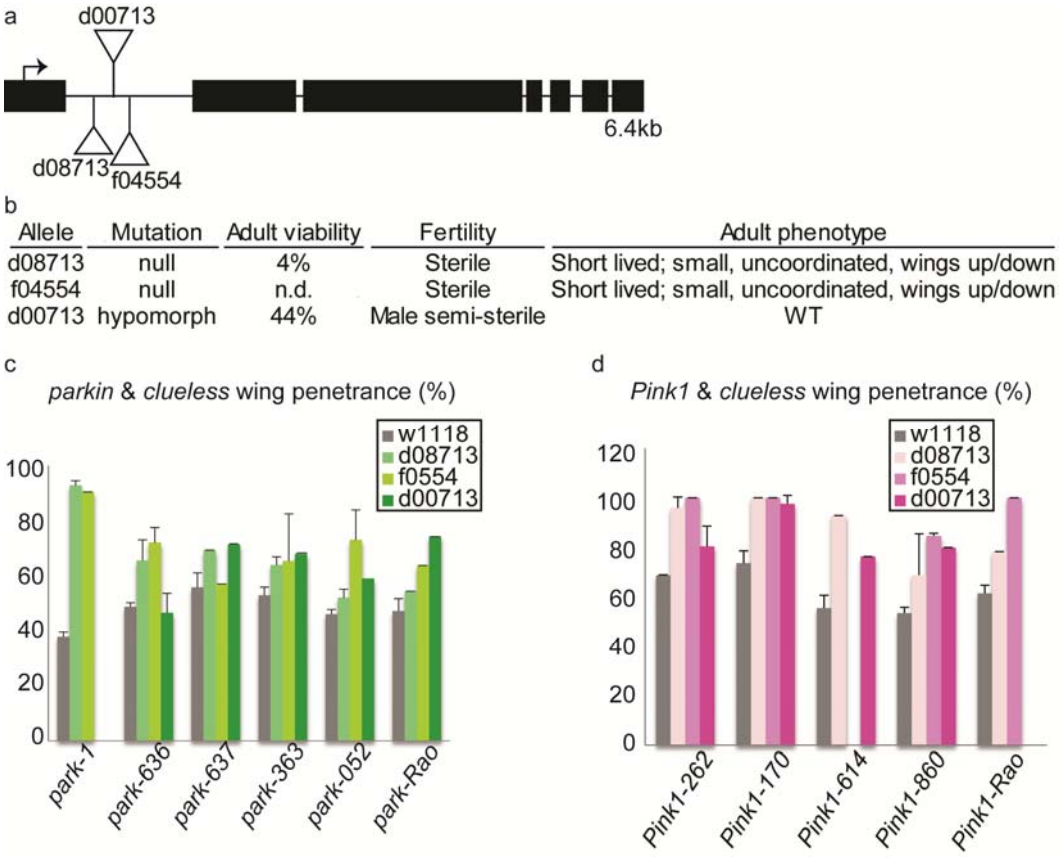


**Figure 3.6 Genetic interactions between *clu*, *park*, and *Pink1*.** **a**, Map of the *clu* locus showing sites of insertion mutation (triangles) and the translation start (arrow). Black boxes are exons (adapted from Cox and Spradling, 2009). **b**, *Clueless* alleles and associated phenotypes observed in a previous study (Cox and Spradling, 2009). **c**, Summary of the *clueless* interactions with multiple *parkin* alleles. **d**, Summary of the *clueless* interactions with multiple *Pink1* alleles. This data was obtained in collaboration with the Artavanis-Tsakonas lab with all experiments performed by Mark Kankel.

### 3.2.4 CLU1 interaction and domain analysis

To better understand how CLU1 might be influencing the PINK1/PARKIN pathway, we created a 293T cell line stably expressing CLU1-C-HA-Flag (Figure 3.7b). Via anti-HA immunoprecipitation, we purified CLU1 with and without 1 hour of CCCP treatment. Using AP-MS in conjunction with the *CompPASS* proteomics software platform, we attempted to identify high confidence CLU1-interacting proteins. Unexpectedly, CLU1 interacted with very little both in the presence and absence of depolarization; indeed, we did not identify PINK1 as a high confidence interacting protein (Supplementary Table 11). We considered the possibility that C-terminal tagging of CLU1 might have interfered with its ability to interact with binding partners or with proper folding or localization of the protein. To address this potential issue, we created a 293T cell line stably expressing N-HA-Flag-CLU1. However, AP-MS analysis again produced no reproducible interactors for CLU1, suggesting that ectopically tagging CLU1 may not be a suitable way in which to study the protein. Alternatively, we may not have captured CLU1 under conditions which allow its interactions to occur, though transient transfection of N-MYC-CLU1 did validate interaction with PINK1 (Figure 3.5).

In an effort to characterize CLU1 and dissect its interaction with PINK1, we constructed truncation mutants of CLU1. We examined the protein sequence of CLU1 to identify any known or potential domains in addition to the TPR repeats and CLU domain. Truncations were designed based on alignment of human CLU1 with the Drosophila *clueless* protein (Figure 3.7a). We created five truncation mutants spanning the whole protein, including isolated CLU domain and TPR motif mutants expressed as C-terminally HA-Flag-tagged proteins. Similarly to the full-length protein, AP-MS analysis of the CLU1 domains did not reveal any high confidence interacting proteins (Supplementary Table 11).

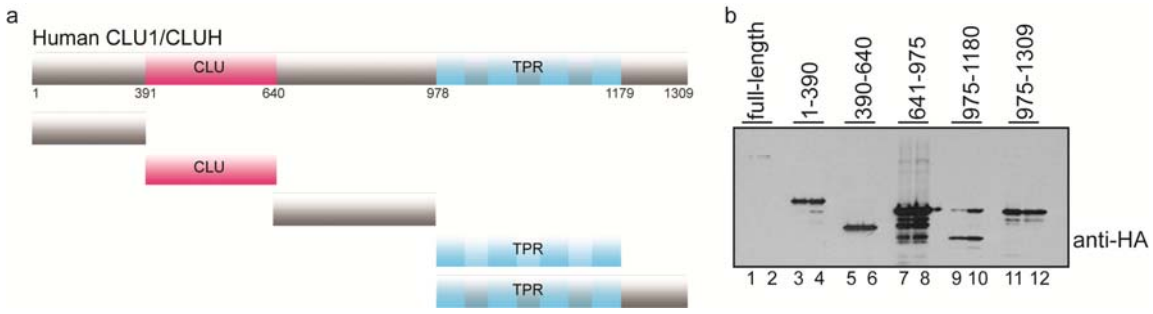


**Figure 3.7 CLU1 constructs used in this study. a**, Full-length human CLU1 and truncation mutants used in AP-MS experiments. **b**, 293T cell extracts immunoblotted to detect CLU1 C-HA-Flag-tagged constructs used for AP-MS experiments.

### 3.2.5 Depletion of CLU1 alters mitochondrial morphology

To elaborate on the role of CLU1 in mitochondrial maintenance, we use RNAi to deplete CLU1 in HeLa cells for 72 hours, after which cells were fixed for immunofluorescence depolarization. We found that loss of CLU1 led to alterations in mitochondrial morphology in comparison to control siRNA-treated cells (Figure 3.8). Additionally, the total amount of mitochondria per cell appeared to be increased in cells treated with CLU1 siRNA. Likewise, the network of mitochondria was expanded throughout the cell and seemingly more fragmented than in control cells, consistent with a role for CLU1 in mitochondrial dynamics independently of PARKIN. CLU1 was also included in our RNAi screen for PARKIN interactors (Chapter 2.2.8) and scored as a positive in the screen for increasing total mitochondrial area after depletion (Figure 2.22), thus validating our original finding.

### 3.2.6 CLU1 may affect PINK1 activity

We have established that CLU1 interacts genetically with both PINK1 and PARKIN, interacts physically with PINK1, and appears to be necessary for maintenance of normal mitochondrial morphology. Both because it interacts with PINK1 in the presence and absence of mitochondrial depolarization and contains a TPR domain, often involved in protein-protein

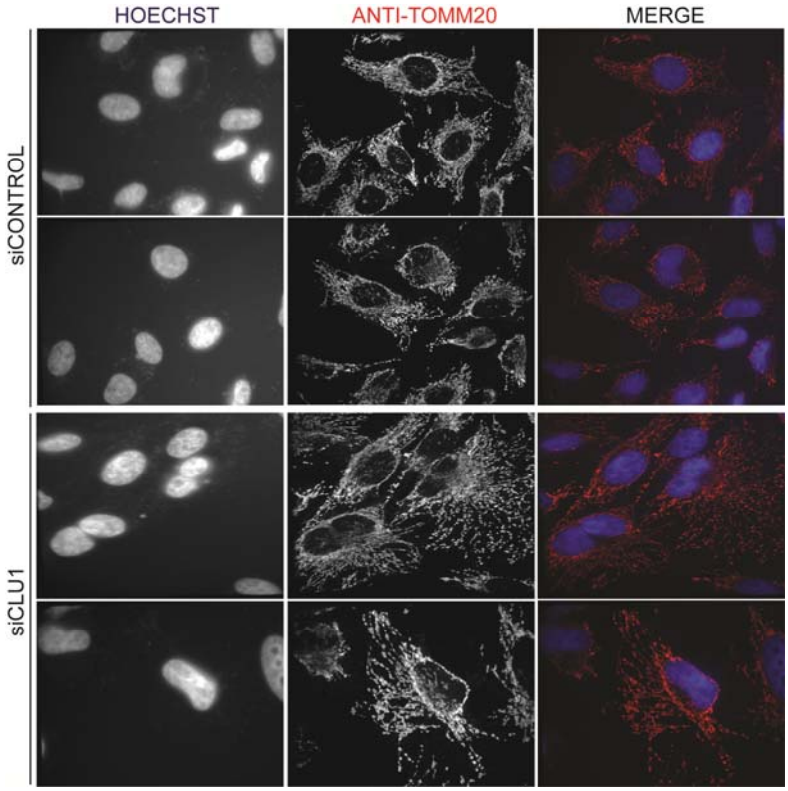


**Figure 3.8 Effects of CLU1 depletion on mitochondrial organization.** Mitochondrial marker, TOMM20, is used to stain the mitochondria in HeLa cells.

interaction or scaffolding, we believe that CLU1 may control the activity status or localization properties of PINK1. To determine whether PINK1 activity is affected by loss of CLU1, we treated HeLa cells with siRNA targeting CLU1, followed by transient transfection of MYC-PARKIN 24 h later. Finally, at 72 hours post-siRNA transfection, we treated cells with 1 h of CCCP (10μM) or CCCP (10μM) and Btz (1μM). Depletion of CLU1 did not affect processing of PINK1 after mitochondrial depolarization, however, total levels of PINK1 appear to be slightly reduced upon immunoblotting (Figure 3.9a). Ubiquitylation of MFN2, catalyzed by PARKIN in a PINK1-dependent manner after CCCP treatment, is a useful readout of PINK1 activity. MFN2 ubiquitylation was reduced upon CLU1 depletion, though not completely abolished; however, we did not achieve complete knockdown of the highly expressed CLU1 protein (Figure 3.9a). We then examined the effects of PINK1 depletion on CLU1. As expected siRNA targeting PINK1 abolished MFN2 ubiquitylation (Figure 3.9b). However, we also noted that CLU1 levels were

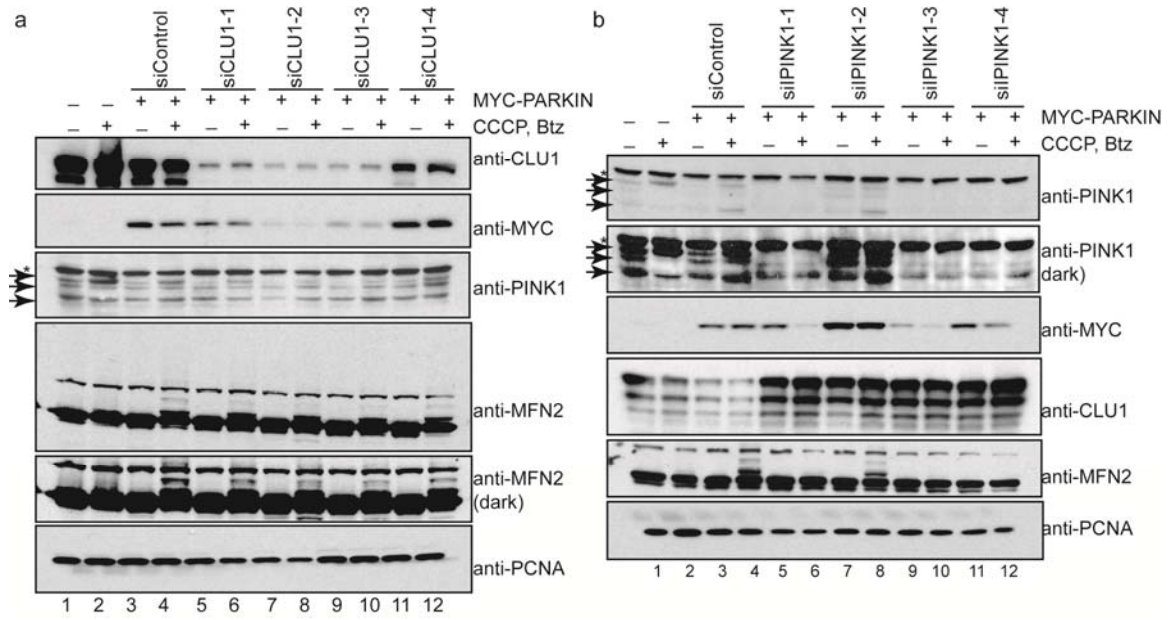


**Figure 3.9 Effects of CLU1 depletion in HeLa cells. a**, siRNA-mediated depletion of CLU1 in HeLa cells diminished MFN2 ubiquitylation and may decrease total PINK1 and PARKIN levels. **b**, siRNA-mediated depletion of PINK1 in HeLa cells abolishes MFN2 ubiquitylation. PINK1 loss appears to increase total levels of CLU1 and may decrease total PARKIN levels. Cells are treated with 1 h of CCCP (10μM) or CCCP (10μM) and Btz (1μM). *, non-specific band recognized by α-PINK1 antibody. Arrows indicate PINK1 forms (full-length, 63kD; ΔMTS, 60kD; and PARL-cleaved, 52kD).

drastically increased in the absence of PINK1 (Figure 3.9b). It is possible that CLU1 and PINK1 may physically interact in a manner that supports the other's stability, though we need further studies to fully understand this data. Of interest, we also noted that MYC-PARKIN levels varied considerably in the absence of PINK1 and CLU1, corresponding to the degree of knockdown (Figure 3.9a, b). There have been a few reports suggesting that PINK1 regulates total PARKIN cellular levels (Um et al., 2009), however, until we repeat this result in cells stably expressing PARKIN, we cannot rule out variability due to transfection.

### 3.3 Discussion

Loss-of-function mutations in PINK1 are associated with genetic Parkinson's disease (Valente et al., 2004). PINK1 and PARKIN have been shown to function in the same pathway to maintain mitochondrial fitness thus further supporting the model for mitochondrial dysfunction in Parkinson's disease. The process of PINK1 and PARKIN-mediated remodeling of the

mitochondrial membrane after depolarization is an important step in the progression of mitophagy and our aim is to better understand how this signaling is regulated. We know that the PINK1 kinase can recruit PARKIN to the mitochondria to facilitate ubiquitylation on the mitochondria after membrane depolarization, however, it is currently being debated as to whether PINK1-dependent phosphorylation of PARKIN is direct or if another substrate might contribute toward mitochondrial translocation and activity of Parkin. Here we describe the results of PINK1 interaction proteomics both before and after mitochondrial depolarization, revealing the context in which PINK1 functions in cultured cells.

Our analysis revealed an interaction with the translocase of the outer membrane complex (Figure 3.4b). This interaction was recently reported by another laboratory using native gels to demonstrate that endogenous PINK1 binds the TOMM complex on depolarized mitochondria, a scenario which is proposed to allow rapid reimport of PINK1 in order to rescue repolarized mitochondria from mitophagy (Lazarou et al., 2012). Interestingly, we found that PINK1 interacted with approximately equivalent amounts of TOMM subunits both in the presence and absence of depolarization. It is possible that our method is more sensitive thus more likely to identify the interaction. It is also possible that overexpression of PINK1 in our assay could be increasing the amount of full-length PINK1 available for binding – possibly it is overwhelming the PINK1 processing machinery. However, western blot analysis of our stable C-terminally tagged PINK1 cell lines showed that processing appeared to occur as expected – we saw the expected increase in full-length PINK1 after CCCP treatment and the cleaved 52 kD form after proteasome inhibition (Figure 3.4a). Regardless of this discrepancy, our data is in agreement with the finding that PINK1 strongly interacts with the TOMM complex, with the highest scoring interactors including TOMM40, TOMM70, TOMM22, and TOM20, which was shown to mediate the interaction with PINK1 (Lazarou et al., 2012).

Though the interaction with the translocase was exciting, we were very intrigued by the identification of CLU1 as a candidate PINK1 high confidence interacting protein. Based on the

data available about its role in Drosophila and yeast (Cox and Spradling, 2009; Fields et al., 1998), we think CLU1 may potentially control the activity, localization properties, or cytoskeletal interactions of PINK1. Furthermore, because we showed the genetic interaction between CLU1 and both PINK1 and PARKIN, we expect that CLU1 is important for PINK1-PARKIN function in human cells, as it appears to be in Drosophila. To date, we have confirmed the interaction with PINK1 in two cell types and determined that loss of CLU1 drastically affects mitochondrial morphology and may have an effect on PINK1 activity (Figure 3.5, Figure 3.8, Figure 3.9). Though our study is not yet complete, we are interested in determining in detail how CLU1 is affecting the mitochondria. There are numerous ways in which CLU1 may be linked to the PINK1/PARKIN pathway. First, loss of CLU1 may cause damage to the mitochondria, resulting in loss of membrane potential, thus activating the PINK1/PARKIN response. It is likely that the phenotype observed upon CLU1 knockdown may affect membrane potential similarly to the way MFN1/2 knockout does through an effect on fusion/fission cycles. The increase in total cellular mitochondria that we observe may be the result of a fission defect, possibly a defect late in mitochondrial fission of the MOM, an explanation offered for the phenotype in *cluA*-Dictyostelium (Fields et al., 2002). However, we do observe a direct interaction of PINK1 with CLU1, suggesting that the relationship between these proteins is more than just indirect activation of PINK1 by mitochondrial damage.

A second way in which CLU1 might be affecting PINK1 is through a scaffolding or regulatory role, which might ultimately affect PINK1 activity. The CLU domain and TPR repeats found in CLU1 are highly conserved in eukaryotic CLU1 orthologs, indicating that they are likely extremely important for CLU1 function. In fact, rescue of the null requires the full-length protein in Dictyostelium, further underscoring the importance of each domain, however, the precise function of the CLU domain remains unknown (Fields et al., 2002). In Dictyostelium, *cluA* may regulate interaction with microtubules (Fields et al., 2002). A dysregulated interaction with microtubules could also explain the mitochondrial clustering seen in yeast and Dictyostelium

upon knockout. Mitochondrial movement is regulated by engagement of plus-end-directed Kinesin motors and minus-end-directed Dynein motors. Because most membranous organelles are moved around the cell by trafficking via microtubules, any interference with this pathway could easily lead to abnormally situated or possibly unhealthy mitochondria – proper mitochondrial movement and distribution are critical for their localized function in cell metabolism, growth, and survival. CLU1 is thought to be a cytoplasmic protein; therefore, we need to understand where it might be interacting with PINK1. It is possible that CLU1, PARKIN, and PINK1 interact at the mitochondrial interface with motor proteins on microtubules thus potentially regulating mitochondrial movement by bridging different motors and transport systems. Such regulation can also be important for maintenance of healthy mitochondria. For example, fusion events can occur when two mitochondria are in close proximity, allowing exchange of soluble intermembrane and matrix proteins (Liu et al., 2009b). Furthermore, fusion can allow damaged mitochondria to merge with healthy mitochondria and be restored through mixing of contents. These events both require and promote mitochondrial motility and contribute fundamentally to mitochondrial maintenance. Furthermore, mitochondria are typically found distributed along cytoplasmic microtubules and evidence has shown that intact microtubule/mitochondrial interaction may be necessary for proper mitochondrial biogenesis (Karbowski et al., 2001).

In the case of neurons, loss of the ability to transport and localize mitochondria correctly could be particularly deleterious. Research has shown that disruption of microtubules decreases membrane potential and alters $Ca^{2+}$ levels in neuronal mitochondria in addition to interfering with necessary mitochondrial and ER contacts mediated by microtubules (Mironov et al., 2005). Additionally, microtubules are required for axonal transport of mitochondria, a pathway to which PINK1 and PARKIN have already been linked through interaction with RHOT1 and kinesin heavy chain (Wang et al., 2011b). The tetratricopeptide repeats present in CLU1 also suggest that it may play some sort of scaffolding role as they are primarily found to mediate protein-

protein interaction, often contributing to the assembly of multiprotein complexes (Das et al., 1998). TPR repeat regions are involved in a variety of biological processes, including mitochondrial protein transport – they are found in TOMM70 and thought to be required for recruitment of soluble proteins to the mitochondrial surface essential for maintaining mitochondrial shape (Kondo-Okamoto et al., 2008). It is possible that CLU1 may play a role in linking PINK1 and PARKIN with the microtubule network and possibly contribute to mitochondrial homeostasis. Further studies are necessary to determine how loss of CLU1 may affect mitochondrial membrane potential as well as motility.

Our first approach for studying CLU1 though interaction proteomics has proven challenging since CLU1 did not appear to reproducibly interact with any proteins. Furthermore, truncation mutants designed to examine the individual domains also showed few reproducible interactors. It may be that expressing a tagged version of CLU1 interferes with either its own folding or its potential scaffolding function. We will need to perform further experiments using different approaches to understand CLU1's functions. Amongst the data necessary to collect includes determining how loss of CLU1 affects membrane potential, cell cycle, and PINK1 localization. Fractionation experiments or native gel assays from whole cell lysate will be useful in determining CLU1 interactors. Because the mechanism by which PINK1 recruits PARKIN to mitochondria is still unclear, we will determine whether loss of CLU1 affects the kinetics of PARKIN recruitment to mitochondria after PINK1 activation, a possibility supported by the interaction data from *Drosophila*. Additionally, we are developing an in vitro kinase which will allow us to examine PINK1 activity using phosphorylation of PARKIN as a readout. We are using a baculovirus produced in the Shokat lab expressing PINK1 together with chaperone protein TRAP1, which allows active PINK1 kinase to be purified.

PINK1 acts as a pivotal regulator of mitochondrial quality control through numerous avenues. In conjunction with PARKIN and the autophagy machinery, PINK1 effectively removes unhealthy mitochondria from the cell. Failure of this ultimate stage of quality control leads to cell

death. Therefore, identification and characterization of PINK1 interacting proteins, such as CLU1, is also critical in understanding how cells maintain a healthy mitochondrial population. Thus, PINK1, and potentially CLU1, plays a fundamental, multifactorial role in mitochondrial homeostasis, study of which will prove effective for better understanding the pathology and treatment of Parkinson's disease.

# CHAPTER 4

**Significance and Future Directions**

## 4.1 Significance

Mutations in PARKIN or PINK1 are the most common causes of recessive familial parkinsonism. These proteins form a mitochondria quality control pathway that identifies dysfunctional mitochondria, isolates them from the mitochondrial network, and promotes their degradation by autophagy. Our study provides the first quantitative description of the PARKIN-modified proteome, including the identification of hundreds of ubiquitylation sites in candidate PARKIN targets. This information holds the potential to reveal countless aspects of mitochondrial quality control and regulation, some of which we have started to explore and develop for future projects. Additionally, we have demonstrated that diGly capture proteomics can be used to identify substrates of a single E3 in a signal-dependent manner. Additionally, we have established numerous assays, including a new approach for studying PARKIN-dependent ubiquitin transfer to MOM substrates *in vitro*, which will allow the lab to continue to explore the wealth of data our study has produced. Our data physically links PARKIN targets to mitophagy and quantitatively describes the magnitude of depolarization-dependent ubiquitylation. Furthermore, we have created a map depicting the topology and landscape of PARKIN action on the MOM as well as on an assortment of previously unrecognized cytoplasmic proteins. Finally, we have created a web resource which provides public access to all of our diGly data. We hope this will provide a valuable resource for the PARKIN field, which can be used to interrogate the structural biology and dynamic changes that occur in the PARKIN-modified proteome.

In parallel, we have sought to expand current knowledge of PINK1's role in this pathway and have identified a novel interactor, CLU1, shown to regulate mitochondrial morphology in lower eukaryotes. Our data suggests that CLU1 may function to regulate PINK1 activity and contributes to mitochondrial maintenance in mammalian cells. This protein may represent a newly identified node of regulation for the PINK1/PARKIN pathway which we have yet to fully understand. Though our work is removed from the direct alleviation of the distress of a

Parkinson's-afflicted patient, we believe that in order to truly treat or attempt to cure Parkinson's, it is essential to understand the molecular basis of the disease. Though great advances in managing Parkinson's disease have been made in the last few decades, dopamine replacement remains the most potent drug for controlling PD symptoms. However, it is associated with numerous side-effects after prolonged treatment, including loss of efficacy. Knowledge of the contributions of disparate genetic and environmental factors to development of PD continues to be expanded, thus highlighting the need for individualized and tailored treatment options. This further underscores the need to fully understand the molecular origins of the disease. We began with a global approach to define the altered landscape of the cellular proteome upon mitochondrial depolarization. The role of mitochondrial dysfunction in neurodegenerative disease is currently an area of intense study since perturbation of these vital organelles can affect energy production, free radical generation, $Ca^{2+}$ buffering, and cell death, ultimately leading to the failure of dopaminergic neurons in Parkinson's disease. Our approach has helped us identify numerous new subjects of interest spanning the entirety of the PINK1/PARKIN pathway which will be introduced in the following section.

The roles of PARKIN and PINK1 have been established in the turnover of damaged mitochondria and possibly other processes linked with reactive oxygen species and even tumorigenesis. Nevertheless, the actual physiological substrates of PARKIN's ubiquitin ligase activity important for its quality control functions have been poorly defined until now. We expect the compendium of validated PARKIN targets we have constructed to have significant impact in the field. Because the majority of previously published PARKIN targets have not been successfully validated, it has been difficult to move forward with an understanding of PARKIN function and potential therapeutic modalities. Our studies have provided a validated list of candidate substrates for further analysis by the field. We also believe it will be incredibly useful to develop reagents (i.e. antibodies or proteomic standards) that will allow detection of ubiquitylation of validated PARKIN targets in various disease tissues, potentially revealing

defects in the PARKIN system in a clinical setting. Finally, the ultimate application of our work would be to provide opportunities for development of therapeutics that circumvent a role for PARKIN or PINK1 in promoting mitochondrial and neuronal health.

## 4.2 Future Directions

### 4.2.1 CALCOCO2, TAX1BP1, LC3C, and TBC1D15 may link mitochondria and autophagy machinery

Despite extensive investigation by numerous groups, much of the detail of the mitophagy pathway – from specific steps in initiation to details of autophagy regulation – remains a mystery. Though it will involve effort from multiple labs and many years to construct a full and detailed map of the pathway, we have selected a number of pressing unanswered questions on which to focus our future studies. In order to place in context the PARKIN substrates that we have identified, we intend to further develop our RNAi-screening strategy. We have identified proteins which may be important in the initial translocation of PARKIN to the mitochondria as well as proteins which may have a role in the overall progression of mitophagy. We intend to follow-up on the initial list of hits for both screens through targeted studies of the individual genes of interest. One way to do this will include examining the requirement for PARKIN-mediated ubiquitination of these candidate substrates via RNAi depletion experiments in conjunction with rescue using substrates lacking the lysine of interest. Certain subsets of these genes are of particular interest, particularly those which may play roles as autophagy adaptors (TAX1BP1, CALCOCO2, and SQSTM1).

TAX1BP1 and CALCOCO2/NDP52 are structurally related and may work together to bridge ubiquitylated mitochondria with the autophagy machinery. CALCOCO2 was shown to interact with the ATG8 protein LC3C via an LC3-interacting region (LIR) to promote autophagic clearance of *Salmonella* (Thurston et al., 2009). Staining of LC3 is often used to demonstrate colocalization of a protein or organelle of interest with autophagosomes; however, though some studies have demonstrated colocalization of damaged mitochondria and LC3B, the degree of

overlap is generally unimpressive. We believe this may be because LC3C, for which efficient antibodies do not yet exist, may actually be the ATG8 protein associated with mitophagy. Both TAX1BP1 and CALCOCO2 are highly enriched in purified autophagosomes and immunofluorescence experiments indicate that the endogenous proteins colocalize with autophagosomes (Newman et al., 2012; Thurston et al., 2009). In support of a role for these proteins, we have found that both CALCOCO2 and TAX1BP1 are ubiquitylated in a PARKIN-dependent manner and associate stably with PARKIN in the presence of BafA. In addition, TBC1D15, a candidate RAB GAP, is ubiquitylated in a PARKIN-dependent manner, interacts with FIS1 on the MOM (Onoue et al., 2012), binds PARKIN in the presence of BafA, and interacts with the ATG8 isoform GABARAP in a LIR-dependent manner (Behrends et al., 2010). Our preliminary RNAi-mediated depletion experiments suggest that loss of LC3C or the combined absence of CALCOCO2 and TAX1BP1 results in a delay in clearance of mitochondria. In combination with LC3C depletion and colocalization experiments, we hope to show that these proteins are involved in mitochondrial clustering or targeting the delivery of ubiquitylated mitochondria to the autophagosome for destruction.

### 4.2.2 Non-specific ubiquitylation on the mitochondrial surface may trigger mitophagy

We have repeatedly identified a cohort of mitochondrial outer membrane proteins as both substrates and interactors of PARKIN; therefore, it seems that PARKIN could be targeting a specific population of proteins after mitochondrial depolarization. However, though it is very possible that PARKIN does recognize specific substrates, perhaps through cooperation with varied E2 or scaffolding proteins, we cannot rule out the possibility that once activated, PARKIN may ubiquitylate nonspecifically. Using motif-x, we were unable to identify any pattern similarities in the ubiquitylation sites of Class 1 PARKIN targets, the highest confidence substrates. Additionally, ubiquitylation occurred on α-helices, β-sheets, and globular domains of these proteins with the most apparent similarity being that many were located on the

mitochondrial outer membrane. This has led us to consider the possibility that ubiquitin density on mitochondria as opposed to site-specific ubiquitylation is central to mitophagy. Fusion of a ubiquitin G76V mutant to peroxisomal membrane proteins was shown to be sufficient to induce their selective autophagy if ubiquitin was extended into the cytosol (Kim et al., 2008a), supporting the notion that this process may be regulated more by the presence of ubiquitin rather than exactly where the ubiquitin is conjugated.

To attempt to test this alternative hypothesis, we are developing reagents to use a chemical dimerizer approach to directly examine the effects of targeting ubiquitin to the mitochondria in the absence of depolarization. Similar to a previously published report (Komatsu et al., 2010), we have created cell lines expressing TOM20-YFP-FRB which dimerizes with CFP-FKBP-ubiquitin upon the addition of a rapalog, thus promoting recruitment of the FKBP construct to the mitochondrial outer membrane. This approach has been attempted by one group using transient co-transfection of UbG76V-EGFP-FKBP and a FRB-FIS1 construct (Narendra et al., 2010a). Though ubiquitin was observed at the mitochondrial membrane, no detectable reduction in mitochondrial mass was observed after 24 hours of rapalog treatment. We intend to further optimize this approach, first by stably expressing all of the FRB and FKBP constructs in HeLa cells to reduce variability inherent in transient transfection. Second, we are developing a variety of constructs that will allow us to test this model using recruitment of various types of ubiquitin chains to the MOM. We will fuse the FKBP protein to non-hydrolyzable tetra Ub or mono-Ub, or to degrons that are constitutively ubiquitylated with the desired chain types, thus allowing us to create a system in which levels of ubiquitin on the MOM can be temporally controlled independently of depolarization. Because PARKIN appears to be capable of constructing both K48- and K63-linked chains, we will attempt to target both of these chain types to the mitochondria. CFP-FKBP will be expressed in fusion with a degron from surfactant protein C (SPC) that is recognized by the WW-domain of the NEDD4 ubiquitin ligase, a constitutively active E3 (Conkright et al., 2010; Kotorashvili et al., 2009). A well-characterized

lysine residue in SPC will serve as the site of constitutive K63 poly-ubiquitylation, which can be targeted to the mitochondria upon the addition of a rapalog. We will also attempt to create K48-linked chains at the mitochondria using a similar approach employing the fusion of CFP-FKBP with a constitutively phosphorylated transferable degron containing lysine recipient sites for SCF-βTRCP from Vpu (phosphorylated by CK1) or employ an auxin-inducible degron (AID) system which uses a small molecule to conditionally control ubiquitin chain assembly (Estrabaud et al., 2007; Nishimura et al., 2009). If we are able to successfully observe ubiquitylation at the mitochondria, we will be able to use this system to measure the kinetics and saturation of the ubiquitin/degron-CFP-FKBP loading onto mitochondria (with and without BafA to block degradation) as well as mitochondrial clustering, total area, and co-localization of mitochondria with ATG8-positive autophagosomes as a measure of mitophagy. This effort will allow us to address our alternative hypothesis that ubiquitin density rather than site-specific ubiquitylation is the rate-limiting signal in mitophagy.

However, the induction and progression of mitophagy is likely not quite so simple. Some proteins, for example, MFN1/2, are degraded in a PARKIN-dependent manner prior to mitophagic clearance of mitochondria. There must be some way in which these proteins are being targeted for degradation while others create a signal for autophagy. This may be through the different chain linkages which PARKIN is presumably attaching to these proteins, thus highlighting another area of interest.

### 4.2.3 Determination of PARKIN chain linkages *in vivo* and *in vitro* PARKIN activation and mechanism

One extremely important aspect of PARKIN biology which needs to be better understood is the type of ubiquitin chain linkages PARKIN creates and how PARKIN directs construction of these specific linkages on, presumably, specific substrates. An understanding of the functional and mechanistic basis for chain-linkage specific PARKIN-mediated poly-ubiquitylation will provide us with an understanding of the molecular mechanisms underlying PARKIN function

and how PD mutations might affect mitochondrial homeostasis. Investigation of this question is linked to improving our understanding of how PARKIN is activated and the enzymatic mechanism though which PARKIN ligase activity is controlled. We have proposed a few ways in which to explore these questions which combine proteomic and genetic approaches.

Previous work has shown that PARKIN may catalyze K6-, K27-, K48- and K63-linked chains (Chan et al., 2011; Durcan et al., 2011; Geisler et al., 2010). It is a mystery and also somewhat controversial as to how one E3 ligase is able to do this; however, little is actually known about the mechanism of PARKIN activity. Ubiquitin chain-type specific antibodies have been used in the past to examine PARKIN substrates, but at present, antibodies targeting only 3 out of 7 chain types are available. We want to systematically and quantitatively examine the ubiquitin chains present after PARKIN activation using multiplex AQUA proteomics the employ heavy-labeled diGly peptides corresponding to the 7 possible lysine linkages in ubiquitin (Kirkpatrick et al., 2005a). We believe we can examine the types of chains present on purified mitochondria as well as purified PARKIN substrates, and PARKIN itself. Furthermore, we can combine AQUA proteomics with our *in vitro* ubiquitylation system to precisely and quantitatively monitor PARKIN-dependent chain formation.

### 4.2.4 Mechanism of PARKIN activation and effects of disease mutations

The study of how PARKIN directs specific chain linkages is intertwined with the investigation of PARKIN enzymatic function on a mechanistic level. The mechanism of the RING-IBR-RING family of E3 ligases, of which PARKIN is a member, is poorly understood. Furthermore, the recent identification of a HECT-like active site in PARKIN demonstrates the enigmatic nature of this enzyme. Dissection of the enzymatic mechanism by which PARKIN functions and determining whether it behaves *in vivo* as it has been shown to *in vitro* is crucial. We have already discussed recent studies which suggest that PARKIN exists in an auto-inhibited form until activation. Our data supports the model that upon mitochondrial damage,

PARKIN becomes activated in a process that requires phosphorylation by PINK1 (likely on multiple sites) and the active site Cys of PARKIN. We will further investigate this process in cells and *in vitro* while optimizing the *in vitro* ubiquitylation system we have already developed in combination with biochemical and cell biological assays.

It is still unclear how PARKIN's E3 function is activated in response to mitochondrial damage and, once activated, how PARKIN maintains substrate specificity and chain linkage specificity. Ser65 of PARKIN, which lies within the UBL domain, was recently reported as a PINK1 phosphorylation site required for the activation of ubiquitin transfer *in vitro*. However, we have found that Ser65 is not absolutely required for PARKIN recruitment to mitochondria, ubiquitylation of MFN2, or association with a host of ubiquitylation targets Indeed, we have found that removal of the UBL domain resulted in increased interaction of PARKIN with MOM proteins, however, upon depolarization, this mutant was further stimulated, suggesting that there is an activating signal that occurs outside of the UBL domain. We have found additional phosphorylation sites as well as ubiquitylation sites within PARKIN which we believe may be important in its activation and are in the process of creating point mutations in these sites in order to determine their effects which we will test both *in vivo* and *in vitro*.

We can perform these assays in parallel with functional studies using an array of PD-patient derived PARKIN mutations. To determine how particular PARKIN mutants are defective, we will assess the kinetics of translocation via microscopy as well as activity *in vitro*, thus also allowing the use of quantitative proteomics to determine the kinetics and type of ubiquitin chain assembly. We already have a panel of 9 different PARKIN patient mutations spanning the length of the protein (R33G, R42P, K161N, K211N, T240R, R275W, G328E, G430D and C431F) stably expressed in multiple cell lines with which we can begin these analyses. Though these targeted analyses, we can contribute towards an understanding of how these mutations impact PARKIN activity and disease progression. Taken together, these studies will help us expose the functional roles and complexity of the PARKIN-modified proteome and provide new

insights into PARKIN's mechanism of action, which may also be applicable to other RING-IBR-RING family members.

### 4.2.5 Role of PARKIN-mediated ubiquitylation on mitochondrial trafficking and fusion

Ubiquitylation is often associated with protein degradation as an end point; however, ubiquitin operates in dynamic signaling systems whose ultimate function is often non-degradative but regulatory. We know that PARKIN and PINK1 are key components of the signaling pathway that controls mitochondrial homeostasis after depolarization. This regulation is carried out both by targeted protein degradation and alterations in mitochondrial dynamics. For example, known targets of PARKIN include the mitochondrial outer membrane proteins, MFN1/2 and the RHOT1/2 Miro GTPases, which alter mitochondrial fission-fusion cycles and trafficking on microtubules respectively (Chen et al., 2003; Wang et al., 2011b). Ubiquitylation and degradation of the Mitofusin proteins is thought to halt fusion-fission cycles, thus promoting sequestration of the damaged population of mitochondria which can then be efficiently targeted by the autophagy machinery. Furthermore, RHOT1 and RHOT2 regulate kinesin-dependent mitochondrial trafficking on microtubules and are targeted for ubiquitin dependent turnover by the PINK1-PARKIN pathway after mitochondrial damage (Glater et al., 2006).

A critical factor in demonstrating the utility of the data we have generated is to reveal the biological significance of ubiquitylation sites identified on PARKIN-modified proteins. To begin this process, we want to evaluate the effects of site-specific ubiquitylation of MFN1/2 and RHOT1/2. We have created arginine point mutations for all of the lysines found modified via QdiGly analysis in these proteins and will test whether the kinetics of turnover in HeLa cells is affected or blocked completely after mitochondrial depolarization. Examination of functional effects of site mutations in the Mitofusin proteins will be tested via observation of mitochondrial dynamics and fragmentation after depolarization to determine whether the kinetics of these processes are altered. We will also collaborate with the Schwarz lab (Children's Hospital) to test

the effects of Lys-to-Arg mutations in RHOT1/2 on mitochondrial trafficking on microtubules in axons of hippocampal neurons using live-cell imaging. If these sites are important, we would expect to observe a loss in mitochondrial trafficking upon PARKIN activation.

### 4.2.6 Role of CLU1 in mitochondrial homeostasis and the PARKIN and PINK1 pathway

Much of chapter three focused on the identification of a novel PINK1 interacting protein, CLU1, which is genetically implicated in mitochondrial dysfunction in mammals and *Drosophila* and which appears to be required for proper mitochondrial morphology. We do not yet fully understand the role of CLU1 in these processes and therefore plan to continue to explore and characterize it. There are a number of questions to address, including whether CLU1 may be a PINK1 substrate, if it truly affects PINK1 kinase activity, and how it is regulating mitochondrial morphology. We intend to address these and further questions using the assays we have developed to test CLU1 effects on PINK1 and PARKIN activity *in vivo* and *in vitro.* Additionally, we will address whether CLU is required for PARKIN-mediated ubiquitylation events

### 4.2.7 The need to study the PARKIN/PINK1 pathway in neurons

Cell culture models are indisputably useful in discerning the molecular mechanisms of biological pathways. Because mitochondrial quality control is universally important, studying it in numerous cell types allows us to determine those aspects of the pathways which are generally important as well as those that may be cell- or tissue-type specific. To advance the Parkinson's field faster, our data now needs to be applied to more physiological models of disease. Though Parkinson's disease elicits systemic effects as evidenced by global defects in null animal models, much of the impairment of motor function may develop in part due to the accumulation of mitochondrial damage in neurons, thus it is essential to validate our data in these cell types as well as begin functional studies. It is not clear why neurons of the substantia nigra are so sensitive to the triggers of PD, be they genetic or environmental, thus highlighting the need to study the PINK1/PARKIN pathway in relevant cell types. Determination of the PARKIN

ubiquitylome in primary cells, such as neurons, would likely be very technically challenging. Therefore, the lab will attempt profiling of PARKIN targets in iPS cells derived from PD patient fibroblasts harboring a PARKIN deletion mutation. This approach will allow us to validate and extend our site-specific data and test these sites and identified substrates via cell biological assays in relevant models.

### 4.2.8 Concluding remarks

There are so many fascinating aspects of the PINK1/PARKIN pathway that have not yet been well defined, and undoubtedly many more that have not even been identified. Our contribution to this field includes the systematic analysis of PARKIN substrates and interacting proteins and the development of a comprehensive compendium of PARKIN targets, which we hope will serve as a resource for the PD field. Along the way, we have also explored more focused areas of PARKIN and PINK1 biology illuminating the complexity of PARKIN regulation and perhaps creating as many new questions about the pathway as we have addressed. Evidence clearly demonstrates the crucial role of specific mitochondrial functions in maintaining neuronal integrity, emphasizing the need to understand the molecular basis of mitochondrial maintenance and the mechanisms and targets of the PINK1-PARKIN pathway. The overall driving force of our research persists - the pressing need for insight into the pathogenesis of PD in order to accelerate understanding of PARKIN, PINK1, and mitochondrial homeostasis in Parkinson’s disease.

# CHAPTER 5

## Materials and Methods

**Cell culture**

For all experiments excluding SILAC, 293T and HeLa cells were grown at 37°C in Dulbecco's Modified Eagle medium (DMEM) supplemented with 10% (v/v) FBS (Gibco).

**Antibodies**

The antibodies used are as follows: anti-HA (Covance, 16B12), anti-PCNA (Santa Cruz, sc-56), anti-TOMM70, (Proteintech, 14528-1); anti-MFN2, (Epitomics, 3272-1 or Sigma, WH0009927M3); anti-ADRM1, (Enzo Scientific, BML-PW9910); anti-Rpn10, (Enzo Scientific, BML-PW9250); anti-HK1, (Cell Signaling, C35C4); anti-PSMD2, (Affinity BioReagents, PA1-964); anti-PARKIN, (PRK8, Santa Cruz, sc-32282); anti-Myc, (9E10, Santa Cruz); anti-TOMM20 (Santa Cruz, FL-145 ); and anti-PINK1 (Novus Biologicals, BC100-494).

**Plasmids**

DONR223-open reading frames (ORFs) were either harvested from the mammalian genome collection (MGC) or were cloned from cDNA vectors (Open Biosystems, MGC) by PCR with KOD polymerase (Novagen). The wild-type PARKIN ORF was a gift from Brenda Schulman. PCR products were cloned in pDONR223 using the Gateway system (Invitrogen). For stable expression vectors, ORFs were recombined into the appropriate recipient/destination vector using λ-recombinase. All open reading frames were sequence validated.

**BP reactions**

2µl of PCR product, 1µl DONR (150ng/µl), 2µl 5X BP buffer (100mM Tris-HCl, pH 7.5; 20mM EDTA; 30mM spermidine; 25% glycerol; 225mM NaCl), and 1µl BP enzyme were mixed with H2O to 10µl. The reactions were incubated at RT for several hours or overnight. Reaction products were then transformed into 20µl of competent DH5alpha cells and plated on Spectinomycin. Individual colonies were picked, miniprepped, and sequence verified. ORFs in pDONR were sequenced using M13 For (-21) and M13 Reverse (Invitrogen).

**LR Reactions**

1µl of DONR plasmid, 1µl destination/recipient plasmid (150ng/µl), 1µl 5X LR buffer 1µl H2O, and 1µl LR clonase were mixed and incubate at RT for several hours or overnight. Reaction products were transformed into competent DH5alpha cells and plate on Carbenicillin. Individual colonies were picked, miniprepped, and verified by BsrGI digest (NEB). For viral production, ORFS were cloned into either MSCV-N-HA-Flag-GAW-IP (Gateway Ires-Puro), pHAGE-N-HA-Flag-GAW, pHAGE-C-HA-Flag-GAW, or pHAGE-N-eGFP-GAW.

**Site-Directed Mutagenesis**

pDONR223-PARKIN was used as a template for PCR with KOD polymerase (Novagen). The reaction was performed as described by the manufacturer except 5uM of each primer was used; primers are listed in Table 5.1. PCR reaction products were incubated with 2µl DpnI for several hours to overnight at 37°C. 2µl of the DpnI-treated PCR products were transformed into 20µl competent DH5alpha cells and plate on Spectinomycin. Single colonies were picked, prepped, and sequence verified.

**Sample preparation for diGly capture**

HCT116, HeLa or SH-SY5Y cells ($10^8$) were grown in lysine-free DMEM supplemented with 10% dialysed FBS (v/v) (Gibco), 2 mM L-glutamine, 1% (v/v) penicillin/streptomycin (Gibco) and light (K0) lysine (50 µg $ml^{-1}$), which contained no heavy isotopes. Heavy media was the same except the light lysine was replaced with K8-lysine (L-Lysine:2 HCl (u-13C6, 99%, u-15N2, 99%) (Cambridge Isotopes) at the same concentration (Kim et al., 2011)**.** Where indicated, cells were treated with Btz (1 µM), CCCP (10 µM), and/or BafA (50 nM) for the times indicated. After the indicated treatments, heavy and light cells were mixed 1:1 by cell number and lysed in 8 ml of denaturing lysis buffer (8 M urea, 50 mM Tris pH 8.2, 75 mM NaCl, protease inhibitors (EDTA-free), Roche). Samples were incubated on ice for 10 min and then

**Table 5.1 DNA primers for site-directed mutagenesis used in this study.**
For = forward, Rev = reverse.

| Construct | Primer | 5' - 3' |
|---|---|---|
| PARKIN S65A | For | TTGTGACCTGGATCAGCAGGCCATTGTTCACATTGTGCAG |
| | Rev | CTGCACAATGTGAACAATGGCCTGCTGATCCAGGTCACAA |
| PARKIN S65E | For | GAATTGTGACCTGGATCAGCAGGAGATTGTTCACATTGTGCAGAGAC |
| | Rev | GTCTCTGCACAATGTGAACAATCTCCTGCTGATCCAGGTCACAATTC |
| PARKIN K27R | For | ACACCAGCATCTTCCAGCTCAGGGAGGTGGTTG |
| | Rev | CAACCACCTCCCTGAGCTGGAAGATGCTGGTGT |
| PARKIN K27A | For | CCAGCATCTTCCAGCTCGCGGAGGTGGTTGCTAAGC |
| | Rev | GCTTAGCAACCACCTCCGCGAGCTGGAAGATGCTGG |
| PARKIN K48R | For | CGTGTGATTTTCGCAGGGAGGGAGCTGAGGAAT |
| | Rev | ATTCCTCAGCTCCCTCCCTGCGAAAATCACACG |
| PARKIN K48A | For | CGTGTGATTTTCGCAGGGGCGGAGCTGAGGAATGACTG |
| | Rev | CAGTCATTCCTCAGCTCCGCCCCTGCGAAAATCACACG |
| PARKIN UBL | For | TGGAGAAAAGGTCAAGAAATGTAGCCAACTTTCTTGTACAAAGTTGTCCCC |
| | Rev | GGGGACAACTTTGTACAAGAAAGTTGGCTACATTTCTTGACCTTTTCTCCA |
| PARKIN R33G | For | GGTGGTTGCTAAGCAACAGGGGGTTCCGG |
| | Rev | CCGGAACCCCCTGTTGCTTAGCAACCACC |
| PARKIN R42P | For | CGGCTGACCAGTTGCCTGTGATTTTCGCAGG |
| | Rev | CCTGCGAAAATCACAGGCAACTGGTCAGCCG |
| PARKIN K161N | For | AGTGCAGCCGGGAAATCTCAGGGTACAGTG |
| | Rev | CACTGTACCCTGAGATTTCCCGGCTGCACT |
| PARKIN K211N | For | GGACTAGTGCAGAATTTTTCTTTAATTGTGGAGCACACC |
| | Rev | GGTGTGCTCCACAATTAAAGAAAAATTCTGCACTAGTCC |
| PARKIN T240R | For | AGTCGGAACATCACTTGCATTAGGTGCACAGACGT |
| | Rev | ACGTCTGTGCACCTAATGCAAGTGATGTTCCGACT |
| PARKIN R275W | For | CTGTGTGACAAGACTCAATGATTGGCAGTTTGTTCACG |
| | Rev | CGTGAACAAACTGCCAATCATTGAGTCTTGTCACACAG |
| PARKIN G328E | For | TGTCCTGCAGATGGAGGGCGTGTTATGCC |
| | Rev | GGCATAACACGCCCTCCATCTGCAGGACA |
| PARKIN G430D | For | CAGTGGAAAAAAAATGGAGACTGCATGCACATGAAGTG |
| | Rev | CACTTCATGTGCATGCAGTCTCCATTTTTTTCCACTG |
| PARKIN C431F | For | TGGAAAAAAAATGGAGGCTTCATGCACATGAAGTGTCC |
| | Rev | GGACACTTCATGTGCATGAAGCCTCCATTTTTTTCCA |
| PARKIN C431S | For | GTGGAAAAAAAATGGAGGCAGCATGCACATGAAGTGTC |
| | Rev | GACACTTCATGTGCATGCTGCCTCCATTTTTTTCCAC |
| CLU1 1-390 | For | GGGGACAACTTTGTACAAAAAAGTTGGCATGCTCTTAAACGGGGACT |
| | Rev | GGGGACAACTTTGTACAAGAAAGTTGGGGTGAAGTCGCTGTGCAC |
| CLU1 390-640 | For | GGGGACAACTTTGTACAAAAAAGTTGGCATGACCGCGGCAGCCACCAGG |
| | Rev | GGGGACAACTTTGTACAAGAAAGTTGGGGAGGGGGTCTCCAGCTG |
| CLU1 641-975 | For | GGGGACAACTTTGTACAAAAAAGTTGGCATGTCCTCCCTGGAAAATGGT |
| | Rev | GGGGACAACTTTGTACAAGAAAGTTGGGGCCTTGGGGTTGACGTG |
| CLU1 975-1180 | For | GGGGACAACTTTGTACAAAAAAGTTGGCATGGCCTCGGATGCCTTCCATT |
| | Rev | GGGGACAACTTTGTACAAGAAAGTTGGCAGCTGCGTCTTGTAGATGGT |
| CLU1 975-1309 | For | GGGGACAACTTTGTACAAAAAAGTTGGCATGGCCTCGGATGCCTTCCATT |
| | Rev | GGGGACAACTTTGTACAAGAAAGTTGGGTATCCCTGCACGCTCGGA |

sonicated with 3 × 10 s pulses. We typically obtained 30–50 mg of total protein. Lysates were digested with trypsin as described previously with one modification (Villen and Gygi, 2008). Prior to trypsin digestion, lysates were diluted 1:1 with 50 mM Tris pH 8.2 to lower the urea concentration to 4 M and digested with 10 ng $\mu l^{-1}$ Lys-C (Wako) for 2 h at room temperature.

**Immunoprecipitation of diGly containing peptides**

Lyophilized peptides from 30–50 mg of digested proteins were resuspended in 1.3 ml of IAP buffer (50 mM MOPS pH 7.4, 10 mM $Na_2HPO_4$, 50 mM NaCl) and centrifuged at 14,000*g* for 5 min to remove any insoluble materials. The supernatant was incubated with anti-diGly antibody coupled to protein A agarose or acrylamide beads for 1 h at 4 °C and washed with IAP buffer 3× and once with PBS as described previously (Kim et al., 2011). Peptides were eluted by treatment with 50 µl of 5% formic acid for 10 min twice. The eluted peptides were desalted using C18 stage-tip method and resuspended in 5% formic acid before mass spectrometric analysis. Lysates were subjected to immunoprecipitation sequentially two or four times, unless otherwise noted in Supplementary Table 1.

**Mass spectrometry analysis of diGly peptides**

Peptides were separated on 100 µm × 20 cm C18 reversed phase (Maccel C18 3m 200A˚ , The Nest Group) with a 165 min gradient of 6% to 27% acetonitrile in 0.125% formic acid (Haas et al., 2006). The twenty most intense peaks from each full mass spectrometry (MS) scan acquired in the Orbitrap Velos (Thermo) were selected for MS/MS (see RAW files for specific settings).

Sequest-based identification using a Human UNIPROT database followed by a target decoy-based linear discriminant analysis was used for peptide and protein identification as described (Eng et al., 1994; Huttlin et al., 2010; Kim et al., 2011). Localization of diGly sites used a modified version of the *A*-score algorithm (Beausoleil et al., 2006) as described (Kim et al., 2011). *A*-scores > 13 were considered localized. SILAC-based site quantification and signal-to-noise was performed as described previously (Kim et al., 2011) by using extracted ion chromatograms. The heavy- and light-labelled peptides from each search were subsequently combined using custom scripts. Other parameters used for database searching include: 50 p.p.m. precursor mass tolerance; 1.0 Da product ion mass tolerance; tryptic digestion with up

to three missed cleavages; and variable oxidation of Met (+15.994946). For an individual peptide to be used for quantification of sites and proteins, it had to meet one of two conditions: (1) both heavy and light isotopic envelopes must be detected with signal-to-noise ratios above 5.0; and (2) one isotopic envelope (heavy or light) must have a signal-to-noise ratio above 10.0. Equal mixing ratios for heavy to light cells were confirmed by calculating the mean $\log_2$(H:L) ratios in non-diGly non-lysine containing peptides and subtracting that from the corresponding $\log_2$(H:L) diGly ratios if necessary. Keratins were removed from site lists. Contributions of peptide identifications to various protein isoforms were condensed into a single UniProt descriptor using principles of parsimony.

**Interaction Proteomics**

Interaction proteomics was performed essentially as described previously, but with small modifications (Sowa et al., 2009). Briefly, 293T or HeLa cells were transduced with a lentiviral vector expressing HA–Flag–PARKIN (NP_004553.2), PINK1 (NP_115785.1), CLU1 (NP_056044.3), or the designated PARKIN or CLU1 mutants, and stable cell lines selected in puromycin. Cells from 4 × 15 cm dishes at 80% confluence were treated with CCCP (10 μM) (Sigma Aldrich), Btz (1 μM), and/or BafA (50 nM) (Sigma Aldrich) as indicated. Btz was a gift from Millennium Pharmaceuticals. After the indicated time, cells were collected and lysed in 3 ml of 50 mM Tris-HCl (pH 7.4), 150 mM NaCl, 0.5% Nonidet P40, and protease inhibitors. Cleared lysates were filtered through 0.45μm spin filters (Millipore Ultrafree-CL) and immunoprecipitated with 30 μl anti-HA resin (Sigma). Complexes were washed 4× with lysis buffer, exchanged into PBS for a further three washes, eluted with HA peptide, reductively carboxymethylated, and precipitated with 10% trichloroacetic acid (TCA)**.** TCA-precipitated proteins were trypsinized, purified with Empore C18 extraction media (3 M), and analyzed by liquid chromatography-tandem mass spectrometry (LC-MS/MS) with a LTQ-Velos linear ion trap mass spectrometer (Thermo) with an 18 $cm^3$ 125 μm (ID) C18 column and a 50 min 8–26% acetonitrile gradient.

All AP–MS experiments in 293T cells were performed in biological duplicates and for each biological experiment, complexes were analyzed twice by LC-MS to generate technical duplicates. AP–MS experiments in HeLa cells were performed on a single IP but with technical duplicates. Spectra were searched with Sequest against a target-decoy human tryptic UniProt-based peptide database, and these results were loaded into the Comparative Proteomics Analysis Software Suite (CompPASS) to identify high confidence candidate interacting proteins (HCIPs) (Sowa et al., 2009). Here, average assembled peptide spectral matches (APSMs) for each identified protein were used to determine weighted and normalized $D^N$-scores ($WD^N$-score) and *Z*-scores in a comparative analysis using a statistics table derived from analogous AP–MS data for 166 unrelated proteins. The $D^N$-score measures the reproducibility, abundance and frequency of individual proteins detected in each individual analysis.

To identify PARKIN-associated proteins, we filtered proteins at a 2% false discovery rate for those with a $WD^N$-score ≥ 1.0, *Z*-score ≥ 5, and average assembled peptide spectral matches (APSMs) ≥ 2 in both biological duplicates. In addition to the initially identified proteins, APSMs for interactors with $WD^N$-scores greater than 1 under at least one condition examined, or with a *Z*-score greater than 10 in both biological duplicates, were plotted in heat map form using Multi-experiment Viewer software (MeV). Due to space limitations, a subset of proteins which had a $WD^N$-score ≥ 1.0 in at least one experiment were omitted from Figures 2.12 and 2.14 but are contained in Supplementary Tables 3 and 4. TAX1BP1 that was identified in PARKIN immunoprecipitates and also found to be ubiquitylated but did not pass the stringent cut-off for passing our scoring scheme was also displayed in the heat map. We note that whereas several proteins passed the $WD^N$-score cut-off for PARKIN-associated proteins in the absence of depolarization in individual experiments, there was essentially no overlap within biological duplicates (Supplementary Table 4). In addition, for proteins with a maximum of 1–3 spectral counts, it is possible that those proteins were missed under some conditions due to stochastic sampling of low abundance proteins by LC-MS (for example, CYB5R3, TOM22, and

RHOT1 with wild-type PARKIN at 8 h post-CCCP in the presence versus the absence of BafA, Figure 2.12. The following proteins were identified in only 1 biological duplicate as being associated with PARKIN but were included in the heat map (Figure 2.12) as they are also present as Class 1 diGly targets: SQSTM1, TAX1BP1, TBC1D15, MYO6, VCP, RHOT2, HK2, MDH2, CYB5R3 and ACSL4.

For phosphoproteomic analysis, sequest-based identification using a Human UNIPROT database followed by a target decoy-based linear discriminant analysis was used for peptide and protein identification as described (Eng et al., 1994; Huttlin et al., 2010; Kim et al., 2011). Localization of phosphorylation sites used a modified version of the *A*-score algorithm (Beausoleil et al., 2006; Kim et al., 2011). *A*-scores/ Modscores > 13 were considered localized. Parameters used for database searching include: 2.0 Da product ion mass tolerance; tryptic digestion with up to two missed cleavages; carboxymethylation of Cys (57.021463), variable oxidation of Met (+15.994946), and phosphorylation of Ser, Thr, or Tyr (79.966330.

**Protein Interaction**

To validate interactions between PARKIN and candidate interacting proteins, 293T cells stably expressing HA–Flag–PARKIN were either left untreated or treated with CCCP (10 μM) or CCCP (10 μM) and Btz (1 μM) for 1 h. Extracts (50 mM Tris-HCl (pH 7.4), 150 mM NaCl, 0.5% Nonidet P40, and protease inhibitors) from cells were subjected to immunoprecipitation with anti-Flag resin (M2 agarose; Sigma), and washed complexes subjected to immunoblotting with the indicated antibodies. To examine MFN2 ubiquitylation, extracts from cells lysed in denaturing lysis buffer (8 M urea, 75 mM NaCl, 50 mM Tris (pH 8.0), and protease inhibitors) expressing the indicated HA–Flag–PARKIN mutant proteins were separated on a 4–12% gradient SDS-polyacrylamide gel (PAGE) and blotted with anti-HA or anti-MFN2. To examine PARKIN levels in the cell lines used, cells were lysed in denaturing lysis buffer and protease inhibitors and extracts subjected to SDS–PAGE and immunoblotting. To examine ubiquitylation

of candidate PARKIN substrates by immunoblotting, HCT116 cell lines stably expressing the candidate substrates C-terminally tagged with HA–Flag epitopes were transfected with either control siRNA or an siRNA targeting *PARKIN* After 72 h, cells were treated with CCCP (10 μM) with or without Btz to block proteasomal turnover of targets. At the indicated times, cells were lysed in 8 M urea and subjected to immunoblotting using anti-HA antibodies. Identical gels were run and probed with anti-PCNA as a loading control.

To validate interactions between PINK1 and CLU1, the indicated proteins were expressed in 293T or HeLa cells and lysed in lysis buffer (50 mM Tris-HCl (pH 7.4), 150 mM NaCl, 0.5% Nonidet P40, and protease inhibitors) and subjected to immunoprecipitation with anti-Myc resin (Sigma). Washed complexes were subjected to immunoblotting with the indicated antibodies.

**Virus Production**

For retroviral MSCV vectors, DNA was mixed 2:1:1 (MSCV-DEST:pCG-VSVG:pCG-GagPol) and transfected with Transit 293 Transfection Reagent (Mirus) into 293T cells. Media was changed 24 hours post-transfection and virus was harvest 48 hours post-transfection. Virus was filtered through 0.45μM filters and added to plated cells in the presence of 8mg/ml of polybrene. Twenty-four hours after infection, media was changed and 48 hours after infection, cells were split into the appropriate selection media.

For lentiviral pHAGE vectors, DNA was mixed 2:0.5:0.5:0.5:0.5 (pHAGE-DEST: HDM-Tat1b: HDM-VSVG: RC-CMV-Rev1b: HDM-Hgpm2). Virus was produced as described above.

***In* vitro ubiquitylation**

Purification of PARKIN: 293T cells stably expressing N-HA-PARKIN WT or C431S were treated with CCCP (10 μM) or CCCP (10 μM) and Btz (1 μM) for 1 h and lysed in 50 mM Tris-HCl (pH 7.4), 150 mM NaCl, 0.5% Nonidet P40, 1uM ubiquitin aldehyde, 1mM β-

glycerophosphate, 1mM NaF, 0.1uM Okadeic Acid, 1mM DTT, and protease inhibitors. Cleared lysates were filtered through 0.45µm spin filters (Millipore Ultrafree-CL) and immunoprecipitated with 80 µl anti-HA resin (Sigma) for 1h at 4°C followed by 4 washes with lysis buffer and washed into *in vitro* ubiquitylation buffer (500mM Tris-HCl, pH 7.4, 500mM NaCl, 10µM ZnCl2, 1mM B-glycerophosphate, 1mM NaF, 0.1µM Okadeic Acid , protease inhibitors) twice. Purification of mitochondria from HeLa cells was as performed as described in (Bozidis et al., 2007) with minor modifications including treatment with CCCP (10 µM) for 1 h. *In vitro* ubiquitylation reactions were performed using HA agarose conjugated HA-PARKIN (5µl), E1 ubiquitin-activating enzyme (3.6µM) (Boston Biochem), UbcH7 (100µM), ubiquitin (10-50µM) (Boston Biochem), 1 µM ubiquitin aldehyde (Boston Biochem), energy mix (200mM creatine phosphate, 2µg/µl creatine phosphokinase), 1 mM dithiothreitol, 2 mM ATP, 100nM Btz, 1mM B-glycerophosphate, protease inhibitors, and 50-100µg purified mitochondria. Reactions were incubated at 32°C for 1-2 hours.

**RNAi**

RNAimax (Invitrogen) was used for reverse siRNA transfections (20nM or 30nM as noted) according to the manufacturer's instructions. siRNAs used were from Dharmacon and sequences are provided by the ICCB screening facility upon request.

**siRNA screen transfection and PARKIN immunofluorescence**

For the primary siRNA screen, clonal HeLa cells stably expressing N-HA-Flag-PARKIN were reverse transfected in Evotec 384-well, black, clear-bottom plates (Perkin Elmer) in one siRNA-one well format with four individual siRNAs for each gene (Thermo Fisher). The siRNA was dispensed in quadruplicate directly into empty 384-well plates to achieve a final concentration of 30 nM. A mixture of Lipofectamine RNAiMAX/OptiMEM (Invitrogen) was then added to the wells and the plates were briefly centrifuged; the complex was incubated at room

temperature for 15 min. HeLa-PARKIN cells were trypsinized, counted and 3000 cells were added to each well. Each plate also contained Universal Negative Control, PARKIN and PINK1 siRNAs as negative and positive controls (Thermo Fisher). Plates were briefly centrifuged and incubated at 37°C for 72 hours to achieve maximum penetrance of the siRNA phenotype.

Following incubation, media was aspirated and plates were either untreated or treated with either 2 hour 10μM CCCP (translocation screen) or 24 hours 10μM CCCP (mitophagy screen, treatment was initiated 48 hours post transfection). Cells were washed once with PBS, fixed in 4% paraformaldehyde/ PBS (15 min at RT), washed, and permeabilized with 0.5% Triton X-100 in PBS (10 min, RT). Cells were washed with PBS and then blocked in 1% BSA in PBS (1 hour, RT). Cells were incubated with anti-HA (Covance) and anti-TOMM20 (Santa Cruz Biotech) for 1 hour at RT, and then washed 3 times in wash buffer (10 mM Tris-Cl pH 7.5, 150 mM NaCl, 1% FBS and 2 mM EDTA pH 8.0). Cells were incubated with Alexa Fluor goat anti-mouse 488 and Alexa Fluor goat anti-rabbit 562 (Invitrogen) for 1 hour at RT and then washed 3 times with wash buffer. Nuclei were stained with Hoechst 33342, 5 min at RT (Molecular Probes/Invitrogen). Cells were stained with HCS CellMask Deep Red Stain (Invitrogen) to delineate cell boundaries and facilitate downstream image analysis.

**Image Acquisition and Analysis**

Plates were imaged using the ImageXpress Micro (IXM) automated High Content epifluorescent microscope in the Institute of Chemistry and Cell Biology (ICCB) at Harvard Medical School. Eight fields per well were selected for image capture using a 20X lens. A custom MATLAB script was developed by Tiao Xie of the Image and Data Analysis Core (IDAC) at Harvard Medical School to aid in image analysis. For both screens, 1) the total number of cells, 2) mean nuclear area, 3) mean cell area were determined on a per field as well as per well basis. For the PARKIN translocation screen, the percent of HA-PARKIN that colocalized with mitochondria (TOMM20 staining) was determined. Cells that did not express PARKIN (on

average < 5%) were determined on a per field basis based the background staining intensity and discounted from the analysis. For the PARKIN translocation screen, genes were classified as Class 1 if depletion resulted in >=75% loss of translocation or Class 2 if depletion resulted in >=50% loss of translocation. Genes were further classified based on how many siRNAs out of four gave a positive result.

For the Mitophagy screen, the mean mitochondrial area (based on TOMM20 staining) was calculated and normalized for cell thickness using the HCS CellMask staining profile. Residual mitochondrial staining that overlapped with nuclei was subtracted from the analysis. The mean mitochondrial area and the standard deviation for the quadruplicate wells were calculated and hits from the screen were classified based on thresholds determined by siPINK1, siPARKIN, and siControl experiments. Class 1 proteins, thresholded on mean mitochondrial area in siPINK1-treated cells showed the most drastic effect on mitophagy progression. Class 2 proteins were thresholded on siPARKIN-treated cells and showed a milder defect. Within each class of proteins, genes were further classified based on how many siRNAs out of four gave a positive result. For measurement of increased mitophagy, mean mitochondrial area was compared to siControl-treated cells. Further details are contained in Supplementary Table 8.

**Immunofluorescence staining and microscopy**

To examine the localization of PARKIN and various PARKIN mutants, HeLa cells stably expressing HA–Flag-tagged proteins were plated on No.1 coverslips, treated with CCCP (10 μM, 1 h), and fixed with 4% paraformaldehyde before immunofluorescence using anti-HA to detect PARKIN proteins and anti-TOMM20 to detect mitochondria. All images were collected with a Yokogawa CSU-X1 spinning disk confocal on a Nikon Ti-E inverted microscope equipped with ×100 Plan Apo numerical aperture 1.4 objective lens. HA–PARKIN fluorescence was excited with the 491 nm line (selected with an AOTF) from Spectral Applied Precision LMM-7 solid-state laser launch. Emission was collected with a quad band pass polychroic mirror

(Semrock) and a Chroma ET525/50m emissions filter. TOMM20 fluorescence was excited with the 561 nm line from the LMM-7 launch, and emission collected with the Semrock polychroic and a Chroma ET620/60m emission filter. Images were acquired with a Hamamatsu ORCA-AG cooled CCD camera controlled with MetaMorph 7 software. Nine *z*-series optical sections were collected with a step size of 0.2 μm, using the internal Nikon Ti-E focus motor. *z*-series were deconvolved using AutoQuant blind deconvolution software, and are displayed as maximum *z*-projections. Gamma and brightness were adjusted on displayed images (identically for compared image sets) and percent colocalization was calculated by thresholding for signal at least 4 standard deviations above background in a single *z* slice (identically for compared image sets) using MetaMorph 7 software (Supplementary Table 6).

**Structural analysis of ubiquitylation sites and web portal**

Using the UniProt identifier for each protein identified, the corresponding PDB file(s) (if available) were determined using data from the UniProt to PDB cross-reference table (http://www.ebi.ac.uk/pdbe/docs/sifts/quick.html). The amino acid position in the structure corresponding to each ubiquitylation site was calculated based on their relative position in the structure using the information provided by the cross reference table. Data for each experiment was stored in MySQL tables, which are used when accessing the data via the web portal. For rendering of the structural information via the web portal, Jmol: an open-source Java viewer for chemical structures in 3D (http://www.jmol.org/) was used. Access to the web portal is available at harper.hms.harvard.edu.

**Gene ontology**

Gene ontology analysis was performed using DAVID (Huang da et al., 2009a, b). Additional sub-cellular localization parameters as designated in Figure 2.9b were performed manually using MITOCARTA, Human Protein Atlas, and GenBank.

**Fly stocks**

The following fly stocks were used: *tubulin-GAL4*, *UAS-parkin-RNAi/TM6B*, GAL80 tubulin-GAL4, *UAS-PINK1-RNAi* /TM6B, Tb, *GAL80,* clueless [d08713]/CyO, clueless [f04554]/CyO, and clueless [d00713]/CyO.

# CHAPTER 6

## References

Abbas, N., Lucking, C.B., Ricard, S., Durr, A., Bonifati, V., De Michele, G., Bouley, S., Vaughan, J.R., Gasser, T., Marconi, R.*, et al.* (1999). A wide variety of mutations in the parkin gene are responsible for autosomal recessive parkinsonism in Europe. French Parkinson's Disease Genetics Study Group and the European Consortium on Genetic Susceptibility in Parkinson's Disease. Human molecular genetics *8*, 567-574.

Al Rawi, S., Louvet-Vallee, S., Djeddi, A., Sachse, M., Culetto, E., Hajjar, C., Boyd, L., Legouis, R., and Galy, V. (2011). Postfertilization autophagy of sperm organelles prevents paternal mitochondrial DNA transmission. Science *334*, 1144-1147.

Arbuthnott, G.W., and Wickens, J. (2007). Space, time and dopamine. Trends in neurosciences *30*, 62-69.

Argenzio, E., Bange, T., Oldrini, B., Bianchi, F., Peesari, R., Mari, S., Di Fiore, P.P., Mann, M., and Polo, S. (2011). Proteomic snapshot of the EGF-induced ubiquitin network. Molecular systems biology *7*, 462.

Ashrafi, G., and Schwarz, T.L. (2013). The pathways of mitophagy for quality control and clearance of mitochondria. Cell death and differentiation *20*, 31-42.

Beasley, S.A., Hristova, V.A., and Shaw, G.S. (2007). Structure of the Parkin in-between-ring domain provides insights for E3-ligase dysfunction in autosomal recessive Parkinson's disease. Proceedings of the National Academy of Sciences of the United States of America *104*, 3095-3100.

Beausoleil, S.A., Villen, J., Gerber, S.A., Rush, J., and Gygi, S.P. (2006). A probability-based approach for high-throughput protein phosphorylation analysis and site localization. Nature biotechnology *24*, 1285-1292.

Becker, D., Richter, J., Tocilescu, M.A., Przedborski, S., and Voos, W. (2012). Pink1 kinase and its membrane potential (Deltapsi)-dependent cleavage product both localize to outer mitochondrial membrane by unique targeting mode. The Journal of biological chemistry *287*, 22969-22987.

Behrends, C., Sowa, M.E., Gygi, S.P., and Harper, J.W. (2010). Network organization of the human autophagy system. Nature *466*, 68-76.

Bennett, E.J., Bence, N.F., Jayakumar, R., and Kopito, R.R. (2005). Global impairment of the ubiquitin-proteasome system by nuclear or cytoplasmic protein aggregates precedes inclusion body formation. Molecular cell *17*, 351-365.

Bennett, E.J., Shaler, T.A., Woodman, B., Ryu, K.Y., Zaitseva, T.S., Becker, C.H., Bates, G.P., Schulman, H., and Kopito, R.R. (2007). Global changes to the ubiquitin system in Huntington's disease. Nature *448*, 704-708.

Berger, K.H., and Yaffe, M.P. (1996). Mitochondrial distribution and inheritance. Experientia *52*, 1111-1116.

Betarbet, R., Sherer, T.B., MacKenzie, G., Garcia-Osuna, M., Panov, A.V., and Greenamyre, J.T. (2000). Chronic systemic pesticide exposure reproduces features of Parkinson's disease. Nature neuroscience *3*, 1301-1306.

Borland, M.K., Trimmer, P.A., Rubinstein, J.D., Keeney, P.M., Mohanakumar, K., Liu, L., and Bennett, J.P., Jr. (2008). Chronic, low-dose rotenone reproduces Lewy neurites found in early stages of Parkinson's disease, reduces mitochondrial movement and slowly kills differentiated SH-SY5Y neural cells. Molecular neurodegeneration *3*, 21.

Bozidis, P., Williamson, C.D., and Colberg-Poley, A.M. (2007). Isolation of endoplasmic reticulum, mitochondria, and mitochondria-associated membrane fractions from transfected cells and from human cytomegalovirus-infected primary fibroblasts. Current protocols in cell biology / editorial board, Juan S Bonifacino [et al] *Chapter 3*, Unit 3 27.

Browning, K.S., Gallie, D.R., Hershey, J.W., Hinnebusch, A.G., Maitra, U., Merrick, W.C., and Norbury, C. (2001). Unified nomenclature for the subunits of eukaryotic initiation factor 3. Trends in biochemical sciences *26*, 284.

Burchell, L., Chaugule, V.K., and Walden, H. (2012). Small, N-terminal tags activate Parkin E3 ubiquitin ligase activity by disrupting its autoinhibited conformation. PloS one *7*, e34748.

Cai, Q., Zakaria, H.M., and Sheng, Z.H. (2012a). Long time-lapse imaging reveals unique features of PARK2/Parkin-mediated mitophagy in mature cortical neurons. Autophagy *8*, 976-978.

Cai, Q., Zakaria, H.M., Simone, A., and Sheng, Z.H. (2012b). Spatial parkin translocation and degradation of damaged mitochondria via mitophagy in live cortical neurons. Current biology : CB *22*, 545-552.

Canet-Aviles, R.M., Wilson, M.A., Miller, D.W., Ahmad, R., McLendon, C., Bandyopadhyay, S., Baptista, M.J., Ringe, D., Petsko, G.A., and Cookson, M.R. (2004). The Parkinson's disease protein DJ-1 is neuroprotective due to cysteine-sulfinic acid-driven mitochondrial localization. Proceedings of the National Academy of Sciences of the United States of America *101*, 9103-9108.

Cannon, J.R., and Greenamyre, J.T. (2011). The role of environmental exposures in neurodegeneration and neurodegenerative diseases. Toxicological sciences : an official journal of the Society of Toxicology *124*, 225-250.

Capili, A.D., Edghill, E.L., Wu, K., and Borden, K.L. (2004). Structure of the C-terminal RING finger from a RING-IBR-RING/TRIAD motif reveals a novel zinc-binding domain distinct from a RING. Journal of molecular biology *340*, 1117-1129.

Casarejos, M.J., Menendez, J., Solano, R.M., Rodriguez-Navarro, J.A., Garcia de Yebenes, J., and Mena, M.A. (2006). Susceptibility to rotenone is increased in neurons from parkin null mice and is reduced by minocycline. Journal of neurochemistry *97*, 934-946.

Chan, N.C., Salazar, A.M., Pham, A.H., Sweredoski, M.J., Kolawa, N.J., Graham, R.L., Hess, S., and Chan, D.C. (2011). Broad activation of the ubiquitin-proteasome system by Parkin is critical for mitophagy. Human molecular genetics *20*, 1726-1737.

Chaugule, V.K., Burchell, L., Barber, K.R., Sidhu, A., Leslie, S.J., Shaw, G.S., and Walden, H. (2011). Autoregulation of Parkin activity through its ubiquitin-like domain. The EMBO journal *30*, 2853-2867.

Chen, H., Chomyn, A., and Chan, D.C. (2005). Disruption of fusion results in mitochondrial heterogeneity and dysfunction. The Journal of biological chemistry *280*, 26185-26192.

Chen, H., Detmer, S.A., Ewald, A.J., Griffin, E.E., Fraser, S.E., and Chan, D.C. (2003). Mitofusins Mfn1 and Mfn2 coordinately regulate mitochondrial fusion and are essential for embryonic development. The Journal of cell biology *160*, 189-200.

Chew, K.C., Matsuda, N., Saisho, K., Lim, G.G., Chai, C., Tan, H.M., Tanaka, K., and Lim, K.L. (2011). Parkin mediates apparent E2-independent monoubiquitination in vitro and contains an intrinsic activity that catalyzes polyubiquitination. PloS one *6*, e19720.

Choudhary, C., Kumar, C., Gnad, F., Nielsen, M.L., Rehman, M., Walther, T.C., Olsen, J.V., and Mann, M. (2009). Lysine acetylation targets protein complexes and co-regulates major cellular functions. Science *325*, 834-840.

Chu, C.T. (2010). Tickled PINK1: mitochondrial homeostasis and autophagy in recessive Parkinsonism. Biochimica et biophysica acta *1802*, 20-28.

Chu, C.T., Zhu, J., and Dagda, R. (2007). Beclin 1-independent pathway of damage-induced mitophagy and autophagic stress: implications for neurodegeneration and cell death. Autophagy *3*, 663-666.

Ciechanover, A., Elias, S., Heller, H., and Hershko, A. (1982). "Covalent affinity" purification of ubiquitin-activating enzyme. The Journal of biological chemistry *257*, 2537-2542.

Clark, I.E., Dodson, M.W., Jiang, C., Cao, J.H., Huh, J.R., Seol, J.H., Yoo, S.J., Hay, B.A., and Guo, M. (2006). Drosophila pink1 is required for mitochondrial function and interacts genetically with parkin. Nature *441*, 1162-1166.

Cocheme, H.M., and Murphy, M.P. (2008). Complex I is the major site of mitochondrial superoxide production by paraquat. The Journal of biological chemistry *283*, 1786-1798.

Cohen, G. (2000). Oxidative stress, mitochondrial respiration, and Parkinson's disease. Annals of the New York Academy of Sciences *899*, 112-120.

Colombini, M., Blachly-Dyson, E., and Forte, M. (1996). VDAC, a channel in the outer mitochondrial membrane. Ion channels *4*, 169-202.

Conkright, J.J., Apsley, K.S., Martin, E.P., Ridsdale, R., Rice, W.R., Na, C.L., Yang, B., and Weaver, T.E. (2010). Nedd4-2-mediated ubiquitination facilitates processing of surfactant protein-C. American journal of respiratory cell and molecular biology *42*, 181-189.

Cookson, M.R. (2010). DJ-1, PINK1, and their effects on mitochondrial pathways. Movement disorders : official journal of the Movement Disorder Society *25 Suppl 1*, S44-48.

Cookson, M.R., Lockhart, P.J., McLendon, C., O'Farrell, C., Schlossmacher, M., and Farrer, M.J. (2003). RING finger 1 mutations in Parkin produce altered localization of the protein. Human molecular genetics *12*, 2957-2965.

Corti, O., Lesage, S., and Brice, A. (2011). What genetics tells us about the causes and mechanisms of Parkinson's disease. Physiological reviews *91*, 1161-1218.

Cox, R.T., and Spradling, A.C. (2009). Clueless, a conserved Drosophila gene required for mitochondrial subcellular localization, interacts genetically with parkin. Disease models & mechanisms *2*, 490-499.

Cummings, C.J., Reinstein, E., Sun, Y., Antalffy, B., Jiang, Y., Ciechanover, A., Orr, H.T., Beaudet, A.L., and Zoghbi, H.Y. (1999). Mutation of the E6-AP ubiquitin ligase reduces nuclear inclusion frequency while accelerating polyglutamine-induced pathology in SCA1 mice. Neuron *24*, 879-892.

Dachsel, J.C., Lucking, C.B., Deeg, S., Schultz, E., Lalowski, M., Casademunt, E., Corti, O., Hampe, C., Patenge, N., Vaupel, K.*, et al.* (2005). Parkin interacts with the proteasome subunit alpha4. FEBS letters *579*, 3913-3919.

Danielsen, J.M., Sylvestersen, K.B., Bekker-Jensen, S., Szklarczyk, D., Poulsen, J.W., Horn, H., Jensen, L.J., Mailand, N., and Nielsen, M.L. (2011). Mass spectrometric analysis of lysine ubiquitylation reveals promiscuity at site level. Molecular & cellular proteomics : MCP *10*, M110 003590.

Das, A.K., Cohen, P.W., and Barford, D. (1998). The structure of the tetratricopeptide repeats of protein phosphatase 5: implications for TPR-mediated protein-protein interactions. The EMBO journal *17*, 1192-1199.

Dauer, W., and Przedborski, S. (2003). Parkinson's disease: mechanisms and models. Neuron *39*, 889-909.

Dawson, T.M., and Dawson, V.L. (2003). Molecular pathways of neurodegeneration in Parkinson's disease. Science *302*, 819-822.

Dawson, T.M., and Dawson, V.L. (2010). The role of parkin in familial and sporadic Parkinson's disease. Movement disorders : official journal of the Movement Disorder Society *25 Suppl 1*, S32-39.

Deas, E., Plun-Favreau, H., Gandhi, S., Desmond, H., Kjaer, S., Loh, S.H., Renton, A.E., Harvey, R.J., Whitworth, A.J., Martins, L.M.*, et al.* (2011). PINK1 cleavage at position A103 by the mitochondrial protease PARL. Human molecular genetics *20*, 867-879.

Demartino, G.N., and Gillette, T.G. (2007). Proteasomes: machines for all reasons. Cell *129*, 659-662.

Denison, S.R., Wang, F., Becker, N.A., Schule, B., Kock, N., Phillips, L.A., Klein, C., and Smith, D.I. (2003). Alterations in the common fragile site gene Parkin in ovarian and other cancers. Oncogene *22*, 8370-8378.

Deosaran, E., Larsen, K.B., Hua, R., Sargent, G., Wang, Y., Kim, S., Lamark, T., Jauregui, M., Law, K., Lippincott-Schwartz, J*., et al.* (2012). NBR1 acts as an autophagy receptor for peroxisomes. Journal of cell science.

Deshaies, R.J., and Joazeiro, C.A. (2009). RING domain E3 ubiquitin ligases. Annual review of biochemistry *78*, 399-434.

Detmer, S.A., and Chan, D.C. (2007). Functions and dysfunctions of mitochondrial dynamics. Nature reviews Molecular cell biology *8*, 870-879.

Devine, M.J., Plun-Favreau, H., and Wood, N.W. (2011). Parkinson's disease and cancer: two wars, one front. Nature reviews Cancer *11*, 812-823.

DiMauro, S., and Schon, E.A. (2003). Mitochondrial respiratory-chain diseases. The New England journal of medicine *348*, 2656-2668.

Dorsey, E.R., Constantinescu, R., Thompson, J.P., Biglan, K.M., Holloway, R.G., Kieburtz, K., Marshall, F.J., Ravina, B.M., Schifitto, G., Siderowf, A*., et al.* (2007). Projected number of people with Parkinson disease in the most populous nations, 2005 through 2030. Neurology *68*, 384-386.

Durcan, T.M., Kontogiannea, M., Thorarinsdottir, T., Fallon, L., Williams, A.J., Djarmati, A., Fantaneanu, T., Paulson, H.L., and Fon, E.A. (2011). The Machado-Joseph disease-associated mutant form of ataxin-3 regulates parkin ubiquitination and stability. Human molecular genetics *20*, 141-154.

Eisenhaber, B., Chumak, N., Eisenhaber, F., and Hauser, M.T. (2007). The ring between ring fingers (RBR) protein family. Genome biology *8*, 209.

Eng, J.K., McCormack, A.L., and Yates III, J.R. (1994). An approach to correlate tandem mass spectral data of peptides with amino acid sequences in a protein database. Journal of the American Society for Mass Spectrometry *5*, 976-989.

Ernster, L., and Schatz, G. (1981). Mitochondria: a historical review. The Journal of cell biology *91*, 227s-255s.

Estrabaud, E., Le Rouzic, E., Lopez-Verges, S., Morel, M., Belaidouni, N., Benarous, R., Transy, C., Berlioz-Torrent, C., and Margottin-Goguet, F. (2007). Regulated degradation of the HIV-1 Vpu protein through a betaTrCP-independent pathway limits the release of viral particles. PLoS pathogens *3*, e104.

Ewing, R.M., Chu, P., Elisma, F., Li, H., Taylor, P., Climie, S., McBroom-Cerajewski, L., Robinson, M.D., O'Connor, L., Li, M*., et al.* (2007). Large-scale mapping of human protein-protein interactions by mass spectrometry. Molecular systems biology *3*, 89.

Exner, N., Lutz, A.K., Haass, C., and Winklhofer, K.F. (2012). Mitochondrial dysfunction in Parkinson's disease: molecular mechanisms and pathophysiological consequences. The EMBO journal *31*, 3038-3062.

Farrer, M., Chan, P., Chen, R., Tan, L., Lincoln, S., Hernandez, D., Forno, L., Gwinn-Hardy, K., Petrucelli, L., Hussey, J*., et al.* (2001). Lewy bodies and parkinsonism in families with parkin mutations. Annals of neurology *50*, 293-300.

Fields, S.D., Arana, Q., Heuser, J., and Clarke, M. (2002). Mitochondrial membrane dynamics are altered in cluA- mutants of Dictyostelium. Journal of muscle research and cell motility *23*, 829-838.

Fields, S.D., Conrad, M.N., and Clarke, M. (1998). The S. cerevisiae CLU1 and D. discoideum cluA genes are functional homologues that influence mitochondrial morphology and distribution. Journal of cell science *111 ( Pt 12)*, 1717-1727.

Finley, D. (2009). Recognition and processing of ubiquitin-protein conjugates by the proteasome. Annual review of biochemistry *78*, 477-513.

Finley, D., Ulrich, H.D., Sommer, T., and Kaiser, P. (2012). The ubiquitin-proteasome system of Saccharomyces cerevisiae. Genetics *192*, 319-360.

Frederick, R.L., and Shaw, J.M. (2007). Moving mitochondria: establishing distribution of an essential organelle. Traffic *8*, 1668-1675.

Gandhi, S., Muqit, M.M., Stanyer, L., Healy, D.G., Abou-Sleiman, P.M., Hargreaves, I., Heales, S., Ganguly, M., Parsons, L., Lees, A.J*., et al.* (2006). PINK1 protein in normal human brain and Parkinson's disease. Brain : a journal of neurology *129*, 1720-1731.

Geisler, S., Holmstrom, K.M., Skujat, D., Fiesel, F.C., Rothfuss, O.C., Kahle, P.J., and Springer, W. (2010). PINK1/Parkin-mediated mitophagy is dependent on VDAC1 and p62/SQSTM1. Nature cell biology *12*, 119-131.

Giasson, B.I., Duda, J.E., Murray, I.V., Chen, Q., Souza, J.M., Hurtig, H.I., Ischiropoulos, H., Trojanowski, J.Q., and Lee, V.M. (2000). Oxidative damage linked to neurodegeneration by selective alpha-synuclein nitration in synucleinopathy lesions. Science *290*, 985-989.

Glater, E.E., Megeath, L.J., Stowers, R.S., and Schwarz, T.L. (2006). Axonal transport of mitochondria requires milton to recruit kinesin heavy chain and is light chain independent. The Journal of cell biology *173*, 545-557.

Goldberg, M.S., Fleming, S.M., Palacino, J.J., Cepeda, C., Lam, H.A., Bhatnagar, A., Meloni, E.G., Wu, N., Ackerson, L.C., Klapstein, G.J*., et al.* (2003). Parkin-deficient mice exhibit nigrostriatal deficits but not loss of dopaminergic neurons. The Journal of biological chemistry *278*, 43628-43635.

Graham, D.G., Tiffany, S.M., Bell, W.R., Jr., and Gutknecht, W.F. (1978). Autoxidation versus covalent binding of quinones as the mechanism of toxicity of dopamine, 6-hydroxydopamine, and related compounds toward C1300 neuroblastoma cells in vitro. Molecular pharmacology *14*, 644-653.

Greenamyre, J.T., Sherer, T.B., Betarbet, R., and Panov, A.V. (2001). Complex I and Parkinson's disease. IUBMB life *52*, 135-141.

Greene, J.C., Whitworth, A.J., Kuo, I., Andrews, L.A., Feany, M.B., and Pallanck, L.J. (2003). Mitochondrial pathology and apoptotic muscle degeneration in Drosophila parkin mutants. Proceedings of the National Academy of Sciences of the United States of America *100*, 4078-4083.

Guo, X., Macleod, G.T., Wellington, A., Hu, F., Panchumarthi, S., Schoenfield, M., Marin, L., Charlton, M.P., Atwood, H.L., and Zinsmaier, K.E. (2005). The GTPase dMiro is required for axonal transport of mitochondria to Drosophila synapses. Neuron *47*, 379-393.

Haas, W., Faherty, B.K., Gerber, S.A., Elias, J.E., Beausoleil, S.A., Bakalarski, C.E., Li, X., Villen, J., and Gygi, S.P. (2006). Optimization and use of peptide mass measurement accuracy in shotgun proteomics. Molecular & cellular proteomics : MCP *5*, 1326-1337.

Hampe, C., Ardila-Osorio, H., Fournier, M., Brice, A., and Corti, O. (2006). Biochemical analysis of Parkinson's disease-causing variants of Parkin, an E3 ubiquitin-protein ligase with monoubiquitylation capacity. Human molecular genetics *15*, 2059-2075.

Haque, M.E., Mount, M.P., Safarpour, F., Abdel-Messih, E., Callaghan, S., Mazerolle, C., Kitada, T., Slack, R.S., Wallace, V., Shen, J*., et al.* (2012). Inactivation of Pink1 gene in vivo sensitizes dopamine-producing neurons to 1-methyl-4-phenyl-1,2,3,6-tetrahydropyridine (MPTP) and can be rescued by autosomal recessive Parkinson disease genes, Parkin or DJ-1. The Journal of biological chemistry *287*, 23162-23170.

Haque, M.E., Thomas, K.J., D'Souza, C., Callaghan, S., Kitada, T., Slack, R.S., Fraser, P., Cookson, M.R., Tandon, A., and Park, D.S. (2008). Cytoplasmic Pink1 activity protects neurons from dopaminergic neurotoxin MPTP. Proceedings of the National Academy of Sciences of the United States of America *105*, 1716-1721.

Hardy, J. (2010). Genetic analysis of pathways to Parkinson disease. Neuron *68*, 201-206.

Harner, M., Neupert, W., and Deponte, M. (2011). Lateral release of proteins from the TOM complex into the outer membrane of mitochondria. The EMBO journal *30*, 3232-3241.

Hattori, N., Tanaka, M., Ozawa, T., and Mizuno, Y. (1991). Immunohistochemical studies on complexes I, II, III, and IV of mitochondria in Parkinson's disease. Annals of neurology *30*, 563-571.

Hershko, A., and Ciechanover, A. (1998). The ubiquitin system. Annual review of biochemistry *67*, 425-479.

Hershko, A., Heller, H., Elias, S., and Ciechanover, A. (1983). Components of ubiquitin-protein ligase system. Resolution, affinity purification, and role in protein breakdown. The Journal of biological chemistry *258*, 8206-8214.

Hirtz, D., Thurman, D.J., Gwinn-Hardy, K., Mohamed, M., Chaudhuri, A.R., and Zalutsky, R. (2007). How common are the "common" neurologic disorders? Neurology *68*, 326-337.

Hollenbeck, P.J., and Saxton, W.M. (2005). The axonal transport of mitochondria. Journal of cell science *118*, 5411-5419.

Hristova, V.A., Beasley, S.A., Rylett, R.J., and Shaw, G.S. (2009). Identification of a novel Zn2+-binding domain in the autosomal recessive juvenile Parkinson-related E3 ligase parkin. The Journal of biological chemistry *284*, 14978-14986.

Huang da, W., Sherman, B.T., and Lempicki, R.A. (2009a). Bioinformatics enrichment tools: paths toward the comprehensive functional analysis of large gene lists. Nucleic acids research *37*, 1-13.

Huang da, W., Sherman, B.T., and Lempicki, R.A. (2009b). Systematic and integrative analysis of large gene lists using DAVID bioinformatics resources. Nature protocols *4*, 44-57.

Huang, Q., and Figueiredo-Pereira, M.E. (2010). Ubiquitin/proteasome pathway impairment in neurodegeneration: therapeutic implications. Apoptosis : an international journal on programmed cell death *15*, 1292-1311.

Huttlin, E.L., Jedrychowski, M.P., Elias, J.E., Goswami, T., Rad, R., Beausoleil, S.A., Villen, J., Haas, W., Sowa, M.E., and Gygi, S.P. (2010). A tissue-specific atlas of mouse protein phosphorylation and expression. Cell *143*, 1174-1189.

Itakura, E., Kishi-Itakura, C., Koyama-Honda, I., and Mizushima, N. (2012). Structures containing Atg9A and the ULK1 complex independently target depolarized mitochondria at initial stages of Parkin-mediated mitophagy. Journal of cell science *125*, 1488-1499.

Itier, J.M., Ibanez, P., Mena, M.A., Abbas, N., Cohen-Salmon, C., Bohme, G.A., Laville, M., Pratt, J., Corti, O., Pradier, L*., et al.* (2003). Parkin gene inactivation alters behaviour and dopamine neurotransmission in the mouse. Human molecular genetics *12*, 2277-2291.

Itoh, K., Nakamura, K., Iijima, M., and Sesaki, H. (2013). Mitochondrial dynamics in neurodegeneration. Trends in cell biology *23*, 64-71.

Janetzky, B., Hauck, S., Youdim, M.B., Riederer, P., Jellinger, K., Pantucek, F., Zochling, R., Boissl, K.W., and Reichmann, H. (1994). Unaltered aconitase activity, but decreased complex I activity in substantia nigra pars compacta of patients with Parkinson's disease. Neuroscience letters *169*, 126-128.

Jin, S.M., Lazarou, M., Wang, C., Kane, L.A., Narendra, D.P., and Youle, R.J. (2010). Mitochondrial membrane potential regulates PINK1 import and proteolytic destabilization by PARL. The Journal of cell biology *191*, 933-942.

Joselin, A.P., Hewitt, S.J., Callaghan, S.M., Kim, R.H., Chung, Y.H., Mak, T.W., Shen, J., Slack, R.S., and Park, D.S. (2012). ROS-dependent regulation of Parkin and DJ-1 localization during oxidative stress in neurons. Human molecular genetics *21*, 4888-4903.

Kalia, L.V., Kalia, S.K., McLean, P.J., Lozano, A.M., and Lang, A.E. (2012). alpha-Synuclein oligomers and clinical implications for Parkinson disease. Annals of neurology.

Kanki, T., Wang, K., Cao, Y., Baba, M., and Klionsky, D.J. (2009). Atg32 is a mitochondrial protein that confers selectivity during mitophagy. Developmental cell *17*, 98-109.

Kanki, T., Wang, K., and Klionsky, D.J. (2010). A genomic screen for yeast mutants defective in mitophagy. Autophagy *6*, 278-280.

Karbowski, M., Spodnik, J.H., Teranishi, M., Wozniak, M., Nishizawa, Y., Usukura, J., and Wakabayashi, T. (2001). Opposite effects of microtubule-stabilizing and microtubule-destabilizing drugs on biogenesis of mitochondria in mammalian cells. Journal of cell science *114*, 281-291.

Keane, P.C., Kurzawa, M., Blain, P.G., and Morris, C.M. (2011). Mitochondrial dysfunction in Parkinson's disease. Parkinson's disease *2011*, 716871.

Kim, I., Rodriguez-Enriquez, S., and Lemasters, J.J. (2007). Selective degradation of mitochondria by mitophagy. Archives of biochemistry and biophysics *462*, 245-253.

Kim, P.K., Hailey, D.W., Mullen, R.T., and Lippincott-Schwartz, J. (2008a). Ubiquitin signals autophagic degradation of cytosolic proteins and peroxisomes. Proceedings of the National Academy of Sciences of the United States of America *105*, 20567-20574.

Kim, W., Bennett, E.J., Huttlin, E.L., Guo, A., Li, J., Possemato, A., Sowa, M.E., Rad, R., Rush, J., Comb, M.J.*, et al.* (2011). Systematic and quantitative assessment of the ubiquitin-modified proteome. Molecular cell *44*, 325-340.

Kim, Y., Park, J., Kim, S., Song, S., Kwon, S.K., Lee, S.H., Kitada, T., Kim, J.M., and Chung, J. (2008b). PINK1 controls mitochondrial localization of Parkin through direct phosphorylation. Biochemical and biophysical research communications *377*, 975-980.

Kirkin, V., Lamark, T., Sou, Y.S., Bjorkoy, G., Nunn, J.L., Bruun, J.A., Shvets, E., McEwan, D.G., Clausen, T.H., Wild, P.*, et al.* (2009). A role for NBR1 in autophagosomal degradation of ubiquitinated substrates. Molecular cell *33*, 505-516.

Kirkpatrick, D.S., Gerber, S.A., and Gygi, S.P. (2005a). The absolute quantification strategy: a general procedure for the quantification of proteins and post-translational modifications. Methods *35*, 265-273.

Kirkpatrick, D.S., Weldon, S.F., Tsaprailis, G., Liebler, D.C., and Gandolfi, A.J. (2005b). Proteomic identification of ubiquitinated proteins from human cells expressing His-tagged ubiquitin. Proteomics *5*, 2104-2111.

Kitada, T., Asakawa, S., Hattori, N., Matsumine, H., Yamamura, Y., Minoshima, S., Yokochi, M., Mizuno, Y., and Shimizu, N. (1998). Mutations in the parkin gene cause autosomal recessive juvenile parkinsonism. Nature *392*, 605-608.

Komatsu, T., Kukelyansky, I., McCaffery, J.M., Ueno, T., Varela, L.C., and Inoue, T. (2010). Organelle-specific, rapid induction of molecular activities and membrane tethering. Nature methods *7*, 206-208.

Kondapalli, C., Kazlauskaite, A., Zhang, N., Woodroof, H.I., Campbell, D.G., Gourlay, R., Burchell, L., Walden, H., Macartney, T.J., Deak, M.*, et al.* (2012). PINK1 is activated by mitochondrial membrane potential depolarization and stimulates Parkin E3 ligase activity by phosphorylating Serine 65. Open biology *2*, 120080.

Kondo-Okamoto, N., Shaw, J.M., and Okamoto, K. (2008). Tetratricopeptide repeat proteins Tom70 and Tom71 mediate yeast mitochondrial morphogenesis. EMBO reports *9*, 63-69.

Kotorashvili, A., Russo, S.J., Mulugeta, S., Guttentag, S., and Beers, M.F. (2009). Anterograde transport of surfactant protein C proprotein to distal processing compartments requires PPDY-mediated association with Nedd4 ubiquitin ligases. The Journal of biological chemistry *284*, 16667-16678.

Kulathu, Y., and Komander, D. (2012). Atypical ubiquitylation - the unexplored world of polyubiquitin beyond Lys48 and Lys63 linkages. Nature reviews Molecular cell biology *13*, 508-523.

Lamark, T., Kirkin, V., Dikic, I., and Johansen, T. (2009). NBR1 and p62 as cargo receptors for selective autophagy of ubiquitinated targets. Cell cycle *8*, 1986-1990.

Langston, J.W., Ballard, P., Tetrud, J.W., and Irwin, I. (1983). Chronic Parkinsonism in humans due to a product of meperidine-analog synthesis. Science *219*, 979-980.

Lazarou, M., Jin, S.M., Kane, L.A., and Youle, R.J. (2012). Role of PINK1 binding to the TOM complex and alternate intracellular membranes in recruitment and activation of the E3 ligase Parkin. Developmental cell *22*, 320-333.

Lazarou, M., Narendra, D.P., Jin, S.M., Tekle, E., Banerjee, S., and Youle, R.J. (2013). PINK1 drives Parkin self-association and HECT-like E3 activity upstream of mitochondrial binding. The Journal of cell biology *200*, 163-172.

Lee, K.A., Hammerle, L.P., Andrews, P.S., Stokes, M.P., Mustelin, T., Silva, J.C., Black, R.A., and Doedens, J.R. (2011). Ubiquitin ligase substrate identification through quantitative proteomics at both the protein and peptide levels. The Journal of biological chemistry *286*, 41530-41538.

Lemasters, J.J., and Holmuhamedov, E. (2006). Voltage-dependent anion channel (VDAC) as mitochondrial governator--thinking outside the box. Biochimica et biophysica acta *1762*, 181-190.

Levine, B., and Klionsky, D.J. (2004). Development by self-digestion: molecular mechanisms and biological functions of autophagy. Developmental cell *6*, 463-477.

Levine, B., Mizushima, N., and Virgin, H.W. (2011). Autophagy in immunity and inflammation. Nature *469*, 323-335.

Liang, C.L., Wang, T.T., Luby-Phelps, K., and German, D.C. (2007). Mitochondria mass is low in mouse substantia nigra dopamine neurons: implications for Parkinson's disease. Experimental neurology *203*, 370-380.

Liesa, M., Palacin, M., and Zorzano, A. (2009). Mitochondrial dynamics in mammalian health and disease. Physiological reviews *89*, 799-845.

Lim, K.L., Dawson, V.L., and Dawson, T.M. (2002). The genetics of Parkinson's disease. Current neurology and neuroscience reports *2*, 439-446.

Lin, W., and Kang, U.J. (2008). Characterization of PINK1 processing, stability, and subcellular localization. Journal of neurochemistry *106*, 464-474.

Liu, S., Sawada, T., Lee, S., Yu, W., Silverio, G., Alapatt, P., Millan, I., Shen, A., Saxton, W., Kanao, T*., et al.* (2012). Parkinson's disease-associated kinase PINK1 regulates Miro protein level and axonal transport of mitochondria. PLoS genetics *8*, e1002537.

Liu, W., Vives-Bauza, C., Acin-Perez, R., Yamamoto, A., Tan, Y., Li, Y., Magrane, J., Stavarache, M.A., Shaffer, S., Chang, S*., et al.* (2009a). PINK1 defect causes mitochondrial dysfunction, proteasomal deficit and alpha-synuclein aggregation in cell culture models of Parkinson's disease. PloS one *4*, e4597.

Liu, X., Weaver, D., Shirihai, O., and Hajnoczky, G. (2009b). Mitochondrial 'kiss-and-run': interplay between mitochondrial motility and fusion-fission dynamics. The EMBO journal *28*, 3074-3089.

Lopes, F.M., Schroder, R., da Frota, M.L., Jr., Zanotto-Filho, A., Muller, C.B., Pires, A.S., Meurer, R.T., Colpo, G.D., Gelain, D.P., Kapczinski, F*., et al.* (2010). Comparison between proliferative and neuron-like SH-SY5Y cells as an in vitro model for Parkinson disease studies. Brain research *1337*, 85-94.

Lu, X.H., Fleming, S.M., Meurers, B., Ackerson, L.C., Mortazavi, F., Lo, V., Hernandez, D., Sulzer, D., Jackson, G.R., Maidment, N.T*., et al.* (2009). Bacterial artificial chromosome transgenic mice expressing a truncated mutant parkin exhibit age-dependent hypokinetic motor deficits, dopaminergic neuron degeneration, and accumulation of proteinase K-resistant alpha-synuclein. The Journal of neuroscience : the official journal of the Society for Neuroscience *29*, 1962-1976.

Malkus, K.A., Tsika, E., and Ischiropoulos, H. (2009). Oxidative modifications, mitochondrial dysfunction, and impaired protein degradation in Parkinson's disease: how neurons are lost in the Bermuda triangle. Molecular neurodegeneration *4*, 24.

Marin, I., Lucas, J.I., Gradilla, A.C., and Ferrus, A. (2004). Parkin and relatives: the RBR family of ubiquitin ligases. Physiological genomics *17*, 253-263.

Martin, I., Dawson, V.L., and Dawson, T.M. (2011). Recent advances in the genetics of Parkinson's disease. Annual review of genomics and human genetics *12*, 301-325.

Matsuda, N., Kitami, T., Suzuki, T., Mizuno, Y., Hattori, N., and Tanaka, K. (2006). Diverse effects of pathogenic mutations of Parkin that catalyze multiple monoubiquitylation in vitro. The Journal of biological chemistry *281*, 3204-3209.

Matsuda, N., Sato, S., Shiba, K., Okatsu, K., Saisho, K., Gautier, C.A., Sou, Y.S., Saiki, S., Kawajiri, S., Sato, F.*, et al.* (2010). PINK1 stabilized by mitochondrial depolarization recruits Parkin to damaged mitochondria and activates latent Parkin for mitophagy. The Journal of cell biology *189*, 211-221.

Matsuda, W., Furuta, T., Nakamura, K.C., Hioki, H., Fujiyama, F., Arai, R., and Kaneko, T. (2009). Single nigrostriatal dopaminergic neurons form widely spread and highly dense axonal arborizations in the neostriatum. The Journal of neuroscience : the official journal of the Society for Neuroscience *29*, 444-453.

Matsumoto, M., Hatakeyama, S., Oyamada, K., Oda, Y., Nishimura, T., and Nakayama, K.I. (2005). Large-scale analysis of the human ubiquitin-related proteome. Proteomics *5*, 4145-4151.

McCoy, M.K., and Cookson, M.R. (2011). DJ-1 regulation of mitochondrial function and autophagy through oxidative stress. Autophagy *7*, 531-532.

McNaught, K.S., Perl, D.P., Brownell, A.L., and Olanow, C.W. (2004). Systemic exposure to proteasome inhibitors causes a progressive model of Parkinson's disease. Annals of neurology *56*, 149-162.

Meierhofer, D., Wang, X., Huang, L., and Kaiser, P. (2008). Quantitative analysis of global ubiquitination in HeLa cells by mass spectrometry. Journal of proteome research *7*, 4566-4576.

Meissner, C., Lorenz, H., Weihofen, A., Selkoe, D.J., and Lemberg, M.K. (2011). The mitochondrial intramembrane protease PARL cleaves human Pink1 to regulate Pink1 trafficking. Journal of neurochemistry *117*, 856-867.

Metzger, M.B., Hristova, V.A., and Weissman, A.M. (2012). HECT and RING finger families of E3 ubiquitin ligases at a glance. Journal of cell science *125*, 531-537.

Mills, R.D., Sim, C.H., Mok, S.S., Mulhern, T.D., Culvenor, J.G., and Cheng, H.C. (2008). Biochemical aspects of the neuroprotective mechanism of PTEN-induced kinase-1 (PINK1). Journal of neurochemistry *105*, 18-33.

Mironov, S.L., Ivannikov, M.V., and Johansson, M. (2005). [Ca2+]i signaling between mitochondria and endoplasmic reticulum in neurons is regulated by microtubules. From mitochondrial permeability transition pore to Ca2+-induced Ca2+ release. The Journal of biological chemistry *280*, 715-721.

Mizushima, N. (2007). Autophagy: process and function. Genes & development *21*, 2861-2873.

Moore, D.J. (2006). Parkin: a multifaceted ubiquitin ligase. Biochemical Society transactions *34*, 749-753.

Muqit, M.M., Abou-Sleiman, P.M., Saurin, A.T., Harvey, K., Gandhi, S., Deas, E., Eaton, S., Payne Smith, M.D., Venner, K., Matilla, A.*, et al.* (2006). Altered cleavage and localization of PINK1 to aggresomes in the presence of proteasomal stress. Journal of neurochemistry *98*, 156-169.

Nakatogawa, H., Suzuki, K., Kamada, Y., and Ohsumi, Y. (2009). Dynamics and diversity in autophagy mechanisms: lessons from yeast. Nature reviews Molecular cell biology *10*, 458-467.

Narendra, D., Kane, L.A., Hauser, D.N., Fearnley, I.M., and Youle, R.J. (2010a). p62/SQSTM1 is required for Parkin-induced mitochondrial clustering but not mitophagy; VDAC1 is dispensable for both. Autophagy *6*, 1090-1106.

Narendra, D., Tanaka, A., Suen, D.F., and Youle, R.J. (2008). Parkin is recruited selectively to impaired mitochondria and promotes their autophagy. The Journal of cell biology *183*, 795-803.

Narendra, D., Tanaka, A., Suen, D.F., and Youle, R.J. (2009). Parkin-induced mitophagy in the pathogenesis of Parkinson disease. Autophagy *5*, 706-708.

Narendra, D., Walker, J.E., and Youle, R. (2012). Mitochondrial quality control mediated by PINK1 and Parkin: links to parkinsonism. Cold Spring Harbor perspectives in biology *4*.

Narendra, D.P., Jin, S.M., Tanaka, A., Suen, D.F., Gautier, C.A., Shen, J., Cookson, M.R., and Youle, R.J. (2010b). PINK1 is selectively stabilized on impaired mitochondria to activate Parkin. PLoS biology *8*, e1000298.

Narendra, D.P., and Youle, R.J. (2011). Targeting mitochondrial dysfunction: role for PINK1 and Parkin in mitochondrial quality control. Antioxidants & redox signaling *14*, 1929-1938.

Newman, A.C., Scholefield, C.L., Kemp, A.J., Newman, M., McIver, E.G., Kamal, A., and Wilkinson, S. (2012). TBK1 kinase addiction in lung cancer cells is mediated via autophagy of Tax1bp1/Ndp52 and non-canonical NF-kappaB signalling. PloS one *7*, e50672.

Nicholls, D.G. (2008). Oxidative stress and energy crises in neuronal dysfunction. Annals of the New York Academy of Sciences *1147*, 53-60.

Nicklas, W.J., Youngster, S.K., Kindt, M.V., and Heikkila, R.E. (1987). MPTP, MPP+ and mitochondrial function. Life sciences *40*, 721-729.

Nishimura, K., Fukagawa, T., Takisawa, H., Kakimoto, T., and Kanemaki, M. (2009). An auxin-based degron system for the rapid depletion of proteins in nonplant cells. Nature methods *6*, 917-922.

Nowikovsky, K., Reipert, S., Devenish, R.J., and Schweyen, R.J. (2007). Mdm38 protein depletion causes loss of mitochondrial K+/H+ exchange activity, osmotic swelling and mitophagy. Cell death and differentiation *14*, 1647-1656.

Okamoto, K., and Shaw, J.M. (2005). Mitochondrial morphology and dynamics in yeast and multicellular eukaryotes. Annual review of genetics *39*, 503-536.

Okatsu, K., Oka, T., Iguchi, M., Imamura, K., Kosako, H., Tani, N., Kimura, M., Go, E., Koyano, F., Funayama, M*., et al.* (2012). PINK1 autophosphorylation upon membrane potential dissipation is essential for Parkin recruitment to damaged mitochondria. Nature communications *3*, 1016.

Onoue, K., Jofuku, A., Ban-Ishihara, R., Ishihara, T., Maeda, M., Koshiba, T., Itoh, T., Fukuda, M., Otera, H., Oka, T*., et al.* (2012). Fis1 acts as mitochondrial recruitment factor for TBC1D15 that involved in regulation of mitochondrial morphology. Journal of cell science.

Paisan-Ruiz, C., Guevara, R., Federoff, M., Hanagasi, H., Sina, F., Elahi, E., Schneider, S.A., Schwingenschuh, P., Bajaj, N., Emre, M*., et al.* (2010). Early-onset L-dopa-responsive parkinsonism with pyramidal signs due to ATP13A2, PLA2G6, FBXO7 and spatacsin mutations. Movement disorders : official journal of the Movement Disorder Society *25*, 1791-1800.

Palade, G.E. (1953). An electron microscope study of the mitochondrial structure. The journal of histochemistry and cytochemistry : official journal of the Histochemistry Society *1*, 188-211.

Pallen, M.J. (2011). Time to recognise that mitochondria are bacteria? Trends in microbiology *19*, 58-64.

Park, J., Lee, S.B., Lee, S., Kim, Y., Song, S., Kim, S., Bae, E., Kim, J., Shong, M., Kim, J.M*., et al.* (2006). Mitochondrial dysfunction in Drosophila PINK1 mutants is complemented by parkin. Nature *441*, 1157-1161.

Park, Y.Y., Lee, S., Karbowski, M., Neutzner, A., Youle, R.J., and Cho, H. (2010). Loss of MARCH5 mitochondrial E3 ubiquitin ligase induces cellular senescence through dynamin-related protein 1 and mitofusin 1. Journal of cell science *123*, 619-626.

Parkinson, J. (2002). An essay on the shaking palsy. 1817. The Journal of neuropsychiatry and clinical neurosciences *14*, 223-236; discussion 222.

Peng, J., Schwartz, D., Elias, J.E., Thoreen, C.C., Cheng, D., Marsischky, G., Roelofs, J., Finley, D., and Gygi, S.P. (2003). A proteomics approach to understanding protein ubiquitination. Nature biotechnology *21*, 921-926.

Pickart, C.M., and Cohen, R.E. (2004). Proteasomes and their kin: proteases in the machine age. Nature reviews *5*, 177-187.

Pickart, C.M., and Eddins, M.J. (2004). Ubiquitin: structures, functions, mechanisms. Biochimica et biophysica acta *1695*, 55-72.

Plun-Favreau, H., Klupsch, K., Moisoi, N., Gandhi, S., Kjaer, S., Frith, D., Harvey, K., Deas, E., Harvey, R.J., McDonald, N*., et al.* (2007). The mitochondrial protease HtrA2 is regulated by Parkinson's disease-associated kinase PINK1. Nature cell biology *9*, 1243-1252.

Priault, M., Salin, B., Schaeffer, J., Vallette, F.M., di Rago, J.P., and Martinou, J.C. (2005). Impairing the bioenergetic status and the biogenesis of mitochondria triggers mitophagy in yeast. Cell death and differentiation *12*, 1613-1621.

Pridgeon, J.W., Olzmann, J.A., Chin, L.S., and Li, L. (2007). PINK1 protects against oxidative stress by phosphorylating mitochondrial chaperone TRAP1. PLoS biology *5*, e172.

Rakovic, A., Shurkewitsch, K., Seibler, P., Grunewald, A., Zanon, A., Hagenah, J., Krainc, D., and Klein, C. (2013). Phosphatase and Tensin Homolog (PTEN)-induced Putative Kinase 1 (PINK1)-dependent Ubiquitination of Endogenous Parkin Attenuates Mitophagy: STUDY IN HUMAN PRIMARY FIBROBLASTS AND INDUCED PLURIPOTENT STEM CELL-DERIVED NEURONS. The Journal of biological chemistry *288*, 2223-2237.

Rosen, K.M., Veereshwarayya, V., Moussa, C.E., Fu, Q., Goldberg, M.S., Schlossmacher, M.G., Shen, J., and Querfurth, H.W. (2006). Parkin protects against mitochondrial toxins and beta-amyloid accumulation in skeletal muscle cells. The Journal of biological chemistry *281*, 12809-12816.

Ross, C.A., and Pickart, C.M. (2004). The ubiquitin-proteasome pathway in Parkinson's disease and other neurodegenerative diseases. Trends in cell biology *14*, 703-711.

Safadi, S.S., and Shaw, G.S. (2010). Differential interaction of the E3 ligase parkin with the proteasomal subunit S5a and the endocytic protein Eps15. The Journal of biological chemistry *285*, 1424-1434.

Sagan, L. (1967). On the origin of mitosing cells. Journal of theoretical biology *14*, 255-274.

Sakata, E., Yamaguchi, Y., Kurimoto, E., Kikuchi, J., Yokoyama, S., Yamada, S., Kawahara, H., Yokosawa, H., Hattori, N., Mizuno, Y.*, et al.* (2003). Parkin binds the Rpn10 subunit of 26S proteasomes through its ubiquitin-like domain. EMBO reports *4*, 301-306.

Sandebring, A., Thomas, K.J., Beilina, A., van der Brug, M., Cleland, M.M., Ahmad, R., Miller, D.W., Zambrano, I., Cowburn, R.F., Behbahani, H.*, et al.* (2009). Mitochondrial alterations in PINK1 deficient cells are influenced by calcineurin-dependent dephosphorylation of dynamin-related protein 1. PloS one *4*, e5701.

Sandoval, H., Thiagarajan, P., Dasgupta, S.K., Schumacher, A., Prchal, J.T., Chen, M., and Wang, J. (2008). Essential role for Nix in autophagic maturation of erythroid cells. Nature *454*, 232-235.

Sandy, M.S., Armstrong, M., Tanner, C.M., Daly, A.K., Di Monte, D.A., Langston, J.W., and Idle, J.R. (1996). CYP2D6 allelic frequencies in young-onset Parkinson's disease. Neurology *47*, 225-230.

Sang, T.K., Chang, H.Y., Lawless, G.M., Ratnaparkhi, A., Mee, L., Ackerson, L.C., Maidment, N.T., Krantz, D.E., and Jackson, G.R. (2007). A Drosophila model of mutant human parkin-induced toxicity demonstrates selective loss of dopaminergic neurons and dependence on cellular dopamine. The Journal of neuroscience : the official journal of the Society for Neuroscience *27*, 981-992.

Saudou, F., Finkbeiner, S., Devys, D., and Greenberg, M.E. (1998). Huntingtin acts in the nucleus to induce apoptosis but death does not correlate with the formation of intranuclear inclusions. Cell *95*, 55-66.

Schmidt, O., Harbauer, A.B., Rao, S., Eyrich, B., Zahedi, R.P., Stojanovski, D., Schonfisch, B., Guiard, B., Sickmann, A., Pfanner, N.*, et al.* (2011). Regulation of mitochondrial protein import by cytosolic kinases. Cell *144*, 227-239.

Schwartz, M., and Sabetay, S. (2012). An approach to the continuous dopaminergic stimulation in Parkinson's disease. The Israel Medical Association journal : IMAJ *14*, 175-179.

Schweers, R.L., Zhang, J., Randall, M.S., Loyd, M.R., Li, W., Dorsey, F.C., Kundu, M., Opferman, J.T., Cleveland, J.L., Miller, J.L.*, et al.* (2007). NIX is required for programmed mitochondrial clearance during reticulocyte maturation. Proceedings of the National Academy of Sciences of the United States of America *104*, 19500-19505.

Seibler, P., Graziotto, J., Jeong, H., Simunovic, F., Klein, C., and Krainc, D. (2011). Mitochondrial Parkin recruitment is impaired in neurons derived from mutant PINK1 induced pluripotent stem cells. The Journal of neuroscience : the official journal of the Society for Neuroscience *31*, 5970-5976.

Sha, D., Chin, L.S., and Li, L. (2010). Phosphorylation of parkin by Parkinson disease-linked kinase PINK1 activates parkin E3 ligase function and NF-kappaB signaling. Human molecular genetics *19*, 352-363.

Sheng, Z.H., and Cai, Q. (2012). Mitochondrial transport in neurons: impact on synaptic homeostasis and neurodegeneration. Nature reviews Neuroscience *13*, 77-93.

Sherer, T.B., Kim, J.H., Betarbet, R., and Greenamyre, J.T. (2003). Subcutaneous rotenone exposure causes highly selective dopaminergic degeneration and alpha-synuclein aggregation. Experimental neurology *179*, 9-16.

Shiba, K., Arai, T., Sato, S., Kubo, S., Ohba, Y., Mizuno, Y., and Hattori, N. (2009). Parkin stabilizes PINK1 through direct interaction. Biochemical and biophysical research communications *383*, 331-335.

Shimura, H., Hattori, N., Kubo, S., Mizuno, Y., Asakawa, S., Minoshima, S., Shimizu, N., Iwai, K., Chiba, T., Tanaka, K.*, et al.* (2000). Familial Parkinson disease gene product, parkin, is a ubiquitin-protein ligase. Nature genetics *25*, 302-305.

Shin, J.H., Ko, H.S., Kang, H., Lee, Y., Lee, Y.I., Pletinkova, O., Troconso, J.C., Dawson, V.L., and Dawson, T.M. (2011). PARIS (ZNF746) repression of PGC-1alpha contributes to neurodegeneration in Parkinson's disease. Cell *144*, 689-702.

Shpilka, T., and Elazar, Z. (2012). Essential role for the mammalian ATG8 isoform LC3C in xenophagy. Molecular cell *48*, 325-326.

Smith, D.M., Benaroudj, N., and Goldberg, A. (2006). Proteasomes and their associated ATPases: a destructive combination. Journal of structural biology *156*, 72-83.

Sowa, M.E., Bennett, E.J., Gygi, S.P., and Harper, J.W. (2009). Defining the human deubiquitinating enzyme interaction landscape. Cell *138*, 389-403.

Sun, Y., Vashisht, A.A., Tchieu, J., Wohlschlegel, J.A., and Dreier, L. (2012). Voltage-dependent anion channels (VDACs) recruit Parkin to defective mitochondria to promote mitochondrial autophagy. The Journal of biological chemistry *287*, 40652-40660.

Surmeier, D.J., Guzman, J.N., Sanchez-Padilla, J., and Goldberg, J.A. (2010). What causes the death of dopaminergic neurons in Parkinson's disease? Progress in brain research *183*, 59-77.

Tagwerker, C., Flick, K., Cui, M., Guerrero, C., Dou, Y., Auer, B., Baldi, P., Huang, L., and Kaiser, P. (2006). A tandem affinity tag for two-step purification under fully denaturing conditions: application in ubiquitin profiling and protein complex identification combined with in vivocross-linking. Molecular & cellular proteomics : MCP *5*, 737-748.

Tan, F., Lu, L., Cai, Y., Wang, J., Xie, Y., Wang, L., Gong, Y., Xu, B.E., Wu, J., Luo, Y.*, et al.* (2008). Proteomic analysis of ubiquitinated proteins in normal hepatocyte cell line Chang liver cells. Proteomics *8*, 2885-2896.

Tanaka, A., Cleland, M.M., Xu, S., Narendra, D.P., Suen, D.F., Karbowski, M., and Youle, R.J. (2010). Proteasome and p97 mediate mitophagy and degradation of mitofusins induced by Parkin. The Journal of cell biology *191*, 1367-1380.

Tanaka, K., and Tsurumi, C. (1997). The 26S proteasome: subunits and functions. Molecular biology reports *24*, 3-11.

Thomas, B., and Beal, M.F. (2007). Parkinson's disease. Human molecular genetics *16 Spec No. 2*, R183-194.

Thurston, T.L., Ryzhakov, G., Bloor, S., von Muhlinen, N., and Randow, F. (2009). The TBK1 adaptor and autophagy receptor NDP52 restricts the proliferation of ubiquitin-coated bacteria. Nature immunology *10*, 1215-1221.

Todd, A.M., and Staveley, B.E. (2008). Pink1 suppresses alpha-synuclein-induced phenotypes in a Drosophila model of Parkinson's disease. Genome / National Research Council Canada = Genome / Conseil national de recherches Canada *51*, 1040-1046.

Todd, A.M., and Staveley, B.E. (2012). Expression of Pink1 with alpha-synuclein in the dopaminergic neurons of Drosophila leads to increases in both lifespan and healthspan. Genetics and molecular research : GMR *11*, 1497-1502.

Um, J.W., Im, E., Lee, H.J., Min, B., Yoo, L., Yoo, J., Lubbert, H., Stichel-Gunkel, C., Cho, H.S., Yoon, J.B.*, et al.* (2010). Parkin directly modulates 26S proteasome activity. The Journal of neuroscience : the official journal of the Society for Neuroscience *30*, 11805-11814.

Um, J.W., Stichel-Gunkel, C., Lubbert, H., Lee, G., and Chung, K.C. (2009). Molecular interaction between parkin and PINK1 in mammalian neuronal cells. Molecular and cellular neurosciences *40*, 421-432.

Valente, E.M., Abou-Sleiman, P.M., Caputo, V., Muqit, M.M., Harvey, K., Gispert, S., Ali, Z., Del Turco, D., Bentivoglio, A.R., Healy, D.G.*, et al.* (2004). Hereditary early-onset Parkinson's disease caused by mutations in PINK1. Science *304*, 1158-1160.

Van Laar, V.S., Arnold, B., Cassady, S.J., Chu, C.T., Burton, E.A., and Berman, S.B. (2011). Bioenergetics of neurons inhibit the translocation response of Parkin following rapid mitochondrial depolarization. Human molecular genetics *20*, 927-940.

Villen, J., and Gygi, S.P. (2008). The SCX/IMAC enrichment approach for global phosphorylation analysis by mass spectrometry. Nature protocols *3*, 1630-1638.

Vives-Bauza, C., Zhou, C., Huang, Y., Cui, M., de Vries, R.L., Kim, J., May, J., Tocilescu, M.A., Liu, W., Ko, H.S.*, et al.* (2010). PINK1-dependent recruitment of Parkin to mitochondria in mitophagy. Proceedings of the National Academy of Sciences of the United States of America *107*, 378-383.

Von Coelln, R., Thomas, B., Savitt, J.M., Lim, K.L., Sasaki, M., Hess, E.J., Dawson, V.L., and Dawson, T.M. (2004). Loss of locus coeruleus neurons and reduced startle in parkin null mice. Proceedings of the National Academy of Sciences of the United States of America *101*, 10744-10749.

von Muhlinen, N., Akutsu, M., Ravenhill, B.J., Foeglein, A., Bloor, S., Rutherford, T.J., Freund, S.M., Komander, D., and Randow, F. (2012). LC3C, bound selectively by a noncanonical LIR motif in NDP52, is required for antibacterial autophagy. Molecular cell *48*, 329-342.

Vornlocher, H.P., Hanachi, P., Ribeiro, S., and Hershey, J.W. (1999). A 110-kilodalton subunit of translation initiation factor eIF3 and an associated 135-kilodalton protein are encoded by the Saccharomyces cerevisiae TIF32 and TIF31 genes. The Journal of biological chemistry *274*, 16802-16812.

Wagner, S.A., Beli, P., Weinert, B.T., Nielsen, M.L., Cox, J., Mann, M., and Choudhary, C. (2011). A proteome-wide, quantitative survey of in vivo ubiquitylation sites reveals widespread regulatory roles. Molecular & cellular proteomics : MCP *10*, M111 013284.

Wang, C., Lu, R., Ouyang, X., Ho, M.W., Chia, W., Yu, F., and Lim, K.L. (2007). Drosophila overexpressing parkin R275W mutant exhibits dopaminergic neuron degeneration and mitochondrial abnormalities. The Journal of neuroscience : the official journal of the Society for Neuroscience *27*, 8563-8570.

Wang, C., Tan, J.M., Ho, M.W., Zaiden, N., Wong, S.H., Chew, C.L., Eng, P.W., Lim, T.M., Dawson, T.M., and Lim, K.L. (2005). Alterations in the solubility and intracellular localization of parkin by several familial Parkinson's disease-linked point mutations. Journal of neurochemistry *93*, 422-431.

Wang, H.L., Chou, A.H., Wu, A.S., Chen, S.Y., Weng, Y.H., Kao, Y.C., Yeh, T.H., Chu, P.J., and Lu, C.S. (2011a). PARK6 PINK1 mutants are defective in maintaining mitochondrial membrane potential and inhibiting ROS formation of substantia nigra dopaminergic neurons. Biochimica et biophysica acta *1812*, 674-684.

Wang, X., Winter, D., Ashrafi, G., Schlehe, J., Wong, Y.L., Selkoe, D., Rice, S., Steen, J., LaVoie, M.J., and Schwarz, T.L. (2011b). PINK1 and Parkin target Miro for phosphorylation and degradation to arrest mitochondrial motility. Cell *147*, 893-906.

Wenzel, D.M., Lissounov, A., Brzovic, P.S., and Klevit, R.E. (2011). UBCH7 reactivity profile reveals parkin and HHARI to be RING/HECT hybrids. Nature *474*, 105-108.

Xie, H.R., Hu, L.S., and Li, G.Y. (2010). SH-SY5Y human neuroblastoma cell line: in vitro cell model of dopaminergic neurons in Parkinson's disease. Chinese medical journal *123*, 1086-1092.

Xie, Z., and Klionsky, D.J. (2007). Autophagosome formation: core machinery and adaptations. Nature cell biology *9*, 1102-1109.

Yang, Y., Gehrke, S., Imai, Y., Huang, Z., Ouyang, Y., Wang, J.W., Yang, L., Beal, M.F., Vogel, H., and Lu, B. (2006). Mitochondrial pathology and muscle and dopaminergic neuron degeneration caused by inactivation of Drosophila Pink1 is rescued by Parkin. Proceedings of the National Academy of Sciences of the United States of America *103*, 10793-10798.

Yang, Z., and Klionsky, D.J. (2010a). Eaten alive: a history of macroautophagy. Nature cell biology *12*, 814-822.

Yang, Z., and Klionsky, D.J. (2010b). Mammalian autophagy: core molecular machinery and signaling regulation. Current opinion in cell biology *22*, 124-131.

Yoshii, S.R., Kishi, C., Ishihara, N., and Mizushima, N. (2011). Parkin mediates proteasome-dependent protein degradation and rupture of the outer mitochondrial membrane. The Journal of biological chemistry *286*, 19630-19640.

Zhang, Y., Gao, J., Chung, K.K., Huang, H., Dawson, V.L., and Dawson, T.M. (2000). Parkin functions as an E2-dependent ubiquitin- protein ligase and promotes the degradation of the synaptic vesicle-associated protein, CDCrel-1. Proceedings of the National Academy of Sciences of the United States of America *97*, 13354-13359.

Zhao, T., De Graaff, E., Breedveld, G.J., Loda, A., Severijnen, L.A., Wouters, C.H., Verheijen, F.W., Dekker, M.C., Montagna, P., Willemsen, R*., et al.* (2011). Loss of nuclear activity of the FBXO7 protein in patients with parkinsonian-pyramidal syndrome (PARK15). PloS one *6*, e16983.

Zhou, C., Huang, Y., Shao, Y., May, J., Prou, D., Perier, C., Dauer, W., Schon, E.A., and Przedborski, S. (2008). The kinase domain of mitochondrial PINK1 faces the cytoplasm. Proceedings of the National Academy of Sciences of the United States of America *105*, 12022-12027.

Zhu, Q., Hulen, D., Liu, T., and Clarke, M. (1997). The cluA- mutant of Dictyostelium identifies a novel class of proteins required for dispersion of mitochondria. Proceedings of the National Academy of Sciences of the United States of America *94*, 7308-7313.

## Appendix A: Landscape of the PARKIN-dependent ubiquitylome in response to mitochondrial depolarization

LETTER

doi:10.1038/nature12043

# Landscape of the PARKIN–dependent ubiquitylome in response to mitochondrial depolarization

Shireen A. Sarraf[1], Malavika Raman[1], Virginia Guarani-Pereira[1], Mathew E. Sowa[1], Edward L. Huttlin[1], Steven P. Gygi[1] & J. Wade Harper[1]

**The PARKIN ubiquitin ligase (also known as PARK2) and its regulatory kinase PINK1 (also known as PARK6), often mutated in familial early-onset Parkinson's disease, have central roles in mitochondrial homeostasis and mitophagy[1–3]. Whereas PARKIN is recruited to the mitochondrial outer membrane (MOM) upon depolarization via PINK1 action and can ubiquitylate porin, mitofusin and Miro proteins on the MOM[1,4–11], the full repertoire of PARKIN substrates—the PARKIN-dependent ubiquitylome—remains poorly defined. Here we use quantitative diGly capture proteomics (diGly)[12,13] to elucidate the ubiquitylation site specificity and topology of PARKIN-dependent target modification in response to mitochondrial depolarization. Hundreds of dynamically regulated ubiquitylation sites in dozens of proteins were identified, with strong enrichment for MOM proteins, indicating that PARKIN dramatically alters the ubiquitylation status of the mitochondrial proteome. Using complementary interaction proteomics, we found depolarization-dependent PARKIN association with numerous MOM targets, autophagy receptors, and the proteasome. Mutation of the PARKIN active site residue C431, which has been found mutated in Parkinson's disease patients, largely disrupts these associations. Structural and topological analysis revealed extensive conservation of PARKIN-dependent ubiquitylation sites on cytoplasmic domains in vertebrate and *Drosophila melanogaster* MOM proteins. These studies provide a resource for understanding how the PINK1–PARKIN pathway re-sculpts the proteome to support mitochondrial homeostasis.**

PARKIN, a RING-HECT hybrid E3 ubiquitin ligase[14], is recruited to the MOM in cancer cell lines, mouse embryo fibroblasts (MEFs) and primary neurons to promote mitophagy in response to mitochondrial depolarization[1,2,15,16]. This process requires PINK1, which binds the MOM translocase (TOMM) complex and phosphorylates PARKIN on multiple residues to promote MOM localization and ligase activation[17–20]. The best understood PARKIN substrates are MFN1/2 and RHOT1/2 (MIRO in *Drosophila*), MOM-tethered GTPases whose PARKIN-dependent proteasomal turnover alters fission–fusion cycles and microtubule-dependent trafficking of mitochondria, respectively[1,5–8,10,11]. The MOM porin proteins VDAC1/2/3 are also ubiquitylated by PARKIN, and are required for PARKIN localization on mitochondria through a poorly understood mechanism[9,21]. Proteomic studies of purified mitochondria have also identified additional proteins whose abundance is either decreased or increased upon PARKIN activation or mitochondrial depolarization[1,4], but precisely how these proteins are regulated and the extent to which ubiquitin is involved is unclear. Consequently, we do not have a comprehensive understanding of cellular PARKIN targets, which is critical for elucidating how PARKIN promotes mitochondrial homeostasis. Moreover, for the vast majority of E3 ubiquitin ligases, including PARKIN, the extent to which ubiquitin transfer is site specific and signal dependent is largely unknown, and a global understanding of site specificity across a wide range of substrates is lacking for any E3. Such information is necessary for decoding the cellular and molecular topology of E3 function and for defining how the ubiquitin system re-sculpts the proteome.

We set out to systematically identify cellular PARKIN-dependent ubiquitylation targets and the dynamics of modification in a site-specific manner using quantitative diGly (QdiGly) proteomics. QdiGly merges antibody-based capture of 'diGly remnant'-containing peptides (marking ubiquitylated proteins after trypsinolysis) and stable isotopic labelling with amino acids in culture (SILAC) to identify ubiquitylation sites that are dynamically induced, in this case, upon mitochondrial depolarization[12,13]. To overcome inherent stochastic sampling for low-abundance diGly peptides (see Supplementary Fig. 1a, b)[12,13], we performed 73 control and QdiGly profiling experiments in four cell lines with and without elevated PARKIN levels (~tenfold) (Supplementary Fig. 2a) in a three-tiered manner, varying the length of depolarization with carbonyl cyanide *m*-chlorophenyl hydrazone (CCCP) (Fig. 1a and Supplementary Table 1). In some cases, protein turnover was blocked by proteasome inhibition with bortezomib (Btz) or autophagy inhibition with bafilomycin A (BafA) (Supplementary Table 1). Elevated PARKIN levels were used to increase the likelihood of capturing signal-dependent and mechanistically relevant ubiquitylation events that would otherwise be below the level of detection due to low stoichiometry or abundance.

Using HCT116 cells expressing a haemagglutinin-derived epitope tag (HA)-fused with PARKIN ($HCT116^{PARKIN}$, Tier 1), we performed 34 control and QdiGly experiments (Supplementary Table 1), quantifying 4,772 non-redundant ubiquitylation sites in 1,654 proteins (Fig. 1a, b). In 18 of these experiments using Btz or CCCP/Btz for 1 h, we identified 443 diGly sites (261 proteins) with $\log_2$(heavy:light (H:L)) ratios $\geq 1.0$ (twofold change) in at least one experiment (Fig. 1b, c, Supplementary Fig. 2a–c, Supplementary Tables 1, 2), with a Pearson's correlation of 0.69 for two representative experiments (Supplementary Fig. 2e). Sixteen additional Tier 1 experiments with depolarization times up to 10 h identified 537 non-redundant diGly sites (304 proteins), including 192 diGly sites (138 proteins) also identified at 1 h (Supplementary Fig. 2d). Comparison of $\log_2$(H:L) ratios for 48 Tier 1 sites in 36 proteins at 1 and 8 h post CCCP treatment from parallel experiments revealed persistent or increased ubiquitylation for 34 sites when proteasome activity is blocked (Supplementary Fig. 2f).

To systematically determine PARKIN dependence and compare targets in distinct cell lines, we performed 6 QdiGly experiments in HeLa versus $HeLa^{PARKIN}$ cells (Tier 2) with CCCP/Btz (1 h) and reverse SILAC labelling (Fig. 1a, Supplementary Tables 1, 2). As expected[4–7], CCCP-dependent MFN2 poly-ubiquitylation in HeLa cells required PARKIN expression (Supplementary Fig. 2a). We identified 582 PARKIN-dependent diGly peptides (303 proteins) (Fig. 1b), with a Pearson's correlation of 0.88 for duplicate samples (Supplementary Fig. 2e) and significant overlap across biological triplicates (Fig. 1d). Importantly, 165 diGly sites (99 proteins) were common to Tiers 1 and 2 with 1 h of depolarization (Fig. 1e). This increased to 191 sites (144 proteins) when all Tier1 and Tier 2 data were compared

[1]Department of Cell Biology, Harvard Medical School, 240 Longwood Avenue, Boston, Massachusetts 02115, USA.

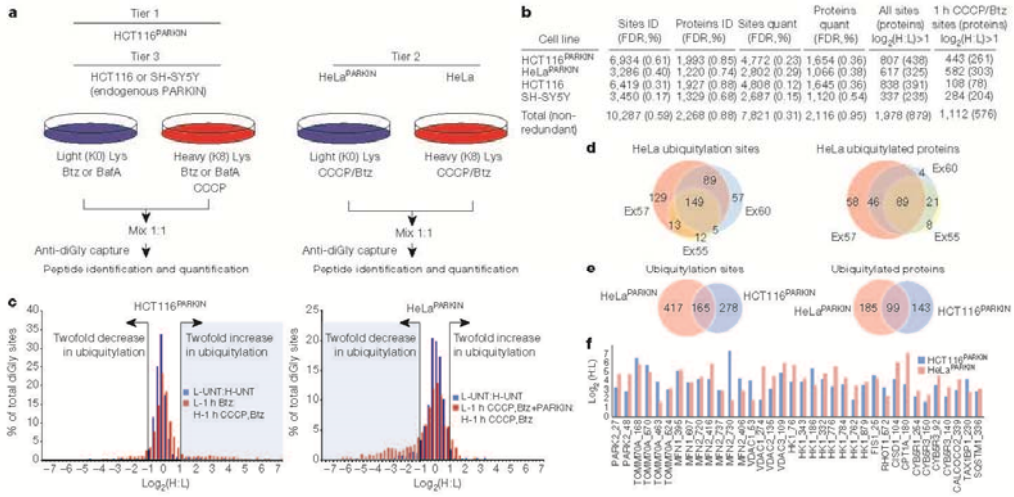


**Figure 1 | QdiGly proteomics for PARKIN-dependent ubiquitylation.** **a**, Proteomics work flow. **b**, diGly sites identified and quantified across 73 experiments. FDR, false discovery rate. **c**, $Log_2$(H:L) plots for quantified diGly peptides for HCT116$^{PARKIN}$ (experiment 17) or HeLa$^{PARKIN}$ (experiment 57) cells (Supplementary Table 2). **d**, Overlap of ubiquitylation sites in HeLa$^{PARKIN}$ biological triplicates (1 h CCCP + Btz) (Supplementary Tables 1, 2). Ex, experiment. **e**, Ubiquitylation site and protein overlap between all HCT116$^{PARKIN}$ and HeLa$^{PARKIN}$ experiments treated with CCCP and Btz for 1 h. **f**, $log_2$(H:L) ratios for selected diGly sites from HCT116$^{PARKIN}$ (Ex17) and HeLa$^{PARKIN}$ (Ex57) (1 h CCCP + Btz).

(Supplementary Table 2). We refer to the overlapping set of ubiquitylation sites with 1 h of depolarization and their associated proteins as Class 1 candidate PARKIN-dependent targets, whereas proteins found in both cell lines but with different sites of ubiquitylation are referred to as Class 2 (Supplementary Table 2). Whereas a twofold increase in H:L ratio was used as a threshold for regulated ubiquitylation, many diGly sites were induced 30–60-fold upon depolarization (Fig. 1f, Supplementary Table 2), indicating highly dynamic target modification via PARKIN.

Class 1 targets were enriched in mitochondrial proteins ($P < 1.76 \times 10^{-17}$), although numerous cytoplasmic proteins were also identified (Fig. 2, Supplementary Fig. 2i). In total, 60 Class 1 and 2 targets were linked with mitochondria or endoplasmic reticulum-type membranes, including 36 MOM proteins. Candidate cytoplasmic targets included proteasome subunits, the VCP/p97 ATPase, and proposed autophagy adaptors (SQSTM1, CALCOCO2 (also known as NDP52), and TAX1BP1).

We next performed 22 control and QdiGly profiling experiments using HCT116 or neuronal SH-SY5Y cells (Tier 3, Fig. 1a, b, Supplementary Tables 1, 2), which show primarily mono-ubiquitylated forms of MFN2 ubiquitylation upon depolarization, apparently due to low levels of endogenous PARKIN (Supplementary Fig. 2a). Cumulatively, 838 diGly sites (391 proteins) in HCT116 and 337 diGly sites (235 proteins) in SH-SY5Y had $log_2$(H:L) $\geq 1.0$ (Fig. 1b), with extensive overlap across Tier 1 and 2 data sets (Supplementary Fig. 2g) and biological triplicates in SH-SY5Y (1 h/CCCP) (Supplementary Fig. 2h). Fifteen sites in 12 Class 1 or 2 targets were found in both cell lines, and 29 and 27 CCCP-dependent diGly sites in 27 and 17 Class 1 or 2 proteins were detected in SH-SY5Y or HCT116 cells, respectively (Fig. 2, Supplementary Tables 1, 2). Additionally, 124 Tier 3 sites were identified in 29 Class 1 or 2 proteins that were distinct from Class 1 sites. Thus, many PARKIN-dependent diGly targets were confirmed at endogenous PARKIN levels. Ubiquitylation of several candidate substrates was demonstrated by immunoblotting, and ubiquitylation was reduced upon small-interfering RNA (siRNA)-mediated depletion of PARKIN for several targets tested (Supplementary Fig. 3a–d).

To complement QdiGly proteomics, we used anti-HA affinity purification–mass spectrometry (AP–MS)[22] to identify depolarization-dependent high-confidence candidate HA–PARKIN-interacting proteins (HCIPs) in duplicate experiments in 293T$^{PARKIN}$ cells (Fig. 3a, Supplementary Fig. 4a, Supplementary Table 3), with further validation in HeLa$^{PARKIN}$ cells (Supplementary Fig. 4b, Supplementary Table 4) (see Methods). Because PARKIN action is dynamic, we examined several time points (1, 4 or 8 h) after depolarization in the presence or absence of Btz or BafA. To allow a semiquantitative assessment of interactions, we compared bait-normalized average assembled peptide spectral matches (APSMs) for proteins that were HCIPs under at least one condition examined unless otherwise noted (Fig. 3a, Supplementary Fig. 4a, Supplementary Tables 3, 4). Without depolarization, no HCIPs were common to both wild-type PARKIN biological duplicates, consistent with PARKIN auto-inhibition before activation[23] (Fig. 3a, Supplementary Text). Remarkably, upon depolarization, four classes of HCIPs were identified in at least one condition examined (Fig. 3a, b): (1) 20 MOM proteins, including MFN1/2, RHOT1/2 and VDACs, HK1/2, the fission protein FIS1 and its interacting protein TBC1D15, and the translocase components TOMM20 and TOMM70; (2) the autophagy adaptors SQSTM1 (also known as p62), CALCOCO2 and TAX1BP1; (3) subunits of the catalytic and regulatory particles of the proteasome; and (4) the VCP (also known as p97) ATPase implicated in MFN1 turnover[7]. Nineteen of the 26 mitochondrial and autophagy proteins and 39 of 40 proteasome subunits found in 293T cells were also identified in at least one condition examined in HeLa cells (Fig. 3b, Supplementary Fig. 4b). Depolarization-dependent interaction of Flag–PARKIN with selected endogenous HCIPs was verified by anti-Flag immunoprecipitation and immunoblotting (Supplementary Fig. 5). Notably, 21 of the 27 mitochondrial and autophagy receptor proteins found associated with PARKIN, as well as eight subunits of the regulatory particle of the proteasome and VCP, were also identified as Class 1 or 2 PARKIN-dependent ubiquitylation targets (Figs 2, 3b, Supplementary Table 2).

PARKIN activation is thought to reverse auto-inhibition by its amino-terminal ubiquitin-like domain (UBL), which has been proposed to


**Figure 2 | PARKIN-dependent ubiquitylation sites revealed by QdiGly proteomics.** Class 1 sites are in black font. Additional sites found in Class 1 proteins are in red ($HCT116^{PARKIN}$) or blue font ($HeLa^{PARKIN}$). Site overlap in HCT116 and/or SH-SY5Y: magenta, orange, and green octagons. Dotted lines: interacting proteins. Rectangles represent Class 2 substrates. Red or blue boxes refer to additional sites identified in either $HCT116^{PARKIN}$ and $HeLa^{PARKIN}$ cells (Supplementary Table 2). MIM, mitochondrial inner membrane. * and *, protein levels decrease or increase, respectively, upon depolarization[4].

sterically hinder ubiquitin-conjugating (E2) enzyme interaction with the catalytic centre[20,23]. We explored the role of these regions in MOM recruitment, MFN2 ubiquitylation, substrate binding and proteasome association by using five mutants (Supplementary Fig. 6a): (1) ΔUBL, lacking the UBL domain (residues 1–80), (2) K27/48R, which blocks ubiquitylation of two regulated diGly sites in the UBL (Fig. 2), (3) S65A and S65E, which block PINK1-dependent phosphorylation of the UBL domain implicated in PARKIN activation *in vitro*[18], and (4) C431S, removing the active site Cys in RING2. The Parkinson's disease patient mutation PARKIN(C431F) fails to localize to mitochondria in response to depolarization[15,20]. Consistent with this, PARKIN(C431S) failed to localize to mitochondria, efficiently poly-ubiquitylate MFN2, or interact robustly with MOM substrates in response to depolarization (Fig. 3a, Supplementary Fig. 6a–d). In contrast, K27/K48R, S65A and S65E mutants showed near wild-type activity for localization, MFN2 ubiquitylation and interaction with MOM proteins at 1 h post

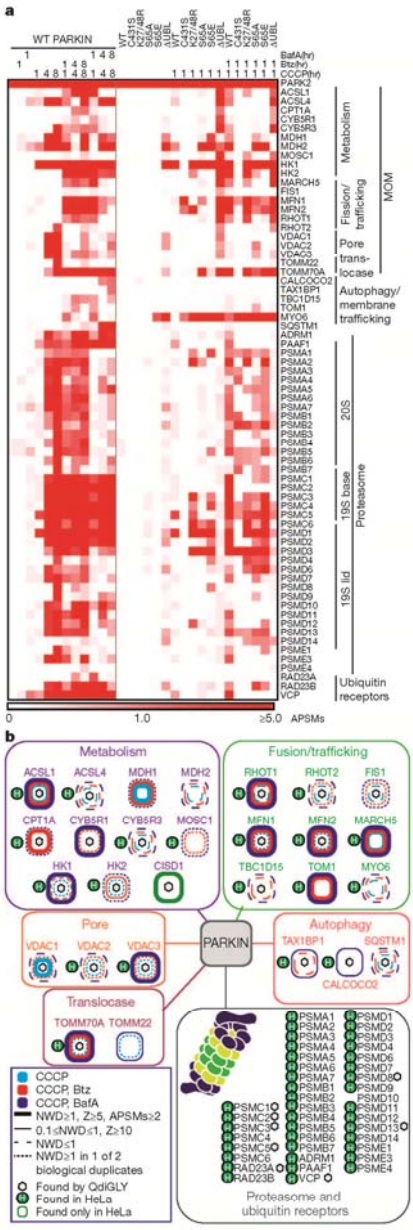


**Figure 3 | PARKIN associates with mitochondrial proteins and the proteasome in response to depolarization. a**, Heat map of HCIPs (represented by APSMs) for HA–Flag–PARKIN and mutants in response to depolarization in 293T cells, with or without Btz or BafA. Proteins indicated had weighted and normalized *D*-scores ≥ 1.0,

*Z*-score ≥ 5, and APSMs ≥ 2 unless otherwise noted (see Methods). **b**, Summary of PARKIN-interacting proteins in 293T and HeLa and integration with diGly sites.

depolarization (Fig. 3a, Supplementary Fig. 6a–d, Supplementary Tables 3, 6), although we cannot rule out a kinetic effect of these mutations. PARKIN(ΔUBL) displayed readily detectable association with MOM substrates in the absence of depolarization, consistent with some loss of auto-inhibition[22], but nevertheless showed enhanced substrate association upon depolarization, indicating residual PINK1 dependence despite the absence of the UBL and S65. However, MFN2 ubiquitylation was reduced compared with wild-type PARKIN, suggesting reduced ubiquitylation activity. PARKIN(ΔUBL) also lacked a robust increase in proteasomal binding (Fig. 3a).

Our data indicate that PARKIN interacts with and promotes the site-specific ubiquitylation of numerous mitochondrial and cytoplasmic proteins, thereby extending previous studies examining abundance of mitochondrially enriched proteins[1,4]. To place candidate PARKIN-dependent ubiquitination targets into a structural and functional framework, we have created an interactive resource that integrates dynamic ubiquitylation data with available structural information (Supplementary Fig. 7b–e and Methods). We explored the spatial relationship between protein localization, structure and conservation for 90 Class 1 sites on 36 candidate PARKIN substrates (Fig. 4a–d, Supplementary Fig. 7a, Supplementary Table 5). We found that 90% of ubiquitylated lysine residues are conserved in mouse (*Mus musculus*), 78% in zebrafish (*Danio rerio*), and 51% in the 29 conserved orthologues in *D. melanogaster*, which harbours an active PARKIN–PINK1 pathway[6]. Moreover, 38% of sites were conserved in all three species, and 22 of 36 proteins have at least one site conserved from human to *D. melanogaster* (Fig. 4a–d, Supplementary Fig. 7a). DiGly sites were observed on multiple structural elements (α-helices, β-sheets and loops) and no obvious sequence motif was identified by MOTIFX, indicating that PARKIN specificity is driven primarily by substrate recruitment and/or proximity rather than specific target sequences.

Of the 17 MOM targets whose structures or membrane orientations are defined, all identified ubiquitylation sites are presented on the cytoplasmic surface (Fig. 4c, d), consistent with the idea that PARKIN resculpts the MOM proteome via its cytoplasmic recruitment. Fifty-nine percent of Class 1 and 2 targets had one or two sites of ubiquitylation, whereas 41% of targets had 3–15 sites that were PARKIN-dependent on the basis of Tier 2 analysis (Supplementary Fig. 7f). Of the eight Class 1 and Class 2 sites identified in MFN1, all but two are located in helical motifs flanking the two carboxy-terminal membrane-spanning regions, indicating localized ubiquitylation (Fig. 2 and Fig. 4d). We detected 14 Class 1 and 2 sites in HK1, but unlike MFN1, these sites were comparatively delocalized across both globular domains in HK1 (Fig. 4c). Similarly, TOMM70 was decorated extensively over its 10 cytoplasmic TPR motifs (Figs 2, 4d). Although we cannot exclude the possibility that some ubiquitylation events occur downstream of PARKIN activation, the fact that we find many of the targets as PARKIN-interacting proteins (Fig. 3b) is consistent with direct ubiquitylation (see Supplementary Text). An understanding of how PARKIN ubiquitylates topologically diverse proteins and domains within proteins requires further study but will be facilitated by the site-specificity data reported here.

PARKIN seems to promote rapid turnover of some targets but not others. In total, 12 of the Class 1 and 2 proteins identified here (see Fig. 2), like MFN1/2 and RHOT1/2[1,4,7,10,11], probably undergo proteasomal turnover, including C1QBP1 (Supplementary Fig. 3c, d), FIS1 and CISD1, as their total levels are also decreased upon PARKIN activation[1,4]. In contrast, previous studies[4] have identified 50 preferentially cytoplasmic proteins or protein complexes that are enriched in mitochondria in response to depolarization. Consistent with this, we identified 11 of these proteins or components of protein complexes as Class 1 or 2 targets (Fig. 2 and Supplementary Fig. 7g), possibly reflecting an under-appreciated dynamic recruitment process affecting mitochondrial homeostasis. These include the autophagy adaptor p62, previously linked with mitochondrial clustering after damage[24], as well as TBC1D15 and DNML1, which are known to interact with FIS1 to regulate fission–fusion cycles[25]. In addition to p62, we also identified candidate autophagy receptors, CALCOCO2 and TAX1BP1, which are ubiquitylated upon depolarization and associate with PARKIN in the presence of BafA (Figs 2, 3). Because CALCOCO2 has been shown to target bacteria for autophagy[26], it is an attractive candidate for involvement in mitophagy. We speculate that these related autophagy adaptor proteins may be dynamically recruited to the MOM and may link the depolarization response to the recruitment of autophagy machinery. Additionally, it is possible that additional cytoplasmic proteins identified here as PARKIN-dependent targets are transiently recruited to mitochondria but below the level of detection in previous studies. It is also likely that ubiquitylation of PARKIN targets alters their enzymatic properties or functions before their turnover by the proteasome or autophagy. Potential PARKIN-regulated functions include: (1) fission–fusion cycles (FIS1, TBC1D15), (2) small molecule transport (VDACs), (3) apoptosis (FKBP8, MCL1, BAX), (4) iron-sulphur shuttling (CISD1), (5) protein translocation (TOMM70) or (6) proteasome assembly or activity (PSMC subunits) (see Supplementary Text)[25,27].

This work provides systematic target identification and ubiquitylation site-specificity for PARKIN, thereby revealing the diversity and complexity of PARKIN function on the MOM and in the cytoplasm. This resource will enable the development of methods that detect specific diGly sites in PARKIN targets *in situ*, thus enabling a deeper understanding of how PARKIN controls mitochondrial homeostasis in tissues relevant to Parkinson's disease.

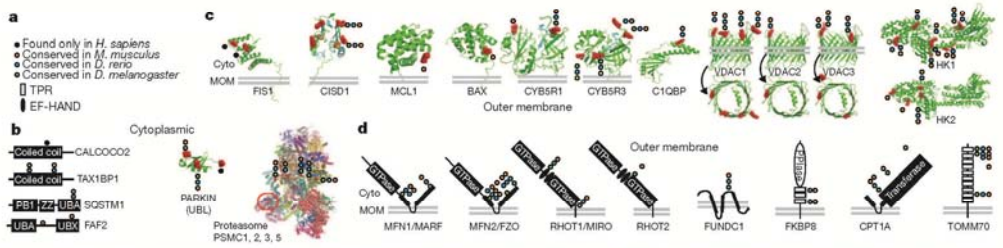


**Figure 4 | Structural anatomy and conservation of PARKIN-dependent diGly sites.** Structures or domain schematics are shown for Class 1 depolarization and PARKIN-dependent diGly sites (PDB codes, Supplementary Table 5). **a**, Legend for colour-coded circles that indicate the conservation of Lys at homologous positions in *M. musculus*, *D. rerio* and *D. melanogaster* (Supplementary Table 5). For structures, regulated sites are shown in red space-filled models. **b**, Cytoplasmic proteins. RPN10, red circle. **c**, MOM proteins with structures. **d**, MOM proteins without structures.

## METHODS SUMMARY

Cells were grown in Lys(K)-free DMEM/dialysed fetal bovine serum, with light (K0) or heavy (K8) Lys (50 μg ml$^{-1}$)[12], and treated with Btz (1 μM), CCCP (10 μM), and/or BafA (50 nM). Mixed cells were lysed in 8 M urea, 75 mM NaCl, 50 mM Tris HCl (pH 8.2), and tryptic/LysC peptides immunoprecipitated with anti-diGly-Protein A (Cell Signaling Technologies) (1 h, 4 °C), typically with 2–4 sequential immunoprecipitations (Supplementary Table 1)[12]. Peptides and ubiquitylation sites were identified by liquid chromatography-tandem mass spectrometry (see Methods)[12]. Extracted ion chromatograms were used for quantification and signal-to-noise measurements[12]. Interaction proteomics used 293T or HeLa cells stably expressing HA–Flag–PARKIN (or mutants) and *CompPASS* to identify HCIPs[22].

**Full Methods** and any associated references are available in the online version of the paper.

**Received 11 November 2012; accepted 26 February 2013.**
**Published online 17 March 2013.**

1. Narendra, D., Walker, J. E. & Youle, R. Mitochondrial quality control mediated by PINK1 and Parkin: links to parkinsonism. *Cold Spring Harb. Perspect. Biol.* **4,** a011338 (2012).
2. Youle, R. J. & Narendra, D. P. Mechanisms of mitophagy. *Nature Rev. Mol. Cell Biol.* **12,** 9–14 (2011).
3. Dawson, T. M. & Dawson, V. L. The role of parkin in familial and sporadic Parkinson's disease. *Mov. Disord.* **25** (Suppl 1), S32–S39 (2010).
4. Chan, N. C. *et al.* Broad activation of the ubiquitin-proteasome system by Parkin is critical for mitophagy. *Hum. Mol. Genet.* **20,** 1726–1737 (2011).
5. Glauser, L., Sonnay, S., Stafa, K. & Moore, D. J. Parkin promotes the ubiquitination and degradation of the mitochondrial fusion factor mitofusin 1. *J. Neurochem.* **118,** 636–645 (2011).
6. Ziviani, E., Tao, R. N. & Whitworth, A. J. *Drosophila* parkin requires PINK1 for mitochondrial translocation and ubiquitinates mitofusin. *Proc. Natl Acad. Sci. USA* **107,** 5018–5023 (2010).
7. Tanaka, A. *et al.* Proteasome and p97 mediate mitophagy and degradation of mitofusins induced by Parkin. *J. Cell Biol.* **191,** 1367–1380 (2010).
8. Poole, A. C., Thomas, R. E., Yu, S., Vincow, E. S. & Pallanck, L. The mitochondrial fusion-promoting factor mitofusin is a substrate of the PINK1/parkin pathway. *PLoS ONE* **5,** e10054 (2010).
9. Sun, Y., Vashisht, A. A., Tchieu, J., Wohlschlegel, J. A. & Dreier, L. VDACs recruit Parkin to defective mitochondria to promote mitochondrial autophagy. *J. Biol. Chem.* **287,** 40652–40660 (2012).
10. Wang, X. *et al.* PINK1 and Parkin target Miro for phosphorylation and degradation to arrest mitochondrial motility. *Cell* **147,** 893–906 (2011).
11. Liu, S. *et al.* Parkinson's disease-associated kinase PINK1 regulates Miro protein level and axonal transport of mitochondria. *PLoS Genet.* **8,** e1002537 (2012).
12. Kim, W. *et al.* Systematic and quantitative assessment of the ubiquitin-modified proteome. *Mol. Cell* **44,** 325–340 (2011).
13. Wagner, S. A. *et al.* A proteome-wide, quantitative survey of *in vivo* ubiquitylation sites reveals widespread regulatory roles. *Mol. Cell Proteomics* **10,** M111.013284 (2011).
14. Wenzel, D. M., Lissounov, A., Brzovic, P. S. & Klevit, R. E. UbcH7-reactivity profile reveals Parkin and HHARI to be RING/HECT hybrids. *Nature* **474,** 105–108 (2011).
15. Joselin, A. P. *et al.* ROS-dependent regulation of Parkin and DJ-1 localization during oxidative stress in neurons. *Hum. Mol. Genet.* **21,** 4888–4903 (2012).
16. Narendra, D., Tanaka, A., Suen, D. F. & Youle, R. J. Parkin is recruited selectively to impaired mitochondria and promotes their autophagy. *J. Cell Biol.* **183,** 795–803 (2008).
17. Lazarou, M., Jin, S. M., Kane, L. A. & Youle, R. J. Role of PINK1 binding to the TOM complex and alternate intracellular membranes in recruitment and activation of the E3 ligase Parkin. *Dev. Cell* **22,** 320–333 (2012).
18. Kondapalli, C. *et al.* PINK1 is activated by mitochondrial membrane potential depolarization and stimulates Parkin E3 ligase activity by phosphorylating Serine 65. *Open Biol.* **2,** 120080 (2012).
19. Sha, D., Chin, L. S. & Li, L. Phosphorylation of parkin by Parkinson disease-linked kinase PINK1 activates parkin E3 ligase function and NF-κB signaling. *Hum. Mol. Genet.* **19,** 352–363 (2010).
20. Lazarou, M. *et al.* PINK1 drives Parkin self-association and HECT-like E3 activity upstream of mitochondrial binding. *J. Cell Biol.* **200,** 163–172 (2013).
21. Geisler, S. *et al.* PINK1/Parkin-mediated mitophagy is dependent on VDAC1 and p62/SQSTM1. *Nature Cell Biol.* **12,** 119–131 (2010).
22. Sowa, M. E., Bennett, E. J., Gygi, S. P. & Harper, J. W. Defining the human deubiquitinating enzyme interaction landscape. *Cell* **138,** 389–403 (2009).
23. Chaugule, V. K. *et al.* Autoregulation of Parkin activity through its ubiquitin-like domain. *EMBO J.* **30,** 2853–2867 (2011).
24. Narendra, D., Kane, L. A., Hauser, D. N., Fearnley, I. M. & Youle, R. J. p62/SQSTM1 is required for Parkin-induced mitochondrial clustering but not mitophagy; VDAC1 is dispensable for both. *Autophagy* **6,** 1090–1106 (2010).
25. Onoue, K. *et al.* Fis1 acts as mitochondrial recruitment factor for TBC1D15 that is involved in regulation of mitochondrial morphology. *J. Cell Sci.* http://dx.doi.org/10.1242/jcs.111211 (2012).
26. von Muhlinen, N. *et al.* LC3C, bound selectively by a noncanonical LIR motif in NDP52, is required for antibacterial autophagy. *Mol. Cell* **48,** 329–342 (2012).
27. Huang, P., Galloway, C. A. & Yoon, Y. Control of mitochondrial morphology through differential interactions of mitochondrial fusion and fission proteins. *PLoS ONE* **6,** e20655 (2011).

**Supplementary Information** is available in the online version of the paper.

**Acknowledgements** We thank W. Kim for LC-MS and for development of QdiGly profiling, R. Kunz for peptide purification, J. Lydeard, S. Hayes and A. White for proteomics, M. Comb and S. Beausoleil (Cell Signaling Technologies) for antibodies, Nikon Imaging Center (Harvard Medical School) for microscopy, and D. Finley and B. Schulman for discussions. Supported by NIH grants GM070565 and GM095567 to J.W.H., GM067945 to S.P.G., CA139885 to M.R., and the Michael J. Fox Foundation for Parkinson's Research to J.W.H.

**Author Contributions** S.A.S. and J.W.H. conceived the experiments. S.A.S. performed QdiGly profiling, biochemical, and interaction experiments and analysis. S.A.S., M.R. and V.G.-P. performed cell biological experiments. M.E.S. designed site visualization software. E.L.H. and S.P.G. provided proteomics software and analysis. S.A.S. and J.W.H. wrote the manuscript. All authors assisted in editing the manuscript.

**Author Information** Reprints and permissions information is available at www.nature.com/reprints. The authors declare no competing financial interests. Readers are welcome to comment on the online version of the paper. Correspondence and requests for materials should be addressed to J.W.H. (wade_harper@hms.harvard.edu).

## METHODS

**Sample preparation for diGly capture.** HCT116, HeLa or SH-SY5Y cells ($10^8$) were grown in lysine-free DMEM supplemented with 10% dialysed FBS (Gibco), 2 mM L-glutamine, 1% penicillin/streptomycin (Gibco), and light (K0) lysine (50 μg ml$^{-1}$), which contained no heavy isotopes[12]. Heavy media was the same except the light lysine was replaced with heavy (K8, 8 Da heavier) lysine (L-lysine:2HCl (U-$^{13}$C6, 99%, U-$^{15}$N2, 99%); Cambridge Isotopes) at the same concentration. Where indicated, cells were treated with Btz (1 μM), CCCP (10 μM), and/or BafA (50 nM) for the times indicated. Btz was a gift from Millennium Pharmaceuticals. After the indicated treatments, heavy and light cells were mixed 1:1 by cell number and lysed in 8 ml of denaturing lysis buffer (8 M urea, 50 mM Tris (pH 8.2), 75 mM NaCl, protease inhibitors (EDTA-free), Roche)[12]. Samples were incubated on ice for 10 min and then sonicated with 3 × 10 s pulses. We typically obtained 30–50 mg of total protein. Lysates were digested with trypsin as described previously[26] with one modification. Prior to trypsin digestion, lysates were diluted 1:1 with 50 mM Tris (pH 8.2) to lower the urea concentration to 4 M and digested with 10 ng μl$^{-1}$ Lys-C (Wako) for 2 h at room temperature.

**Immunoprecipitation of diGly containing peptides.** Lyophilized peptides from 30–50 mg of digested proteins were resuspended in 1.3 ml of IAP buffer (50 mM MOPS (pH 7.4), 10 mM $Na_2HPO_4$, 50 mM NaCl) and centrifuged at 14,000*g* for 5 min to remove any insoluble materials. The supernatant was incubated with anti-diGly antibody coupled to protein A agarose or acrylamide beads for 1 h at 4 °C and washed with IAP buffer 3 × and once with PBS as described previously[12]. Peptides were eluted by treatment with 50 μl of 5% formic acid for 10 min twice. The eluted peptides were desalted using C18 stage-tip method and resuspended in 5% formic acid before mass spectrometric analysis. Lysates were subjected to immunoprecipitation sequentially two or four times, unless otherwise noted in Supplementary Table 1.

**Mass spectrometry analysis of diGly peptides.** Peptides were separated on 100 μm × 20 cm C18 reversed phase (Maccel C18 3μ 200 Å, The Nest Group) with a 165 min gradient of 6% to 27% acetonitrile in 0.125% formic acid[29]. The twenty most intense peaks from each full mass spectrometry (MS) scan acquired in the Orbitrap Velos (Thermo) were selected for MS/MS (see RAW files for specific settings).

Sequest-based identification using a Human UNIPROT database followed by a target decoy-based linear discriminant analysis was used for peptide and protein identification as described[12,30,31]. Localization of diGly sites used a modified version of the *A*-score algorithm[32] as described[12]. *A*-scores > 13 were considered localized. SILAC-based site quantification and signal-to-noise was performed as described previously[12] by using extracted ion chromatograms. The heavy- and light-labelled peptides from each search were subsequently combined using custom scripts. Other parameters used for database searching include: 50 p.p.m. precursor mass tolerance; 1.0 Da product ion mass tolerance; tryptic digestion with up to three missed cleavages; and variable oxidation of Met (+15.994946). For an individual peptide to be used for quantification of sites and proteins, it had to meet one of two conditions: (1) both heavy and light isotopic envelopes must be detected with signal-to-noise ratios above 5.0; and (2) one isotopic envelope (heavy or light) must have a signal-to-noise ratio above 10.0. Equal mixing ratios for heavy to light cells were confirmed by calculating the mean $\log_2$(H:L) ratios in non-diGly non-lysine containing peptides and subtracting that from the corresponding $\log_2$(H:L) diGly ratios if necessary. Keratins were removed from site lists. Contributions of peptide identifications to various protein isoforms were condensed into a single UniProt descriptor using principles of parsimony. Mass spectrometry RAW files are available upon request.

**Interaction proteomics.** Interaction proteomics was performed essentially as described previously, but with small modifications[22]. Briefly, 293T or HeLa cells were transduced with a lentiviral vector expressing HA–Flag–PARKIN (NP_004553.2) or the designated PARKIN mutants, and stable cell lines selected in puromycin. Cells from 4 × 15 cm dishes at 80% confluence were treated with CCCP (10 μM), Btz (1 μM), and/or BafA (50 nM) as indicated and after the indicated time, cells were collected and lysed in 3 ml of 50 mM Tris-HCl (pH 7.4), 150 mM NaCl, 0.5% Nonidet P40, and protease inhibitors. Cleared lysates were filtered through 0.45−μm spin filters (Millipore Ultrafree-CL) and immunoprecipitated with 30 μl anti-HA resin (Sigma). Complexes were washed 4× with lysis buffer, exchanged into PBS for a further three washes, eluted with HA peptide, reductively carboxymethylated, and precipitated with 10% trichloroacetic acid (TCA). TCA-precipitated proteins were trypsinized, purified with Empore C18 extraction media (3 M), and analysed by liquid chromatography-tandem mass spectrometry (LC-MS/MS) with a LTQ-Velos linear ion trap mass spectrometer (Thermo) with an 18 cm$^3$ 125 μm (ID) C18 column and a 50 min 8–26% acetonitrile gradient. All AP–MS experiments in 293T cells were performed in biological duplicates and for each biological experiment, complexes were analysed twice by LC-MS to generate technical duplicates. AP–MS experiments in HeLa cells were performed on a single IP but with technical duplicates. Spectra were searched with Sequest against a target-decoy human tryptic UniProt-based peptide database, and these results were loaded into the Comparative Proteomics Analysis Software Suite (CompPASS) to identify high confidence candidate interacting proteins (HCIPs)[33]. Here, a statistics table derived from analogous AP–MS data for 166 unrelated proteins was used to determine weighted and normalized *D*-scores (WD$^N$-score) as well as *Z*-scores based on spectral counts. The *D*-score measures the reproducibility, abundance and frequency of individual proteins detected in each individual analysis.

To identify PARKIN-associated proteins, we filtered proteins at a 2% false discovery rate for those with a WD$^N$-score ≥ 1.0, *Z*-score ≥ 5, and average assembled peptide spectral matches (APSMs) ≥ 2 in both biological duplicates. In addition to the initially identified proteins, APSMs for interactors with WD$^N$-scores greater than 1 under at least one condition examined, or with a *Z*-score greater than 10 in both biological duplicates, were plotted in heat map form using Multi-experiment Viewer software (MeV). Due to space limitations, a subset of proteins which had a WD$^N$-score ≥ 1.0 in at least one experiment were omitted from Fig. 3 but are contained in the heat maps in Supplementary Fig. 4 as well as Supplementary Tables 3 and 4. TAX1BP1 that was identified in PARKIN immunoprecipitates and also found to be ubiquitylated but did not pass the stringent cut-off for passing our scoring scheme was also displayed in the heat map. We note that whereas several proteins passed the WD$^N$-score cut-off for PARKIN-associated proteins in the absence of depolarization in individual experiments, there was essentially no overlap within biological duplicates (Supplementary Table 4). In addition, for proteins with a maximum of 1–3 spectral counts, it is possible that those proteins were missed under some conditions due to stochastic sampling of low abundance proteins by LC-MS (for example, CYB5R3, TOM22, and RHOT1 with wild-type PARKIN at 8 h post-CCCP in the presence versus the absence of BafA, Fig. 3a). The following proteins were identified in only 1 biological duplicate as being associated with PARKIN but were included in the heat map (Fig. 3a) as they are also present as Class 1 diGly targets: SQSTM1, TAX1BP1, TBC1D15, MYO6, VCP, RHOT2, HK2, MDH2, CYB5R3 and ACSL4.

**Immunological methods and microscopy.** To validate interactions between PARKIN and candidate interacting proteins (Supplementary Fig. 3), 293T cells stably expressing HA–Flag–PARKIN were either left untreated or treated with CCCP (10 μM) or CCCP (10 μM) and Btz (1 μM) for 1 h. Extracts (50 mM Tris-HCl (pH 7.4), 150 mM NaCl, 0.5% Nonidet P40, and protease inhibitors) from cells were subjected to immunoprecipitation with anti-Flag resin (M2 agarose; Sigma), and washed complexes subjected to immunoblotting with the indicated antibodies. To examine MFN2 ubiquitylation, extracts from cells lysed in denaturing lysis buffer (8 M urea, 75 mM NaCl, 50 mM Tris (pH 8.0), and protease inhibitors) expressing the indicated HA–Flag–PARKIN mutant proteins were separated on a 4–12% gradient SDS-polyacrylamide gel (PAGE) and blotted with anti-HA or anti-MFN2. To examine PARKIN levels in the cell lines used (Supplementary Fig. 1), cells were lysed in denaturing lysis buffer and protease inhibitors and extracts subjected to SDS–PAGE and immunoblotting. To examine ubiquitylation of candidate PARKIN substrates by immunoblotting, HCT116 cell lines stably expressing the candidate substrates C-terminally tagged with HA–Flag epitopes were transfected with either control siRNA or an siRNA targeting *PARKIN* (1: 5′-GGAGUGCAGUGCCGUAUUU-3′, 2: 5′-GUAAAGAAGCGUACCAUGA-3′, 3: 5′-GGAGCCAUCGCCUAUGAAA-3′, 4: 5′-GUAAAGAAGCGUACCAUGA-3′, Thermo Scientific). After 72 h, cells were treated with CCCP (10 μM) with or without Btz to block proteasomal turnover of targets. At the indicated times, cells were lysed in 8 M urea and subjected to immunoblotting using anti-HA antibodies. Identical gels were run and probed with anti-PCNA as a loading control. The antibodies used are as follows: anti-TOMM70, (Proteintech, 14528-1); anti-MFN2, (Epitomics, 3272-1 or Sigma, WH0009927M3); anti-ADRM1, (Enzo Scientific, BML-PW9910); anti-Rpn10, (Enzo Scientific, BML-PW9250); anti-HK1, (Cell Signaling, C35C4); anti-PSMD2, (Affinity BioReagents, PA1-964); anti-PARKIN, (PRK8, Santa Cruz, sc-32282).

To examine the localization of PARKIN and various PARKIN mutants, HeLa cells stably expressing HA–Flag-tagged proteins were plated on No.1 coverslips, treated with CCCP (10 μM, 1 h), and fixed with 4% paraformaldehyde before immunofluorescence using anti-HA to detect PARKIN proteins and anti-TOMM20 to detect mitochondria. All images were collected with a Yokogawa CSU-X1 spinning disk confocal on a Nikon Ti-E inverted microscope equipped with ×100 Plan Apo numerical aperture 1.4 objective lens. HA–PARKIN fluorescence was excited with the 491 nm line (selected with an AOTF) from Spectral Applied Precision LMM-7 solid-state laser launch. Emission was collected with a quad band pass polychroic mirror (Semrock) and a Chroma ET525/50m emissions filter. TOMM20 fluorescence was excited with the 561 nm line from the LMM-7 launch, and emission collected with the Semrock polychroic and a

Chroma ET620/60m emission filter. Images were acquired with a Hamamatsu ORCA-AG cooled CCD camera controlled with MetaMorph 7 software. Nine *z*-series optical sections were collected with a step size of 0.2 μm, using the internal Nikon Ti-E focus motor. *z*-series were deconvolved using AutoQuant blind deconvolution software, and are displayed as maximum *z*-projections. Gamma and brightness were adjusted on displayed images (identically for compared image sets) and percent colocalization was calculated by thresholding for signal at least 4 standard deviations above background in a single *z* slice (identically for compared image sets) using MetaMorph 7 software (Supplementary Table 6).

**Structural analysis of ubiquitylation sites and web portal.** Using the UniProt identifier for each protein identified, the corresponding PDB file(s) (if available) were determined using data from the UniProt to PDB cross-reference table (http://www.ebi.ac.uk/pdbe/docs/sifts/quick.html). The amino acid position in the structure corresponding to each ubiquitylation site was calculated based on their relative position in the structure using the information provided by the cross reference table. Data for each experiment was stored in MySQL tables, which are used when accessing the data via the web portal. For rendering of the structural information via the web portal, Jmol: an open-source Java viewer for chemical structures in 3D (http://www.jmol.org/) was used. Access to the web portal is available at harper.hms.harvard.edu.

**Gene ontology.** Gene ontology analysis was performed using DAVID[33]. Additional sub-cellular localization parameters as designated in Fig. 2 were performed manually using MITOCARTA, Human Protein Atlas, and GenBank.


28. Villén, J. & Gygi, S. P. The SCX/IMAC enrichment approach for global phosphorylation analysis by mass spectrometry. *Nature Protocols* **3,** 1630–1638 (2008).
29. Haas, W. *et al.* Optimization and use of peptide mass measurement accuracy in shotgun proteomics. *Mol. Cell. Proteomics* **5,** 1326–1337 (2006).
30. Huttlin, E. L. *et al.* A tissue-specific atlas of mouse protein phosphorylation and expression. *Cell* **143,** 1174–1189 (2010).
31. Eng, J. K., McCormack, A. L. & Yates, J. R. III. An approach to correlate tandem mass spectral data of peptides with amino acid sequences in a protein database. *J. Am. Soc. Mass Spectrom.* **5,** 976–989 (1994).
32. Beausoleil, S. A., Villen, J., Gerber, S. A., Rush, J. & Gygi, S. P. A probability-based approach for high-throughput protein phosphorylation analysis and site localization. *Nature Biotechnol.* **24,** 1285–1292 (2006).
33. Huang, D. W., Sherman, B. T. & Lempicki, R. A. Systematic and integrative analysis of large gene lists using DAVID bioinformatics resources. *Nature Protocols* **4,** 44–57 (2009).

doi:10.1038/nature12043

**TABLE OF CONTENTS**

**a**

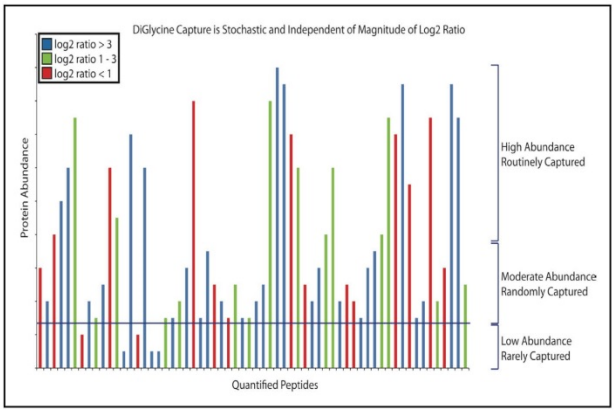


**b**

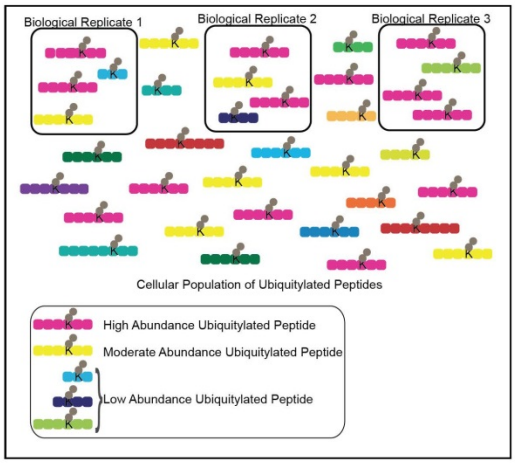


**Figure S1**. Schematic representation of stochasticity in the diGLY capture approach. **a**, Schematic displaying the basis for stochastic retrieval of low abundance peptides that nevertheless have high log2 (H:L) ratios in a SILAC experiment. Abundant proteins may be routinely sampled by diGLY antibody regardless of their log2 (H:L) ratio but lower abundance proteins may be rarely captured, even though they may be highly regulated in response to a signal (log2 (H:L) ratio >3). Thus, multiple experiments may be required to substantially sample a wide cross section of ubiquitylation sites. **b**, Basis for stochastic capture of peptides across biological replicates, with peptides from abundant proteins being detected routinely whereas peptides for low abundance proteins are only captured within a subset of experiments.

**a**

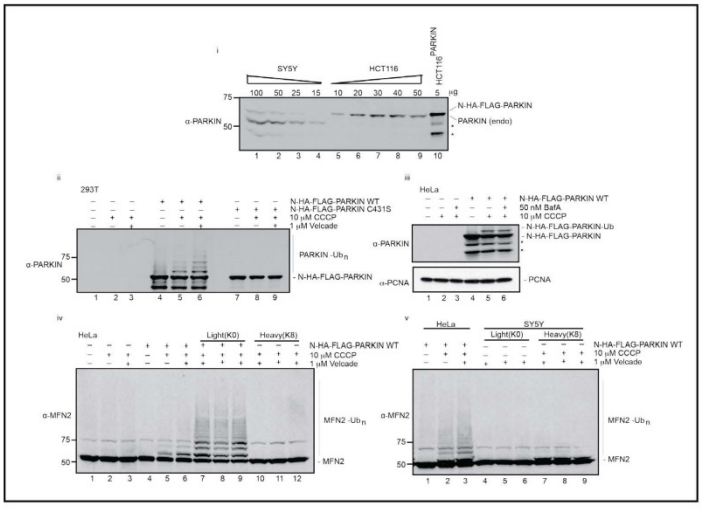
SY5Y
HCT116
HCT116PARKIN
α-PARKIN
N-HA-FLAG-PARKIN
PARKIN (endo)
293T
N-HA-FLAG-PARKIN WT
N-HA-FLAG-PARKIN C431S
10 μM CCCP
1 μM Velcade
PARKIN -Ubn
N-HA-FLAG-PARKIN
HeLa
50 nM BafA
N-HA-FLAG-PARKIN-Ub
α-PCNA
PCNA
Light(K0)
Heavy(K8)
α-MFN2
MFN2 -Ubn
MFN2

**b**

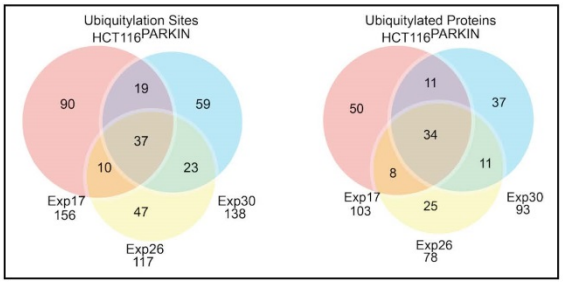
Ubiquitylation Sites
HCT116PARKIN
90
19
59
37
10
23
Exp17
156
47
Exp30
138
Exp26
117
Ubiquitylated Proteins
HCT116PARKIN
50
11
37
34
8
11
Exp17
103
25
Exp30
93
Exp26
78

**c**

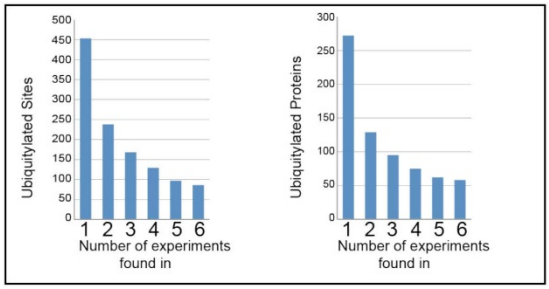
Ubiquitylated Sites
Number of experiments found in
Ubiquitylated Proteins
Number of experiments found in

**d**

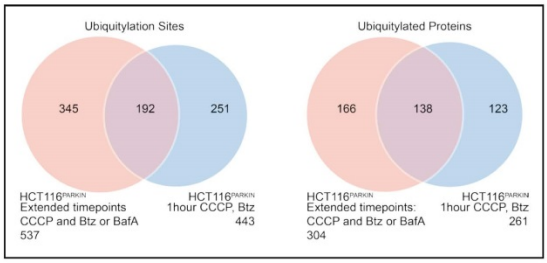
Ubiquitylation Sites
345
192
251
HCT116PARKIN
Extended timepoints
CCCP and Btz or BafA
537
HCT116PARKIN
1hour CCCP, Btz
443
Ubiquitylated Proteins
166
138
123
HCT116PARKIN
Extended timepoints:
CCCP and Btz or BafA
304
HCT116PARKIN
1hour CCCP, Btz
261

**e**

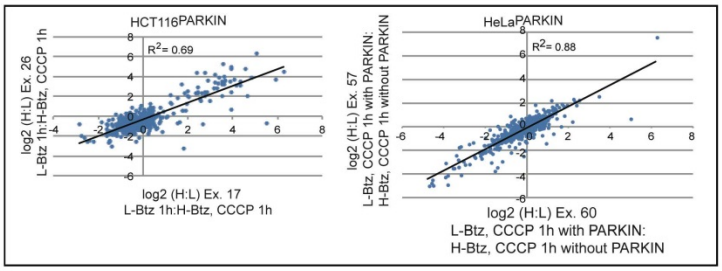
HCT116PARKIN
R2= 0.69
log2 (H:L) Ex. 26
L-Btz 1h:H-Btz, CCCP 1h
log2 (H:L) Ex. 17
L-Btz 1h:H-Btz, CCCP 1h
HeLaPARKIN
R2= 0.88
log2 (H:L) Ex. 57
L-Btz, CCCP 1h with PARKIN:
H-Btz, CCCP 1h without PARKIN
log2 (H:L) Ex. 60
L-Btz, CCCP 1h with PARKIN:
H-Btz, CCCP 1h without PARKIN

**f**

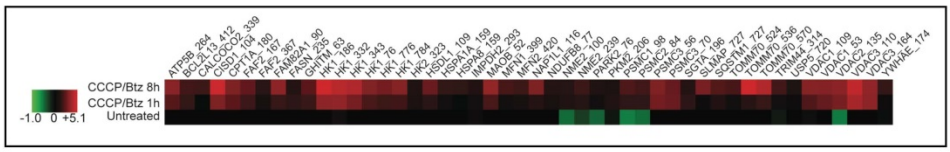
CCCP/Btz 8h
CCCP/Btz 1h
Untreated
-1.0 0 +5.1

**g**

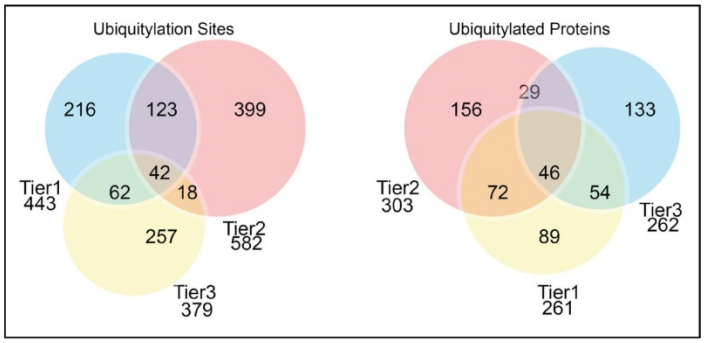
Ubiquitylation Sites
216
123
399
42
62
18
257
Tier1
443
Tier2
582
Tier3
379
Ubiquitylated Proteins
156
29
133
46
72
54
89
Tier2
303
Tier3
262
Tier1
261

**h**

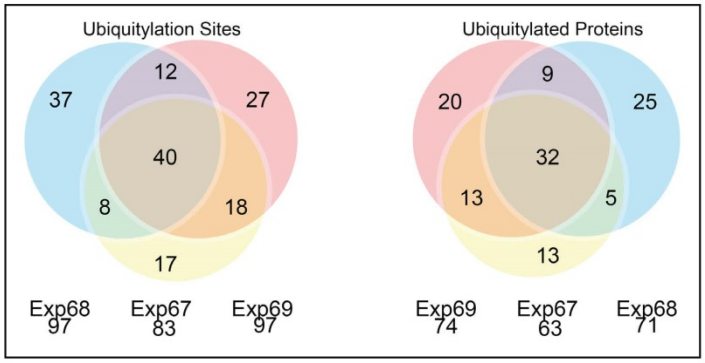


**i**

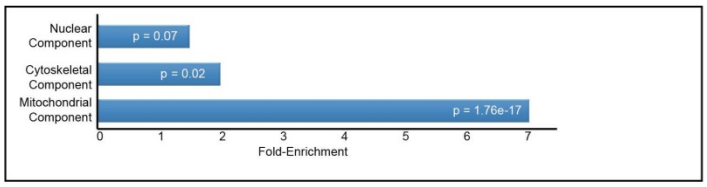


**Figure S2**. Analysis of the PARKIN-dependent ubiquitin modified proteome. **a**, Characterization of PARKIN expression in cell lines employed in this study. Extracts from the indicated cell lines were subjected to SDS-PAGE and immunoblotting with anti-PARKIN antibodies. Panel i) Determination of the relative levels of PARKIN in SH-SY5Y, HCT116, and HCT116$^{PARKIN}$ cell lines. ii-iii) Characterization of N-HA-FLAG-PARKIN expression in 293T and HeLa cells used for interaction proteomics. iv) Demonstration of MFN2 ubiquitylation in HeLa$^{PARKIN}$ cells used for QdiGLY profiling. v) Demonstration of MFN2 ubiquitylation in SH-SY5Y cells used for QdiGLY profiling. *, PARKIN breakdown product. **b**, Venn diagrams for the 3 deepest HCT116$^{PARKIN}$ QdiGLY datasets with a treatment of 10 μM CCCP, 1 μM Btz, for 1 h. **c**, Distribution of ubiquitylation sites (log2(H:L)≥1) and proteins identified up to 6 times across 18 independent HCT116$^{PARKIN}$ QdiGLY experiments (1h CCCP + Btz). **d**, Overlap between ubiquitylation sites and proteins for the various extended time point HCT116$^{PARKIN}$ QdiGLY profiling experiments and the HCT116$^{PARKIN}$ 1h QdiGLY profiling experiments. See Table S1 for conditions of the extended timecourse experiments. **e**, Pearson's Correlation plots for 2 representative QdiGLY experiments from HCT116$^{PARKIN}$ cells (left panel)and HeLa$^{PARKIN}$ cells (right panel). **f**, Heatmap of Log2(H:L) values for selected diGLY peptides from untreated HCT116$^{PARKIN}$ cells and at 1 and 8 h post CCCP treatment. Data are shown for those peptides that were quantified at both time points and in which at least one time point had a log2(H:L) value ≥1.0. **g**, Overlap between Tier 1, 2 and 3 experiments (1h CCCP/Btz). Venn diagram corresponds to diGLY sites with log2(H:L)≥1.0 and their corresponding proteins. **h**, Overlap between triplicate QdiGLY profiling experiments in SH-SY5Y cells with CCCP/Btz for 1 h. **i**, Class 1 target Gene Ontology Enrichment.

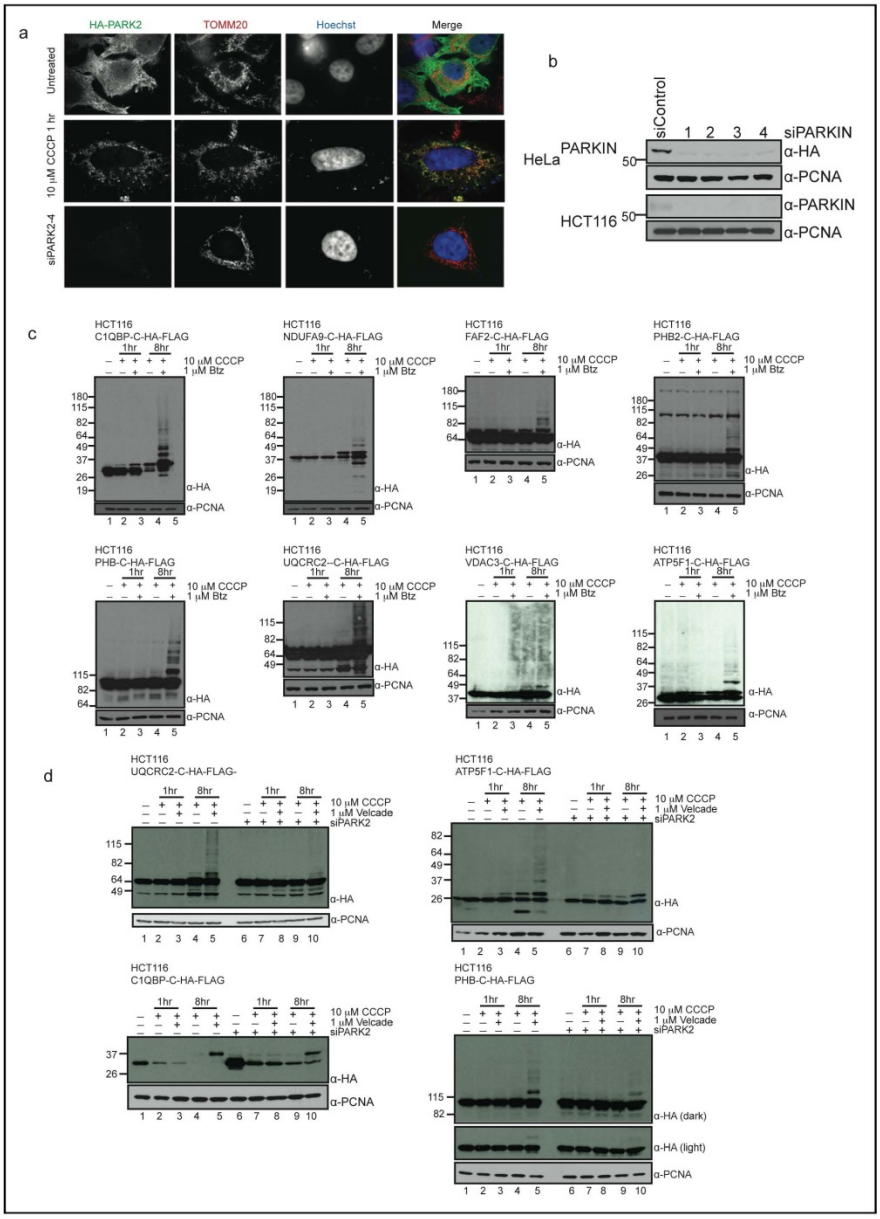


**Figure S3**. Validation of candidate PARKIN targets.
**a,** Validation of siRNAs targeting PARKIN by immunoflourescence. HeLa cells stably expressing HA-FLAG-PARKIN were transfected with PARKIN siRNAs and the

depletion of PARKIN examined by confocal microscopy after immunostaining with anti-HA and anti-TOMM20 antibodies. Nuclei were stained with Hoechst dye.

**b**, Validation of siRNAs targeting PARKIN by immunoblotting. The indicated siRNAs were transfected into HCT116 expressing endogenous levels of PARKIN or HeLa cells stably expressing HA-FLAG-PARKIN cells and after 72 h, cell extracts were immunoblotted with anti-PARKIN, anti-HA, or anti-PCNA antibodies.

**c**, HCT116 cells stably expressing the indicated candidate PARKIN targets as C-terminal HA-FLAG-tagged fusions were treated with CCCP (10 μM) and/or Btz (1 μM) for the indicated period of time prior to harvesting proteins in 8 M urea. Extracts were subjected to immunoblotting with the indicated antibodies.

**d**, HCT116 cells stably expressing the indicated candidate PARKIN targets as C-terminal HA-FLAG-tagged fusions were transiently transfected with either control siRNA or a validated siRNA targeting PARKIN. After 72 h, cells were treated with CCCP (10 μM) and/or Btz (1 μM) for the indicated period of time prior to harvesting proteins in 8 M urea. Extracts were subjected to immunoblotting with the indicated antibodies.

**a**

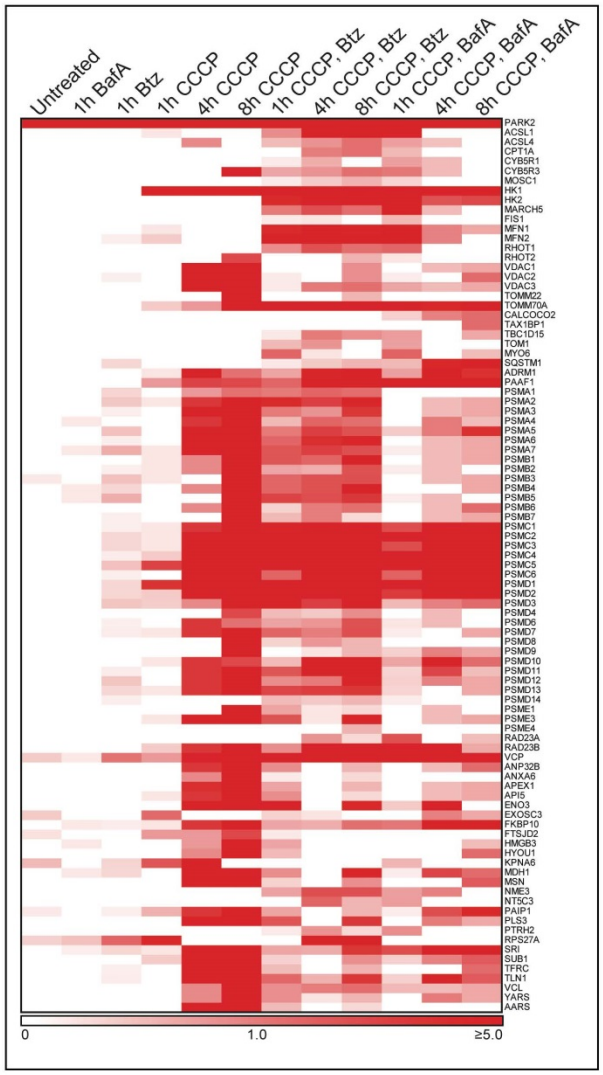
Untreated
1h BafA
1h Btz
1h CCCP
4h CCCP
8h CCCP
1h CCCP, Btz
4h CCCP, Btz
8h CCCP, Btz
1h CCCP, BafA
4h CCCP, BafA
8h CCCP, BafA
PARK2
ACSL1
ACSL4
CPT1A
CYB5R1
CYB5R3
MOSC1
HK1
HK2
MARCH5
FIS1
MFN1
MFN2
RHOT1
RHOT2
VDAC1
VDAC2
VDAC3
TOMM22
TOMM70A
CALCOCO2
TAX1BP1
TBC1D15
TOM1
MYO6
SQSTM1
ADRM1
PAAF1
PSMA1
PSMA2
PSMA3
PSMA4
PSMA5
PSMA6
PSMA7
PSMB1
PSMB2
PSMB3
PSMB4
PSMB5
PSMB6
PSMB7
PSMC1
PSMC2
PSMC3
PSMC4
PSMC5
PSMC6
PSMD1
PSMD2
PSMD3
PSMD4
PSMD5
PSMD7
PSMD8
PSMD9
PSMD10
PSMD11
PSMD12
PSMD13
PSMD14
PSME1
PSME3
PSME4
RAD23A
RAD23B
VCP
ANP32B
ANXA6
APEX1
API5
ENO3
EXOSC3
FKBP10
FTSJD2
HMGB3
HYOU1
KPNA6
MDH1
MSN
NME3
NT5C3
PAIP1
PLS3
PTRH2
RPS27A
SRI
SUB1
TFRC
TLN1
VCL
YARS
AARS
0
1.0
≥5.0

b

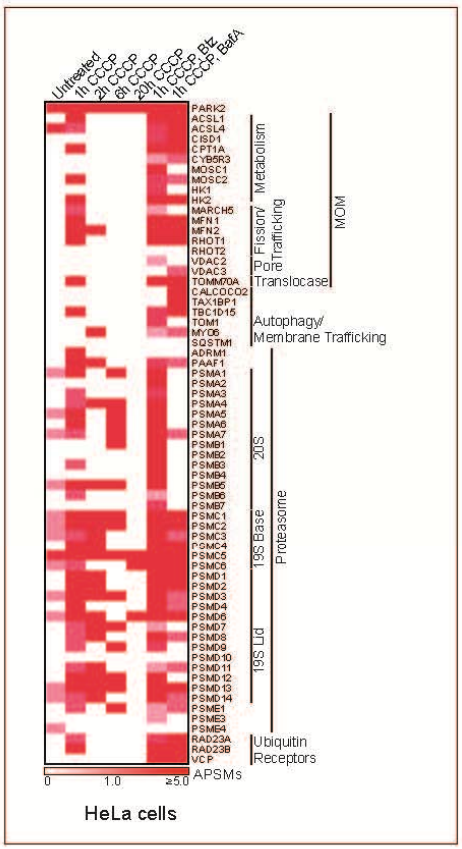


**Figure S4.** Heatmaps of PARKIN-interacting proteins in 293T and HeLa cells. **a**, Heatmaps for WT PARKIN interacting proteins in 293T cells (biological duplicates) with a $WD^N$-score ≥1.0, Z ≥ 5, APSMs ≥ 2, unless otherwise noted (see FULL METHODS). The heatmap reflects APSMs. **b**, Heat map of HA-FLAG-PARKIN interacting proteins (HCIPs) in response to depolarization in HeLa cells, with or without treatment with Btz or BafA. Proteins indicated had $WD^N$-scores ≥ 1.0 or a Z-score ≥ 10 unless otherwise noted (see FULL METHODS). The heatmap reflects APSMs.

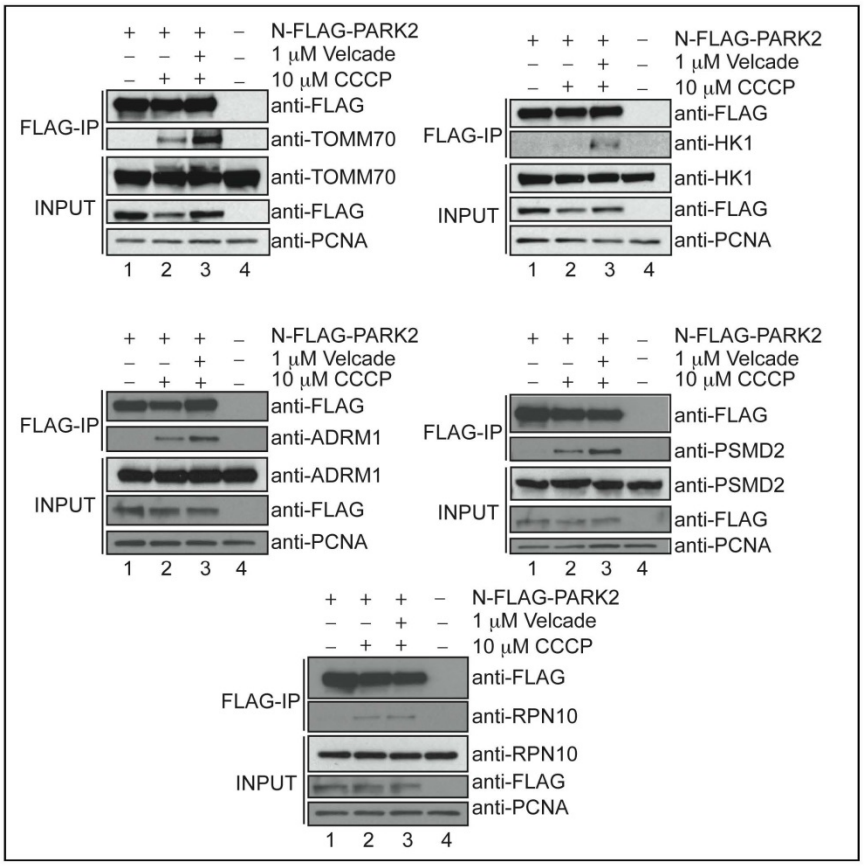


**Figure S5**. Validation of PARKIN interaction with TOMM70, HK1, and proteasomal subunits ADRM1, RPN10, and PSMD2. Extracts from 293T cells stably expressing HA-FLAG-PARKIN with or without treatment with CCCP (10 μM) or CCCP and Btz (Velcade) (1 μM) were immunoprecipitated with anti-FLAG antibodies and immunoblotted with the indicated antibodies. Anti-PCNA was used as a loading control.

**a**

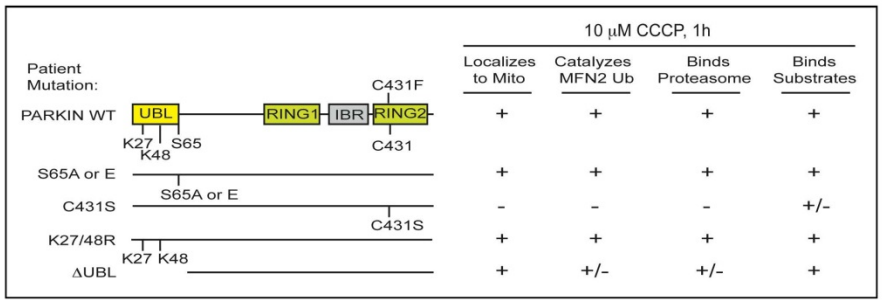
10 μM CCCP, 1h
Patient Mutation:
Localizes to Mito
Catalyzes MFN2 Ub
Binds Proteasome
Binds Substrates
C431F
PARKIN WT
UBL
RING1
IBR
RING2
K27
K48
S65
C431
S65A or E
C431S
K27/48R
ΔUBL
+
-
+/-

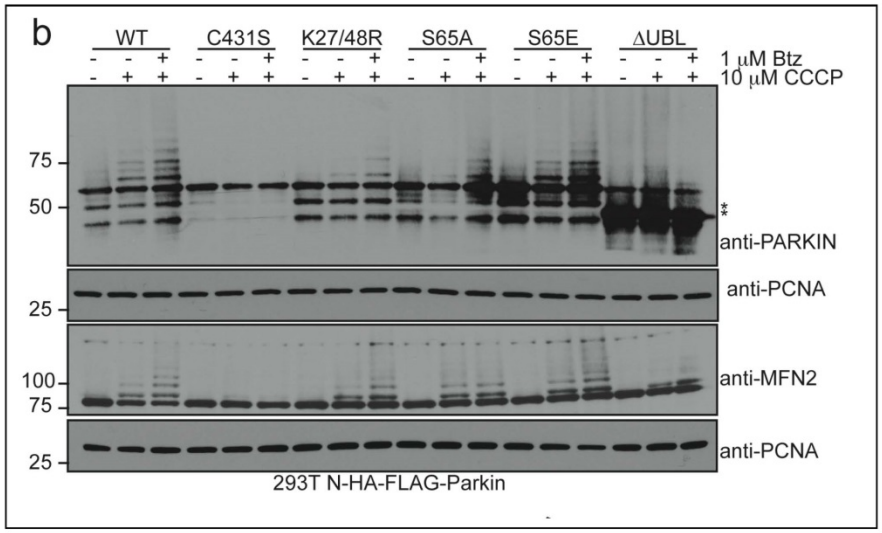
b
WT
C431S
K27/48R
S65A
S65E
ΔUBL
1 μM Btz
10 μM CCCP
75
50
25
100
75
25
anti-PARKIN
anti-PCNA
anti-MFN2
anti-PCNA
293T N-HA-FLAG-Parkin

**c**

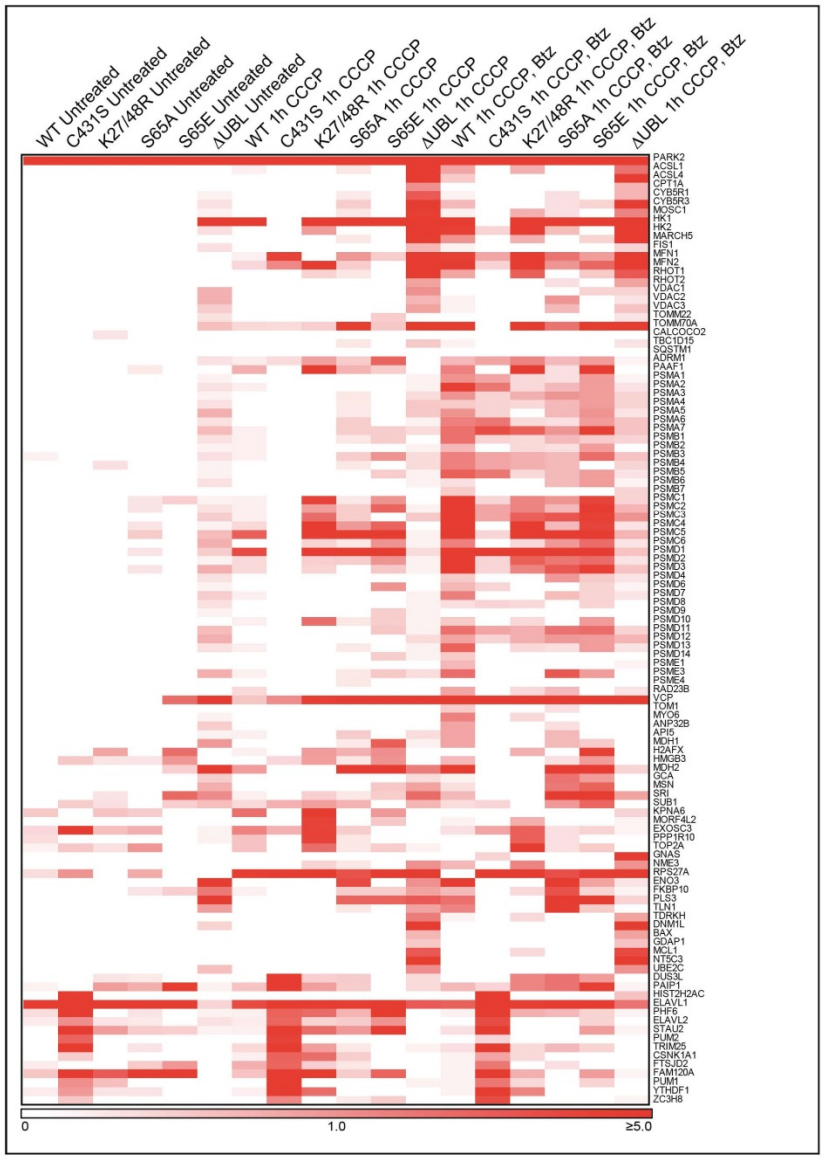
WT Untreated
C431S Untreated
K27/48R Untreated
S65A Untreated
S65E Untreated
ΔUBL Untreated
WT 1h CCCP
C431S 1h CCCP
K27/48R 1h CCCP
S65A 1h CCCP
S65E 1h CCCP
ΔUBL 1h CCCP
WT 1h CCCP, Btz
C431S 1h CCCP, Btz
K27/48R 1h CCCP, Btz
S65A 1h CCCP, Btz
S65E 1h CCCP, Btz
ΔUBL 1h CCCP, Btz
PARK2
ACSL1
ACSL4
CPT1A
CYB5R1
CYB5R3
MOSC1
HK1
HK2
MARCH5
FIS1
MFN1
MFN2
RHOT1
RHOT2
VDAC1
VDAC2
VDAC3
TOMM22
TOMM70A
CALCOCO2
TBC1D15
SQSTM1
ADRM1
PAAF1
PSMA1
PSMA2
PSMA3
PSMA4
PSMA5
PSMA6
PSMA7
PSMB1
PSMB2
PSMB3
PSMB4
PSMB5
PSMB6
PSMB7
PSMC1
PSMC2
PSMC3
PSMC4
PSMC5
PSMC6
PSMD1
PSMD2
PSMD3
PSMD4
PSMD6
PSMD7
PSMD8
PSMD9
PSMD10
PSMD11
PSMD12
PSMD13
PSMD14
PSME1
PSME3
PSME4
RAD23B
VCP
TOM1
MYO6
ANP32B
API5
MDH1
H2AFX
HMGB3
MDH2
GCA
MSN
SRI
SUB1
KPNA6
MORF4L2
EXOSC3
PPP1R10
TOP2A
GNAS
NME3
RPS27A
ENO3
FKBP10
PLS3
TLN1
TDRKH
DNM1L
BAX
GDAP1
MCL1
NT5C3
UBE2C
DUS3L
PAIP1
HIST2H2AC
ELAVL1
PHF6
ELAVL2
STAU2
PUM2
TRIM25
CSNK1A1
FTSJD2
FAM120A
PUM1
YTHDF1
ZC3H8
0
1.0
≥5.0

**d**

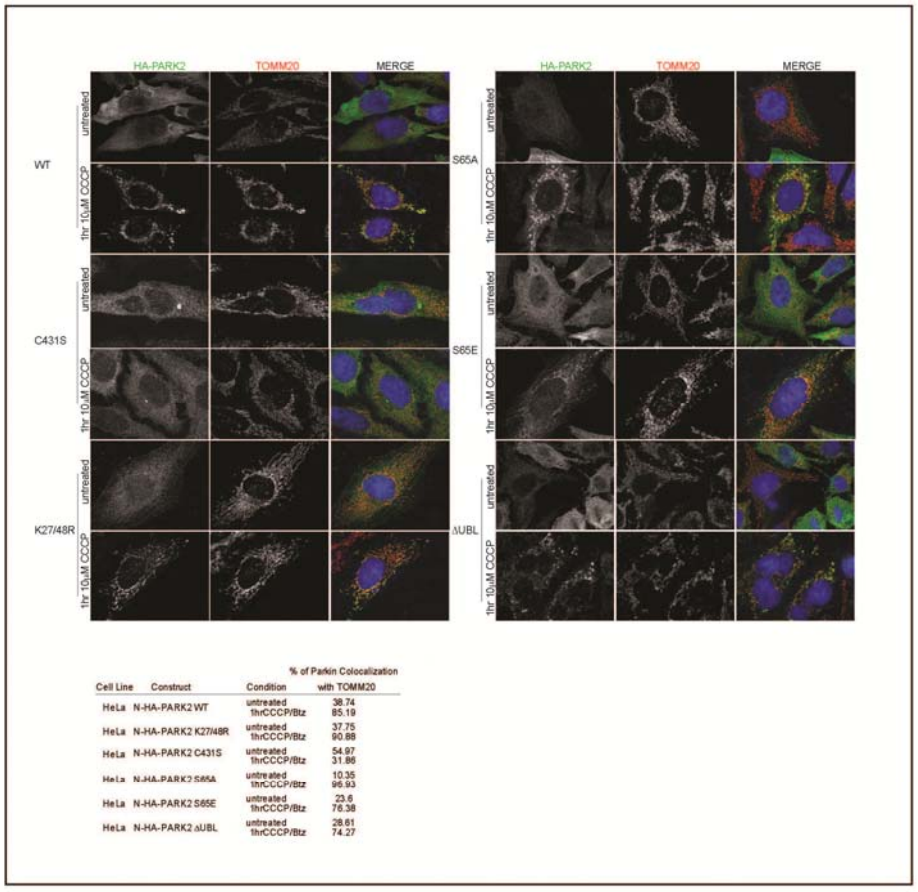


| Cell Line | Construct | Condition | % of Parkin Colocalization with TOMM20 |
|---|---|---|---|
| HeLa | N-HA-PARK2 WT | untreated | 38.74 |
| | | 1hrCCCP/Btz | 85.19 |
| HeLa | N-HA-PARK2 K27/48R | untreated | 37.75 |
| | | 1hrCCCP/Btz | 90.88 |
| HeLa | N-HA-PARK2 C431S | untreated | 54.97 |
| | | 1hrCCCP/Btz | 31.86 |
| HeLa | N-HA-PARK2 S65A | untreated | 10.35 |
| | | 1hrCCCP/Btz | 96.93 |
| HeLa | N-HA-PARK2 S65E | untreated | 23.6 |
| | | 1hrCCCP/Btz | 76.38 |
| HeLa | N-HA-PARK2 ΔUBL | untreated | 28.61 |
| | | 1hrCCCP/Btz | 74.27 |

**Figure S6.** Functional properties and interaction partners of PARKIN mutants. **a**, Summary of functional experiments on selected PARKIN mutant proteins. ΔUBL-PARKIN, residues 81-465. **b**, MFN2 ubiquitylation by selected PARKIN mutants in 293T cells. *, PARKIN breakdown products. **c,** Heatmaps for a series of interacting proteins with a $WD^N$-score $\geq 1.0$, Z-score $\geq 5$, APSMs $\geq 2$, and found in biological duplicates for various PARKIN mutants, unless otherwise noted (see FULL METHODS). **d**, Localization of PARKIN and selected mutants to mitochondria in response to depolarization. HeLa cells stably expressing wild-type PARKIN or the indicated PARKIN mutants as HA-FLAG fusion proteins were treated with CCCP (10 μM, 1h), cells were fixed, stained with anti-HA (green) and anti-TOMM20 (red), and nuclei stained with Hoechst 33342. Images of representative cells were collected using a Nikon confocal microscope.

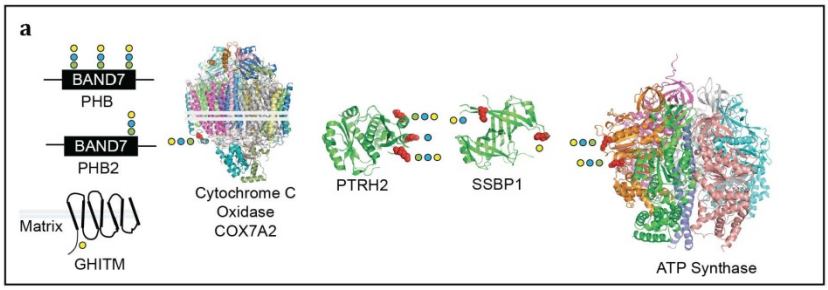
a
BAND7
PHB
BAND7
PHB2
Matrix
GHITM
Cytochrome C
Oxidase
COX7A2
PTRH2
SSBP1
ATP Synthase

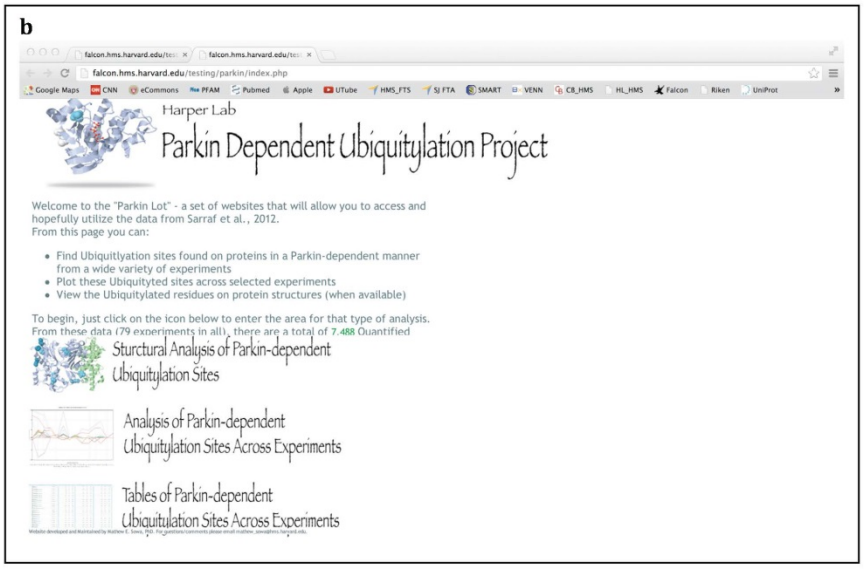
b
falcon.hms.harvard.edu/testing/parkin/index.php
Harper Lab
Parkin Dependent Ubiquitylation Project
Welcome to the "Parkin Lot" - a set of websites that will allow you to access and hopefully utilize the data from Sarraf et al., 2012.
From this page you can:
Find Ubiquitlyation sites found on proteins in a Parkin-dependent manner from a wide variety of experiments
Plot these Ubiquityted sites across selected experiments
View the Ubiquitylated residues on protein structures (when available)
To begin, just click on the icon below to enter the area for that type of analysis.
Sturctural Analysis of Parkin-dependent Ubiquitylation Sites
Analysis of Parkin-dependent Ubiquitylation Sites Across Experiments
Tables of Parkin-dependent Ubiquitulation Sites Across Experiments

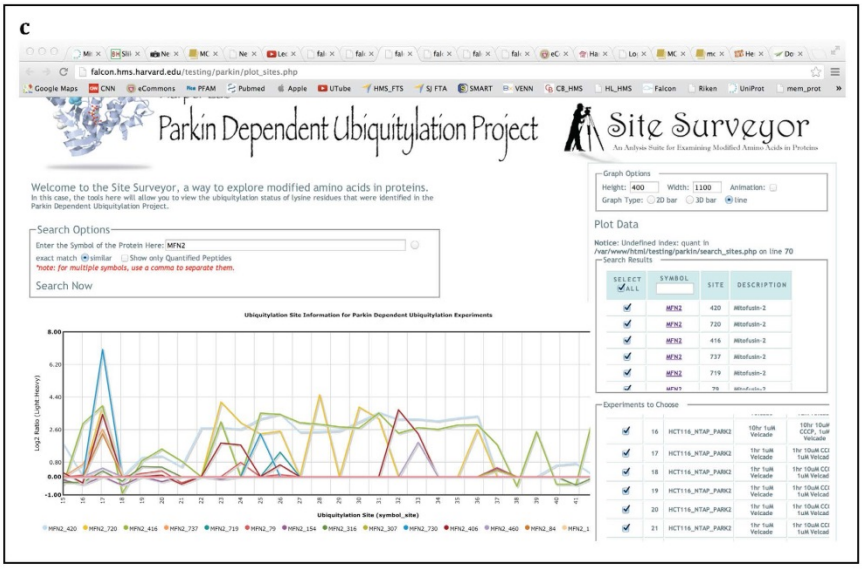
c
falcon.hms.harvard.edu/testing/parkin/plot_sites.php
Parkin Dependent Ubiquitylation Project
Site Surveyor
An Analysis Suite for Examining Modified Amino Acids in Proteins
Welcome to the Site Surveyor, a way to explore modified amino acids in proteins.
In this case, the tools here will allow you to view the ubiquitylation status of lysine residues that were identified in the Parkin Dependent Ubiquitylation Project.
Search Options
Enter the Symbol of the Protein Here: MFN2
exact match similar Show only Quantified Peptides
*note: for multiple symbols, use a comma to separate them.
Search Now
Ubiquitylation Site Information for Parkin Dependent Ubiquitylation Experiments
Log2 Ratio (Light:Heavy)
Ubiquitylation Site (symbol_site)
Graph Options
Height: 400 Width: 1100 Animation:
Graph Type: 2D bar 3D bar line
Plot Data
Notice: Undefined index: quant in /var/www/html/testing/parkin/search_sites.php on line 70
Search Results
SELECT ALL
SYMBOL
SITE
DESCRIPTION
MFN2 420 Mitofusin-2
MFN2 720 Mitofusin-2
MFN2 416 Mitofusin-2
MFN2 737 Mitofusin-2
MFN2 719 Mitofusin-2
Experiments to Choose

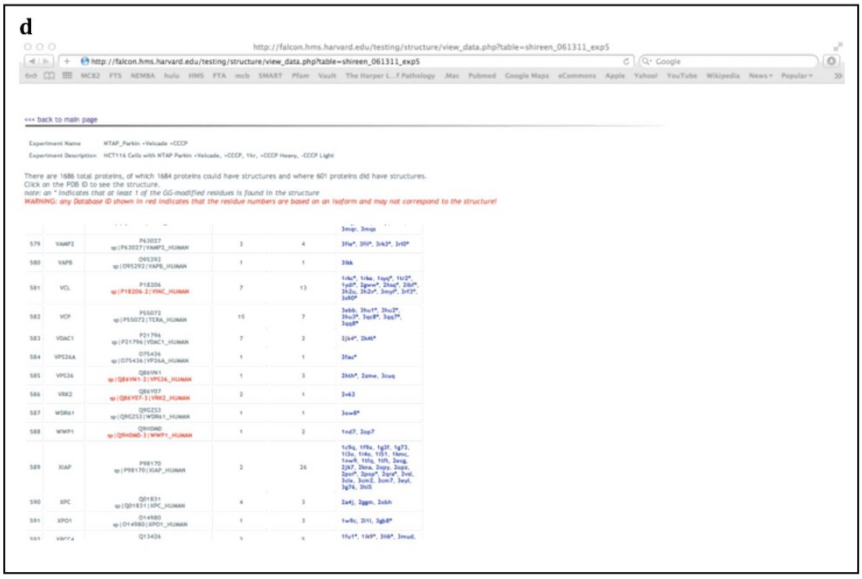
d
http://falcon.hms.harvard.edu/testing/structure/view_data.php?table=shireen_061311_exp5
<<< back to main page
There are 1686 total proteins, of which 1684 proteins could have structures and where 601 proteins did have structures.
Click on the PDB ID to see the structure.
note: an * indicates that at least 1 of the GG-modified residues is found in the structure
WARNING: any Database ID shown in red indicates that the residue numbers are based on an isoform and may not correspond to the structure!

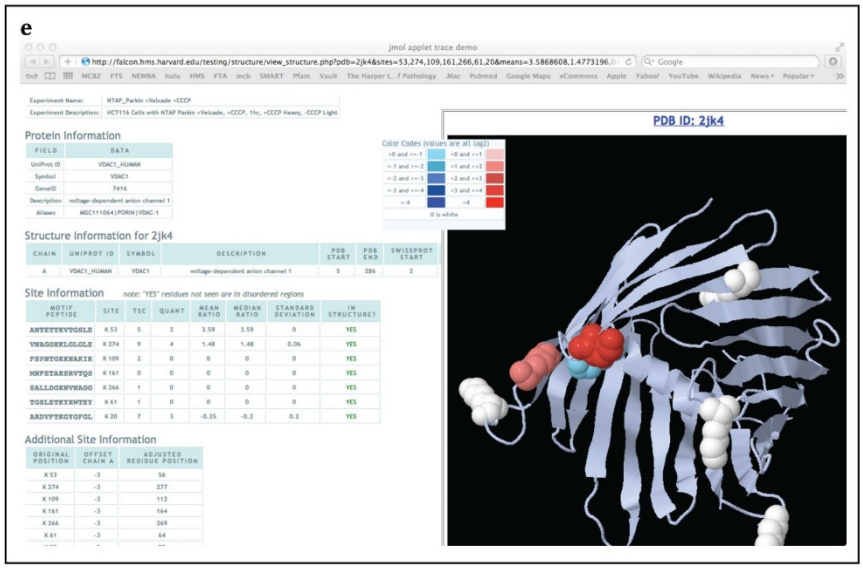
e
jmol applet trace demo
PDB ID: 2jk4
Protein Information
Structure Information for 2jk4
Site Information
Additional Site Information

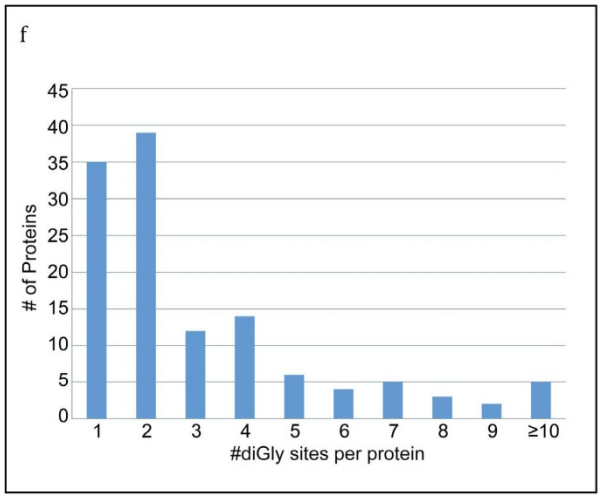
f
# of Proteins
#diGly sites per protein
0
5
10
15
20
25
30
35
40
45
1
2
3
4
5
6
7
8
9
≥10

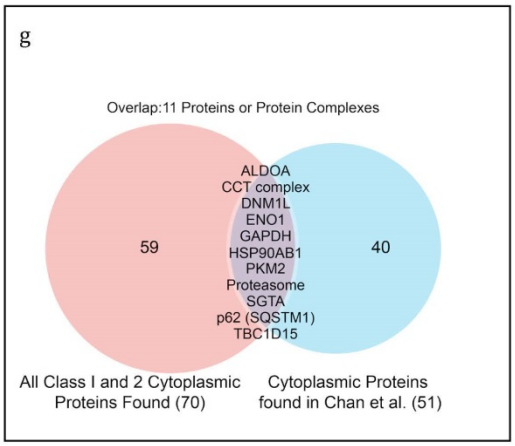


**Figure S7**. Structural analysis of mitochondrial inner membrane and matrix candidate PARKIN substrates and a Web-tool for interrogation and structural analysis of candidate PARKIN targets. **a**, Structures or domain schematics are shown for depolarization and PARKIN-dependent diGLY sites [log2(H:L) ≥ 1.0] (PDB codes, Table S5). Color-coded circles (as detailed in Figure 4a in the main paper) indicate the conservation of Lys at the homologous position in *M. musculus*, *D. rerio*, and *D. melanogaster* (Table S5). For structures, regulated sites are shown in red space-filled models. **b**, Web tool. In order to aid in the analysis of the PARKIN-dependent ubiquitin modified proteome, a web-based tool was developed for retrieval, plotting of data for individual sites across multiple experiments, and visualization of structures for candidate PARKIN targets. On the front page (panel b), you can enter 3 analysis areas: structural analysis, plotting of ubiquitylation sites across experiments, and access to tables and retrieval of data. Panel **c** shows an example of a plot of log2 SILAC ratios for a MFN2 site across several experiments using Site-Surveyor. For structural analysis, individual experiments can be selected from the drop-down menu, which then populates a table collecting PDB identifiers for proteins having structures in the PDB (see Panel d). Individual PDB identifiers are linked to a page, which collects relevant quantitative proteomics data (principally the log2 ratio for identified and quantified peptides and the peptide sequences), and displays the structure in a new window, allowing 3-D rotation and visualization (Panel **e**). Lysines that were identified as ubiquitylated are shown in space-filling models and are color-coded based on the log2 ratio for regulated sites (sites showing an increased diGLY ratio in red. Sites that are identified but are not quantified are shown in white. This web-tool can be accessed at http://harper.hms.harvard.edu. **f**, Distribution of the number of Class 1 and 2 ubiquitylation sites identified across all Class 1 and 2 targets. **g**, Comparison between cytoplasmic proteins identified as PARKIN targets (Class 1 and 2) in this study, and proteins whose abundance accumulated in mitochondria as determined by SILAC-based proteomics.[4]

**Supplemental Text**

**Comparison of depolarization-dependent interaction data with historical studies**

Using interaction proteomics, we identified a reproducible cohort of depolarization-dependent PARKIN-interacting proteins, many of which are mitochondrial, consistent with the model of PINK1-dependent recruitment of PARKIN to the mitochondria after damage. Identification of ubiquitylation sites on many of these proteins via QdiGly analysis further supports the view that these proteins both interact with and are substrates of PARKIN. However, a number of candidate PARKIN binding proteins and substrates reported prior to the discovery of this PINK1-dependent conversion of PARKIN from an inactive to active form - including CCNE, AIMP2, DJ-1, and RANBP2 (Ref 3) - were not detected here, and some of these interactions have been called into question as PARKIN targets based on other grounds.[3] In contrast, activated PARKIN displays robust signal-dependent association with MOM-derived proteins, consistent with a primary role in mitochondrial ubiquitylation in response to this particular type of cellular challenge.[1]

**Potential impact of MOM ubiquitylation by PARKIN on the activity of individual proteins**

Previous studies indicate that PINK1 interacts stably with the TOMM complex[17]. Together with our findings that TOMM70 and TOMM22 are depolarization-dependent PARKIN-interacting proteins as well as the identification of PARKIN-dependent ubiquitylation sites on TOMM70 (Figure 2b), these data suggest that the TOMM complex may serve as a nexus for regulation of PARKIN by PINK1. Additionally, translocase function, for example, interaction with transport substrates, may be dynamically altered by ubiquitylation of numerous TPR repeats in TOMM70 (Figure 4c).

In addition to modification of MOM proteins, we also observed modification of proteins resident in the MIM or matrix (Figure 2 and S7a). Ubiquitylation of these proteins may reflect disruption of mitochondrial structure, which either allows MIM or matrix proteins to escape or permits ubiquitylation machinery access to these compartments; notably, the extent of ubiquitylation often increased substantially at longer timepoints following depolarization (Table S2).[36] However, we cannot exclude the possibility that PARKIN's association with the TOMM complex allows ubiquitylation of proteins whose transport is stalled as a result of depolarization or PARKIN-dependent TOMM70 ubiquitylation. If this occurs, the repeated identification of the same subset of sites in multiple experiments employing 1h of depolarization would suggest a highly stereotypical ubiquitylation mechanism.

Also of interest, we identified ubiquitylation sites in each of three ATPase subunits of the regulatory particle of the proteasome (PSMC1/RPT2, PSMC2/RPT1, and PSMC3/RPT5) (Figure 2, Figure 4b). These ubiquitylation events occur within extended helices that form coiled-coils with neighboring RPT subunits and are clustered together on a surface of the regulatory particle that is proximal to the RPN10 subunit (Figure 4b). Previous studies indicate that the C-terminal UIM domain of RPN10 associates with the UBL domain of PARKIN.[37] Thus, our finding that association of PARKIN with the proteasome is greatly stimulated by mitochondrial depolarization (Figure 3a) suggests

that PSMC ubiquitylation is likely linked to assembly of PARKIN with the proteasome, as association of PARKIN with the RPN10 subunit is likely to favor ubiquitylation of nearby PSMC subunits (Figure 4e). Determination of whether this modification affects proteasome assembly or function downstream of PARKIN activation or is merely a "bystander effect" is crucial to resolve.

**Relationship of PARKIN to other potential ubiquitin ligases acting on mitochondria.**

We have identified numerous proteins on the MOM and in the cytoplasm that are ubiquitylated in a depolarization and PARKIN-dependent manner. In addition, we demonstrated that a substantial fraction of these proteins are captured as PARKIN-associated proteins by affinity chromatography-MS. However, we did not detect a substantial number of candidate substrates in association with PARKIN. This could reflect low abundance, difficulty in extraction from the MOM, or transient association with PARKIN. However, we are not able to conclude that all depolarization and PARKIN-dependent proteins are direct substrates. Another prominent mitochondrial E3 is MARCH5. Interestingly, we have identified MARCH5 as a PARKIN-associated protein (Figure 3a,b), although we did not identify any PARKIN and depolarization-dependent ubiquitylation sites in MARCH5. Previous studies have implicated MARCH5 in cell cycle dependent control of MFN1 turnover. While we cannot rule out a role for MARCH5 in ubiquitylation events seen here, our studies did not directly examine cell cycle dependent changes in ubiquityaltion-site occupancy. Further studies are necessary to test the involvement of MARCH5 in the PARKIN-dependent ubiquitin modified proteome.

Using the QdiGLY approach, we have identified a wide cross-section of candidate PARKIN substrates. This work, together with previous studies summarized above, supports a model wherein PINK1-dependent recruitment to PARKIN allows its interactions with and ubiquitylation of numerous MOM proteins, likely resulting in widespread alterations in protein-protein interactions and turnover rates for many key mitochondrial proteins. Targeted studies within the cellular context of PD are required to elucidate the key PARKIN targets whose ubiquitylation is necessary for proper mitochondrial quality control and will be aided by the PARKIN target landscape reported here.

36 Yoshii, S. R., Kishi, C., Ishihara, N. & Mizushima, N. Parkin Mediates Proteasome-dependent Protein Degradation and Rupture of the Outer Mitochondrial Membrane. *J Biol Chem* **286**, 19630-19640, (2011).

37 Sakata, E. *et al*. Parkin binds the Rpn10 subunit of 26S proteasomes through its ubiquitin-like domain. *EMBO Rep* **4**, 301-306, (2003).

38 Park YY, Cho H. Mitofusin 1 is degraded at G2/M phase through ubiquitylation by MARCH5. *Cell Div*. 7:25. doi: 10.1186/1747-1028-7-25 (2012).